Synthesis and Applications of Cellulose Derivatives for Drug Delivery

Joyann Audrene Marks

Dissertation submitted to the faculty of the Virginia Polytechnic Institute and State University in partial fulfillment of the requirements for the degree of

Doctor of Philosophy

In

Macromolecular Science and Engineering

Kevin J. Edgar, Chair

Maren Roman

Lynne S. Taylor

Judy S. Riffle

S. Richard Turner

August 5, 2015

Blacksburg, VA

Keywords: pairwise blends, amorphous solid dispersion, oral drug delivery, cellulose esters, bioavailability, cationic cellulose, extrusion

Synthesis and Applications of Cellulose Derivatives for Drug Delivery

Joyann Audrene Marks

ABSTRACT

In an effort to produce new derivatives of cellulose for drug delivery applications, methods were developed to regioselectively modify C-6 halo cellulose esters to produce cationic derivatives via nucleophilic substitution. Reaction of C-6 substituted bromo and iodo cellulose with trialkylated amines and phosphines produced new cationic ammonium and phosphonium cellulose derivatives which can be explored as delivery agents for nucleic acids, proteins and other anionic drug molecules. It was anticipated that these new derivatives would not only be capable of complexing anionic drug molecules but would have greatly improved aqueous solubility compared to their precursors. The phosphonium derivatives described in this work are an obvious example of such improved solubility properties.

Given the importance of cellulose derivatives in making amorphous dispersions with critical drugs, it has also been important to analyze commercially available polymers for the potential impact in oral drug delivery formulations. To do so pairwise blends of cellulosics and synthetic polymers commonly used as excipients were tested for miscibility using techniques such as DSC, mDSC, FTIR and film clarity. Miscible combinations highlight the potential to use combinations of polymers currently available commercially to provide drug delivery solutions for specific drug formulations.

The use of melt extrusion in processing some of these drug/polymer dispersions provides a means of highlighting the capability for the use of these cellulosics in melt extruded amorphous dispersions. This solvent free, high pressure method significantly reduces cost and time and can be applied on a large scale. The analysis of long chain cellulose esters and ultimately the novel omega carboxy esters for melt processability significantly impacts the possibilities available for use of those excellent drug delivery agents on a much larger scale.

Dedication

For my mother -You have always been my rock and continue to be despite your illness. I am thankful for you and for all the encouraging words and prayers that have pushed me throughout this journey. Thank you for always being my ultimate motivation. I love you.

Acknowledgements

I would first like to express sincere gratitude to my advisor Dr. Kevin J. Edgar who has been a source of encouragement, guidance and inspiration for me throughout this journey. He has displayed great patience and understanding throughout the course of this work and has always been available to assist in providing much needed guidance throughout my time at Virginia Tech. I am eternally grateful for the opportunity to pursue my PhD under his mentorship and have gained a wealth of knowledge and opportunities during this time. I will always be grateful to him and his wife for their welcoming and encouraging nature.

I am also grateful to the members of my graduate committee, Dr. Judy S. Riffle, Dr. Maren Roman, Dr. S. Richard Turner and Dr. Lynne S. Taylor for their guidance and suggestions that have proven very valuable throughout my research.

I must say a big thank you to all my colleagues in the Cellulose Research group and Taylor group past and present who have played vital roles in my time at Virginia Tech. They have provided great advice, engaging discussions and made time spent both in and out of lab an enjoyable one.

I am grateful to the Macromolecules and Interface Institute (MII), Sustainable Biomaterials and the Institute for Critical Technology and Applied Science (ICTAS) for academic, financial and facilities support and thankful for funding provided by NSF Fund DMR-1308276. I am also immensely thankful for the help of various other students, professors and support staff in these and the Chemistry department who have been instrumental in providing necessary instrumentation and instruction.

I must also acknowledge the encouraging professors at Fisk University who supported me throughout my undergraduate career and have continued to provide mentorship and advice throughout my PhD work.

I am forever grateful for the patience, love and prayers of my immediate and extended family who have been my source of strength and of unconditional support.

A big thank you to my dearest friends who have been like family, brightening some of the darkest moments along the way, praying for me and with me and providing much needed encouragement.

Finally I am grateful to my Lord Jesus Christ, my ever present source of peace and guidance.

Attribution

Several colleagues aided in data collection and research for the chapters within this dissertation. A brief description of their contributions is included here.

Dr. Kevin J. Edgar was the principal investigator and was a primary contributor in the planning, organizing, and directing of the projects described in this dissertation.

Chapter 3: Pairwise Polymer Blends for Oral Drug Delivery

Dr. Lynne Taylor is a collaborator in the Department of Industrial and Physical Pharmacy at Purdue University and served as a coauthor on this paper.

Dr. Lindsay Wegiel at Purdue University (Taylor Group) assisted with FTIR analyses described under section 3.3.5 and served as a co-author on this paper.

Dr. Bruce Orler at Virginia Tech (Moore Group) assisted with the DSC analyses described under section 3.3.4.

Chapter 4: Cationic Cellulose Derivatives for Drug Delivery: Synthetic Pathways to Regioselectively Substituted Ammonium and Phosphonium Derivatives

Preliminary findings of Dr. S. Carter Fox at Virginia Tech (Edgar Group) assisted in research development for the results presented and he is a coauthor on the manuscript to be submitted for publication.

Chapter 5: 6-Carboxycellulose Acetate Butyrate as a Novel Polymer for Amorphous Solid Dispersion and Extrusion

Ms. Ruoran Zhang and Ms. Brittany Nichols at Virginia Tech (Edgar Group) assisted in data collection for the results presented in Chapter 5.

Dr. Ann Norris at Virginia Tech (Department of Sustainable Biomaterials) assisted with XRD analyses described under section 5.3.8.

Table of contents

List of Figures

List of Schemes

List of Tables

Chapter 1: Research Introduction

Cellulose is an extremely versatile polymer, and is the basis for derivatives that have many important applications, including in textiles, paper making, coatings and also in drug delivery. Successfully applying cellulose in these regards requires a strong understanding of how the structure of the polysaccharide relates to its function. The synthesis of new derivatives of cellulose has been critical to these efforts and has permitted the application of cellulose in new and innovative ways. This research has not only sought to develop techniques for synthesizing new derivatives of cellulose but also to explore the applications of cellulose derivatives using various techniques related to making amorphous solid dispersions with critical drug molecules. An overarching theme of this research is centered on improving the methods of making formulations for drug delivery and providing derivatives that have the potential to act as improved matrix polymers for those applications.

In light of the importance of understanding more about the structure/property relationships of cellulose, regioselective modification has provided important information on this subject. The type of substituent as well as the distribution of these substituents along the polysaccharide chain can influence the resulting physical properties. Greater understanding of these physical properties is crucial to applications in drug delivery. There are two major focal points of this research; the synthesis of cationic cellulose derivatives of cellulose for use in drug delivery formulations with anionic drug molecules, and more broadly the examination of cellulose derivatives as matrix materials for drug delivery applications. This research will describe efforts to synthesize these regioselectively modified cationic cellulose derivatives with potential applications in drug and gene delivery and seek to understand some of the properties of

the resulting polysaccharides. A substantial focus will also be given to the use of cellulosic derivatives as amorphous matrix formulations for drug delivery through amorphous dispersions and melt extruded formulations.

Halogenation of cellulose at C-6 will be utilized to provide a facile route to regioselectively substituted quaternary ammonium and phosphonium derivatives that are expected to provide options for complexing and delivering anionic drugs. These new polysaccharide derivatives have similar potential applications in drug delivery as amine containing polysaccharides like chitosan and heparin. These derivatives are also attractive due to their potential as paracellular permeability enhancers (PPEs) for tight junction opening and for the delivery of nucleic acids and other anionic drug actives similar to applications for chitosan and other cationic polymers. The potential benefits of pairwise blends of cellulose derivatives with other well-known polymer entities and the utilization of novel cellulose derivatives with superior properties for crystallization inhibition of target drugs are examined in this research. Combining the favorable properties of two polymers has historically been an important method of producing diverse polymeric materials. This concept has been applied to amorphous formulations for drug delivery and has provided very promising candidates. An extensive study on the characteristics of polymer blends of well-known matrix polymers as well as novel cellulose derivatives is important for enhancing the database of effective amorphous matrix formulations currently available.

As new excipients are synthesized and examined for use in drug delivery formulations, there is also a challenge of processing these formulations using techniques that are efficient, safe and economically viable. Melt extrusion is used commercially to generate pharmaceutical products that can be easily shaped into tablet formulations for oral drug delivery or implantable

devices. Melt extrusion is advantageous based on its lower cost due to absence of solvent, higher yields and more consistent product once optimal conditions are determined for extrusion of a particular pharmaceutical product. Melt extrusion is used to achieve a solid dispersion from a highly crystalline, poorly soluble drug through combination with a suitable polymeric material. This research examines the melt processability of drug/polymer blends containing some commercially available as well as novel cellulosics from our lab formulated with commonly used poorly soluble pharmaceuticals. The novel cellulosics are long chain omega carboxycellulose esters. These highly substituted cellulose esters are less prone to crosslinking reactions and instability at higher temperatures due to interchange reactions between hydroxyl and carboxylic acid groups in the backbone of OH/COOH containing polymers. These reactions include transesterification between carboxylic acid groups on adjacent chains and esterification reactions between carboxylic acid groups and free hydroxyls along the cellulose chain. These transesterification reactions are common in some cellulose ethers like carboxy methyl cellulose (CMC) at high temperatures. Internal plasticization of longer chain cellulose esters also provides lower glass transition temperatures to give broader processing windows for the derivatives and enable processing at lower temperatures. This helps to minimize the thermal degradation of the cellulose esters during processing.

An outline for this dissertation is as follows: **Chapter 2** will review some of the fundamentals concerning the properties and applications of cellulose. It will give a detailed review of regioselective modifications performed on cellulose. The chapter will also discuss the use of cellulose derivatives in drug delivery applications as well as some of the processing methods and analytical techniques used to evaluate those drug delivery formulations. **Chapter 3** will then present investigations of pairwise polymer blends of some commercially available

cellulosics, synthetic excipients and a novel cellulose omega carboxy ester. This chapter will highlight some pairwise blends that are very promising for the delivery of poorly aqueous soluble drugs and could provide solutions to the high cost of synthesizing new derivatives to cater to the differences in individual drug molecules. **Chapter 4** will then discuss the synthesis of cationic cellulose derivatives through reactions with trialkylated amines and phosphines to provide new agents for permeation enhancement and show the production of water-soluble cellulose derivatives that can be further used for complexing anionic drugs. **Chapter 5** will describe results on the application of 6-carboxycellulose acetate butyrate (CCAB) as a matrix material for amorphous solid dispersion (ASD) formulations with structurally diverse active pharmaceutical ingredients (APIs). This chapter will describe the formulation of CCAB/drug formulations as well as examine the practicality of melt processing dispersions of this novel polymer with poorly water-soluble pharmaceuticals in an effort to decrease crystallinity, improve solubility and give improved delivery of the drugs. **Chapter 6** will conclude with a summary of the research results discussed in this dissertation and give some suggestions for future work.

Chapter 2: Literature review

2.1 Introduction

Cellulose is one of the most abundant natural polymers found on earth. This polymer is found primarily in plants and is produced by some microorganisms. It is a versatile polymer that has many applications in textiles, paper making, and drug delivery. In order to take advantage of this versatile polymer it is important to understand how its structure relates to its functionality; synthesis of derivatives of cellulose has contributed greatly to such studies. This review will seek to describe some of the basic elements regarding cellulose followed by more detailed information about the functionalization of cellulose and the ways in which these derivatives have been studied for potential drug delivery applications. A greater focus will be given to the use of cellulosic derivatives as amorphous matrix formulations for drug delivery and how derivatization can aid in improving such applications.

There are two major focal points of this review; the synthesis of cationic cellulose derivatives for drug delivery applications, and more broadly the examination of cellulose derivatives as matrix materials for drug delivery applications. There will be a brief introduction to the structure and reactivity of cellulose and those elements that most influence the process of making cellulose derivatives including crystallinity, hydrogen bonding, cellulose dissolution and degradation. These are important elements to consider when finding more effective means of derivatizing cellulose to produce novel derivatives for drug delivery applications.

Current methods used for producing regioselectively substituted derivatives of cellulose and those that are most useful for producing derivatives at the C-6 position will be discussed in some detail. Tosylation and C-6 halogenation methods will be considered especially in the context of providing a route to quaternary ammonium and phosphonium cationic derivatives of cellulose which are expected to have great application in complexing and delivering anionic drugs and providing structural analogs of well known cationic and amine containing polymers like chitosan, and glycosaminoglycans like heparin.

Subsequent to the discussion on derivatizing methods, the use of cellulose derivatives as matrix materials for amorphous solid dispersions will be examined in detail. A description of current methods of analyzing such derivatives in this regard as well as the important elements for effective drug release will also be described in this review. As an extension of the examination of cellulose derivatives for drug delivery applications, the potential benefits of making binary

blends of cellulose derivatives with other well-known polymer entities and the utilization of novel cellulose derivatives with superior properties for crystallization inhibition of target drugs will be carefully described. Combining the favorable properties of two polymers has historically been an important method of producing diverse polymeric materials[2]. This concept has been applied to amorphous formulations for drug delivery and has provided very promising candidates. An extensive study on the characteristics of polymer blends of well-known matrix polymers as well as novel cellulose derivatives is important for enhancing the available options of effective amorphous matrix formulations.

2.2 Cellulose

Cellulose is a component of the cell wall of higher plants but it is also produced in some species of bacteria, algae, fungi, amoeba and some sea animals, for example tunicates. The majority of cellulose used commercially and for research initiatives is obtained from plant sources. Cellulose is the primary structural polymer found in trees and other plants. It is a storage polymer for the photosynthetic products of these plants. The annual production of cellulose in nature is about 10^{11} to 10^{12} tons[3]. Cellulose is produced in a relatively pure form from the seed hairs of the cotton plant but the greatest production in nature occurs for the purpose of generating the cell walls in woody plants. Cellulose obtained from these sources differs significantly in crystallinity and this helps to determine how it is utilized (Table 1). Microcrystalline cellulose for example, obtained from plant sources, and having DP between 100 and 300 is used extensively for cellulose derivatization[3-4].

Table 2.1: Cellulose purity and crystallinity from common sources. Heinze, T.; Liebert, T.; Koschella, A., Esterification of Polysaccharides. Springer: 2006.[5] Used under fair use, 2015.

Type	Glc (%)	Man (%)	Xyl (%)	DP	Crystallinity (%)
Avicel	100	ND	ND	280	61
Prehyd. Sulfate Southern Pine	95	1.6	3.1	800	54
Spruce Sulfite	96	2.0	2.5	800	54
Linters	100	ND	ND	1470	63
Bacterial Cellulose	100	ND	ND	2000-8000	60-90

2.3 The Structure of Cellulose

Cellulose is a linear homopolymer of D-glucose. D-Glucose adopts a stable chair conformation of its pyranose ring with all hydroxyl groups in the equatorial position. Cellulose is biosynthesized by polymerization via condensation reaction, from glucose in the form of the substrate uridine diphosphate (UDP)-glucose, by the cellulose synthase enzyme[6]. The glucose units along the chain are arranged in the ß configuration at the anomeric position and the loss of a molecule of water leads to the use of the term anhydroglucose units (AGUs) to describe each repeat unit in the cellulose backbone. The linkages between the anhydroglucose units are thus described as ß - (1→4)-glycosidic bonds. Every other AGU along the polymer backbone is arranged at a 180° angle to its neighboring units; the structural repeat unit of the cellulose chain thus comprises two AGUs and is classified as cellobiose. The regularly repeating nature of the chain coupled with the presence of three free hydroxyl groups on C-2, C-3, and C-6 helps to form an extensive hydrogen-bonding network that is supported by both intermolecular and intramolecular hydrogen bonding interactions. In the context of degree of polymerization however, determination is made based on the number of AGUs versus the number of repeat units present. The chain ends of cellulose consist of a free hydroxyl group on C-4 at the non-reducing end of the chain and a hydroxyl group on C-1 at the reducing end of the chain. The hemiacetal at the reducing end has an equilibrium concentration of the alpha and beta anomers as well as the open chain aldehyde form[3].

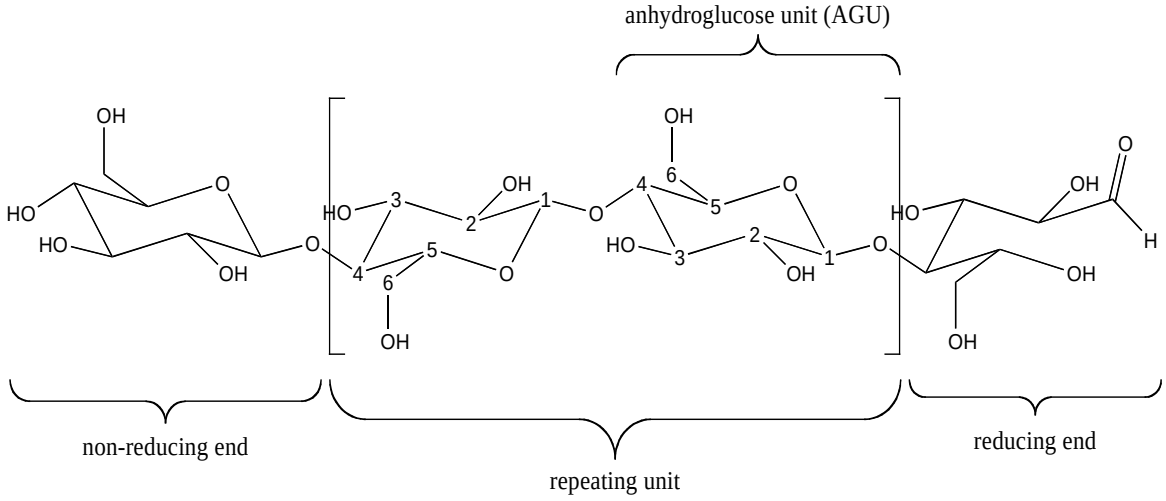

Figure 2.1: Structure of cellulose with numbered carbon atoms

2.4 Hydrogen bonding and crystallinity

The highly regular structure of cellulose and the presence of the hydrogen-bonding network contribute strongly to the physical characteristics and reactivity of the polymer[3]. Cellulose is known to be a highly crystalline material containing different crystalline morphs. This crystallinity renders cellulose insoluble in water and in a number of organic solvents[4b, 7]. Compared to cellulose, the solubility of cellobiose in water is about 12g/100 g solution at 25ºC. While cellulose is very hygroscopic and can swell in water, it is highly insoluble under aqueous conditions[3]. This suggests that there are other fundamental properties of the polymer that interfere with its dissolution ability. In an effort to take advantage of the more favorable non-toxic, biodegradable and biocompatible properties of cellulosic materials, dissolution is a key step to making useful derivatives[8]. The crystalline behavior of cellulose has therefore been widely studied in order to garner information about how best to overcome the barriers of high crystallinity and dissolve this most critical polymer[9].

Cellulose is a polydisperse polymer and as such the order of the macromolecules in a single cellulose fiber may not be uniform throughout. In fact, morphological studies have revealed that there exist regions of both low order as well as high crystalline order throughout the fibril structure. These low order regions are called amorphous regions and are often targeted to initiate hydrolytic and degradative pathways for cellulose[3].

The naturally occurring crystalline form of cellulose is cellulose I. Cellulose I is found as two distinct crystal phases, Iα and Iβ. Iα is most commonly found in the cell walls of some algae and in bacterial cellulose while Iβ has been found in tunicates and higher plants including major cellulose sources like cotton and wood. Cellulose Iα can be partially transformed to Iβ by annealing the polymer between 260° to 280°C [3, 10]. Iα is reported to be the most thermodynamically stable form of cellulose I[11]. Cellulose II or regenerated cellulose, has been described as having some improved properties including greater strength versus cellulose I which makes it more suitable for use in making textiles and other pulp derived materials[3,12]. Cellulose II is produced from the mercerization of cellulose[13] and results in the rotation of the D-glucose residues about the glycosidic bonds[14]. This results in reduced cohesion in cellulose II, with increased amorphous regions and greater accessibility to alkali for increased reactivity in anionic reactions[14-15]. Cellulose I, in the form of microcrystalline cellulose, is typically used for making cellulose derivatives[16]. Cellulose I possesses greater reactivity in acid catalyzed esterification

reactions than Cellulose II and this is largely related to more availability of hydroxyl groups within the structure to participate in these reactions[17]. Cellulose II and I may also be treated to produce other crystalline phases of the polymer[3].

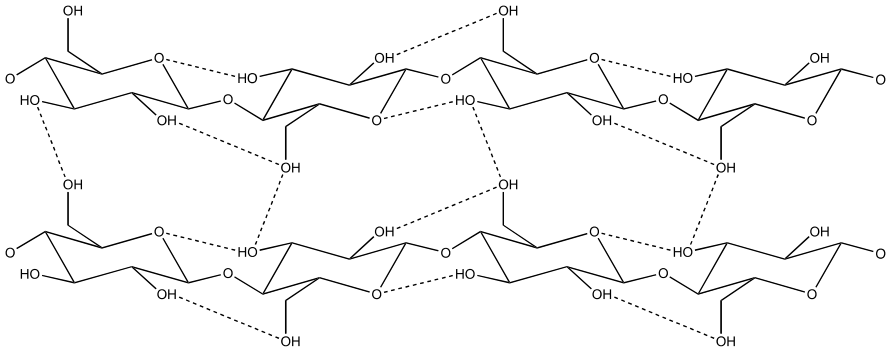

Figure 2.2: Depiction of hydrogen bonding in cellulose 1

2.5 Chemical Modification of Cellulose

As mentioned before, cellulose has very limited solubility in most simple organic solvents and is virtually insoluble in water. However to take advantage of the properties of cellulose, derivatization is a necessary step. Cellulose contains 3 free hydroxyl groups per AGU; these hydroxyl groups can be completely or partially converted to, for example, ether or ester linkages. The partial or complete conversion of these hydroxyl groups helps to reduce the regularity of the chain, reduce hydrogen bonding and produce improved solubility in organic solvents. When cellulose is chemically modified, we describe the extent of modification using the term degree of substitution (DS), defined as the number of positions modified per monosaccharide. The possibility for derivatization at 3 hydroxyl positions (excluding end groups, whose contribution is trivial for high degree of polymerization (DP) derivatives) gives a maximum DS of 3.0. For partial conversion of hydroxyl groups in the polymer, DS can range from 0-3.0 where 1.0 suggests an average of 1 substituted hydroxyl group per AGU and 2.0 suggests an average of 2 substituted groups per AGU.

Over the years, a great deal of research has been focused on finding suitable and effective solvents for cellulose. These solvents are typically divided into derivatizing and non-derivatizing solvents. Depending on the application, these solvent systems have met with varying degrees of success. Cellulose is capable of dissolution through chemical modification, or through solvation

in certain specific multicomponent protic or aqueous media as well as in non-aqueous, non-derivatizing media. There are a number of heterogeneous as well as homogeneous methods available for cellulose dissolution with more emphasis being placed on methods that are homogeneous in nature[3].

2.5.1 Cellulose Swelling

The swelling of cellulose is a key step to the activation of cellulose for dissolution. In order for dissolution under heterogeneous and homogenous conditions to take place, the ability of cellulose to swell in protic solvents inclusive of water is important for 'activating' the polymer for dissolution. Without this much needed activation step, only surface layer reactions are likely to occur. These solvents are capable of interfering with the hydrogen bonding within the less ordered and more accessible amorphous regions of cellulose and thus prime the polymer for dissolution. However, in some cases, the crystalline portions of the polymer are also affected. Recent studies have been able to establish relationships between the supramolecular structure of cellulose; including the size of its crystallites as well as arrangement of the chains, and its ability to swell or dissolve in various solvents. In order to functionalize cellulose, homogenous reactions are most desired. This ensures greatest access of reagents to the free hydroxyl groups for enhanced reactivity and by extension higher degrees of substitution (DS)[3, 18].

Due to the hygroscopic nature of cellulose, swelling in the presence of water is a common occurrence. There is interaction between the hydroxyl groups of cellulose and water molecules. The interaction of cellulose with water and the degree of swelling depend on conditions such as temperature and the amount of water that is already present in the polymer. The swelling of cellulose in water has been frequently used as an activation step for solvent exchange with liquids of decreased polarities[3, 18a].

The swelling of cellulose in alkaline media has also been examined. Chemical interaction between the hydroxyl groups of cellulose and the ion dipoles of sodium hydroxide helps to cleave and thus reduce the presence of intra and intermolecular H-bonding. The swelling of cellulose in alkali greatly influences the composition of the amorphous and crystalline portions of the polymer. In the case of aqueous base (NaOH), the uptake of solvent has been shown to modify the structure of the cellulosic material including decreased size of crystallites, enhanced micropore volumes in the supramolecular structure and higher disorder of the hydroxymethyl

groups bonded to C-5 of each AGU. In the case of polar aprotic solvents, correlation between water content and the dissolution behavior has been established. Researchers believe that a combination of supramolecular modification and reduced interpolymer hydrogen bonding (due to competing hydrogen bonding to the polar protic or aprotic solvents), which result from swelling of cellulose, play important roles in enhancing dissolution[18b].

Cellulose has a high tendency to swell in polar liquids, including water, liquid ammonia, ethanolamine, ethanol, dimethylsulfoxide (DMSO), dimethylformamide (DMF), and dimethylacetamide (DMAc). In solvents that are more capable of competing with the interpolymer hydrogen bonding like DMSO, formamide and ethanolamine, the extent of swelling is much larger compared to water[3].

2.5.2 Cellulose Dissolution

Of particular interest to researchers is the relationship between a solvent's ability to swell cellulose and the capability for dissolution. There are solvents that are able to dissolve cellulose with minimal swelling capability and vice versa. Researchers estimate that this divide is influenced by factors like % crystallinity, DP and the polymer concentration in the solution. Several dissolution methods have been developed for cellulose that involve dipolar interactions with the hydroxyl groups along the polymer chain. This allows for the reduction of the hydrogen-bonding network between the chains and produces greater availability of the hydroxyl groups for derivatization. Most of the methods developed involve very specific procedures, are able to dissolve relatively low concentrations of cellulose (usually <10%) and may produce some degradation of the polymer chain. Some degradative pathways are described in the following section[3]. Cellulose dissolution methods can be broadly segmented into derivatizing systems and non-derivatizing systems. Non-derivatizing solvents give dissolution only by intermolecular interaction while derivatizing systems are capable of dissolution by chemical reaction to form an unstable ether, ester or acetal derivative. A common derivatizing method is the use of CS_2/NaOH/ H_2O to produce cellulose xanthate. Non-derivatizing solvents include DMAc/LiCl[8b], DMSO/tetrabutyl ammonium fluoride (TBAF)[8c, 19], and ionic liquids[8d]. The use of CS_2 was an early development in cellulose dissolution that was later discovered to produce serious pollution. Since then, the aim has been to develop dissolution methods that are 'green' methods and do not necessarily produce a functionalized product of cellulose[3,20].

The dissolution of cellulose has been reported in aqueous NaOH solutions containing 8~10 wt% of cellulose at 4° C. This data has been reported on non-crystalline cellulose having relatively low molecular weight (DP lower than 250). Reaction of cellulose with CS_2 in NaOH is an initially heterogeneous process where cellulose is held in the solvent during which 'ripening' or swelling of the polymer takes place in order to enhance dissolution[21]. The method of producing xanthate, which is a useful form of cellulose used to provide rayon fiber, involves the use of NaOH followed by reaction with carbon disulfide. The dissolution conditions for cellulose in aqueous NaOH are very narrow and do not facilitate effective synthetic work. Under acidic conditions, cellulose can also be dissolved via derivatization. For example, the reaction of concentrated sulfuric acid with cellulose involves hydrolysis of the polymer and production of the sulfated derivative at (but not exclusively at) the C-6 position. Cellulose nitrate and sulfate are two such derivatives, made through reaction with organic acids that have been of interest in cellulose chemistry. However, the use of acid media results in rapid cleavage of the polymer and reduces the molecular weight extensively. This will be discussed further in a subsequent section of this review.

Non-derivatizing solvents have been of primary interest for lab scale cellulose functionalization. While there are numerous systems that have been developed over the years, the use of DMAc/LiCl, DMSO/TBAF, and ionic liquid systems are of more recent significance. Greater focus will therefore be given for these systems as part of this review[3, 20,21].

The McCormick group first reported the use of DMAc/LiCl in 1979[22]. DMAc/LiCl is widely used for cellulose dissolution today and is suitable for a wide variety of reactions. For high molecular weight samples, up to 4 wt% solutions can be achieved while 15 wt% solutions can be achieved for much lower molecular weight samples. Dissolution in DMAc/LiCl can be achieved either by solvent exchange or by heat activation methods. The labor-intensive nature and unfavorable moisture retention are disadvantages of the solvent exchange method using DMAc, water and methanol. For water sensitive reactions like esterification, the retention of moisture is undesirable. The mild solvent exchange method, however, prevents the degradation of the polymer chain that is a disadvantage of the heat activation method. Heat activation of cellulose in DMAc involves heating the mixture to between 120° and 160° C for 1- 2 hours. During this period, DMAc is able to penetrate and swell the supramolecular structure of cellulose. Cellulose dissolves on addition of LiCl while cooling[3,20,22]. Recent studies on this

method have demonstrated that progressive degradation of the polymer can occur by heat activation and this causes a yellowing of the cellulose solution. Two processes have proven responsible for this phenomenon. Thermal endwise peeling of the reducing ends in the form of furan derivatives is thought to slowly reduce the DP of the polymer while the cleavage of glycosidic bonds by the N,N dimethylketeniminium cation, formed from DMAc, produces more extensive DP loss. The keteniminium cation is highly electrophilic and attacks the glycosidic bonds to produce a ketene hemiaminal derivative on the polymer backbone that undergoes secondary hydrolysis (Figure 3). These keteniminium cations are thought to be present above 80°C in solutions with [cellulose] as low as 0.5 wt%[23]. For this reason, temperature control is an important consideration when heating cellulose in DMAc for dissolution. While LiCl is the best salt for cellulose dissolution in DMAc, LiBr may also be substituted but dissolves considerably less cellulose. The use of LiBr is nonetheless preferred for bromination reactions of cellulose[8b, 24]. The more basic chloride ion in LiCl easily displaces the bromide ion by nucleophilic substitution and thus presents a barrier to achieving high degree of bromide substitution at C-6. Chloride ions are stronger nucleophiles in dipolar aprotic solvents like DMAc[25]. Attempted bromination of microcrystalline cellulose using NBS/Ph_3P in LiCl/DMAc produced 6-chloro-6-deoxycellulose almost exclusively. This is attributed to preferential nucleophilic substitution by the more basic chloride ion on the phosphonium salt intermediate of cellulose (Cell – O – $P^+Ph_3X^-$)[8b]. The use of 1,3-dimethyl-2-imidazolinone (DMI) has also been explored in place of DMAc solvent. DMI has demonstrated high efficiency for etherification reactions compared to other homogeneous solvent systems. Studies show that DMI is more stable under basic conditions than DMAc even though DMAc is commonly used in reactions using added base[26].

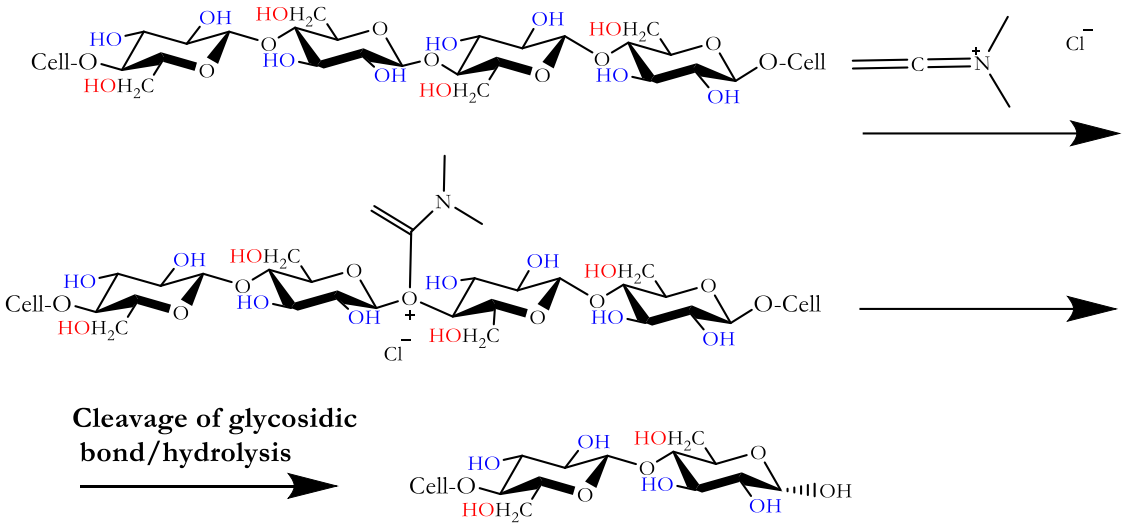

Figure 2.3: Hydrolysis of cellulose by reaction with electrophilic dimethyl keteniminium cation[23b]

The development of a non-derivatizing solvent system for cellulose having DP up to 650 using DMSO containing TBAF trihydrate (TBAF·3H_2O) was an important discovery. This system is capable of dissolving cellulose within 15 minutes at room temperature[3, 20, 27]. In this system, an activation step is not necessary. DMSO/TBAF is very useful and convenient but can prove disadvantageous when carrying out water- sensitive reactions. The TBAF waters of hydration may impact effective esterification of cellulose due to competing hydrolytic reactions[3, 18a, 27]. The instability of anhydrous TBAF has discouraged most efforts to dry it; however synthesis of TBAF *in situ* from tetrabutylammonium cyanide has been reported in the literature[19]. More recent studies have also demonstrated that use of the DMSO/TBAF solvent system in reactions with cellulose esters produces regioselective deacylation mainly at the C-2 and C-3 positions. Deacylation at the secondary alcohol ester positions has been attributed to a ketene mechanism, while deacylation of the primary alcohol ester is due to general base catalysis by the fluoride ion of TBAF [28]. These factors prevent effective high DS cellulose esterification in DMSO/TBAF, and especially hinder incorporation of acyl groups at the C-2 or C-3 positions[29].

Ionic liquids have received a good deal of attention in the last few years. These salts of organic amines have been touted as 'green' solvents that have little or no vapor pressure and can be recovered for reuse. These ionic liquids have low melting points (< 100° C by definition) and can be ideal for dissolution of hydrophobic molecules due to the presence of hydrophobic substituents. One drawback of these solvents however is the high cost and the great efficiency

needed to recover the products of reaction in order to reutilize the solvent. The ionic liquids (ILs) which have been given greatest focus for polysaccharides are imidazolium ILs. The literature reveals that ILs have great utility as cellulose solvents. Efficient esterification has been shown in 1-alkyl-3-methylimidazolium chloride after 5 minutes at 100° C and high DS values can be achieved for cellulose acetates using either an acid chloride or anhydride. The use of this IL does not require activation of cellulose[3, 20, 30]. 1-Butyl-3-methylimidazolium chloride ($Bmim^+Cl^-$) is one of the most effective solvents for cellulose. In 2006, Schlufter et al.[31] reported the complete dissolution of high molecular weight bacterial cellulose (DP ~ 6500) within 20 mins at 80° C without degradation of the polymer chain. Up to 25 wt % solutions have been reported in $Bmim^+Cl^-$. A summary of the dissolution properties of several ILs is shown in the table below. The recovery of ILs after functionalization of cellulose can be easily performed by addition of a non-solvent and filtration of product followed by the evaporation of the non-solvent. Degradation of cellulose in IL solvent systems has been found to be minimal under certain conditions including in the presence of a base for etherification reactions, by use of a protective gas like nitrogen, and it has also been observed that minimal degradation occurs for cellulose of DP < 1000 when carrying out acylation reactions. One potential issue is that for reactions in ILs, the presence of water can have a strongly deleterious effect on cellulose solubility; in some cases even 1% water can cause cellulose to be insoluble[20, 30b].

Table 2.2: Solubility of cellulose in various imidazolium ionic liquids. Fox, S. C. Regioselective Synthesis of Novel Cellulose Derivatives for Drug Delivery. Virginia Polytechnic Institute and State University, 2011[32]. Used under fair use, 2015

Cation structure:

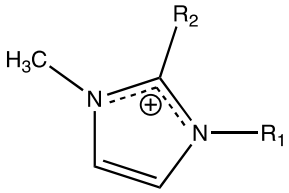

R_1	R_2	Anion	Cellulose DP	Temperature (°C)	Cellulose concentration (wt.%)	Reference [1]
Ethyl	H	Cl^-	286	90	12	Barthel and Heinze 2006
Allyl	H	Cl^-	650	80	14.5	Zhang, et al. 2005
Butyl	H	Cl^-	286	83	18	Heinze, et al. 2005
Butyl	H	Cl^-	593	83	13	Heinze, et al. 2005
Butyl	H	Cl^-	1198	83	10	Heinze, et al. 2005
Butyl	H	Cl^-	≈ 1,000	100	10	Swatloski, et al. 2002
Butyl	H	Cl^-	≈ 1,000	Microwave heating	25	Swatloski, et al. 2002
Ethyl	H	Ac^-	586	90 – 130	13.5	Kosan, et al. 2008
Butyl	H	Br^-	≈ 1,000	Microwave heating	5 - 7	Swatloski, et al. 2002
Butyl	H	SCN^-	≈ 1,000	Microwave heating	5 - 7	Swatloski, et al. 2002
Butyl	H	Ac^-	586	90 – 130	13.2	Kosan, et al. 2008
Hexyl	H	Cl^-	≈ 1,000	100	5	Swatloski, et al. 2002
Butyl	Methyl	Cl^-	377	80	9	Barthel and Heinze 2006
Allyl	Methyl	Br^-	286	80	12	Barthel and Heinze 2006

2.5.3 Cellulose Degradation

The sources of cellulose degradation most significant to lab scale derivatization of cellulose are acid-catalyzed hydrolysis, enzymatic hydrolysis, alkaline degradation and oxidative degradation. Cellulose degradation can be desirable, for example by providing small molecules for fuel like glucose and other furan derivatives. However, in the functionalization of cellulose, maintenance of high DP values to retain the physical properties of cellulose is often important. Degradation along the cellulose backbone can lead to the formation of new functional groups that can heavily affect solubility in common cellulose solvent systems. Degradation begins

primarily in the amorphous regions of the polymer and levels off at a minimum DP depending on the crystallinity of the sample[3].

Acid-catalyzed hydrolysis of cellulose involves the hydrolytic cleavage of glycosidic bonds between two AGUs. This reaction is catalyzed by, e.g., mineral acids including sulfuric acid and phosphoric acid. The bridging oxygen of the glycosidic bond is first protonated by the acid catalyst and results in the formation of a cation at the anomeric position. Subsequent attack by water generates two cellulose chain ends with the recovery of the acid catalyst. The random cleavage along the polymer chain produces rapid loss in DP[3].

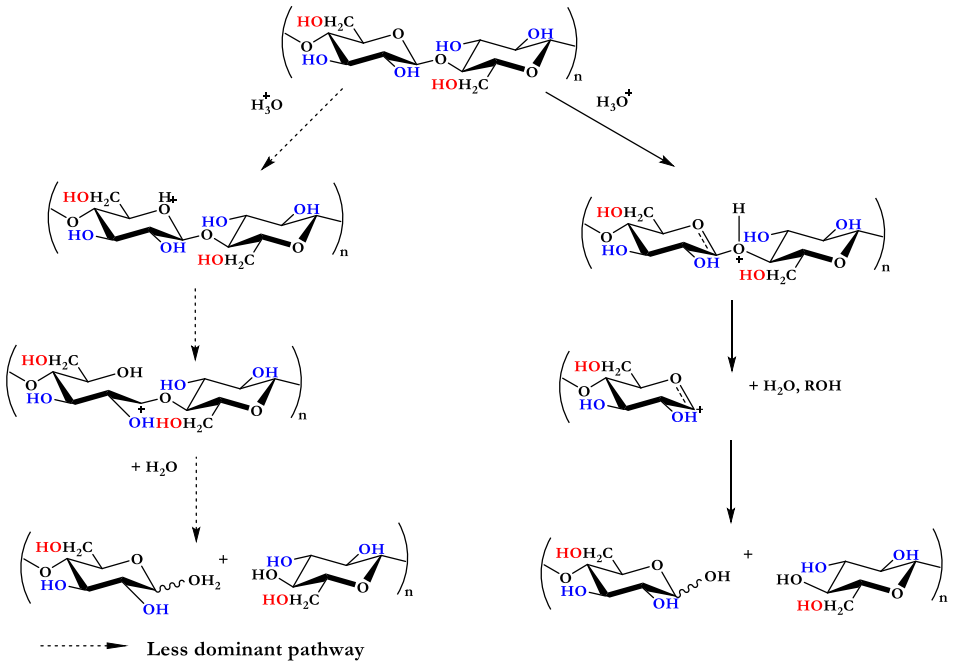

Scheme 2.1: Acid hydrolysis of cellulose

Enzymatic hydrolysis is the biologically relevant pathway for degradation of cellulose. Bacteria and fungi are the most relevant degrading organisms. This enzymatic hydrolysis is carried out by cellulases that are secreted by various bacterial and fungal strains[33]. The cellulolytic enzyme system consists of endoglucanases (which cleave the polymer statistically), exoglucanases that are capable of splitting off cellobiose units from the chain ends, and beta-1,4-glucosidases which degrade cellobiose to glucose. Enzymatic hydrolysis can take place in dilute aqueous systems in the pH range of 4 to 9. The mechanism of hydrolysis is believed to follow an acid catalyzed process in the active site of the cellulase. Enzymatic hydrolysis by cellulases also occurs for water-soluble cellulose derivatives having small substituent groups with low to

medium DS values[34]. The hydrolysis of carboxymethyl cellulose and methylcellulose has also been studied using cellulase enzymes[3].

Cellulose is also susceptible to a 'peeling' reaction in the presence of alkali. At temperatures above 150°C, monosaccharides are cleaved from the reducing end of the polymer chain. Compared to acid hydrolysis, this method results in a much slower reduction in DP for cellulosic samples. In the presence of the alkali and heat, the end AGU undergoes hemiacetal ring opening and undergoes a series of proton eliminations beta to the aldehyde group. This depolymerization reaction can be stunted by conversion of the enolate intermediate into an aldonic acid by beta hydroxyl elimination.

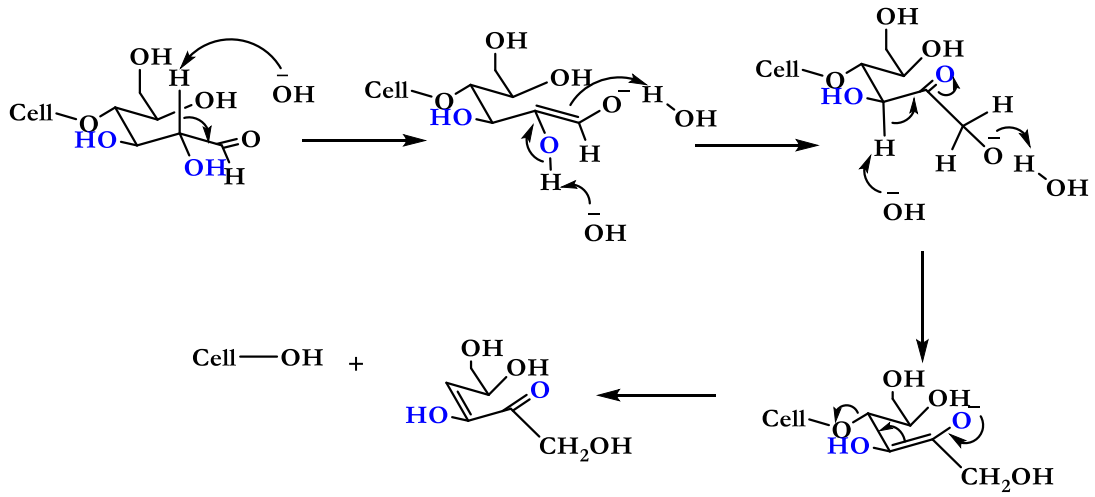

Scheme 2.2: Alkaline hydrolysis of Cellulose

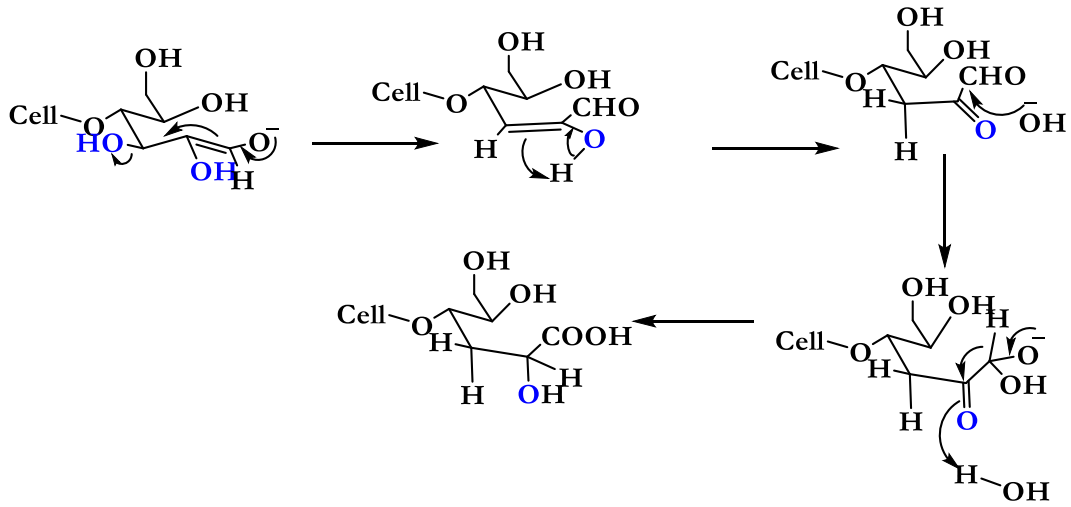

Scheme 2.3: Competing reaction to form aldonic acid derivative

2.5.4 Thermal Degradation of Cellulose and Cellulose derivatives

At elevated temperatures, cellulose and its derivatives are subject to pyrolysis. While the mechanisms by which cellulose pyrolysis takes place are often somewhat ambiguous, examination of derivatives of cellulose can shed some light on possible mechanisms[35]. Thermal degradation of cellulose and its derivatives has been studied extensively using thermal gravimetric analysis (TGA) and accompanying techniques like Fourier transform infrared (FTIR), gas chromatography (GC) and mass spectrometry (MS)[35-36]. One of the earlier studies on cellulose pyrolysis suggested that the thermal decomposition of cellulose can be represented by two competing processes. The first is thought to take place at low temperatures and slow heating rates to produce anhydrocellulose at temperatures below 280°C. The water lost can be from that absorbed by the cellulose and then by beta elimination from the cellulose hydroxyl groups. At temperatures above 280°C, a competitive 'unzipping' of the remaining cellulose takes place leading to tar formation. The further decomposition of anhydrocellulose leads to char and gas formation. This scheme has been reexamined over the years to yield the model described in Figure 2.4 below. This model presents the idea of 'activated cellulose' that is formed at low temperature (259-295°C) through the depolymerization process. This active cellulose can then undergo competitive reactions to produce either char and gas or volatile compounds. At high temperatures (above 295°C) however, there is no 'activation period' and cellulose is instead decomposed to form volatile compounds and char and gas[35].

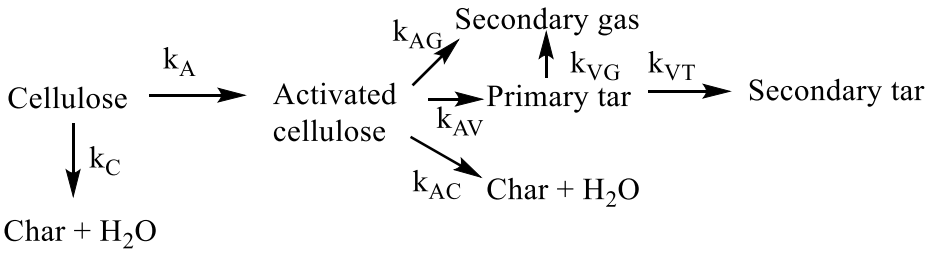

Figure 2.4 Kinetic model for cellulose pyrolysis[35]

It is reported in the literature that there are at least fifty nine volatile products from the thermal decomposition of cellulose[37]. The volatile compounds that are generated upon pyrolysis of cellulose under moderate and high temperatures include: some C5-C6 ring containing compounds (pyrans and furans), aliphatic oxygen containing C2-4 organic compounds and other

light hydrocarbons and gases. Some that are especially relevant as feedstock for fuels and chemical production include levoglucosan, furfural, hydroxyacetaldehyde, acetol, carbon monoxide and carbon dioxide. The chemical structures of some of these compounds are depicted in Figure 2.5.

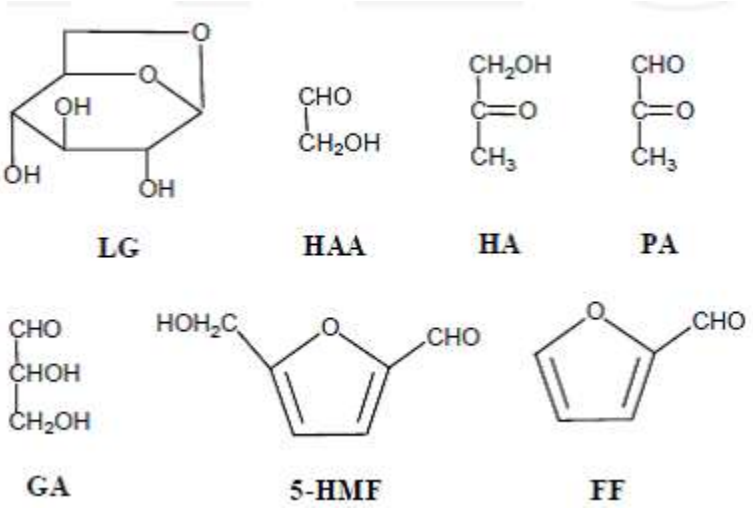

Figure 2.5: The chemical structures of typical compounds from cellulose pyrolysis. LG: levoglucosan, HAA: hydroxyacetaldehyde, HA: Hydroxyacetone, PA: pyruvic aldehyde, GA: glyceraldehyde, 5-HMF: 5-hydroxymethyl-furfural and FF: furfural[35].

The char formation from pyrolysis of cellulose is thought to result from the conversion of cellulose to condensed aromatic structures and ultimately char[36a] while other studies suggest that char formation is also a result of the repolymerization of volatile compounds like levuglucosan[35]. Levoglucosan is a major product formed from cellulose pyrolysis with yields varying between 3 and 63%[36a]. The high yields of levoglucosan are thought to originate from its greater stability compared to other products that degrade much faster. The decomposition of cellulose to levoglucosan occurs through an initial partial decomposition of cellulose which is then subjected to internal nucleophilic attack by hydroxyl to form a 1, 2 epoxide followed by cleavage of the epoxide with the formation of a 1, 6-anhydroglucose linkage. Free levoglucosan can then be formed from hydrolysis or repetition of this process in an adjacent glucose unit[36a]. This mechanism is summarized in Figure 2.6.

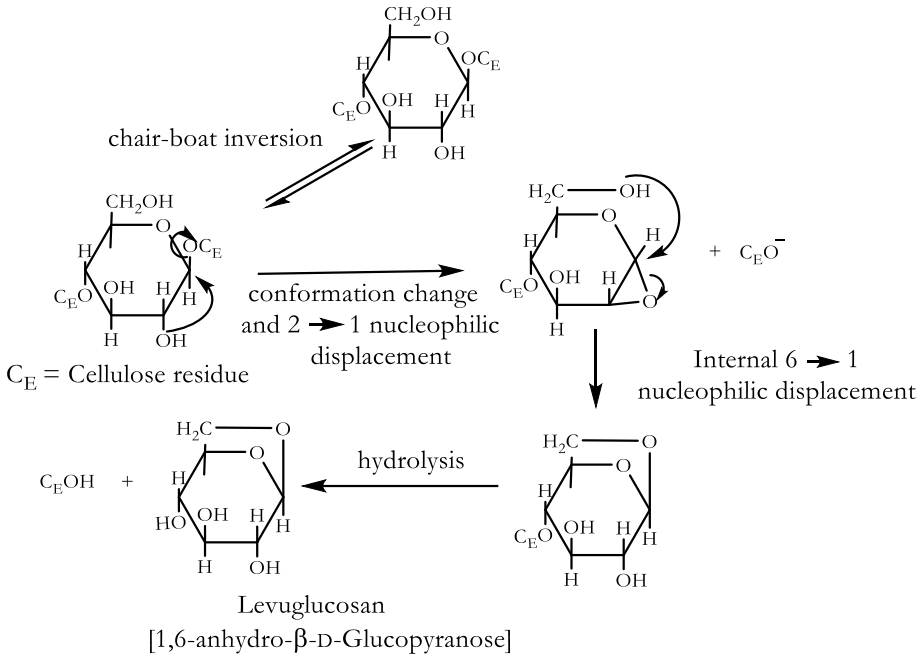

Figure 2.6: Conversion of cellulose directly to levoglucosan[36a]

The thermal properties of cellulose derivatives are affected by the type of and degree of substitution of the substituent groups (whether acyl or ether groups), the crystallinity of the derivative, the side chain length, degree of substitution as well as the heating rates employed in the analyses[36a-d, 37-38]. The thermal stability of such derivatives is very important in the context of their applications. These derivatives may encounter elevated temperatures in microcompounding or processing, for example in hot melt extrusion. Cellulose itself decomposes before it melts and is not melt processable. While it is important to understand the possible degradative properties of cellulose itself, the thermal degradation mechanisms of its derivatives are very important for melt processing applications. It has been reported that lower molecular weights and crystallinity of cellulose and its derivatives have destabilizing effects on the polymers[36d, 38] due to the reduced order of the molecules.

Cellulose aldonic acids have shown much faster degradation at lower temperatures than ethers, esters or cotton cellulose[39]. It is hypothesized that the ring structure of the anhydroglucose units on cellulose is weakened considerably by the oxidation of the primary hydroxyl. This results in thermal degradation to produce mainly water, carbon dioxide, carbon monoxide and only small amounts of the other volatile compounds that are typical products of cellulose degradation[39].

Cellulose esters are also prone to degradation at elevated temperatures due to their labile ester linkages, however there are reported cases of improved stability compared to microcrystalline cellulose[36c]. This improved stability was attributed to the ability of the fatty acid side chains, in a regular arrangement, to form a new ordered structure having increased thermal stability. The internal plasticization from the ester substituents on cellulose derivatives typically provides improved thermal properties in the way of measurable softening temperatures and better processing capabilities compared to cellulose[40]. Thermal degradation studies of cellulose esters have also revealed that thermal stability of the esters decreases with an increase in chain length for C2-C5[32] but higher degree of substitution usually correlates with greater stability[41]. Thermal degradation typically begins with cleavage of the acid for example at ~300°C for acetic acid from cellulose triacetate[32]. The generated acid then catalyzes the dehydration reaction which upon complete removal of the ester groups forms a C=C conjugated system that generates char[32] (Figure 2.7). Short chain cellulose esters like cellulose acetate typically have a narrow window between their softening and decomposition temperatures that can limit their applications considerably[36c]. Cellulose acetate usually requires addition of plasticizer for thermomolding due to its high glass transition temperature[42]. However, applications of long chain linear cellulose esters are much more varied due to their decreased glass transition temperatures. The aliphatic ester chain acts as an internal plasticizer of the cellulose derivative and produces a broader processing window between the softening and decomposition temperatures of the polymer[42-43]. The lower processing temperatures for longer chain esters are also critical for preventing the evolution of acid during melt extrusion. The free acid could potentially react with the drug or other excipients contained in the formulation. Hydroxypropyl methyl cellulose acetate succinate (HPMCAS) for example is recommended for extrusion only below 140° C due to release of acetic and succinic acid at elevated temperatures[44].

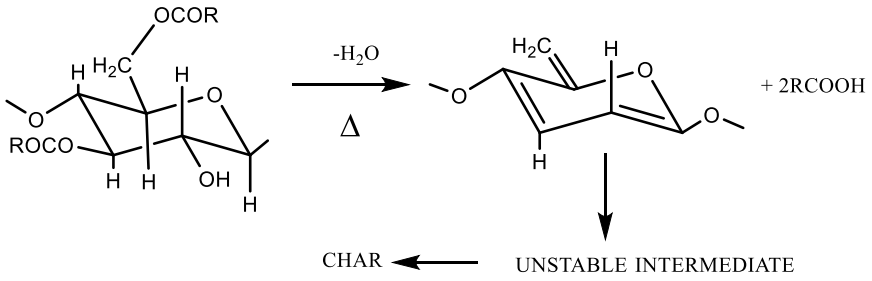

Figure 2.7: Mechanism of thermal degradation of cellulose acetate. Adapted from Tosh[32].

Cellulose ethers are known for low melting/softening temperatures and good processability[45]. Their thermal stability is also influenced by the substituents present, degree of substitution and substituent chain length similar to cellulose esters. They are prone to initial dehydration followed by the production of carbon dioxide, unsaturated compounds, as well as aldehyde and alcohol products at higher temperatures[46].

Derivatives of cellulose containing both hydroxyl and carboxyl functional groups are prone to crosslinking reactions at elevated temperatures[36a]. High temperatures promote esterification reactions between hydroxyl and carboxyl groups along the polymer backbone. While the crosslinking of cellulosics can prove useful in the context of making packaging materials with decreased water sensitivity[47], it may present a challenge for the use of these derivatives in applications like drug delivery[44b].

2.5.5 Reactivity of Cellulose

The free hydroxyl groups along the polymer backbone in the C-2, C-3 and C-6 positions determine the reactivity of the polymer. The reactivity of the individual hydroxyl groups plays a large part in determining the efficiency of reactions geared at selectively functionalizing cellulose at only one or 2 positions on each AGU. Compared to those of small molecules and even those of monosaccharides, all the hydroxyl groups of cellulose have low reactivity due to extensive hydrogen bonding, crystallinity, and approach angles that are restricted by the bulk of the linear polymer chain. The C-2 hydroxyl group is most susceptible to deprotonation as a result of the electron withdrawing effects of the two electronegative oxygen species connected to the anomeric carbon. Thus the C-2 OH is often the most reactive in etherification reactions while the least sterically hindered C-6 hydroxyl is most reactive in esterification reactions. For reactions employing bulky reagents, the C-6 position is usually favored due to steric hindrance[3].

2.6 Regioselective Derivatization of Cellulose

The functionalization of cellulose at one or two specific hydroxyl groups on each AGU has been described as regioselective derivatization. This type of functionalization is important for controlling the properties of cellulose derivatives and helps to determine the potential usage

of the polymers in different areas like drug delivery. For drug delivery applications, the ability to correctly predict and describe the substitution pattern along the polymer backbone is important for getting a drug delivery system into clinical trials. In order to produce derivatives that have more predictable substitution patterns, protecting group strategies, which help to control the site at which chemical substitution occurs, have been employed. Some of the methods studied are highly selective for certain hydroxyl groups based on factors such as the steric bulk of the reagent, and its electrophilicity. Published methods include regioselective tritylation, silylation, tosylation and halogenation[3]. For the purpose of this review, greater focus will be given to the C-6 activating strategies including tosylation and halogenation. Tritylation is important in the context that the bulky reagent trityl chloride reacts preferentially with the C-6 hydroxyl group that is least sterically hindered, with high DS. The sterically hindered C-2 and C-3 hydroxyl groups can be functionalized separately from the C-6 hydroxyl group and the trityl groups can later be removed from the C-6 position by acid hydrolysis in the event that substituents at the C-2 and C-3 are stable under acid conditions [48].

For the synthesis of derivatives that are exclusively substituted at the C-3 position or at the C-2 and C-3 positions, silylation is an interesting method of choice. Under heterogeneous conditions, reaction of cellulose with thexyldimethylsilyl chloride (TDMS-Cl), the bulky silyl derivative can preferentially functionalize the C-6 hydroxyl group with DS values up to 0.99. Under homogeneous conditions however, both the least sterically hindered and most acidic hydroxyl (C-6 and C-2) can be substituted up to DS values of 2. These predictable substitution behaviors give greater possibility of derivatizing the C-3 or C-3 and C-2 hydroxyls independently of the primary hydroxyl. The silyl group can be subsequently removed by treatment with TBAF as fluoride ions catalyze the removal of the silyl group[49].

2.6.1 Tosylation

Tosyl chloride (p-toluenesulfonyl chloride) is another protecting group agent, which has been heavily utilized. Tosylation is most selective for the C-6 position but can produce some substitution at C-3 and C-2. While not as highly selective, the fact that the tosyl group is an excellent leaving group gives it great application in nucleophilic displacement reactions at C-6[50]. While tosylation had been previously demonstrated with cellulosics, the successful demonstration of cellulose tosylation in DMAc/LiCl in the late 1980s by McCormick and Callais

spurred more extensive utilization of the method[51]. Tosylation chemistry has subsequently been used to produce a number of substituted derivatives of cellulose. It has been utilized to introduce an azido group in order to perform 'click' chemistry on cellulose and attach different molecules. The tosyl cellulose derivative is most commonly synthesized using anhydrous solvents, DMAc/LiCl and even ionic liquids[52]. Initial work on tosyl cellulose synthesis in DMAc/LiCl used pyridine as the organic base. However, competing synthesis of chlorodeoxycellulose encouraged the use of the much stronger organic base triethylamine (TEA) that would discourage nucleophilic substitution by the chloride ion to produce chlorodeoxy cellulose. There are two (2) proposed explanations for this phenomenon; TEA has the ability to form a tetrahedral intermediate with the adduct of DMAc and tosyl chloride in contrast to pyridine. This tetrahedral intermediate is more susceptible to nucleophilic substitution to form tosyl cellulose. In addition, the more hydrophobic triethylammonium ion associates more strongly with chloride ions than do pyridinium ions. Chloride ions in the presence of pyridine base are therefore more available to react with tosylcellulose by nucleophilic displacement reaction to give chlorodeoxycellulose[53].

Early attempts to control the total DS of tosyl groups on cellulose in homogeneous reactions used DMAc/LiCl. Tosylates of cellulose having DS values in the range 0.4 -2.3 were synthesized by varying the molar equivalents of tosyl chloride used, and their solubility in various solvents determined. A DS value of 0.9 afforded derivatives that were soluble in polar aprotic solvents like DMSO, DMAc, and DMF while DS values up to 1.4 were soluble in acetone, dioxane, and tetrahydrofuran. Above DS(1.8) derivatives with solubility in additional solvents like chloroform and dichloromethane were produced. However, attempts to exclusively tosylate cellulose at C-6 have been unsuccessful; reaction of the C-6 tosylates with iodide ions reveals that there are residual tosylate substituents on the secondary hydroxyl groups as well. Tosylation at C-6 exclusively was found for derivatives of low DS (0.46), but at higher DS values there was increased substitution at the secondary hydroxyl groups of cellulose. Tosylation at C-6 was determined to be complete at a DS (~1.4)[50a]. Tosylation chemistry is therefore not as selective for the C-6 position as are reactions with sterically demanding trityl and silyl chlorides. It is also extremely difficult to remove the tosyl group from the C-2 positions via nucleophilic substitution reactions. This also presents a challenge of using this method especially for purposes of drug delivery where exact determination of structure and substitution patterns may be needed[52, 54].

Despite these drawbacks, in more recent publications, tosyl cellulose has been found to be very useful for producing amino, azido and trialkylammonium derivatives of cellulose in an effort to produce cationic derivatives of cellulose. In 2001, Heinze et al. [52] reported the synthesis of 6-deoxy-6-amino cellulose derivatives by reaction with chiral amines. Tosyl cellulose, with a DS of 0.74 and 1.29 was reacted with R, S enantiomers and a racemic mixture of 1-phenylethylamine in DMF with added water. Various analytical techniques including NMR, FTIR, elemental analyses and optical rotation studies revealed that the chirality of the starting cellulose backbone did not affect its reactivity with the different enantiomers of the chiral amine reagent. Building on a study conducted by Kern et al.[55] where cationic polyelectrolytes, with the ability to complex polyanions, of 6-deoxy-6-pyridinium cellulose were produced, Koschella et al.[54a] later demonstrated the synthesis of 6-deoxy-6-ammonium cellulose by reaction of tosyl cellulose with tertiary amines in a DMF/H_2O solvent system. Tosyl celluloses of DS 0.74 and 1.02 were reacted with TEA, N,N-dimethyl-1,3-diaminopropane and 2,4,6-tris(N,N-dimethylaminomethyl)phenol via nucleophilic substitution reactions. Reaction of tosyl cellulose with TEA produced both water soluble and insoluble derivatives with the soluble derivatives having much lower sulfur content. The soluble derivatives were produced in the presence of between 23 and 37 vol % water. The assumption is made that higher water content stimulates reaction of water with the amine to produce nucleophilic hydroxyl ions (pK_a values ~15.7 and 10.8 for water and TEA respectively)[56]. These ions are then capable of hydrolyzing off the tosyloxy groups to form hydroxyl moieties at the substituted carbon positions. This results in an increase in polarity of the polymer and increases solubility in water. Bulk reaction of tosyl cellulose (DS 0.74) with 27 vol % water and 5 molar equivalents of TEA successfully produced a water soluble ammonium derivative with DS (ammonium) 0.20 with some residual tosyl groups (DS 0.17). The bulkier tertiary amines N,N-dimethyl-1,3-diaminopropane and 2,4,6-tris(N,N-dimethylaminomethyl) phenol produced water soluble derivatives with higher DS values in the range 0.27 - 0.50. Each derivative product contained a water insoluble portion that was thought to originate from cross-linking between the bulky amino groups along the polymer backbone[54a].

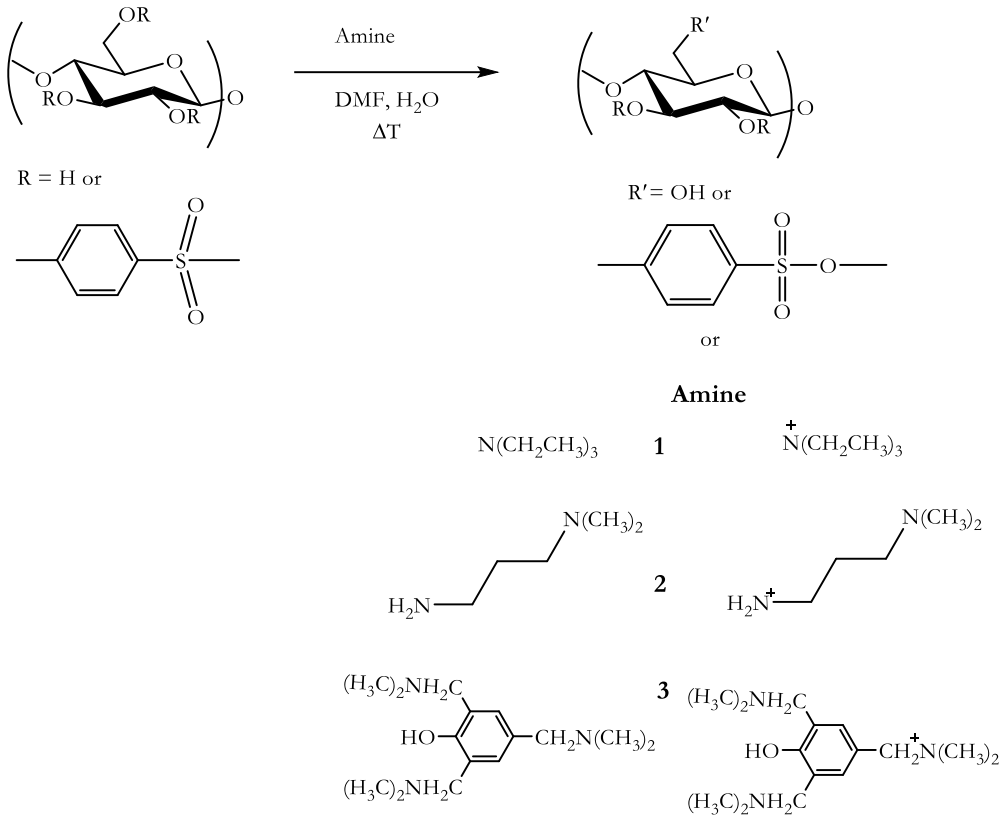

Scheme 2.4: Conversion of p-toluenesulfonyl cellulose with TEA (1), N,N- dimethyl-1,3-diaminopropane (2), and 2,4,6-tris(N,N-dimethyl- aminomethyl)phenol (3). Adapted from Koschella et al. [54a]

Tosylation chemistry has been used to introduce a variety of groups. Liu and Baumann[57] reported the completely regioselective introduction of amino groups at the C-6 position of cellulose in 2002. The 6-deoxy-6-amino-cellulose derivative (DS 1.0) was also used to produce 6-N-sulfonated and 6-N-carboxymethylated cellulose derivatives. First they synthesized a tosyl cellulose derivative that was completely tosylated at C-6 and partially at C-2 and C-3. Nucleophilic substitution with NaN_3 at low temperatures (~50 versus 100°C) replaced the tosyl groups at C-6 with azido groups while subsequent reduction with $LiAlH_4$ reduced the C-6 azido to amino groups while also completely removing the C-2 and C-3 tosyl groups. Sulfonated and carboxymethylated derivatives were thereafter produced from the amino derivative by reaction with sodium carbonate/$SO_3 \cdot NMe_3$ complex (solvent: water) and aqueous

cyanoborohydride/glyoxylic acid monohydrate /NaOH (solvent: water) respectively. Complete regioselectivity was reported for these derivatives and confirmed via ^{13}C NMR and FTIR. The sulfonated and carboxymethylated derivatives have potential application for structure-function studies due to similarity in structure to chitosan as well as to the class of biologically active polysaccharides known as glycosaminoglycans which includes the anticoagulant heparin. The uses of chitosan and the potential for chitosan analogs or structurally similar cationic cellulose derivatives will be discussed more extensively in a later section.

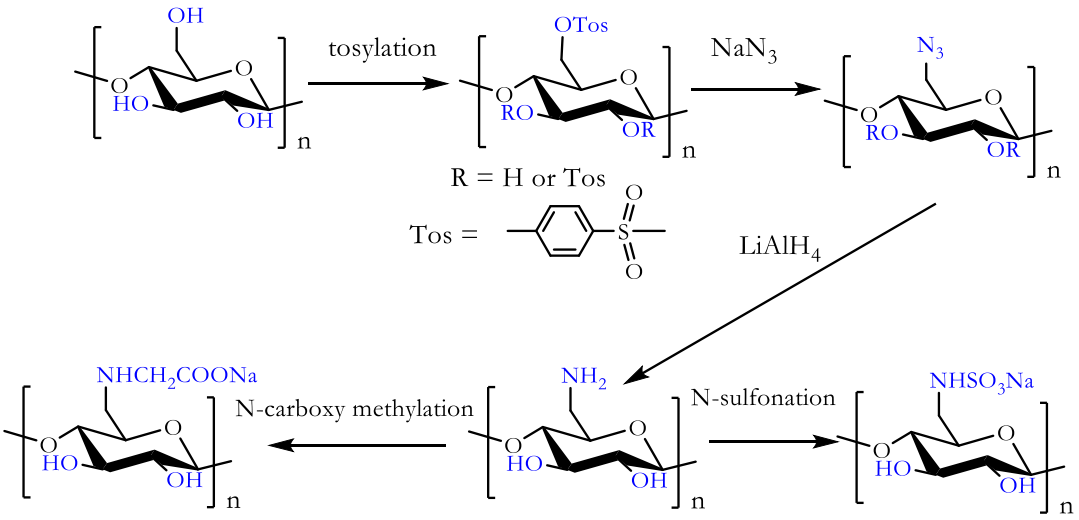

Scheme 2.5: Regioselective synthesis of 6-deoxy-6-amino cellulose and its N-sulfonated and N-carboxymethylated derivatives[57]

More recent developments in tosylation chemistry have been aimed at improving the utility of tosylation by experimenting with various solvent systems. Tosylation of microcrystalline cellulose has been reported by Granstrom in the ionic liquid 1-allyl-3-methylimidazolium chloride (AMIMCl) with DS (0.84) achieved after ~ 48 h at 10°C [57]. A comprehensive study was recently published by Gericke et al.[50b] that examines the factors necessary for control of cellulose tosylation in ionic liquids (ILs) and the properties of the most useful cosolvents. Attempts to synthesize the tosylated product described by Granstrom were not successful and the method was subsequently modified by addition of an organic cosolvent like DMI or DMF to achieve energy efficient homogenous reaction conditions at 25°C and shortened reaction times between 8-16 h. DS values up to 0.97 were achieved with small amounts of C-6 chloride substitution. The

tosylation of cellulose has also been reported in aqueous sodium hydroxide or sodium chloride with TEA as the base in an effort to devise a 'green' method for production of the derivative. DS values ranging form 0.1 to 1.7 have been reported, obtained by adjusting the molar ratio of tosyl chloride/AGU[58].

2.6.2 Direct regioselective halogenation

Halides present another interesting family of C-6 activating and protecting groups, and also act as good leaving groups for nucleophilic substitution to produce other more interesting derivatives. C-6 halogenation is an important strategy for achieving regioselective substitution on cellulose. In 1992, Furuhata published an article that described the direct regioselective bromination of cellulose at the C-6 position by dissolving microcrystalline cellulose in DMAc/LiBr, followed by reaction with triphenylphosphine (Ph_3P) and N-bromosuccinimide (NBS) [8b]. DS values up to 0.91 were achieved. Matsui et al.[59] also demonstrated the bromination of microcrystalline cellulose in LiBr-Me_2NCOMe and treated with NBS/Ph_3P to give a brominated product of DS 0.98 in 91 % yield. One drawback of these methods however was the fact that the C-6 brominated derivative is virtually insoluble in most organic solvents. Fox was later able to develop a protocol which involved the one pot synthesis of 6-deoxy-6-bromo-2,3-di-O-acylated derivatives from microcrystalline cellulose which have enhanced solubility in a variety of organic solvents. Bromide DS of 1.04 was achieved with over 90 % yield[24]. Usov et al.[60] had already brominated the 2,3 di-O-acetyl derivative of cellulose with subsequent deacetylation to produce a brominated derivative with DS of 0.8, however the 6-deoxy-6-bromo-2,3-acylated derivatives recently synthesized have greater solubility and application as starting materials for synthesis of new cellulose derivatives. In fact, the use of NaCN and NaN_3 in nucleophilic displacement reactions with 6-deoxy-6-bromo-2, 3-acylated cellulose derivatives to produce azido and cyano C-6 cellulose esters having DS values up to 0.92 has been demonstrated[24]. Matsui et al. [59] have also reported the synthesis of 6-deoxy-6-azido cellulose with DS (0.96) via heterogeneous reaction of 6-deoxy-6-bromo cellulose with NaN_3 in Me_2SO. The azido derivative can be subsequently reduced to the amino derivative by reaction with $NaBH_4$ in much higher yield than with $LiAlH_4$ (89% versus 44 %). Similar reduction chemistry has been used previously to produce 6-deoxy-6-amino chitosan derivatives[61]. Staudinger

reduction has also provided a successful route to the production of amino and amido cellulose esters from highly selective reduction of the 6 azido group of 6-azido 2,3-acylated cellulose ester starting materials using triphenylphosphine and water with little loss of the ester groups at the C-2 and C-3 positions[62,].

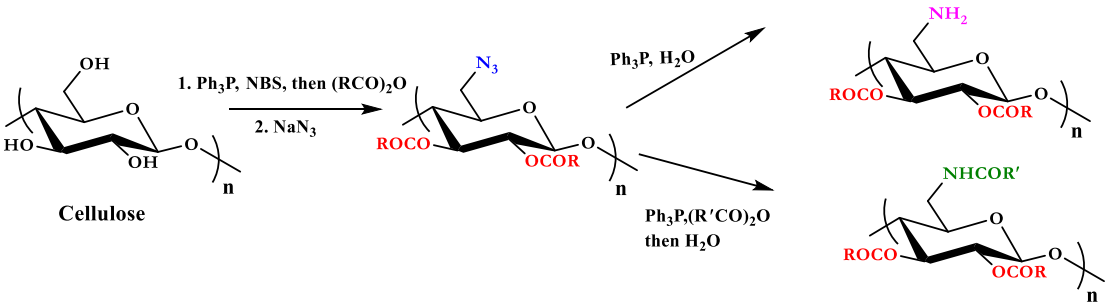

Scheme 2.6: Adapted from[62]: Synthesis of azido, amino, and amido derivatives from brominated cellulose ester starting materials

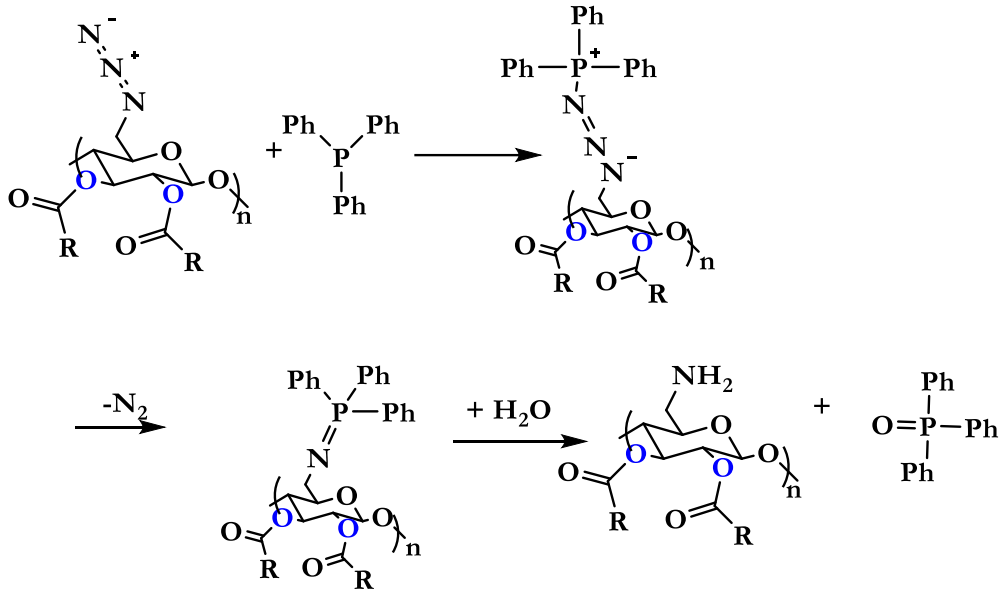

Scheme 2.7: Staudinger reduction of azido cellulose esters

The Staudinger reduction had previously been successfully reported for the conversion of 6-deoxy-6-azido amylose to 6-deoxy-6-amino amylose[63]. The amino derivatives of cellulose are highly insoluble in water but these potential chitosan analogs (**Figure 2.8**) provide great insight

into the possibility of providing quaternized ammonium and phosphonium derivatives from 6-azido-2, 3-acylated cellulose esters which would likely be novel polymer matrix materials for complexing anionic drugs like doxorubicin HCl and fexofenadine HCl[62].

Chitosan (fully deacylated) 6-amino-6-deoxy-cellulose

Figure 2.8: Chemical structure of chitosan and 6-amino-6-deoxy-cellulose

2.6.3 Cationic Derivatives in drug delivery

In recent years, cationic polysaccharides have been a major area of focus due to the large number of applications in drug delivery, especially for highly insoluble anionic drugs like doxorubicin HCl and sensitive anionic species like nuclei acids. Chitosan has been a template for the behavior of cationic polysaccharides and is most heavily targeted for such applications. However, recently, other naturally occurring polysaccharides have been derivatized in an effort to produce analogs of chitosan. These include amylose, dextran, pullulan and cellulose [62-63].

Chitosan is based upon a naturally occurring polysaccharide, chitin, which is a linear homopolymer of β-(1→4) linked N-acetylglucosamine. The glucosamine functionality of chitin has been associated with hepatoprotective[64] and antihypoxic effects[65] as well as preventing inflammation[65], all of which are useful biological functions. Recent reports have also linked acetyl glucosamine to having anti-tumor effects [66]. Chitin derived from the waste products of the shrimp and crab industries can be deacylated under alkaline conditions (conc. NaOH) to produce linear co-polymers of β-(1→4) linked 2-amino-2-deoxy-β-D-glucopyranose and β-(1→4) linked N-acetylglucosamine, with various degrees of deacetylation (proportions of glucosamine). This deacetylation product is known as chitosan. Unlike the more insoluble chitin, the copolymer-like nature of chitosan, which typically is not completely deacetylated, promotes a reduction in crystallinity and an increase in solubility[66,67]. Chitosan and its derivatives have also been shown to feature antimicrobial activity, with a proven effectiveness against *Staphylococcus aureus*,

epidermis, and *haemolyticus* bacterial strains. These gram-positive bacteria are commonly found in the body in locales that are often susceptible to various types of wounds including the skin and oral cavity[68]. Chitosan and its derivatives have a plethora of wound healing benefits associated with their use including hemostatic enhancement, biocompatibility, bioadhesive ability, aiding in regenerating connective tissue, and acting as a bacteriocide[68a].

At slightly acidic pH, the amino groups of chitosan are protonated to render a positively charged polymer. With a pKa of 6.5, chitosan is soluble in pH conditions lower than its pKa and when protonated is able to increase the permeability of peptide drugs across mucosal epithelia; it acts as an effective absorption enhancer in specific regions of the intestinal lumen[69]. The amino groups along the polysaccharide backbone are believed to increase interaction with anionic molecules that are found in mucus or on the surface of cells. For drug and gene delivery applications, chitosan is able to complex and encapsulate anionic nucleic acids and certain proteins through electrostatic interactions. This interaction is capable of protecting the compounds from degradative enzymes within the body[70]. Chitosan can enhance the absorption of drugs across the gastrointestinal (GI) epithelial membrane through the opening of tight junctions[69, 71].

Tight junctions are important in the intestinal framework as they provide a barrier to the passive movement of fluids, electrolytes, cells and large molecules through the paracellular membrane. In an effort to increase permeation across the epithelial membrane especially for hydrophilic macromolecules of therapeutic significance, paracellular permeability enhancers (PPEs) are often sought to temporarily alter the integrity of tight junctions and allow for more effective transport[69, 72].

It was Illum et al. [73] who in 1994 first reported the results of a study that showed the ability of chitosan to promote absorption of small polar molecules, peptides and proteins including insulin across nasal epithelia in rats and sheep. A subsequent report by Artursson et al.[74] showed increased paracellular permeability of mannitol across Caco-2-intestinal epithelia. These were two of the first studies to describe the absorption enhancement properties of chitosan and attributed the observed permeability increase to the widening of tight junctions as well as the bioadhesive properties of chitosan.

While studies have described chitosan as a useful vehicle for therapeutic applications, its limited solubility at neutral pH and inability to target specific areas of the intestine like the ileum or jejunum greatly limit its efficiency in comparison to the best synthetic vehicles available[75]. In

order to solve this problem, researchers have synthesized new derivatives of chitosan as well as derivatized various other polysaccharides in order to access similar properties of chitosan[76]. Derivatization of the amine groups on chitosan has procured quaternized chitosan derivatives, having permanent positive charges, that give greater solubility in a wider pH range and show promising capabilities for enhancing absorption of hydrophilic drugs at pH values similar to the environment of the intestine (pH 6.4-7.5)[69, 72]. *N*,*N*,*N*-Trimethyl chitosan chloride (TMC) has been synthesized and tested for its efficiency as a absorption enhancer compared to chitosan HCl salt. TMC was tested as a permeation enhancer for the peptide drug buserelin and mannitol across Caco-2 cells at neutral pH values. Confocal laser scanning microscopy was used to show the opening of the tight junctions by TMC to give increased transport of the drug[77]. Chitosan is also an excellent film former and mucoadhesive polymer that has been utilized as a coating for alginate beads in a number of controlled release drug delivery applications[78] or as a carrier matrix in the form of chitosan HCl for the controlled release of insulin[73, 79]. Chitosan has also been considered for organ specific drug targeting including liver, colon, kidney and lung. For example, in colonic delivery, chitosan plays an important role in protecting therapeutic agents that would otherwise be susceptible to the harsh conditions of the upper GI tract, specifically directing them to the colon by means of localization of chitinase enzymes in the colon, that biodegrade the polysaccharide[80]. Chitosan can also be conjugated with 'targeting' hydrophobic molecules to produce an amphiphilic molecule that is capable of self-assembly. These self-assembled particles can be used to encapsulate and deliver hydrophobic drugs to a specific site[81]. Chitosan can also be chemically attached to prodrugs via easily cleavable functional linkers and targeted to a specific site in the body [81-82].

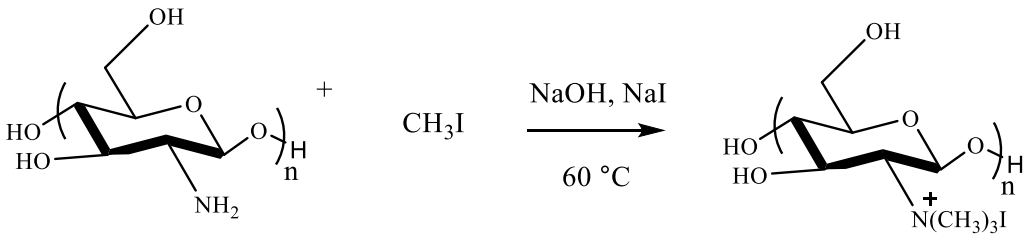

Scheme 2.8: Synthesis of N-trimethyl chitosan chloride[76]

Synthesis of quaternized phosphonium derivatives is another important area in which cationic cellulose derivatives can be produced. While very little is found in the literature about attempts to make phosphonium derivatives of cellulose, such derivatization has been explored for chitosan

and synthetic polymer entities. Phosphonium derivatives of cellulose were reported in 1982[83] but very little has otherwise been published on this subject. In this study, carboxyl containing cellulose derivatives with 1, 2 and 3 carboxyl groups as well as carboxymethylcellulose (CMC) were reacted with tri(hydroxymethyl)phosphine (THMP) and alkylene oxides or aldehydes, in water and DMF. By varying the molar ratios of the reagents, the authors reported up to 98% conversion of the carboxyl groups; increased phosphorus content in β and α hydroxyalkylphosphonium cellulose derivatives was confirmed by elemental analyses. Most derivatives were water insoluble but increasing phosphorus content of derivatives also increased solubility. However, insufficient analytical data presented makes it difficult to evaluate the results of the experiment[83]. Synthetic phosphonium derivatives like quaternized triphenylphosphonium-modified polyphenylene oxide (PPh_3 -PPO) have shown excellent antibacterial activity against *Staphylococcus epidermidis* and *Escherichia coli* while some quaternary phosphonium derived compounds have shown anticancer activity[84],[85]. Water-soluble phosphonium derivatives of chitosan have been produced by first reacting chitosan with 1-hydroxybenzotriazole (HOBt) in water[84]. The solubilized chitosan is thereafter mixed with (2-carboxyethyl) triphenylphosphonium chloride (CTPC) followed by 1-ethyl-3-(3-dimethylaminopropyl) carbodiimide hydrochloride (EDC·HCl) to produce the quaternized derivative. The water-soluble derivatives synthesized show low toxicity toward mouse fibroblast cells and are currently being studied for potential drug applications[84].

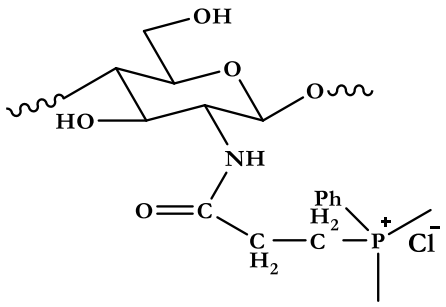

Figure 2.9: Quaternized phosphonium derivative of chitosan. Adapted from[84].

If new reaction pathways are successfully devised for producing both quaternized ammonium and phosphonium derivatives of cellulose, there would be greater possibility of

adding more novel polysaccharide derivatives to the pool of currently available drug delivery agents.

2.6.4 Conclusions

There are a variety of derivatization methods that currently produce cellulose derivatives that have novel properties that can be applied to the delivery of various drugs. However, the broad range of properties of drugs and drug candidates ensures that one specific type of polymer will not always be capable of effectively complexing, releasing or interacting with every new type of drug. For this reason, new polymer candidates are needed to fill in the gaps where needed. Tosylation and halogenation of cellulose present two strategies that have been most utilized for C-6 derivatization and have shown great promise in their ability to produce cationic derivatives of cellulose that may have similar or superior activity to known cationic biopolymers like chitosan. Of the two, halogenation is most specific for C-6 targeting and is a promising technique for expanding the portfolio of novel cellulose derivatives.

2.7 Cellulose Derivatives in Oral Drug Delivery

There are a variety of methods currently available for the delivery of drugs and biologically relevant polymers have been used extensively to help improve these delivery methods. Oral drug delivery is however one of the most patient compliant methods of drug delivery. Compared to the use of injections, intravenous treatment and others, oral delivery provides the patient with the convenience of on-the-go treatment, reduction in cost from more expensive in-patient treatments and does not require much patient supervision for administration. Some routes for drug administration and their pros and cons are summarized in Table 3. While being most conducive to patient compliance, oral drug delivery also suffers from disadvantages brought on by the nature of the drugs on the market and their ability to be absorbed across the intestinal membrane, potential degradation in the GI tract and the potential side effects from high dosages needed to compensate for low drug bioavailability. Bioavailability refers to the percent of the administrated dose of the drug that actually reaches the blood stream intact and is available to act on the target site.

Drugs are greatly affected by metabolic enzymes through oral administration[86]. As these drugs are required to traverse the gastrointestinal tract and cross the gastrointestinal epithelia in

order to reach the blood stream, as a result of oral administration, they come in contact with various transport and metabolic proteins that may modify and/or eliminate the drug, by efflux back into the GI tract, before it reaches its target[87]. In some cases, the drug used may be a substrate for metabolic proteins and efflux pumps on the surface of enterocytes (absorptive intestinal cells) like P-glycoprotein (P-gp) or Cytochrome P_{450} 3A4 (CYP3A4)[87-88].

Table 2.3: Advantages and disadvantages of various drug administration routes[86-89]. Fox, S. C. Regioselective Synthesis of Novel Cellulose Derivatives for Drug Delivery. Virginia Polytechnic Institute and State University, 2011[32]. Used under fair use, 2015.

Route of Administration	Advantages	Disadvantages
Oral	High patient acceptance Self-administered Very little discomfort Used for a wide range of drugs	Potential degradation of drugs in the GI tract Poorly aqueous-soluble drugs --- low bioavailability Poorly membrane-permeable drugs --- low bioavailability First (1st) pass metabolism in liver
Injections	100% bioavailability High control over dosage Fast-acting- important for acute care situations	More expensive Discomfort to the patient Generally requires trained personnel i.e. nurse or doctor Sterility concerns during administration Mode of drug-vehicle clearance from circulation must be precisely understood
Transdermal	Excellent patient acceptance Self-administered Sustained delivery of drug	Difficulty of passive diffusion through the skin ---- limited to lipophilic drugs that can penetrate the skin Potential for skin irritation
Inhalation	Self-administered Drug absorbed rapidly Fast-acting	Control over dosage ----variable inhalation process Requires rigid control of aerosol droplet size

Many of the various drug candidates that are studied and tested today suffer from very poor water solubility[87]. So too do many of the most potent anticancer and antivirals like ritonavir and paclitaxel. Though research into new drug candidates has increased as research methods improve, the actual figures for drugs that are marketed commercially have not seen the same level of increase. Poor aqueous solubility of these candidates leads to very poor bioavailability in the blood stream that comprises about 83% water content.

Studies on drug bioavailability have shown that there are two main factors that are most influential to this property: aqueous solubility as well as the rate of permeation through the lipid bilayer. The Biopharmaceutical Classification System (BCS) is a four-point system based on the level of permeability and aqueous solubility of different drugs. Class 2 drugs having low solubility but high permeability have been heavily targeted for increasing aqueous solubility and thus bioavailability[90]. For improving the two main factors influencing bioavailability, the use of solid dispersions, nanoparticles, complexation by substituted cyclodextrins, formulation with liposomes, use of enteric coatings, osmotic pumps, and manipulation of crystallinity are just a few of the methods used[89c, 91].

In order to be effective, a drug delivery system must be able to satisfy some basic criteria. It must, where necessary, isolate the drug from the acidic environment of the stomach that contains multiple digestive enzymes whose action could destroy the drug long before it is able to be absorbed into the blood stream. The drug delivery system must also have the ability to dissolve or swell in the aqueous environment within the GI tract. The drug itself must be able to permeate through the lipid bilayer and evade the metabolic enzymes that lie in wait, avoid being excreted from or metabolized in the liver and remain soluble in the blood stream long enough for greatest efficacy in target organ and the delivery system must have some means of being cleared from the body. It should also, where appropriate, be capable of providing sustained or zero order release of the drug over a period of a couple hours to days, maintaining drug plasma concentrations at therapeutic versus cytotoxic levels **(Figure 2.10)**. This chapter will focus more exclusively on the use of solid dispersions or amorphous matrix formulations (used interchangeably from here on) in this capacity of producing effective drug delivery systems[87,89c].

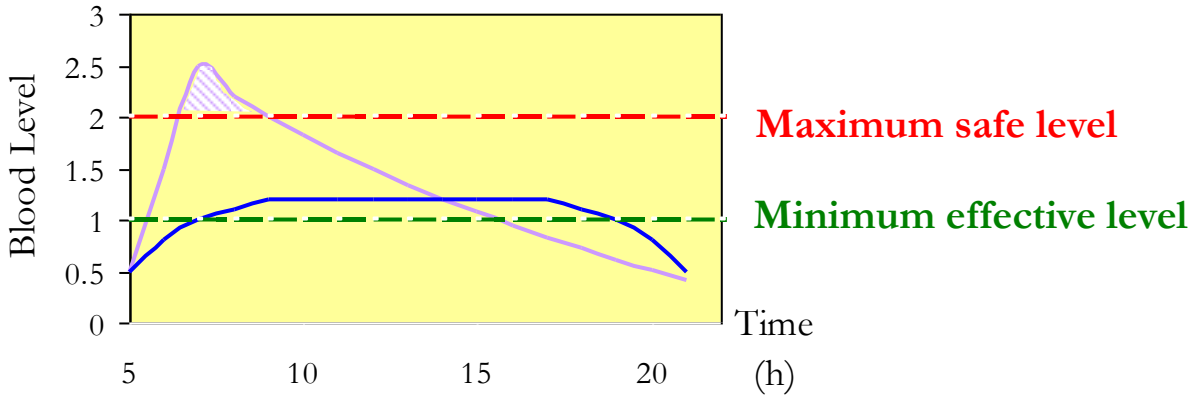

Figure 2.10: Zero-order release profile of the plasma concentration of a drug over time following administration of an oral dosage form (e.g. tablet or capsule). Jones, D. S., *Pharmaceutical Applications of Polymers for Drug Delivery*. iSmithers Rapra Publishing: 2004; Vol. 15, p 124[88]. Used under fair use, 2015.

2.7.1 Amorphous Solid Dispersions

Given the importance of drug solubility for therapeutic activity, the use of amorphous forms of a poorly aqueous soluble drug active to produce supersaturated solutions has become an important means of improving the delivery of poorly soluble drugs. Supersaturation describes the phenomenon whereby the solution concentration exceeds the equilibrium solubility. If the enhanced concentrations of the drug can be maintained for long enough, enhanced absorption of the drug will occur and will result in improved bioavailability. A solid dispersion describes the dissolution or entrapment of a drug substance inside a polymer carrier. These polymer carriers are usually hydrophilic polymers that have the ability to provide effective interaction with an aqueous environment. In order to disrupt the high crystallinity of most drug substances, it is important that the polymer carrier is miscible with the drug. This phenomenon ensures that there is complete molecular mixing of the two substances. Complete molecular mixing of the polymer and drug disrupts the crystal lattice of the drug and prevents further nucleation sites from developing in the dispersion, thus reducing crystallinity. The lack of crystallinity promotes greater dissolution, increasing drug bioavailability where solubility is the or an important barrier (BCS drug classifications II and IV respectively). High polymer T_g is also an important consideration for restricting the mobility of the drug in the solid matrix. High humidity conditions may cause a plasticizing effect on the polymer and drug blend and reduce the formulation T_g. The drug/polymer combination should also be stable to time with regard to drug crystallization. Over a period of months to years, there needs to be a significant window between

formulation T_g and ambient temperature that enables stability of the drug vs. recrystallization from the blend by inhibiting the drug's migration through the polymer matrix. This window between formulation T_g and ambient temperature should be large enough such that the drug will remain amorphous under those conditions for an extended period of time, even when ambient temperature and humidity reach high levels. It is also theorized that if the drug is not entirely amorphous in the formulation, small areas of crystallinity can act as sites for additional crystal growth. This in turn can also reduce the time period over which the stored drug formulation can still remain effective[92]. Thus, high blend T_g is most desirable to resist the effects of moisture (and/or drug) plasticization, and deliver a formulation that effectively solubilizes and stabilizes a target drug[93]. The task of finding suitable polymer matrices can be daunting; non-toxicity, high T_g, miscibility with a mostly hydrophobic drug, as well as possession of an effective drug release mechanism are just some of the characteristics required. Coupled with these, it is important that the drug and polymer formulation be stable enough for transport, have high glass transition temperature to prevent drug migration, and the drug itself should certainly be amorphous as well[92, 94].

2.7.2 Preparation and analysis of amorphous solid dispersions (ASDs)

These amorphous formulations can typically be made in several ways. The target drug and polymer can be dissolved in a common solvent. The solid dispersion can then be achieved through evaporation of the solvent through film casting, rotary evaporation, or by spray drying the mixture to obtain micron-sized particles of the polymer/drug blend in powder form. Co-precipitation and extrusion are also very common methods of obtaining polymer blends for drug delivery applications.

Evaporation of the solvent through film casting is a relatively simple method and can give easy analysis of films for clarity; this would give a first indication of possible miscibility of polymer blends. However, the drying process during film casting is relatively slow and samples are more susceptible to phase separation due to differences in relative solubility of different polymer entities in the chosen solvent. Rotary evaporation is usually very useful with small amounts of material, however recovery of the samples can be extremely difficult especially when glassy films are formed. Co-precipitation of the drug and the polymer in a non-solvent can also be used to obtain solid dispersions. Considerable experimentation may be necessary to optimize

the co-precipitation conditions to maximize drug and polymer recovery, and control the percent drug in the blend. Co-precipitation has also been achieved in the literature by using a supercritical anti-solvent (SAS) precipitation. This involves the use of an organic solvent and carbon dioxide as the precipitating non-solvent. The SAS process has been used to produce micro and nanoparticles (of uniform sizes) using cellulose based polymer blends[93].

Commercial uses of polymer blends, including the use of cellulose based polymers, requires a cost effective means of producing and processing material on a large scale. For pharmaceutical applications, micro compounding is an extrusion method that is used to test formulations on the lab scale. This method can use very small volumes (15 to 5 mL or less) in a twin-screw extruder system having specific design parameters. Micro compounders have a recirculation mode and a conical shape. In a typical continuous twin extruder system, it would be difficult to obtain complete mixing of such small volumes. Micro compounders thus provide the benefit of using a twin extruder type system, are easily filled and cleaned, and allow small amounts of expensive materials to be processed in a just a short period of time[95]. Most natural polysaccharides cannot be melt-processed as they degrade on or before melting; this is certainly the case with cellulose. Many of the blends using these polymers are also designed specifically for incorporating drugs that may be very temperature sensitive. Therefore aqueous blending has thus been more widely used for preparing blends of these polymers for biomedical applications[96].

These dispersions are usually analyzed using differential scanning calorimetry (DSC), Fourier transform infrared (FTIR) and X-ray diffraction (XRD) to verify the miscibility of the combination. DSC provides useful information about the thermal properties of the dispersion. A single T_g can indicate a miscible blend while a decrease in T_g relative to the individual components can indicate that one component has a plasticizing effect. XRD can be used to identify crystalline phases of the dispersion and can be used for comparison with a highly crystalline drug to indicate when the ASD has in fact resulted in an amorphous drug/polymer combination. FTIR gives useful information about favorable interactions like hydrogen bonding between the drug and polymer entity which are usually characterized by broadening and shifts in any hydroxyl, amine, or carbonyl peaks, or those of other functional groups present in the IR spectrum[69c7397].

2.7.3 Drug Release

While the method used to produce and characterize these dispersions is vital to an effective ASD, it is also extremely important that the polymer-drug formulation is capable of stabilizing the drug upon dissolution and release from the matrix. It is widely understood that increased solubility of the drug due to crystallinity suppression can produce a supersaturated drug solution upon release[98]. The supersaturated solution is important for delivering poorly soluble drugs as it also promotes more complete absorption of the drug relative to the saturated solution due to greater thermodynamic activity[72b]. If the polymer of choice is incapable of stabilizing the drug in solution, the likelihood that precipitation of the drug will occur increases greatly. One challenge for individuals working in drug delivery is to find a single polymer that displays all the needed characteristics at once. While polymers such as polyethylene glycol (PEG) and poly (vinylpyrrolidone) (PVP) have been widely examined for their solubility enhancement properties, PEG is limited by its tendency to crystallize while PVP does not fare very well in stabilizing some drug actives from recrystallization[98b, 99]. The highly hydrophilic and hygroscopic nature of PVP is sometimes disadvantageous as a carrier as it is easily solubilized in the stomach, resulting in rapid drug release. The challenge to find more effective polymer matrix materials has left the door wide open for cellulosic derivatives to be used, and many have shown very promising results. This has also led to a focus on the use of blends of polymers for drug delivery applications [72b, 92].

The use of amorphous matrices for producing supersaturated drug solutions is becoming a much more common approach in drug delivery. A caveat of this approach is that bioavailability enhancement of the drug is only possible if enhanced concentrations of the drug can be maintained long enough to permit enhanced absorption of the drug. When the drug is released from the dosage form and the solution is sufficiently supersaturated, the formulation may fail due to the driving force for recrystallization of the drug to achieve equilibrium conditions. Given the thermodynamic driving force for recrystallization of the drug from the supersaturated solution, it is important to consider the processes involved and to find effective means of controlling them[72b, 98a, 100]. Studies have outlined that two processes, nucleation and crystal growth, are critical to drug crystallization. If these processes can be inhibited, supersaturation of the drug can be maintained for a more physiologically relevant time and the absorption of the drug can be improved. Even small concentrations of a polymeric compound can play an important role in

affecting nucleation and crystal growth rates[72b]. As such, some polymers have been revealed to be crystallization inhibitors that can have a big impact on the nucleation and crystal growth rates of a drug. Some of these commercially available inhibitors include PVP, PEG and hydroxypropylmethyl cellulose (HPMC, also called hypromellose). More recently, cellulose acetate adipate propionates, sebacates and suberates have been explored for potential applications in inhibiting the crystal growth of the critical antiviral ritonavir[72b, 101].

The use of polysaccharides in ASDs has significant benefits. The benign nature of polysaccharides ensures that toxicity is negligible. The relatively polar, high molecular weight polysaccharides are incapable of crossing the epithelial membranes; in the case of cellulose, human beings do not possess the cellulase enzymes needed to digest the polymer. The degradation products of the polysaccharides used in drug delivery are also known to be non-toxic in nature. Cellulosic polymers like CMCAB, HPMC and HPMCAS have been studied under many conditions and in some cases have shown zero order release behavior (sustained release over several hours) using drug actives including aspirin, ibuprofen, fexofenadine HCl and griseofulvin among others[89c, 92, 97b]. Just a few years ago, collaborators from Eastman Chemical Company conducted a thorough study on the dissolution of poorly aqueous soluble drugs like aspirin, ibuprofen, glyburide, griseofulvin and the poorly adsorbable drug fexofenadine HCl from CMCAB matrices. A variety of methods were used to prepare solid dispersions of drug and polymer inclusive of spray drying, co-precipitation, rotary evaporation as well as film casting. The crystallinity of the dispersions was evaluated by X-ray diffraction and release studies conducted in simulated intestinal fluid at pH 6.8. The release was also evaluated at pH 1.2 (model for gastric pH). The results indicated that there was much faster, pH controlled release at intestinal pH versus the stomach and enhanced solubility of at least two of the target drugs resulted. This was a promising indication that this type of formulation had potential to enhance the solubility of poorly aqueously soluble drugs. However unexplained phenomena including the reduced solubility of fexofenadine HCl indicate that there is much more work to be done to evaluate potential formulations for drug delivery applications[92]. In the context of pH controlled release, the ability of these cellulosic polymers to swell or dissolve at pH 6-7 to create a means through which water can diffuse and dissolve the drug is also a critical benefit for drug delivery applications. In some cases, the release of drug actives in the stomach may also be beneficial for

treating gastric disorders including ulcers that typically require the administration of antibiotic drugs.

The release of the flavonoid quercetin was also recently evaluated in three (3) cellulosic polymer matrices as well as PVP[102]. The powerful antioxidant, which has also been associated with anti-inflammatory, antibacterial and antiviral effects, is poorly soluble in water and has low bioavailability[103]. ASDs of quercetin in HPMCAS, CMCAB, cellulose acetate adipate propionate (CAAdP) and PVP were prepared using a spray drying technique. These ASDs were amorphous up to 50 % of the drug and exhibited slow, pH-controlled release from the polysaccharide matrices but fast, complete release from PVP even at stomach pH. All the matrices provide sufficient stability of the flavonoid vs. crystallization from solution but only PVP was capable of stabilizing the flavonoid against chemical degradation. This is a promising example of the use of polymer matrices for tailoring the release of a poorly soluble therapeutic[102].

The antiviral ritonavir has also been a major focus of ongoing efforts to use ASDs to help improve the aqueous solubility and by extension the bioavailability of poorly aqueous soluble drugs. Ritonavir is a potent drug that suffers from toxicity due to the high dosages needed to ensure that efficient concentrations of the drug get into the blood stream. Efforts to find an ASD that is most efficient for delivery of ritonavir are ongoing but promising results are being reported. In studies published recently from collaborations between researchers at Virginia Tech and Purdue, more information is being garnered about the properties of cellulosic and synthetic polymers that most influence the solution crystal growth rate of ritonavir[94, 98a, 98b, 104]. Based on a study conducted that utilized thirty-four (34) polymers[98b], cellulosic polymers were found to be most efficient at inhibiting the crystal growth from supersaturated solutions of the drug/polymer formulation at pH 6.8. In fact, a novel and newly synthesized cellulose acetate adipate propionate (CAAdP) was found to be most effective at inhibiting crystal growth based on an initial study. It was surmised that some of the properties contributing to enhanced inhibition of crystal growth include: moderate levels of hydrophobicity, rigidity of the polymer structure, and amphiphilicity of novel derivatives that help to promote adsorption of the polymers onto the crystal faces of ritonavir and thus prevent additional crystal growth formation. This provides great insight into some of the interactions between drug and polymer that are necessary to produce effective therapeutic formulations[98b].

Modification of cellulose has produced derivatives containing pendant carboxyl groups that can provide pH-controlled release of drugs. Carboxyl and amino functional groups are most important in the context of pH-controlled release. Cellulose ester derivatives like CMCAB, HPMCAS and newly synthesized cellulose ester adipate, sebacate or suberate derivatives contain pendant carboxyl groups that can provide release of drugs in the desired pH range (in the intestine versus the stomach)[97b]. The pendant groups along the cellulose backbone also provide an important means of solubilizing different drug actives. The presence of carboxyl groups can aid interaction with amine containing drugs while the degree of hydrophobicity or hydrophilicity of the groups can help to improve interaction with more hydrophobic or hydrophilic drugs[105]. In some cases, the presence of a cationic or anionic cellulose derivative can also be an excellent means of improving interaction between anionic or cationic drugs. The use of cationic ammonium or phosphonium derivatives of cellulose could greatly aid the solubility and improve the release of anionic drugs like the anti-cancer agent doxorubicin and the peptide drug buserelin. In many cases, combinations of polymers with favorable characteristics can prove useful to providing formulations that have superior characteristics to single polymer ASD systems[104, 106]. The next section of this review will seek to describe the potential benefits of blending polymer entities for use in amorphous formulations.

2.7.4 Polymer Blends

The idea of using one or more polymers as matrix materials for amorphous formulations has taken off in the last couple years. In many cases, the use of two or more polymers helps provide an intermediate value between the more favorable properties of each matrix material and in cohort the two can have potentially revolutionary effects on the stabilization of the drug in solid and solution states and give favorable drug release properties. Binary blending of polymers provides an avenue for remedying poor mechanical properties that may be exhibited by some polymers from renewable resources and also may offset the expense of using synthetic biodegradable polymers in various applications[96]. This also provides a unique way to utilize combinations of polymers that already have an established history of human use, with new polymers having exceptional properties[89c].

There are certain characteristics that are usually exhibited by compatible blends that are miscible. They display microscopic homogeneity that is manifested in optical clarity of films,

uniform physical properties, and a single T_g that varies linearly based on the percent composition of each component[107]. The detection of a single T_g in the blend supports the hypothesis that there is no phase separation of the components in the amorphous regions, and suggests that the 'scale of homogeneity' is less than a couple of tens of nanometers[108].

In order to capitalize on the best properties of different polymers, early work with cellulose blends involved the use of cellulose derivatives with other polysaccharides like starch, synthetic polymers like PVP, and those made from renewable resources like poly(lactic)acid (PLA) and poly(ε-caprolactone). In fact, poly(ε-caprolactone) has shown excellent compatibility with various polymers and is often used in blend applications. Starch and cellulose acetate blends were made by reactive extrusion by Warth et al.[109] in 1997. Cellulose-2.5-acetate was processed by reactive extrusion (REX) in a process which grafted cyclic lactones unto the surface of the polysaccharide, hydroxyl functionalized plasticizer and optional filler was added before organosolv lignin, starch, cellulose and chitin were included for reinforcement of the resulting fibers. It was also reported that adding fillers during the REX process greatly enhanced the compatibility between oligolactone-modified cellulose acetate and fillers. This was a gateway to greater use of oligolactones for blending with cellulose derivatives[96, 109]. In a number of examples, starch/cellulose blends have been seen to be extremely effective for drug delivery or other biomedical functions. There are examples in the literature where thermoplastic hydrogels for use as bone cements or as drug delivery carriers have been made through blending starch with cellulose acetate to produce miscible blends that are further modified using acrylates[110]. In one example, hydrogels of commercially available starch/cellulose acetate blends were produced by free radical polymerization with methyl acrylate or an acrylic monomer[110a]. Partially biodegradable bone cements were made in the mentioned cases. In another, aqueous blends of methylcellulose and starch were made by casting or extrusion with added plasticizers to yield favorable results [110c]. Edible films incorporating microcrystalline cellulose, methylcellulose, cornstarch and polyols have also been reported. There were significant shifts in the properties of the films based on the percentage of the components. Increase in water or polyol content resulted in increased elongation capacity while increased cellulose content significantly increased the tensile strength and decreased the transmission of water vapor through the films[111]. There are many such cases demonstrating excellent results of blending two or more polymers with cellulose[96, 112].

Cellulose derivatives have also shown considerable compatibility with poly(3-hydroxybutyrate) (PHB), a degradable aliphatic polyester. Blends of ethyl cellulose and PHB have shown composition-dependent single glass transitions and no crystallization versus what is typical when only PHB is present. SEM studies indicated that there was no phase separation of the polymer components. Cellulose derivatives have attracted much interest for their compatibility with PHB[113]. PHB binary blends with cellulose propionate (CP) have also been found to afford single T_g, miscible blends with marked improvement in ductility vs. the PHB component[114].

In the literature, most of the binary blends produced have involved pairs of amorphous polymers, which may be more likely to be compatible than crystalline polymers. However, modification of polymers which crystallize by blending with amorphous or other crystallizable polymers is thought to be an effective way to produce more diverse materials which may show marked differences in properties from the original polymers combined. While most cellulosic polymers may have very high glass transition and melt temperatures, or may degrade before melting and thus be difficult to process, some aliphatic polyesters like polylactones lack mechanical strength and ductility and are easily affected by heat due to low melting temperatures[108b]. It is with these properties in mind that many researchers have reported the blending of the semi-crystalline polymer poly(ε-caprolactone) (PCL) with cellulose esters. Blends of PCL with cellulose diacetate (CDA), cellulose acetate butyrate (CAB), and cellulose triacetate (CTA) provided what appear to be partially miscible and immiscible blends. The blends were prepared by film casting from a solution of the polymers and evaporating the solvent at room temperature. Double melting endotherms were seen for PCL-CAB using DSC. Despite immiscibility, all the studied blends demonstrated decreased crystallinity with increasing cellulose acetate content. While a number of useful techniques were employed for the mentioned study, including DSC, dynamic mechanical analysis (DMA), and wide-angle X-ray scattering (WAXS) techniques, the method the investigators used for preparing the blends can provide somewhat unreliable or misleading results. Slow evaporation of the solvent can produce phase separation of the polymer entities[115], due not necessarily to immiscibility of the polymers, but rather to differential affinity for the solvent. In 2008, a comprehensive look at the miscibility and crystallization behavior of blends of cellulose alkanoates and PCL was also conducted[108b]. The cellulose esters involved in the study were cellulose butyrate (CB) (of varying DS values) as

well as cellulose valerate (CV). Cellulose mixed esters (cellulose butyrate valerate (CBV), cellulose propionate valerate (CPV), and cellulose acetate valerate (CAV)) were also studied. The blends were made by film casting from mixed polymer solutions using polymer ratios that varied between 10/90 and 95/5 cellulose ester/PCL. The study determined that CB and CV having four (4) and five (5) carbons and most closely matching the chemical structure of the polylactone showed miscibility at lower DS values (1.85 and 2.15 respectively). A single T_g was observed (DSC) for these combinations. At higher DS values, and higher PCL content, the CB/PCL and CV/PCL blends (DS > 2.0 and 2.2) showed a decrease in the crystallization of the PCL. It is believed that the bulky cellulose esters are more capable of being trapped on the growth faces of the PCL crystals and thus produce dispersed amorphous-like phases in the otherwise crystalline regions. Other cellulose esters demonstrated miscibility at different DS values. Some of this information is summarized in the figure below[108b].

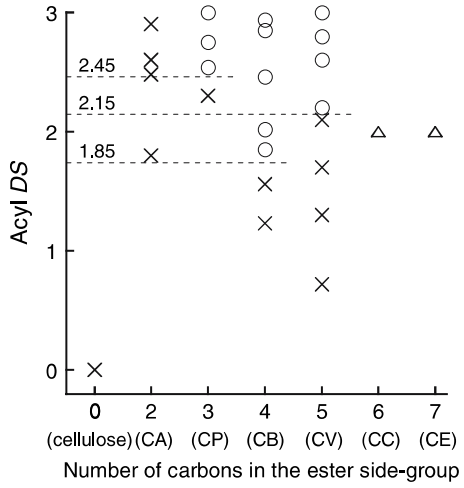

Figure 2.11: Miscibility map for different cellulose alkyl ester/PCL blends as a function of the number of carbons in the side chain and the acyl DS of the cellulosic component. Miscible (circle), immiscible (cross) or partially miscible (triangle). (b) Kusumi, R.; Inoue, Y.; Shirakawa, M.; Miyashita, Y.; Nishio, Y., Cellulose alkyl ester/poly(e-caprolactone) blends: characterization of miscibility and crystallization behaviour. *Cellulose* 2008, *15*, 1-16.[108b]. Used under fair use, 2015

Interesting blends of cellulose and polyethylene glycol (PEG) have also been formulated with potential drug delivery applications. In one such study, PEG and cellulose were blended in ratios ranging between 25 and 85% cellulose. The blends appeared to be miscible by DSC but were not further analyzed for miscibility. The miscible blends were film cast by first using the two polymer components and subsequently a typical drug vitamin C was also included. Cellulose used in the study was of DP 500 and contained 90% α-cellulose. The release studies of the drug

containing films demonstrated temperature and pH dependent release activity. It was concluded that the blend was most suitable for release in acidic media (pH ~ 4) and the temperature sensitive release could be predictably tuned by varying the composition of the polymers. At body temperature, sustained release of vitamin C was seen for a period of at least four (4) hours[116]. PEG and CAB blends have also produced amorphous microspheres that give slow 12 h release of the anti-diabetic drug repaglinide[117].

Eastman Chemical Company was a pioneer in demonstrating the potential for blending cellulosic polymers with PVP and poly (2-ethyl-2-oxazoline) (PEOx). They were able to show that by incorporating just 20 % of PVP or PEOx into blends with cellulose diacetate (to make clear films), they could achieve steady release of dextromethorphan in just a few hours in contrast to the slow release rate for the cellulose diacetate films only[89c]. Later on, a study using blends of two cellulosic polymers would reveal zero order behavior of the same drug over a large range of time. In 2005, Lyu et al.[118] also published work that showed the tuning of release behavior by blending polyvinyl acetate (PVA) and cellulose acetate butyrate (CAB). While the release of dexamethasone from PVA only was very fast, and extremely slow from CAB only, a predictable slowing of the release rate of the drug was seen by adding proportions of CAB to the PVA/drug mixture[118].

Of the greatest significance to this review is a paper published recently in *Crystal Growth and Design*[104]. The study details the formulation of binary blends of cellulosic polymers with synthetic or other cellulosic polymers as well as single polymer matrices in order to pinpoint promising combinations that are applicable to the delivery of the poorly water-soluble antiviral ritonavir. ASDs of 5 synthetic polymers including PVP and PVP vinyl acetate (PVPVA), 3 commercially-available cellulose-based polymers (HPMC, HPMCAS and cellulose acetate phthalate (CAPhth) and 6 newly synthesized cellulose derivative polymers with varying physical and chemical properties with the drug ritonavir were made by co-precipitation and lyophilization. The study included solubility studies that took a detailed look at the crystal growth rate from supersaturated solutions at pH 6.8 and the factors affecting the solution crystal growth of the drug in different formulations. There were thirteen (13) binary combinations examined and ten (10) of those inhibited crystal growth of ritonavir in some way. In those cases, it was found that the combination of two polymers presented more effective inhibition than the individual polymers. PVP for example had no impact on the growth rate of ritonavir when used

alone; however, when combined with CAAdP (cellulose acetate adipate propionate) the ratio of the growth rates increased significantly (growth ratio > 1 shows inhibitory effect on crystallization). Surprisingly enough, it was noticed that not only did the effectiveness of synthetic polymers like PVP increase when combined with cellulosic polymers like CAAdP but there were also synergistic effects of combinations of two (2) cellulosic polymers as well. The most effective combinations from the study were CAAdP /cellulose acetate adipate, and CAAdP (DS Ad 0.85)/ CAAdP (DS Ad 0.33) (difference in DS of adipate). In contrast to the effectiveness of the binary polymer blends on the growth rate of ritonavir, surfactant combinations with cellulose polymers studied significantly decreased the effectiveness of the polymers as growth rate inhibitors of ritonavir. This speaks to the great utility of polymer combinations and the potential for binary cellulose based additives in amorphous formulations for drug delivery applications. Half of the effective combinations included the novel polymer CAAdP that had previously been shown to produce the greatest individual inhibition of crystal growth of all the polymers examined. Combinations of CAAdP with polymers that individually had shown very little effect on the rate of inhibition, like PVP, showed marked improvement in decreasing the rate at which the crystallization of the drug took place. It is theorized that while the cellulosic agent will contribute crystallization inhibition; the presence of PVP in the blend will likely give faster, more streamlined and complete release of the drug. In scenarios where binary additives are used, it is speculated that the two polymers may adsorb onto independent sites of the drug crystals or compete for the same adsorptive sites. Alternatively, the two polymer additives may adsorb at the surface of the drug crystals and form solution complexes. For chemically dissimilar polymer combinations, it is expected that the polymers will adsorb to separate sites and show synergistic effect on inhibiting recrystallization of the drug. For chemically similar polymers, there are two possible considerations for understanding the effect of the combinations. These polymers may compete for adsorptive sites and show very little change in effect compared to the individual polymers, as was observed for HPMCAS/ CAAdP (DS Ad 0.85), or solution complex formation may enhance the effectiveness of the polymer combinations (as seen with CAAdP (DS Ad 0.85)/CAAdP (DS Ad 0.33)). Hydrophobic interaction between the polymers is thought to be a primary mode of complex formation in solution. The degree of hydrophobicity of the polymers used is also critical for effectiveness. Combinations of moderately hydrophobic polymers generally show improved effectiveness in

comparison to the individual polymers. The most hydrophobic polymer combinations may tend to associate in solution, forming highly hydrophobic complexes that will not adsorb to the drug as effectively and will have decreased interaction with the solid-solvent interface. Thus, hydrophilic/hydrophobic balance is an important element of determining polymer combinations with the potential for improved crystal growth inhibition and thus highlighting potential candidates for drug delivery applications[104]. An even more recent study from the Edgar and Taylor groups reveals that certain novel cellulose ω-carboxyalkanoate polymers are superior to CAAdP in inhibiting the crystal growth of ritonavir. Cellulose acetate suberate and cellulose acetate sebacate (CASub and CASeb) contain relatively high DS (DS sub = 0.63; DS seb = 0.57) long □-carboxyalkanoate side chains, and are formed from a relatively hydrophilic cellulose acetate ester. The sebacate and suberate derivatives produced have an optimal level of hydrophobicity that is an important element of their superior performance. The mixed ester cellulose ω-carboxyalkanoate polymers are reported as being 5-fold more effective at inhibiting the crystallization of ritonavir compared to the other cellulosics and non-cellulosics used in the study. It will be important to also determine whether binary blends using these superior polymers produce more promising results for drug delivery as well.

While early studies on polymer blends proved influential, they generally did not focus on utilizing these blends more effectively. More recent publications seem to suggest a trend towards discovering more promising combinations of polymeric agents that will hopefully have a revolutionary effect on the field of drug delivery in the very near future. There is an obvious need to study the potential for blends thoroughly to establish more clearly the potential of different polymer combinations. By utilizing some established polymers like HPMC, HPMCAS, CMCAB, PVP with more recently developed matrix polymers like cellulose adipates and Eudragit E100, the door can be opened even further to show how polymer blends can play significant roles in enhancing the field of drug delivery. The door is also wide open for the synthesis of new derivatives that can provide even greater benefits in drug delivery research.

2.7.5 Concluding remarks

The use of amorphous solid dispersions for oral drug delivery applications continues to be a focal point of research efforts. Crystal growth inhibition, enhanced aqueous solubility and improved release have all been seen for various drug actives using such formulations. The idea

of using blends has also had renewed focus and many researchers believe such blends could potentially be a key to solving many of the problems facing the delivery of poorly soluble, highly crystalline drugs. More information is needed about the properties of different polymer entities in this regard and it is hoped that novel polymers of great significance to drug delivery will continue to be synthesized and successfully applied in the context of commercial usage.

2.8 References

1. (a) Barthel, S.; Heinze, T., Acylation and carbanilation of cellulose in ionic liquids. *Green Chemistry* **2006,** *8* (3), 301-306; (b) Zhang, H.; Wu, J.; Zhang, J.; He, J. S., 1-Allyl-3-methylimidazolium chloride room temperature ionic liquid: A new and powerful nonderivatizing solvent for cellulose. *Macromolecules* **2005,** *38* (20), 8272-8277; (c) Heinze, T.; Schwikal, K.; Barthel, S., Ionic liquids as reaction medium in cellulose functionalization. *Macromolecular Bioscience* **2005,** *5* (6), 520-525; (d) Swatloski, R. P.; Spear, S. K.; Holbrey, J. D.; Rogers, R. D., Dissolution of cellose with ionic liquids. *Journal of the American Chemical Society* **2002,** *124* (18), 4974-4975; (e) Kosan, B.; Michels, C.; Meister, F., Dissolution and forming of cellulose with ionic liquids. *Cellulose* **2008,** *15* (1), 59-66.
2. Robeson, L. M., *Polymer Blends: A Comprehensive Review*. Hanser Gardner Publications: Cincinnati, 2007.
3. Klemm, D., *Comprehensive Cellulose Chemistry: Fundamentals and analytical methods*. Wiley-VCH: 1998.
4. (a) Klemm, D.; Einfeldt, L., Structure design of polysaccharides: Novel concepts, selective syntheses, high value applications. *Macromolecular Symposia* **2001,** *163*, 35-47; (b) Klemm, D.; Heublein, B.; Fink, H. P.; Bohn, A., Cellulose: Fascinating biopolymer and sustainable raw material. *Angewandte Chemie-International Edition* **2005,** *44* (22), 3358-3393.
5. Heinze, T.; Liebert, T.; Koschella, A., *Esterification of Polysaccharides*. Springer: 2006.
6. (a) Saxena, I. M.; Brown, R., Biosynthesis of cellulose. *Progress in Biotechnology* **2001,** *18*, 69-76; (b) Coffey, D. C.; Bell, D. A.; Henderson, A., 5 Cellulose and Cellulose Derivatives. *Food polysaccharides and their applications* **2014,** *160*, 147.
7. O'Sullivan, A. C., Cellulose: the structure slowly unravels. *Cellulose* **1997,** *4* (3), 173-207.
8. (a) Burchard, W., Solubility and solution structure of cellulose derivatives. *Cellulose* **2003,** *10* (3), 213-225; (b) Furuhata, K.-i.; Koganei, K.; Chang, H.-S.; Aoki, N.; Sakamoto, M., Dissolution of cellulose in lithium bromide-organic solvent systems and homogeneous bromination of cellulose with N-bromosuccinimide-triphenylphosphine in lithium bromide-N,N-dimethylacetamide. *Carbohydrate Research* **1992,** *230* (1), 165-177; (c) Ramos, L. A.; Frollini, E.; Heinze, T., Carboxymethylation of cellulose in the new solvent dimethyl sulfoxide/tetrabutylammonium fluoride. *Carbohydrate Polymers* **2005,** *60* (2), 259-267; (d) Zhu, S. D.; Wu, Y. X.; Chen, Q. M.; Yu, Z. N.; Wang, C. W.; Jin, S. W.; Ding, Y. G.; Wu, G., Dissolution of cellulose with ionic liquids and its application: a mini-review. *Green Chemistry* **2006,** *8* (4), 325-327; (e) Bochek, A. M.; Petropavlovsky, G. A.; Kallistov, O. V., Dissolution of Cellulose and Its Derivatives in the Same Solvent, Methylmorpholine-N-Oxide and the Properties of the Resulting Solutions. *Cellulose Chemistry and Technology* **1993,** *27* (2), 137-144; (f) Lu, A.; Zhang, L. N., Advance in solvents of cellulose. *Acta Polymerica Sinica* **2007,** (10), 937-944.

9. (a) Hermans, P.; Weidinger, A., X-ray studies on the crystallinity of cellulose. *Journal of Polymer Science* **1949,** *4* (2), 135-144; (b) Hulleman, S. H.; van Hazendonk, J. M.; van Dam, J. E., Determination of crystallinity in native cellulose from higher plants with diffuse reflectance Fourier transform infrared spectroscopy. *Carbohydrate research* **1994,** *261* (1), 163-172; (c) Thygesen, A.; Oddershede, J.; Lilholt, H.; Thomsen, A. B.; Ståhl, K., On the determination of crystallinity and cellulose content in plant fibres. *Cellulose* **2005,** *12* (6), 563-576.
10. Atalla, R. H.; Vanderhart, D. L., Native Cellulose: A Composite of Two Distinct Crystalline Forms. *Science* **1984,** *223* (4633), 283-285.
11. Yamamoto, H.; Horii, F., CPMAS carbon-13 NMR analysis of the crystal transformation induced for Valonia cellulose by annealing at high temperatures. *Macromolecules* **1993,** *26* (6), 1313-1317.
12. Sasaki, M.; Adschiri, T.; Arai, K., Production of cellulose II from native cellulose by near- and supercritical water solubilization. *Journal of agricultural and food chemistry* **2003,** *51* (18), 5376-5381.
13. (a) Kalia, S.; Sabaa, M., *Polysaccharide based graft copolymers*. Springer: 2013; (b) Okano, T.; Sarko, A., Mercerization of cellulose. II. Alkali–cellulose intermediates and a possible mercerization mechanism. *Journal of applied polymer science* **1985,** *30* (1), 325-332; (c) Fink, H.-P.; Hofmann, D.; Philipp, B., Some aspects of lateral chain order in cellulosics from X-ray scattering. *Cellulose* **1995,** *2* (1), 51-70.
14. Meurant, G., *Advances In Carbohydrate Chemistry*. Elsevier Science: 1964.
15. Sjostrom, E., *Wood Chemistry: Fundamentals and Applications*. Elsevier Science: 2013.
16. Ciolacu, D.; Cazacu, M., Synthesis of New Hydrogels Based on Xanthan and Cellulose Allomorphs. *Cellulose Chemistry and Technology* **2011,** *45* (3-4), 163-169.
17. (a) Urquhart, A., The Reactivity of Cellulose. *Textile Research Journal* **1958,** *28* (2), 159-169; (b) Krassig, H. A., *Cellulose*. Taylor & Francis: 1993.
18. (a) Cuissinat, C.; Navard, P.; Heinze, T., Swelling and dissolution of cellulose, Part V: cellulose derivatives fibres in aqueous systems and ionic liquids. *Cellulose* **2008,** *15* (1), 75-80; (b) El Seoud, O.; Fidale, L.; Ruiz, N.; D'Almeida, M.; Frollini, E., Cellulose swelling by protic solvents: which properties of the biopolymer and the solvent matter? *Cellulose* **2008,** *15* (3), 371-392.
19. Kohler, S.; Heinze, T., New solvents for cellulose: Dimethyl sulfoxide/ammonium fluorides. *Macromolecular Bioscience* **2007,** *7* (3), 307-314.
20. Liebert, T., Cellulose Solvents: Remarkable History, Bright Future. In *Cellulose Solvents: For Analysis, Shaping and Chemical Modification*, American Chemical Society: 2010; Vol. 1033, pp 3-54.
21. Qi, H. S.; Yang, Q. L.; Zhang, L. N.; Liebert, T.; Heinze, T., The dissolution of cellulose in NaOH-based aqueous system by two-step process. *Cellulose* **2011,** *18* (2), 237-245.
22. Mccormick, C. L.; Shen, T. C., A New Cellulose Solvent for Preparing Derivatives under Homogeneous Conditions. *Abstracts of Papers of the American Chemical Society* **1981,** *182* (Aug), 63-&.
23. (a) Rosenau, T.; Potthast, A.; Hofinger, A.; Sixta, H.; Kosma, P., Hydrolytic processes and condensation reactions in the cellulose solvent system N,N-dimethylacetamide/lithium chloride. Part 1. *Holzforschung* **2001,** *55* (6), 661-666; (b) Potthast, A.; Rosenau, T.; Sartori, J.; Sixta, H.; Kosma, P., Hydrolytic processes and condensation reactions in the cellulose solvent system N, N-dimethylacetamide/lithium chloride. Part 2: degradation of cellulose. *Polymer* **2003,** *44* (1), 7-17.

24. Fox, S.; Edgar, K., Synthesis of regioselectively brominated cellulose esters and 6-cyano-6-deoxycellulose esters. . *Cellulose* **2011,** *18*, 1305-1314.
25. Parker, A. J., Protic-dipolar aprotic solvent effects on rates of bimolecular reactions. *Chemical Reviews* **1969,** *69* (1), 1-32.
26. Takaragi, A.; Minoda, M.; Miyamoto, T.; Liu, H.; Zhang, L., Reaction characteristics of cellulose in the LiCl/1,3-dimethyl-2-imidazolidinone solvent system. *Cellulose* **1999,** *6* (2), 93-102.
27. Heinze, T.; Dicke, R.; Koschella, A.; Kull, A. H.; Klohr, E. A.; Koch, W., Effective preparation of cellulose derivatives in a new simple cellulose solvent. *Macromolecular Chemistry and Physics* **2000,** *201* (6), 627-631.
28. Zheng, X.; Gandour, R. D.; Edgar, K. J., Probing the mechanism of TBAF-catalyzed deacylation of cellulose esters. *Biomacromolecules* **2013,** *14* (5), 1388-1394.
29. Xu, D. G.; Edgar, K. J., TBAF and Cellulose Esters: Unexpected Deacylation with Unexpected Regioselectivity. *Biomacromolecules* **2012,** *13* (2), 299-303.
30. (a) Gericke, M.; Fardim, P.; Heinze, T., Ionic Liquids - Promising but Challenging Solvents for Homogeneous Derivatization of Cellulose. *Molecules* **2012,** *17* (6), 7458-7502; (b) Liebert, T.; Heinze, T., Interaction of ionic liquids with polysaccharides 5. Solvents and reaction media for the modification of cellulose. *Bioresources* **2008,** *3* (2), 576-601.
31. Schlufter, K.; Schmauder, H. P.; Dorn, S.; Heinze, T., Efficient homogeneous chemical modification of bacterial cellulose in the ionic liquid 1-N-butyl-3-methylimidazolium chloride. *Macromolecular Rapid Communications* **2006,** *27* (19), 1670-1676.
32. Fox, S. C. Regioselective Synthesis of Novel Cellulose Derivatives for Drug Delivery. Virginia Polytechnic Institute and State University, 2011.
33. Glasser, W. G.; Ravindran, G.; Jain, R. K.; Samaranayake, G.; Todd, J., Comparative Enzyme Biodegradability of Xylan, Cellulose, and Starch Derivatives. *Biotechnology Progress* **1995,** *11* (5), 552-557.
34. (a) Philipp, B.; Stscherbina, D., Enzymatic Degradation of Cellulose Derivatives in Comparison to Cellulose and Lignocellulose. *Papier* **1992,** *46* (12), 710-722; (b) Song, Z.; Hisada, K.; Tabata, I.; Hori, T., Enzymatic hydrolysis of cellulose derivatives, part 1 - Action of cellulase to acetylcelluloses with different degrees of acetyl-substitution. *Sen-I Gakkaishi* **1997,** *53* (12), 526-532.
35. Shen, D.; Xiao, R.; Gu, S.; Zhang, H., The Overview of Thermal Decomposition of Cellulose in Lignocellulosic Biomass. *Edited by Theo van de Ven and John Kadla* **2013**, 193.
36. (a) Molton, P. M.; Demmitt, T. *Reaction mechanisms in cellulose pyrolysis: a literature review*; Battelle Pacific Northwest Labs., Richland, WA (USA): 1977; (b) Alvarez, V. A.; Vazquez, A., Thermal degradation of cellulose derivatives/starch blends and sisal fibre biocomposites. *Polymer Degradation and Stability* **2004,** *84* (1), 13-21; (c) Huang, F.-Y., Thermal properties and thermal degradation of cellulose tri-stearate (CTs). *Polymers* **2012,** *4* (2), 1012-1024; (d) Huang, M. R.; Li, X. G., Thermal degradation of cellulose and cellulose esters. *Journal of applied polymer science* **1998,** *68* (2), 293-304; (e) Jain, R. K.; Lal, K.; Bhatnagar, H. L., A Kinetic-Study of the Thermal-Degradation of Cellulose and Its Derivatives. *Makromolekulare Chemie-Macromolecular Chemistry and Physics* **1982,** *183* (12), 3003-3017; (f) Jandura, P.; Riedl, B.; Kokta, B. V., Thermal degradation behavior of cellulose fibers partially esterified with some long chain organic acids. *Polymer Degradation and Stability* **2000,** *70* (3), 387-394; (g) Jimenez, A.; Ruseckaite, R. A., Binary mixtures based on polycaprolactone and cellulose derivatives -

Thermal degradation and pyrolysis. *Journal of Thermal Analysis and Calorimetry* **2007,** *88* (3), 851-856.
37. Baker, R., Thermal decomposition of cellulose. *Journal of Thermal Analysis and Calorimetry* **1975,** *8* (1), 163-173.
38. Tosh, B., Thermal analysis of cellulose esters prepared from different molecular weight fractions of high a-cellulose pulp. *Indian J Chem Technol* **2011,** *18*, 451-457.
39. Madorsky, S.; Hart, V.; Straus, S., Thermal Degradation of Cellulosic Materials. *Journal of Research of the National Bureau of Standards* **1958,** *60* (4), 343-349.
40. Olabisi, O.; Adewale, K., *Handbook of Thermoplastics*. Taylor & Francis: 1997.
41. Zaikov, G. E.; Monakov, I. U. B.; Jiménez, A., *Homolytic and Heterolytic Reactions: Problems and Solutions*. Nova Science Publishers: 2004.
42. Vaca-Garcia, C.; Gozzelino, G.; Glasser, W. G.; Borredon, M. E., Dynamic mechanical thermal analysis transitions of partially and fully substituted cellulose fatty esters. *Journal of Polymer Science Part B-Polymer Physics* **2003,** *41* (3), 281-288.
43. Malm, C.; Mench, J.; Kendall, D.; Hiatt, G., Aliphatic acid esters of cellulose. Properties. *Industrial & Engineering Chemistry* **1951,** *43* (3), 688-691.
44. (a) Sarode, A. L.; Obara, S.; Tanno, F. K.; Sandhu, H.; Iyer, R.; Shah, N., Stability assessment of hypromellose acetate succinate (HPMCAS) NF for application in hot melt extrusion (HME). *Carbohydrate polymers* **2014,** *101*, 146-153; (b) Meena, A.; Parikh, T.; Gupta, S. S.; Serajuddin, A. T., Investigation of thermal and viscoelastic properties of polymers relevant to hot melt extrusion, II: Cellulosic polymers. *Journal of Excipients and Food Chemicals* **2014,** *5* (1), 46-55.
45. Li, X. G.; Huang, M. R.; Bai, H., Thermal decomposition of cellulose ethers. *Journal of applied polymer science* **1999,** *73* (14), 2927-2936.
46. (a) Biswal, D.; Singh, R., Characterisation of carboxymethyl cellulose and polyacrylamide graft copolymer. *Carbohydrate Polymers* **2004,** *57* (4), 379-387; (b) Zaccaron, C. M.; Oliveira, R. V.; Guiotoku, M.; Pires, A. T.; Soldi, V., Blends of hydroxypropyl methylcellulose and poly (1-vinylpyrrolidone-co-vinyl acetate): Miscibility and thermal stability. *Polymer degradation and stability* **2005,** *90* (1), 21-27.
47. Coma, V.; Sebti, I.; Pardon, P.; Pichavant, F.; Deschamps, A., Film properties from crosslinking of cellulosic derivatives with a polyfunctional carboxylic acid. *Carbohydrate polymers* **2003,** *51* (3), 265-271.
48. (a) Gomez, J. A. C.; Erler, U. W.; Klemm, D. O., 4-methoxy substituted trityl groups in 6-O protection of cellulose: Homogeneous synthesis, characterization, detritylation. *Macromolecular Chemistry and Physics* **1996,** *197* (3), 953-964; (b) Granstrom, M.; Olszewska, A.; Makela, V.; Heikkinen, S.; Kilpelainen, I., A new protection group strategy for cellulose in an ionic liquid: simultaneous protection of two sites to yield 2,6-di-O-substituted mono-p-methoxytrityl cellulose. *Tetrahedron Letters* **2009,** *50* (15), 1744-1747; (c) Kondo, T.; Gray, D. G., The Preparation of O-Methyl-Celluloses and O-Ethyl-Celluloses Having Controlled Distribution of Substituents. *Carbohydrate Research* **1991,** *220*, 173-183.
49. (a) Bontea, D., Solution properties of triphenylsilyl cellulose. *Journal of Applied Polymer Science* **2007,** *103* (2), 1257-1261; (b) Khan, F. Z.; Sakaguchi, T.; Shiotsuki, M.; Nishio, Y.; Masuda, T., Synthesis, characterization, and gas permeation properties of silylated derivatives of ethyl cellulose. *Macromolecules* **2006,** *39* (18), 6025-6030; (c) Kohler, S.; Liebert, T.; Heinze, T., Interactions of ionic liquids with Polysaccharides. VI. Pure cellulose nanoparticles from trimethylsilyl cellulose synthesized in ionic liquids. *Journal of Polymer Science Part a-Polymer*

Chemistry **2008,** *46* (12), 4070-4080; (d) Mormann, W.; Demeter, J.; Wagner, T., Silylcellulose from silylation/desilylation of cellullose in ammonia. *Macromolecular Symposia* **2001,** *163*, 49-57; (e) Philipp, B.; Klemm, D.; Wagenknecht, W., Regioselective Esterification and Etherification of Cellulose and Cellulose Derivatives .2. Synthesis of Cellulose Esters with a Regioselective Distribution of Substituents. *Papier* **1995,** *49* (2), 58-64.
50. (a) Rahn, K.; Diamantoglou, M.; Klemm, D.; Berghmans, H.; Heinze, T., Homogeneous synthesis of cellulose p-toluenesulfonates in N,N-dimethylacetamide/LiCl solvent system. *Angewandte Makromolekulare Chemie* **1996,** *238*, 143-163; (b) Gericke, M.; Schaller, J.; Liebert, T.; Fardim, P.; Meister, F.; Heinze, T.; Network, E. P., Studies on the tosylation of cellulose in mixtures of ionic liquids and a co-solvent. *Carbohydrate Polymers* **2012,** *89* (2), 526-536.
51. Mccormick, C.; Callais, P., Derivatization of cellulose in lithium-chloride and N-N-dimethylacetamide solutions. *Polymer* **1987,** *28*, 2317-2323.
52. Heinze, T.; Koschella, A.; Magdaleno-Maiza, L.; Ulrich, A. S., Nucleophilic displacement reactions on tosyl cellulose by chiral amines. *Polymer Bulletin* **2001,** *46* (1), 7-13.
53. (a) Mccormick, C. L.; Dawsey, T. R., Preparation of Cellulose Derivatives Via Ring-Opening Reactions with Cyclic Reagents in Lithium-Chloride N,N-Dimethylacetamide. *Macromolecules* **1990,** *23* (15), 3606-3610; (b) El Seoud, O. A.; Heinze, T., Organic Esters of Cellulose: New Perspectives for Old Polymers. *Advanced Polymer Science* **2005,** *186*, 103-149.
54. (a) Koschella, A.; Heinze, T., Novel Regioselectively 6-Functionalized Cationic Cellulose Polyelectrolytes Prepared via Cellulose Sulfonates. *Macromolecular Bioscience* **2001,** *1* (5), 178-184; (b) Liu, C.; Baumann, H., Exclusive and complete introduction of amino groups and their N-sulfo and N-carboxymethyl groups into the 6-position of cellulose without the use of protecting groups. *Carbohydrate Research* **2002,** *337* (14), 1297-1307.
55. Kern, H.; Choi, S.; Wenz, G. In *New functional derivatives from 2, 3-di-O-alkyl-celluloses*, Abstracts of papers of the American Chemical Society, American Chemical Society: 1998; pp U3-U3.
56. Clayden, J.; Greeves, N.; Warren, S., *Organic Chemistry*. OUP Oxford: 2012.
57. Granstrom, M.; Kavakka, J.; King, A.; Majoinen, J.; Makela, V.; Helaja, J.; Hietala, S.; Virtanen, T.; Maunu, S. L.; Argyropoulos, D. S.; Kilpelainen, I., Tosylation and acylation of cellulose in 1-allyl-3-methylimidazolium chloride. *Cellulose* **2008,** *15* (3), 481-488.
58. Elchinger, P.-H.; Faugeras, P.-A.; Zerrouki, C.; Montplaisir, D.; Brouillette, F.; Zerrouki, R., Tosylcellulose synthesis in aqueous medium. *Green Chemistry* **2012,** *14* (11), 3126-3131.
59. Matsui, Y.; Ishikawa, J.; Kamitakahara, H.; Takano, T.; Nakatsubo, F., Facile synthesis of 6-amino-6-deoxycellulose. *Carbohydrate Research* **2005,** *340* (7), 1403-1406.
60. Usov, A. I.; Krylova, R. G.; Suleimanova, F. R., Preparation of 6-bromo-6-deoxycellulose and 6-deoxycellulose. *Russian Chemical Bulletin* **1975,** *24* (9), 2009-2011.
61. Furuhata, K.-i.; Arai, N.; Ishizuka, S.; Tseng, H.; Sakamoto, M., Synthesis and reduction of azidodeoxy derivatives of chitin. *Sen'i Gakkaishi* **1998,** *54*, 647-653.
62. Fox, S. C.; Edgar, K. J., Staudinger Reduction Chemistry of Cellulose: Synthesis of Selectively O-Acylated 6-Amino-6-deoxy-cellulose. *Biomacromolecules* **2012,** *13* (4), 992-1001.
63. Cimecioglu, A. L.; Ball, D. H.; Kaplan, D. L.; Huang, S. H., Preparation of Amylose Derivatives Selectively Modified at C-6 - 6-Amino-6-Deoxyamylose. *Macromolecules* **1994,** *27* (11), 2917-2922.
64. (a) Santhosh, S.; Sini, T. K.; Anandan, R.; Mathew, P. T., Effect of chitosan supplementation on antitubercular drugs-induced hepatotoxicity in rats. *Toxicology* **2006,** *219* (1–3), 53-59; (b) Santhosh, S.; Sini, T. K.; Anandan, R.; Mathew, P. T., Hepatoprotective activity of

chitosan against isoniazid and rifampicin-induced toxicity in experimental rats. *European Journal of Pharmacology* **2007,** *572* (1), 69-73.
65. (a) Lim, C. K.; Halim, A. S.; Zainol, I.; Noorsal, K., In vitro evaluation of a biomedical-grade bilayer chitosan porous skin regenerating template as a potential dermal scaffold in skin tissue engineering. *International Journal of Polymer Science* **2011,** *2011*; (b) Pillai, C. K. S.; Sharma, C. P., Review paper: absorbable polymeric surgical sutures: chemistry, production, properties, biodegradability, and performance. *Journal of biomaterials applications* **2010,** *25* (4), 291-366.
66. (a) Jiang, X.; Xin, H.; Gu, J.; Du, F.; Feng, C.; Xie, Y.; Fang, X., Enhanced Antitumor Efficacy by d-Glucosamine-Functionalized and Paclitaxel-Loaded Poly (Ethylene Glycol)-Co-Poly (Trimethylene Carbonate) Polymer Nanoparticles. *Journal of pharmaceutical sciences* **2014,** *103* (5), 1487-1496; (b) Chesnokov, V.; Gong, B.; Sun, C.; Itakura, K., Anti-cancer activity of glucosamine through inhibition of N-linked glycosylation. *Cancer cell international* **2014,** *14* (1), 45.
67. Kumar, M. N. V. R., A review of chitin and chitosan applications. *Reactive and Functional Polymers* **2000,** *46*, 1-27.
68. (a) Krishna, C.; Pillai, S.; Sharma, C. P., Review Paper: Absorbable Polymeric Surgical Sutures: Chemistry, Production, Properties, Biodegradability, and Performance. *Journal of Biomaterials*
Applications **2010,** *25*, 291-366; (b) Dutta, P. K.; Dutta, J.; Tripathi, V. S., Chitin and chitosan: Chemistry, properties and applications. *Journal of Scientific & Industrial Research* **2004,** *63*, 20-31.
69. Thanou, M.; Verhoef, J. C.; Junginger, H. E., Chitosan and its derivatives as intestinal absorption enhancers. *Advanced Drug Delivery Reviews* **2001,** *50, Supplement 1* (0), S91-S101.
70. Lai, W.-F.; Lin, M. C.-M., Nucleic acid delivery with chitosan and its derivatives. *Journal of Controlled Release* **2009,** *134* (3), 158-168.
71. (a) Thanou, M.; Junginger, H. E., *Pharmaceutical Applications of Chitosan and Derivatives.* Marcel Dekker: New York, 2005; (b) Dash, M.; Chiellini, F.; Ottenbrite, R. M.; Chiellini, E., Chitosan: A versatile semi-synthetic polymer in biomedical applications. *Progress in Polymer Science* **2011,** *36* (8), 981-1014.
72. Thanou, M.; Verhoef, J. C.; Junginger, H. E., Oral drug absorption enhancement by chitosan and its derivatives. *Advanced Drug Delivery Reviews* **2001,** *52* (2), 117-126.
73. Illum, L.; Farraj, N. F.; Davis, S. S., Chitosan as a novel nasal delivery system for peptide drugs. *Pharm. Res.* **1994,** *11*, 1186–1189.
74. Artursson, P.; Lindmark, T.; Davis, S. S.; Illum, L., Effect of chitosan on the permeability of monolayers of intestinal epithelial cells (Caco-2). *Pharm. Res.* **1994,** *11*, 1358–1361.
75. Bowman, K.; Leong, K. W., Chitosan nanoparticles for oral drug and gene delivery. *Int J Nanomedicine* **2006,** *1* (1176-9114 (Print)), 117-128.
76. (a) Azzam, T.; Raskin, A.; Makovitzki, A.; Brem, H.; Vierling, P.; Lineal, M.; Domb, A. J., Cationic Polysaccharides for Gene Delivery. *Macromolecules* **2002,** *35* (27), 9947-9953; (b) Nagasaki, T.; Hojo, M.; Uno, A.; Satoh, T.; Koumoto, K.; Mizu, M.; Sakurai, K.; Shinkai, S., Long-Term Expression with a Cationic Polymer Derived from a Natural Polysaccharide: Schizophyllan†. *Bioconjugate Chemistry* **2004,** *15* (2), 249-259; (c) Kamiński, K.; Płonka, M.; Ciejka, J.; Szczubiałka, K.; Nowakowska, M.; Lorkowska, B.; Korbut, R.; Lach, R., Cationic Derivatives of Dextran and Hydroxypropylcellulose as Novel Potential Heparin Antagonists. *Journal of Medicinal Chemistry* **2011,** *54* (19), 6586-6596.

77. Kotze, A. F.; Lueßen, H. L.; de Leeuw, B. J.; de Boer, A. G.; Verhoef, J. C.; Junginger, H. E., N-trimethyl chitosan chloride as a potential absorption enhancer across mucosal surfaces: in vitro evaluation in intestinal epithelial cells (Caco-2). *Pharm. Res.* **1997,** *14*, 1197-1202.
78. (a) Prashanth, K. V. H.; Tharanathan, R. N., Chitin/chitosan: modifications and their unlimited application potential - an overview. *Trends in Food Science & Technology* **2007,** *18* (3), 117-131; (b) Bansal, V.; Sharma, P. K.; Sharma, N.; Pal, O. P.; Malviya, R., Applications of Chitosan and Chitosan Derivatives in Drug Delivery. *Advances in Biological Research* **2011,** *5* (1), 28-37.
79. Bernkop-Schnürch, A.; Kast, C. E., Chemically modified chitosans as enzyme inhibitors. *Advanced Drug Delivery Reviews* **2001,** *52* (2), 127-137.
80. (a) Lorenzo-Lamosa, M. L.; Remuñán-López, C.; Vila-Jato, J. L.; Alonso, M. J., Design of microencapsulated chitosan microspheres for colonic drug delivery. *Journal of Controlled Release* **1998,** *52* (1–2), 109-118; (b) Hejazi, R.; Amiji, M., Chitosan-based gastrointestinal delivery systems. *Journal of Controlled Release* **2003,** *89* (2), 151-165.
81. Park, J. H.; Saravanakumar, G.; Kim, K.; Kwon, I. C., Targeted delivery of low molecular drugs using chitosan and its derivatives. *Advanced Drug Delivery Reviews* **2010,** *62* (1), 28-41.
82. (a) Sonia, T. A.; Sharma, C. P., An overview of natural polymers for oral insulin delivery. *Drug Discovery Today* **2012,** *17* (13-14), 784-792; (b) Sonia, T. A.; Sharma, C. P., Chitosan and Its Derivatives for Drug Delivery Perspective. *Adv. Polym Sci.* **2011,** *243*, 23-54.
83. Khardin, A. P.; Tuzhikov, O. I.; Lemasov, A. I., New phosphorus containing cellulose derivatives. *Polymer Science U.S.S.R.* **1982,** *24* (9), 2115-2120.
84. Wang, L.; Xu, X.; Guo, S.; Peng, Z.; Tang, T., Novel water soluble phosphonium chitosan derivatives: Synthesis, characterization and cytotoxicity studies. *International Journal of Biological Macromolecules* **2011,** *48* (2), 375-380.
85. Kenawy, E.-R.; Abdel-Hay, F. I.; El-Shanshoury, A. E.-R. R.; El-Newehy, M. H., Biologically active polymers: synthesis and antimicrobial activity of modified glycidyl methacrylate polymers having a quaternary ammonium and phosphonium groups. *Journal of Controlled Release* **1998,** *50* (1–3), 145-152.
86. Drugs, C. o., Alternative Routes of Drug Administration—Advantages and Disadvantages (Subject Review). *Pediatrics* **1997,** *100* (1), 143-152.
87. Wu, C. Y.; Benet, L. Z., Predicting drug disposition via application of BCS: Transport/absorption/elimination interplay and development of a biopharmaceutics drug disposition classification system. *Pharmaceutical Research* **2005,** *22* (1), 11-23.
88. Jones, D. S., *Pharmaceutical Applications of Polymers for Drug Delivery*. iSmithers Rapra Publishing: 2004; Vol. 15, p 124.
89. (a) Lipinski, C. A.; Lombardo, F.; Dominy, B. W.; Feeney, P. J., Experimental and computational approaches to estimate solubility and permeability in drug discovery and development settings. *Advanced Drug Delivery Reviews* **1997,** *23* (1–3), 3-25; (b) Behra, A.; Giri, T. K.; Tripathi, D. K.; Ajazuddin; Alexander, A., An Exhaustive Review on Recent Advancement in Pharmaceutical Bioadhesive Used for Systemic Drug Delivery Through Oral Mucosa for Achieving Maximum Pharmacological Response and Effect. *International Journal of Pharmacology* **2012,** *8* (5), 283-305; (c) Edgar, K. J., Cellulose esters in drug delivery. *Cellulose* **2007,** *14* (1), 49-64.
90. Amidon, G. L.; Lennernas, H.; Shah, V. P.; Crison, J. R., A Theoretical Basis for a Biopharmaceutic Drug Classification - the Correlation of in-Vitro Drug Product Dissolution and in-Vivo Bioavailability. *Pharmaceutical Research* **1995,** *12* (3), 413-420.

91. (a) Malm, C. J.; Emerson, J.; Hiatt, G. D., Cellulose acetate phthalate as an enteric coating material. *J Am Pharm Assoc Am Pharm Assoc* **1951,** *40* (10), 520-5; (b) Doelker, E., Cellulose Derivatives. *Advances in Polymer Science* **1993,** *107*, 199-265; (c) Kamel, S.; Ali, N.; Jahangir, K.; Shah, S. M.; El-Gendy, A. A., Pharmaceutical significance of cellulose: A review. *Express Polymer Letters* **2008,** *2* (11), 758-778.
92. Shelton, M. C.; Posey-Dowty, J. D.; Lingerfelt, L.; Kirk, S. K.; Klein, S.; Edgar, K. J., Enhanced dissolution of poorly soluble drugs from solid dispersions in carboxymethylcellulose acetate butyrate matrices. In *Polysaccharide Materials: Performance by Design*, American Chemical Society: 2009; Vol. 1017, pp 93-113.
93. Duarte, A. C.; Gordillo, M. D.; Cardoso, M. M.; Simplicio, A. L.; Duarte, C., M. M., Preparation of ethyl cellulose/methyl cellulose blends by supercritical antisolvent precipitation. *International Journal of Pharmaceutics* **2006,** *311*, 50-54.
94. Liu, H.; Ilevbare, G. A.; Cherniawski, B. P.; Ritchie, E. T.; Taylor, L. S.; Edgar, K. J., Synthesis and structure–property evaluation of cellulose ω-carboxyesters for amorphous solid dispersions. *Carbohydrate Polymers* **2014,** *100* (0), 116-125.
95. Raquez, J.-M.; Narayan, R.; Dubois, P., Recent Advances in Reactive Extrusion Processing of Biodegradable Polymer-Based Compositions. *Macromolecular Materials and Engineering* **2008,** *293* (6), 447-470.
96. Yu, L.; Dean, K.; Li, L., Polymer blends and composites from renewable resources. *Progress in Polymer Science* **2006,** *31* (6), 576-602.
97. (a) Edgar, K. J.; Buchanan, C. M.; Debenham, J. S.; Rundquist, P. A.; Seiler, B. D.; Shelton, M. C.; Tindall, D., Advances in cellulose ester performance and application. *Progress in Polymer Science* **2001,** *26* (9), 1605-1688; (b) Posey-Dowty, J.; Watterson, T.; Wilson, A.; Edgar, K.; Shelton, M.; Lingerfelt, L., Zero- order release formulations using a novel cellulose ester. *Cellulose* **2007,** *14* (1), 73-83; (c) Tanno, F.; Nishiyama, Y.; Kokubo, H.; Obara, S., Evaluation of hypromellose acetate succinate (HPMCAS) as a carrier in solid dispersions. *Drug Development and Industrial Pharmacy* **2004,** *30* (1), 9-17; (d) Alonzo, D. E.; Gao, Y.; Zhou, D. L.; Mo, H. P.; Zhang, G. G. Z.; Taylor, L. S., Dissolution and Precipitation Behavior of Amorphous Solid Dispersions. *Journal of Pharmaceutical Sciences* **2011,** *100* (8), 3316-3331.
98. (a) Ilevbare, G.; Liu, H.; Edgar, K. J.; Taylor, L., Inhibition of Solution Crystal Growth of Ritonavir by Cellulose Polymers–Factors Influencing Polymer Effectiveness. *CrystEngComm* **2012,** *14* (20), 6503-6514; (b) Ilevbare, G. A.; Liu, H. Y.; Edgar, K. J.; Taylor, L. S., Understanding Polymer Properties Important for Crystal Growth Inhibition-Impact of Chemically Diverse Polymers on Solution Crystal Growth of Ritonavir. *Cryst Growth Des* **2012,** *12* (6), 3133-3143; (c) Sharma, A.; Jain, C., Solid dispersion: A promising technique to enhance solubility of poorly water soluble drug. *International Journal of Drug Delivery* **2011,** *3* (2), 149-170.
99. Konno, H.; Handa, T.; Alonzo, D. E.; Taylor, L. S., Effect of polymer type on the dissolution profile of amorphous solid dispersions containing felodipine. *European Journal of Pharmaceutics and Biopharmaceutics* **2008,** *70* (2), 493-499.
100. Hsieh, Y. L.; Ilevbare, G. A.; Van Eerdenbrugh, B.; Box, K. J.; Sanchez-Felix, M. V.; Taylor, L. S., pH-Induced Precipitation Behavior of Weakly Basic Compounds: Determination of Extent and Duration of Supersaturation Using Potentiometric Titration and Correlation to Solid State Properties. *Pharmaceutical Research* **2012**, 1-16.
101. (a) Liu, H. Y.; Kar, N.; Edgar, K. J., Direct synthesis of cellulose adipate derivatives using adipic anhydride. *Cellulose* **2012,** *19* (4), 1279-1293; (b) Wegiel, L. A.; Mauer, L. J.; Edgar, K. J.;

Taylor, L. S., Crystallization of amorphous solid dispersions of resveratrol during preparation and storage-Impact of different polymers. *J Pharm Sci* **2012**.
102. Li, B.; Konecke, S.; Harich, K.; Wegiel, L.; Taylor, L. S.; Edgar, K. J., Solid Dispersion of Quercetin in Cellulose Derivative Matrices Influences both Solubility and Stability. *Carbohydrate Polymers* **2013,** *92* (2), 2033-2040.
103. (a) Igura, K.; Ohta, T.; Kuroda, Y.; Kaji, K., Resveratrol and quercetin inhibit angiogenesis in vitro. *Cancer letters* **2001,** *171* (1), 11-16; (b) Bureau, G.; Longpré, F.; Martinoli, M. G., Resveratrol and quercetin, two natural polyphenols, reduce apoptotic neuronal cell death induced by neuroinflammation. *Journal of neuroscience research* **2008,** *86* (2), 403-410.
104. Ilevbare, G. A.; Liu, H.; Edgar, K. J.; Taylor, L. S., Effect of Binary Additive Combinations on Solution Crystal Growth of the Poorly Water-Soluble Drug, Ritonavir. *Cryst Growth Des* **2012,** *12* (12), 6050-6060.
105. Ilevbare, G. A.; Liu, H.; Edgar, K. J.; Taylor, L. S., Impact of Polymers on Crystal Growth Rate of Structurally Diverse Compounds from Aqueous Solution. *Molecular pharmaceutics* **2013,** *10* (6), 2381-2393.
106. Marks, J. A.; Wegiel, L. A.; Taylor, L. S.; Edgar, K. J., Pairwise Polymer Blends for Oral Drug Delivery. *Journal of pharmaceutical sciences* **2014,** *103* (9), 2871-2883.
107. Moore, G. F.; Saunders, S. M., *Advances in Biodegradable Polymers*. iSmithers Rapra Publishing: 1998.
108. (a) Nishio, Y., *Hyperfine composites of cellulose with synthetic polymers.* Carl Hanser: Munich, 1994; (b) Kusumi, R.; Inoue, Y.; Shirakawa, M.; Miyashita, Y.; Nishio, Y., Cellulose alkyl ester/poly(e-caprolactone) blends: characterization of miscibility and crystallization behaviour. *Cellulose* **2008,** *15*, 1-16.
109. Warth, H.; Mulhaupt, R.; Schatzle, J., Thermoplastic cellulose acetate and cellulose acetate compounds prepared by reactive processing. *J Appl Polym Sci* **1997,** *64*, 231–42.
110. (a) Pereira, C. S.; Cunha, A. M.; Reis, R. L.; Vazquez, B.; San Roman, J., New starch-based thermoplastic hydrogels for use as bone cements or drug-delivery carriers. *J Mater Sci: Mater Med* **1998,** *12*, 825–33; (b) Espigares, I.; Elvira, C.; Mano, J. F.; Va´ zquez, B.; San Roma´ n, J.; Reis, R. L., New partially degradable and bioactive acrylic bone cements based on starch blends and ceramic fillers. *Biomaterials* **2002,** *23*, 1883–95; (c) Arvanitoyannis, I.; Biliaderis, C. G., Physical properties of polyol-plasticized edible blends made of methyl cellulose and soluble starch. *Carbohydrate Polymers* **1999,** *38*, 47–58.
111. Psomiadou, E.; Arvanitoyannis, I.; Yamamoto, N., Edible films made from natural resources; microcrystaloline cellulose (MCC), methylcellulose (MC) and corn starch and polyols—part 2. *Carbohydrate Polymers* **1996,** *31*, 193-204.
112. Xia, F.-X.; Wang, X.-L.; Song, F.; Wang, Y.-Z., A Biobased Blend of Cellulose Diacetate with Starch. *J Polym Environ* **2012,** *20*, 1103-1111.
113. Zhang, L.; Deng, X.; Huang, Z., Miscibility, thermal bahaviour and morphological structure of poly(3-hydroxybutyrate) and ethyl cellulose binary blends. *Polymer* **1997,** *38*, 5379–87.
114. Maekawa, M.; Pearce, R.; Marchessault, R. H.; Manley, R. S. J., Miscibility and tensile properties of poly(b-hydroxybutyrate)-cellulose propionate blend. *Polymer* **1999,** *40*, 1501-5.
115. Vazquez-Torres, H.; Cruuz-Ramos, C. A., Blends of Cellulosic Esters with Poly(caprolactone): Characterization by DSC, DMA, and WAXS. *Journal of Applied Polymer Science* **1994,** *54*, 1141-1159.

116. Shen, Q.; Liu, D., Cellulose/poly(ethylene glycol) blend and its controllable drug release behaviors in vitro. *Carbohydrate Polymers* **2007,** *69*, 293-298

117. Rokhade, A. P.; Patil, S. A.; Belhekar, A. A.; Halligudi, S. B.; Aminabhavi, T. M., Preparation and Evaluation of Cellulose Acetate Butyrate and Poly(ethylene oxide) Blend Microspheres for Gastroretentive Floating Delivery of Repaglinide. *Journal of Applied Polymer Science* **2007,** *105*, 2764-2771.

118. Lyu, S. P.; Sparer, R.; Hobot, C.; Dang, K., Adjusting drug diffusivity using miscible polymer blends. *Journal of Controlled Release* **2005,** *102* (3), 679-687.

Chapter 3: Pairwise Polymer Blends for Oral Drug Delivery

(Used with permission of John Wiley and Sons: Marks, J. A.; Wegiel, L. A.; Taylor, L. S.; Edgar, K. J. (2014), Pairwise Polymer Blends for Oral Drug Delivery. J. Pharm. Sci., 103 (9), 2871-2883.

3.1 Abstract:

Blending polymers with complementary properties holds promise for addressing the diverse, demanding polymer performance requirements in amorphous solid dispersions (ASDs), but we lack comprehensive property understanding for blends of important ASD polymers. Herein we prepare pairwise blends of commercially available polymers polyvinylpyrrolidone (PVP), the cationic acrylate copolymer Eudragit 100 (E100), hydroxypropylmethylcellulose acetate succinate (HPMCAS), carboxymethyl cellulose acetate butyrate (CMCAB), and hypromellose (HPMC), and the new derivative cellulose acetate adipate propionate (CAAdP). This study identifies miscible binary blends that may find use, for example, in ASDs for solubility and bioavailability enhancement of poorly water-soluble drugs. Differential scanning calorimetry (DSC), Fourier transform infrared (FTIR) spectroscopy, and film clarity were used to determine blend miscibility. Several polymer combinations including HPMCAS/PVP, HPMC/CMCAB and PVP/HPMC appear to be miscible in all proportions. In contrast, blends of E100/PVP and E100/HPMC showed a miscibility gap. Combinations of water soluble and hydrophobic polymers like these may permit effective balancing of ASD performance criteria such as release rate and polymer-drug interaction to prevent nucleation and crystal growth of poorly soluble drugs. Miscible polymer combinations described herein will enable further study of their drug delivery capabilities, and provide a potentially valuable set of ASD formulation tools.

3.2 Introduction

Polymers have been extraordinarily important to the development of drug delivery systems and effective pharmaceutical formulations. Polymer functions range from the simple, for example enabling compression of the active and inert ingredients into a tablet with the needed physical properties (e.g. microcrystalline cellulose)[1], to the more demanding, such as enabling pH-controlled release of a medication in order to minimize drug-stomach exposure, (e.g.

cellulose acetate phthalate)[1a, 2], to highly demanding roles such as enabling zero-order drug release (e.g. cellulose acetate).[3] Polysaccharide derivatives including cellulose esters[2a] are useful polymers for drug delivery; they are generally non-toxic, are not absorbed from the gastrointestinal (GI) tract, and can be readily modified to enhance properties critical for drug delivery. In recent times the demands on drug delivery polymers have become greater, including expectations such as more precise timing, greater targeting selectivity, and delivery of compounds with poor solubility and/or permeability. It is often challenging for a single polymer to meet all of the demands for delivery of a particular drug with a diverse set of therapeutic requirements.

Oral drug delivery is a focal point of research on polymeric biomaterials, since it is preferred by patients and is one of the most economical means of drug delivery. Recently there has been strong interest in amorphous solid dispersion (ASD) formulations that suppress crystallization of poorly water-soluble drugs, enhance aqueous solubility, stabilize the drug against recrystallization in both solid and solution phases, and in some cases provide controlled release[4]. These characteristics are especially relevant when delivering insoluble and poorly bioavailable drugs; poor solubility is a substantial impediment to modern drug development[5]. ASD is a promising technology for enhancing solution concentration of these drugs, and indeed is in clinical use, for example in oral formulations of the HIV drug combination, Kaletra (lopinavir and ritonavir)[6,7]. Molecular dispersion of the drug in the polymer matrix eliminates drug crystallinity and drives the formation of a supersaturated solution upon release [8]. The polymer must help stabilize the amorphous drug in the blend as well as in the supersaturated solution after release; typically this requires polymer hydrophobicity to enhance interaction with hydrophobic drugs [9]. At the same time, the formulation must release the drug at an adequate rate; water-soluble polymers like PVP and HPMC have received substantial attention for ASD formulations in part for this reason [10]. A number of studies reveal that HPMC is frequently effective at retarding drug crystal growth when combined in miscible blends with poorly soluble drugs such as felodipine and ritonavir[9a, 11]. PVP has also demonstrated significant utility when used alone or blended with cellulosics for amorphous dispersions with ritonavir, acetaminophen and others[8, 9b, 12]. Water-soluble polymers like PVP help to stabilize the drug after it has dissolved but before it has been absorbed; this is a two-edged sword, since high polymer aqueous solution concentration can also change drug thermodynamic solubility, reducing the extent of

supersaturation and thereby reducing the chemical potential gradient of the drug across the GI epithelium. PVP will also dissolve readily in the acidic milieu of the stomach, which may not be desirable for some drugs (e.g., those that degrade or may tend to recrystallize at low pH). In part for this reason, recently some investigators have focused on carboxyl-containing cellulose derivatives like CAAdP[13] and HPMCAS[14] that are poorly soluble in acidic media but swell or dissolve at neutral pH [15]. Specific interactions between polymer carboxyl groups and drug functional groups (e.g. hydrogen bonding (H-bonding) with amines or amides) can also help to stabilize the drug against crystallization. The high glass transition temperatures (T_gs) of these cellulose derivatives are also useful for ASDs, since they prevent drug mobility and crystallization even when humidity and ambient temperature are high. On the other hand, some of these polymers (e.g. CAAdP or CMCAB) are quite hydrophobic, and so may not release the drug at an adequate rate, or may not dissolve sufficiently at pH 6.8 to stabilize the drug after release. Studies in our labs of the drug clarithromycin, which is subject to acid catalyzed degradation, have shown enhanced chemical stability of the drug in ASDs containing CAAdP. They also demonstrate the difficulty in providing enhanced bioavailability of a target drug using just a single polymer system with hydrophobicity/hydrophilicity, polymer/drug interactions and polymer aqueous solubility playing key roles in manipulating the *in vitro* behavior of the drug-containing ASDs[16].

Researchers have designed new cellulose derivatives in the hopes of achieving a balance in the properties needed for an effective single polymer ASD system[23]. However, criteria like hydrophilicity for enhanced drug release vs. hydrophobicity for enhanced polymer-drug interactions may conflict with one another, challenging the polymer designer. Therefore polymer blending may be an attractive alternative for dealing with deficiencies of existing or novel drug delivery polymers, including those for ASD. Miscible blends of polymer and drug are of great interest, since reduction in the drug domain size to molecular scale decreases the likelihood that the drug will recrystallize from the formulation and revert to its more stable crystalline form[7]. A greater likelihood of producing stable homogenous amorphous systems results from strong H-bonding, dipole-dipole interactions, hydrophobic, acid-base ionic interactions or a combination of interactions between the components[12a, 17]. We hypothesize that by identifying miscible combinations of somewhat hydrophobic polymers with somewhat hydrophilic polymers, the resulting pairwise blends may better address these complex, at times

conflicting requirements for an effective ASD system. The hypothesis is supported by findings that demonstrate more effective crystal growth inhibition by hydrophobic/hydrophilic polymer combinations[12a, 13a]. Polymer blends may in some cases provide synergistic benefits, giving properties that are not just the weighted average of those of component polymers, but that go beyond those of individual components; for example by enhancing solution concentration of poorly soluble drugs beyond that available from dispersion in either individual polymer[18]. It must also be noted that such miscible blends may find use in drug delivery systems other than for those for ASD, and may be useful as well for a much wider variety of applications, for example in coatings or in agricultural films.

There have been relatively few reports of the use of polymer blends in oral drug delivery. Researchers at Eastman Chemical investigated cellulose ester blends with PVP and with poly (2-ethyl-2-oxazoline) (PEOx). They illustrated that by incorporating just 20 % of PVP or PEOx into miscible blends with cellulose diacetate (casting clear films with dextromethorphan incorporated in the blend), effective dextromethorphan release could be achieved in contrast to the impractically slow release rate from films of pure cellulose diacetate[2a]. In 2005, Lyu et al. demonstrated the ability to tune release behavior by blending polyvinyl acetate (PVA) and cellulose acetate butyrate (CAB). While the release of dexamethasone from PVA alone was very fast and from CAB extremely slow, a predictable reduction in the release rate of the drug was achieved by adding increasing proportions of CAB to the PVA/drug mixture[19]. Researchers in Belgium have also demonstrated dissolution enhancement of the antifungal agent itraconazole and the anti-HIV drug UC 781 through various binary combinations of HPMC, polyvinyl pyrrolidone/vinyl acetate copolymer (PVP VA), polyethylene glycol (PEG), E100 and others[20]. Recent studies in our laboratories have highlighted the effectiveness of polymer blends comprised of novel cellulosic polymers including suberate, adipate and sebacate esters of cellulose acetate propionate with commercial cellulose-based and synthetic polymers. Blending two moderately hydrophobic cellulosic polymers, or combining a hydrophobic cellulosic polymer with a more hydrophilic synthetic polymer, afforded synergistic crystal growth inhibition of the poorly soluble CYP-3A4 inhibitor ritonavir[12a, 21].

Several methods exist for determining polymer blend miscibility. To achieve miscibility upon mixing pairs of polymers, a free energy of mixing lower than zero is needed. Based on the thermodynamics of mixing in binary polymer blends, there is predicted to be only a small

combinatorial entropy contribution if only weak intermolecular forces exist between the pair. This may not be enough to ensure blend miscibility; however, miscibility is greatly improved when the paired polymers possess specific interactions including hydrogen bonding that contribute to a favorable free energy of mixing[22]. Several methods are available for assessing blend miscibility, which can be challenging to assess in some cases. Cast films of blends indicate, if they are clear, that there is no phase separation of the components on the micron scale[23], providing initial evidence of miscibility. This evidence can then be used to rule out blends that exhibit very obvious phase separation before carrying out additional analyses. DSC is one of the most widely used methods for investigating blend properties [24], and is useful for determining miscibility of polymers with other polymers and/or with drugs [25]. Phase separation in DSC can typically be detected for domain sizes greater than 20-30 nm[6b]. DSC detects the change in heat capacity of the material and the resultant endothermic baseline shift that typically occurs as the system passes from the glassy to the rubbery state during heating; the glass transition. For blends that are completely mixed at the microscopic level a single glass transition is observed, and is characteristic of a miscible blend. In contrast, immiscible blends will generally show two T_gs, or a single T_g similar to that of one blend component. In cases where the T_gs of the individual components are broad and/or are close to each other (T_g difference $\leq 20°C$), alternative methods such as modulated DSC (MDSC) [26] or solid state nuclear magnetic resonance (ssNMR)[27] may be necessary to resolve or validate transitions seen using conventional DSC.

FTIR spectroscopy is a vital tool for analyzing such polymer blend systems as it is sensitive to any changes in the H-bond network within the polymers and where applicable to the deprotonation status of polymers containing acidic functional groups[24a]. This method detects changes in the vibrational frequencies of specific functional groups within the blended polymers or drug and polymer due to H-bonding or other molecular interactions. These interactions result in significant changes in peak shapes and intensities resulting in peak broadening and in some cases frequency shifts of peaks characteristic of functional groups (e.g. amides, amines, alcohols, carboxylic acids) that can participate in intra- or intermolecular H-bonding.

This study examines changes in T_g through conventional and modulated DSC methods as well as alterations in vibrational frequencies of specific functional groups through FTIR upon blending pairs of polymers, including cellulose and synthetic derivatives, containing a variety of

carboxylic acid, amide, amine, ester and alcohol moieties. Given the promising examples in which binary blends have been shown to enhance the dissolution and stabilization of various drug entities, systematic exploration of ASD polymer miscibility may provide a valuable tool for solving various drug delivery problems. Through investigation of the extent of interactions between polymer pairs, we intend to highlight pairwise blends that will be useful in a variety of drug delivery systems.

3.3 Experimental

3.3.1 Materials

Poly(butyl methacrylate-co-(2- dimethylaminoethyl) methacrylate-co-methyl methacrylate) (Eudragit® E100) was obtained from Degussa, Rohm GmbH and Co., Germany. Poly(vinyl pyrrolidone) (K29/32) and hydroxypropyl methylcellulose (HPMC 2910) were obtained from Sigma-Aldrich. Hydroxypropyl methylcellulose acetate succinate (HPMCAS AS-LG) was from Shin-Etsu Chemical Co., Ltd., Tokyo, Japan. Carboxymethyl cellulose acetate butyrate (CMCAB) was from Eastman Chemical Company. CAAdP was synthesized in our laboratories by the method described by Kar et al.[28]. Methanol, ethanol, dichloromethane, N-methylpyrrolidone (NMP), acetone and tetrahydrofuran (THF) were purchased from Fisher Scientific. All solvents were used as received.

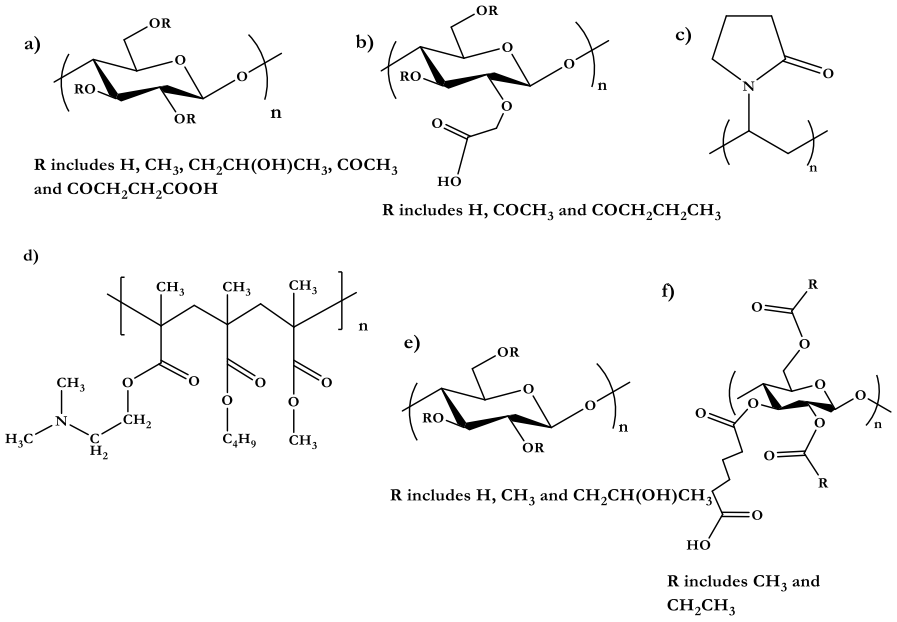

Figure 3.1: Chemical structures of a) HPMCAS b) CMCAB c) PVP d) Eudragit® E100 e) HPMC and f) CAAdP

3.3.2 Methods

3.3.3 Spray-Drying

Powder blend samples were prepared on a Buchi Mini spray dryer B-290. Each polymer pair (1-2 g) was mixed in the ratios 1:2, 1:1 and 2:1 (w:w) and subsequently dissolved in 100 mL solvent (**Table 3.1**). Spray dryer settings of pump at 40%, aspirator at 100% and inlet temperatures of 90 or 214 °C (for NMP samples) were used to produce microparticles of the blended polymers. The temperature was set at least 10 °C above the boiling point of the solvent. Blends containing CAAdP were made by coprecipitation and solvent evaporation methods due to limited polymer supply.

Table 3.1 Solvents for Spray Dried Blends and 50 % CAAdP samples

Polymer A	Polymer B	Solvent
CMCAB	HPMCAS	EtOH/CH_2Cl_2
CMCAB	E100	NMP
CMCAB	PVP	EtOH/CH_2Cl_2
CMCAB	HPMC	MeOH/CH_2Cl_2
CMCAB	CAAdP	Acetone (precipitated in water)
HPMCAS	E100	THF
HPMCAS	PVP	EtOH/CH_2Cl_2
HPMCAS	HPMC	MeOH/CH_2Cl_2
HPMCAS	CAAdP	THF (precipitated in water)
E100	PVP	EtOH/CH_2Cl_2
E100	HPMC	MeOH/CH_2Cl_2
E100	CAAdP	THF (precipitated in water)
PVP	HPMC	MeOH/CH_2Cl_2
PVP	CAAdP	MeOH
HPMC	CAAdP	Acetone/water 90/10 (v/v)

***All mixed solvents were 50/50 (v/v) unless otherwise specified**

3.3.4 Film Casting

A sample (100 mg) of each polymer blend was dissolved in 1-2 mL of the specified solvent mixture in **Table 3.1** (except for E100/HPMCAS blends that were dissolved in DMAc) and cast onto a Teflon-coated glass plate. Films were removed within 10-15 min and dried under vacuum at 50°C for at least 10 h. The dried films were examined for clarity and stored in clear, sterile pouches. For blends containing CAAdP, due to limited polymer availability, 50/50 w/w solutions were made using ~40 mg of polymer in 1-2 mL of solvent and treated as described above.

3.3.5 Differential Scanning Calorimetry (DSC)

Heating curves of 4-10 mg spray-dried powder samples in TA Instruments Tzero aluminum pans were obtained on a TA Instruments Q2000 DSC (New Castle, DE). Samples were first equilibrated at -85 °C for 5 min followed by heating at 20 °C/min to 180 or 200 °C for blends containing higher T_g polymers. Samples were cooled at 20 °C/min to -85°C, then reheated at the same rate. Second heating scan thermograms were evaluated to obtain blend T_g(s). Blends containing HPMC were submitted to temperature modulated DSC (MDSC) with a heating rate of 5 °C/min from -35 °C to 200 or 210 °C and a modulation amplitude of +/- 0.5 °C for 40 s. For these samples reversing heat flow thermograms were evaluated. Blends containing polymers with T_g values differing by < 20 °C were subjected to aging studies to determine whether single or multiple T_gs were present. These samples were heated at 20 °C/min from room temperature (RT) to 205 °C and then quench cooled at 100 °C/min to RT. The samples were then reheated at 20 °C/min from RT to 205 °C after 4, 7, 10, 14 and 21 days. These heating scans were compared to evaluate the thermal properties of these blends. Samples were stored in a desiccator at RT throughout the study.

3.3.6 Fourier Transform Infrared Spectroscopy

Infrared spectra were obtained on spray dried samples in absorbance mode using a Bio-Rad FTS 6000 spectrophotometer equipped with a globar infrared source, KBr beam splitter, and DTGS (d-triglycine sulfate) detector. Spectra of the powdered samples were obtained using a Golden Gate MII attenuated total reflectance (ATR) sampling accessory with a diamond top plate (Specac Inc., Woodstock, GA). Scan range was set from 4000 to 500 cm^{-1} with a 4 cm^{-1}

resolution, and 128 scans were co-added. The absorbance intensity of the spectral region of interest was between 0.6-1.2.

3.3.7 Solubility parameters

Solubility parameter (SP) calculations were used to compare relative polymer hydrophobicity. Larger SP values typically indicate more hydrophilic polymers. The method proposed by Fedors[29] was used to estimate SP. The method uses group additive constants based on polymer structural formulae. The formula used to estimate the SP values is as follows:

$$\delta = \sqrt{\frac{\sum_i \Delta e_i}{\sum_i \Delta v_i}} = \sqrt{\frac{\Delta E_v}{V}} \qquad (1)$$

where the Δe_i and Δv_i are the additive atomic and group contributions for the energy of vaporization and molar volume, respectively. The symbol **δ** indicates the solubility parameter while ΔE_v and V indicate the energy of vaporization and molar volume respectively. The group contributions applicable at 25 °C can be found in reference [29]. For high molecular weight polymers that have glass transitions greater than 25 °C, a small correction factor can be used to account for the deviation in experimentally measured ΔE_v and V and the estimated values. This correction factor is applied to the V values:

$$\Delta v_i = 4n, \quad n < 3 \qquad (2)$$

$$\Delta v_i = 2n, \quad n \geq 3 \qquad (3)$$

where n is the number of main chain skeletal atoms in the smallest repeating unit of the polymer. The SPs of the polymers used for this study are summarized in Table 3.2.

Table 3.2: Properties of the polymers selected for blending: Solubility parameter (SP), glass transition temperature (T_g), weight average molecular weight (M_n) and degree of substitution (DS)

Polymer	*Tg, °C	***M_W g/mol	DS	** SP, MPa $^{1/2}$
E100	48	47,000	-	19.7
HPMCAS	120	18,000	Ac 0.47; OHP 0.25; OMe 1.87; Su 0.40 [30]	22.4[12a]
CMCAB	144	22,000	Ac 0.4; CM 0.3; Bu 1.6[15a]	23.0
HPMC	164	696,720[31]	OHP 0.23; OMe 1.91[32]	22.7[12a]
PVP	178	58,000	-	28.4[12a]
CAAdP	107	17,000 [a]	Ac 0.04; Ad 0.85; Pr 2.09[33]	21.3[12a]

* Tg measured on polymers as received

**SP values calculated by the Fedor's method[29].

*** Molecular weight values obtained from manufacturer unless otherwise indicated.

[a] Molecular weight of CAAdP calculated by size exclusion chromatography (SEC) relative to polystyrene standards[33-34].

[a]Abbreviations: Ac, acetate; Ad, adipate; Bu. Butyl; CM, carboxymethyl; OHP, hydroxypropoxy; OMe, methoxy; Pr, propionate; Su, Succinate

3.4 Results and Discussion:

Five commercially available polymers commonly utilized in drug delivery formulations were selected for the study, along with one newly synthesized cellulose ω-carboxyalkanoate (CAAdP) that has recently shown substantial promise in ASD formulations (**Figure 3.1**)[33, 35]. The synthetic polymers E100 and PVP as well as cellulose-based HPMC are excipients frequently used for ASDs, e.g. of the antiviral drug ritonavir[12a, 36]. More recently, new commercial ASDs containing HPMCAS[37] have been developed while CMCAB has also shown substantial promise in ASD and other formulations[15, 38]. E100 is a cationic copolymer of butyl methacrylate, 2-dimethylaminoethyl methacrylate, and methyl methacrylate. The synthetic polyacrylate contains only H-bonding

acceptor groups; one strong tertiary amine and medium strength ester acceptor groups (**Table 3.3**). The relatively hydrophobic E100 (SP of 19.7) is thus expected to interact best with polymers containing strong H-bond donor groups, like the cellulose derivatives HPMC, HPMCAS, CAAdP, and CMCAB. However, one might suspect that E100 and PVP would form immiscible blends since the pyrrolidone derivative contains only very strong acceptor groups as well. Differences in SP values between the cellulose esters are small, but the presence, amount, and strength of acceptor or donor groups are likely to influence miscibility of such pairs. The difference in solubility parameters between PVP and each cellulose ester is < 7 $MPa^{1/2}$ except for CAAdP with a SP difference of 7.8 $MPa^{1/2}$, suggesting that PVP may form miscible blends with the cellulose esters.

For this study we selected five amorphous polymers that have T_g values between 120 - 180 °C, except for E100 which has a T_g of 48 °C (**Table 3.2**). Higher T_g polymer matrix materials are considered more suitable for ASD formulations and a T_g window of 40 - 50 °C above ambient temperature is desirable to retain the stability of the amorphous formulation over an extended period of time, even in the presence of the drug (which may be a plasticizer) and at high humidity (water is often a plasticizer for cellulose derivatives and other polymers like PVP and PEO)[4].

Table 3.3: Characterization of the H-bond donor and acceptor groups of selected polymers*

Polymer	Group	Hydrogen bond		Donor strength	Acceptor strength (pK_{BHX})
		Donor	Acceptor		
E100	R-C(O)-O-R		Yes		Medium (ethyl acetate 1.07)
	R_3N		Yes		Strong (triethylamine 1.98)
PVP	R-C(O)-N-R_2		Yes		Very strong (1-methyl-2-pyrrolidone 2.38)
CMCAB	R-C(O)-O-H	Yes	Yes	Very strong	Medium (ethyl acetate 1.07)
	R-O-R		Yes		Medium (diethylether 1.01)
	R-O-H	Yes	Yes	Strong	Medium (ethanol 1.02)
HPMC	R-O-R		Yes		Medium (diethylether 1.01)
	R-O-H	Yes	Yes	Strong	Medium (ethanol 1.02)
HPMCAS	R-O-R		Yes		Medium (diethylether 1.01)
	R-C(O)-O-R		Yes		Medium (ethyl acetate 1.07)
	R-O-H	Yes	Yes	Strong	Medium (ethanol 1.02)
	R-C(O)-O-H	Yes	Yes	Very strong	Medium (ethyl acetate 1.07)
CAAdP	R-C(O)-O-R		Yes		Medium (ethyl acetate 1.07)
	R-C(O)-O-H	Yes	Yes	Very strong	Medium (ethyl acetate 1.07)
	R-O-H	Yes	Yes	Strong	Medium (ethanol 1.02)

*Classifications used are comparable to those used in [39] and evaluated based on values found in the database provided by reference [40].

3.4.1 Overall Film Clarity Results

Film casting, while limited by the possibility of polymer phase separation due to solvent partitioning during evaporation, provides a first indication of blend miscibility. A clear film is not conclusive evidence of a miscible blend, but can suggest miscibility and be later verified by further analyses. Of the 35 polymer combinations that were film-cast, all but four produced clear or relatively clear films. Translucent films were produced for all combinations of the synthetic polymers E100 and PVP **(Table 3.4** and **Figure 3.2)**. These two hydrophilic polymers, each containing only H-bonding acceptor groups (see chemical structures shown in **Figure 3.1**), appear to be incompatible and this is revealed in the brittle, translucent nature of the films produced. This immiscibility is also predictable given the large difference in SP values. Visual examination of cast films thus provided preliminary indications that all blends except those of PVP/E100 might be miscible.

Table 3.4: Comparison of Expected versus Observed Tg values and Film Clarity of the Blends

Polymer A	% A	Polymer B	% B	*Expected T_g, °C	Observed T_g(s), °C	Film Clarity	Miscibility
CMCAB	25	HPMCAS	75	125	123	Clear	
	50		50	131	122/139	Clear	p
	75		25	137	134	Clear	
CMCAB	25	E100	75	58	82	Clear	**m**
	50		50	72	101	Clear	
	75		25	96	128	Clear	
CMCAB	25	PVP	75	168	167	Clear	**m**
	50		50	159	159	Clear	
	75		25	151	158	Clear	
CMCAB	25	HPMC	75	158	164	Clear	**m**
	50		50	153	150	Clear	
	75		25	148	144	Clear	
HPMCAS	25	E100	75	57	60	Clear	**m**
	50		50	69	94	Clear	
	75		25	87	110	Clear	
HPMCAS	25	PVP	75	159	160	Clear	**m**
	50		50	143	149	Clear	
	75		25	131	138	Clear	
HPMCAS	25	HPMC	75	150	153	Clear	**m**
	50		50	138	143	Clear	
	75		25	129	130	Clear	
E100	25	PVP	75	106	176/48	Translucent	
	50		50	76	175/48	Translucent	**i**
	75		25	59	175/50	Translucent	
E100	25	HPMC	75	102	**	Clear	
	50		50	74	**	Rel. clear	**i**
	75		25	58	**	Rel. clear	
PVP	25	HPMC	75	167	167	Clear	
	50		50	170	171	Clear	**m**
	75		25	174	172	Clear	
CAAdP	50	CMCAB	50	123	125	Clear	**m**
CAAdP	50	HPMCAS	50	113	114	Clear	**m**
CAAdP	50	E100	50	66	87	Clear	**m**
CAAdP	50	HPMC	50	130	114	Rel. clear	**m**
CAAdP	50	PVP	50	134	132	Clear	**m**

Apparent Miscibility	**m**
Immiscible	**i**
Some compositions miscible	**p**

$$\frac{1}{Tg} = \frac{W_A}{Tg_A} + \frac{W_B}{Tg_B}$$

$$with\ W = weight\ fraction\ of\ polymer\ entity$$

*Expected Tg values are calculated using the Fox Equation[41,42]

** DSC thermograms show strong but not unequivocal evidence for a distinct T_g at or near the T_g of one or more of the polymers

Figure 3.2: Representative examples of translucent (a, 50/50 w/w E100/PVP) and clear films (b, 50/50 w/w CMCAB/PVP) shown here against a dark background.

a **b**

Results from Individual Pairwise Blends
3.4.2 HPMCAS/E100

Table 3.4 compares film clarity and DSC T_g values for polymer pairwise combinations. In the case of HPMCAS/E100 (**Figure 3.3a**), increasing proportions of the lower T_g polymer (E100) result in a weighted decrease in blend T_g by DSC. This combination also produced clear films, confirming compatibility of these two hydrophobic polymers. HPMCAS contains pendant carboxyl groups that help in tuning drug release properties, while the synthetic E100 is an effective excipient for stabilizing drug formulations[39, 43]. The favorable interactions between HPMCAS/E100 appear to be enhanced by the combined DS of 0.65 for the strong to very strong H-bond donor groups of HPMCAS and the H-bond acceptor groups of E100. These interactions are further confirmed by FTIR data that show characteristic broadening of the C=O peaks for HPMCAS/E100 blends relative to the carboxylic acid C=O at 1741 cm^{-1} for HPMCAS and the ester C=O at 1722 cm^{-1} for E100 (**Figure 3.3b**). These interactions also appear to be supplemented by ionic interactions between the cationic E100 and anionic carboxylate of HPMCAS under appropriate pH conditions (pK_a of HPMCAS ~ 5.5)[44]. The nonionized dimethylamino peaks of E100 shown at 2820 and 2770 cm^{-1} in Figure 3.3c appear to participate in ionic interactions with the carboxylic acid group of HPMCAS as evidenced by a decrease in intensity of those peaks as the percentage of HPMCAS is increased in the blend. Figure 3.3c shows evidence of almost complete absence of the E100 dimethylamino peaks at 75% HPMCAS. The small difference in solubility parameters between these polymers also predicted favorable interactions. This suggests that the carbonyl peaks for HPMCAS are reduced in the blends not only due to hydrogen bonds with E100 but also due to evolution of HPMCAS carboxylate groups in the blend.

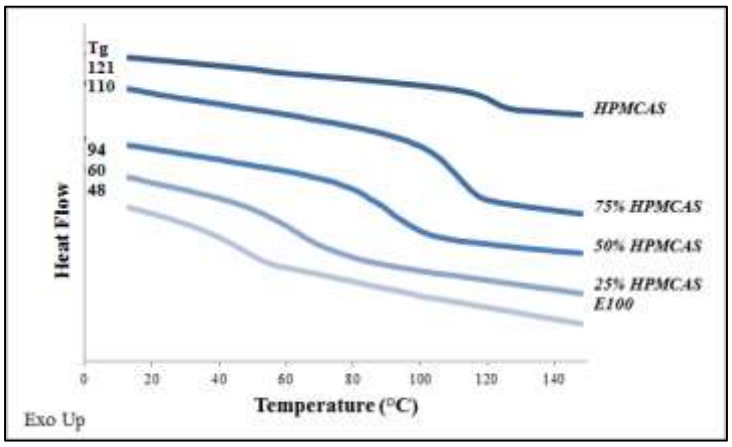

Figure 3.3a: 2nd Heat DSC Thermograms of HPMCAS/E100 blends

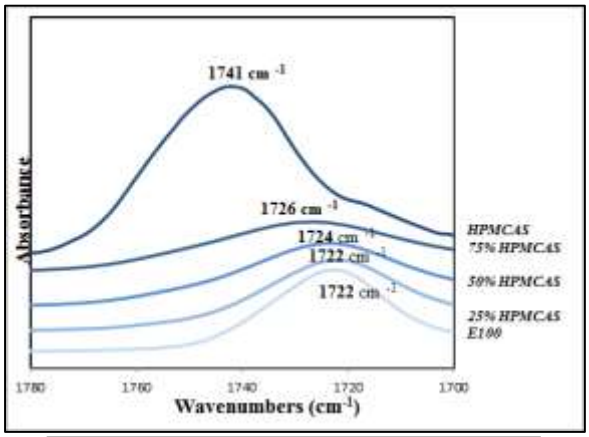

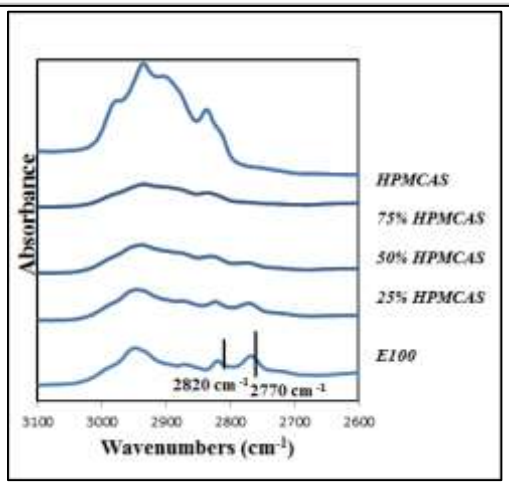

Figure 3.3b and 3.3c. FTIR spectra showing carbonyl shifts for HPMCAS/ E100 blends between 1700 and 1780 as well as 2600 and 3100

3.4.3 PVP/E100

In contrast, evaluation of the thermal properties of PVP/E100 blends that produce translucent films shows, as expected, two distinct glass-rubber transitions near those of the individual polymers (178 and 48°C for PVP and E100 respectively) (**Figure 3.4a**). This combination of an extremely hydrophilic synthetic polymer and the most hydrophobic of those examined in the study yields a blend with a difference in SP values of 8.7 $MPa^{1/2}$; significantly greater than the proposed difference of 7 $MPa^{1/2}$ or less needed to typically produce a miscible blend and support a stable dispersion[24a]. FTIR data for PVP/E100 blends show a very slight shift in the C=O amide stretch at 1659 cm^{-1} for PVP but no shift in the C=O ester stretch at 1722 cm^{-1} for E100. The shifts in PVP are more likely a result of small amounts of moisture interacting with the hygroscopic PVP, rather than from significant interactions between the blended polymers. The fact that neither polymer has strong H-bond donor groups is a likely cause of the observed immiscibility. While studies have underlined the importance of miscible blends in facilitating the most effective drug delivery systems[19, 45], more recent data also demonstrate the utility of immiscible blends for some applications. In a study released this year, Yang et al. described the stabilizing effect of using 50/50 (w/w) immiscible blends of hydrophilic PVP-VA and hydrophobic Eudragit E PO loaded with felodipine via hot melt extrusion to optimize the drug loading ability and mechanical stability of the ASD[46]. The researchers hypothesized that incorporation of the drug into the hydrophilic domains significantly improves drug loading and reduces the tendency for recrystallization. Blending with a hydrophobic polymer increases the overall hydrophobicity of the ASD, reduces the tendency to absorb moisture and promotes the long-term stability of the formulation despite high humidity, temperature and mechanical stresses.

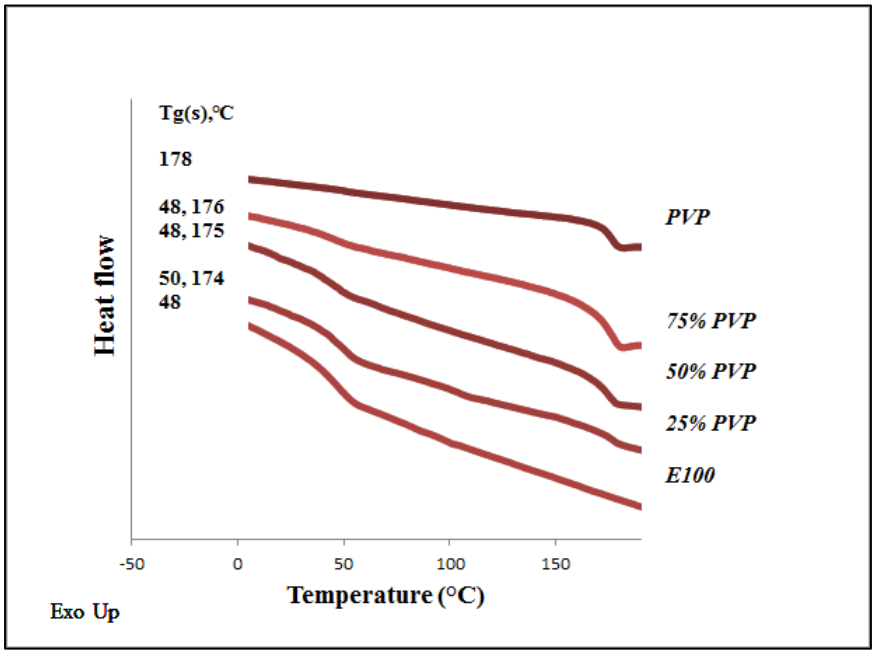

Figure 3.4a. 2nd Heat Thermograms of PVP/E100 blends

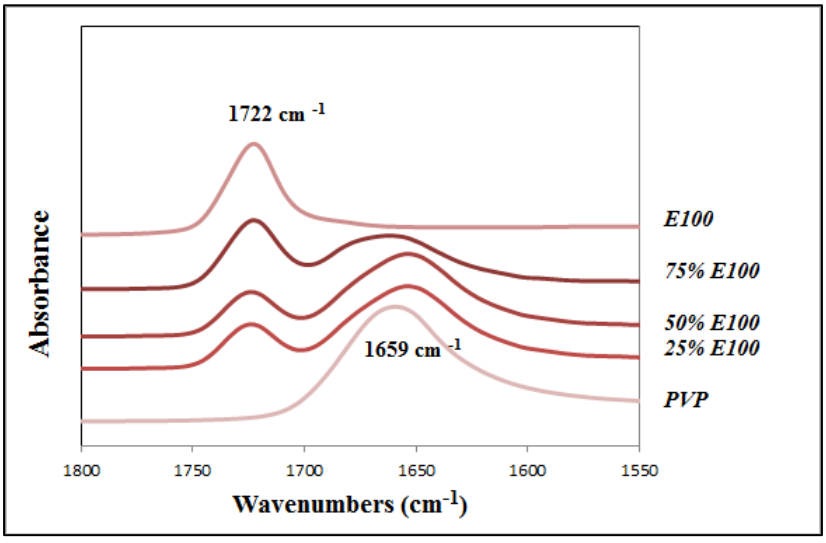

Figure 3.4b. Infrared spectra of PVP/E100 blends in the carbonyl stretch region between 1550-1800 cm^{-1}

3.4.4 HPMC-containing blends

It is very promising that combinations of the water-soluble HPMC with four of the selected polymers appear to be miscible in all combinations. Conventional DSC was not useful for evaluation of HPMC-containing blends. HPMC T_gs tend to be broad (*ca*. 160 to 200 °C) and indistinct, due to the extreme heterogeneity of the HPMC co-polymers. Not only are there four substituent types (hydrogen, methyl, n-propyl and isopropyl), but the reaction with propylene oxide during synthesis of HPMC leads to pendant poly(propylene oxide) chains of various lengths, and various compositions (depending on whether nucleophilic attack on the next propylene oxide monomer occurs at the 1- or 2-carbon of the epoxide). Modulated DSC conditions as described by McPhillips et al. [47] were most effective for thermal analysis of HPMC blends. Reversing heat flow thermograms show single T_g values for blends with HPMCAS, CMCAB and PVP. **Figures 3.5 – 3.7b** show that the measured T_g values for the binary systems varied predictably based on weight composition and were observed between the T_g values of the pure components. There was also high correlation between the predicted and observed T_g values as indicated in **Table 3.4.** These results, combined with the clarity of the associated films as well as relatively small differences in SP values indicate that HPMC blends with HPMCAS, CMCAB and PVP were miscible. These polymer combinations are promising as they highlight HPMC compatibility with a range of polymer matrix types; slightly hydrophilic HPMCAS, more hydrophobic CMCAB and the water-soluble PVP. This creates interesting opportunities for use of HPMC blends in ASD drug delivery systems; for example, blending with CMCAB to enhance release of more hydrophobic drugs, blending with HPMCAS to enhance release and solution stability, or for tuning the crystallization inhibition for highly crystalline and poorly soluble drug actives using PVP.

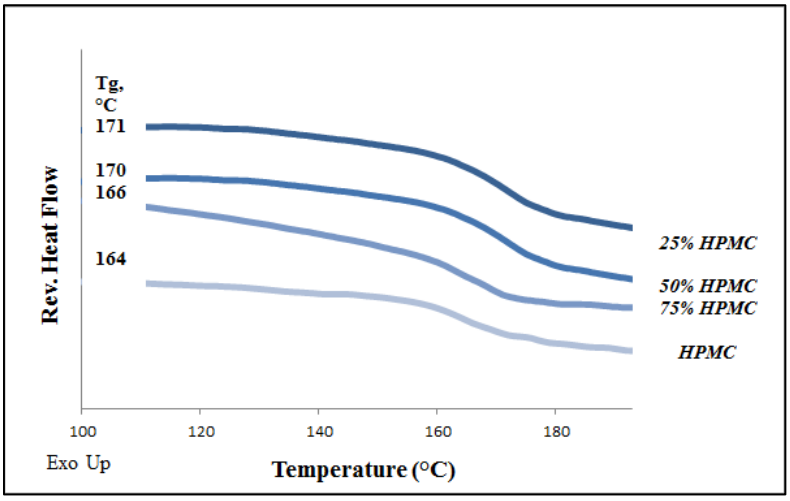

Figure 3.5: MDSC: Reversing heat scans of PVP/HPMC blends

HPMC/ HPMCAS

In addition to the clear blend films and the single T_g's observed near the predicted values, HPMC/HPMCAS blend miscibility is further supported by characteristic broadening and shifts in the C=O and OH stretch regions of the FTIR spectra. While both HPMCAS and HPMC contain relatively weak H-bond donor and acceptor functional groups, FTIR data shows significant broadening and shifting of the OH stretch peaks for HPMC (3471 cm^{-1}) and HPMCAS (3473 cm^{-1}) while C=O stretch peaks broadened and shifted slightly from 1741 cm^{-1} with decreasing HPMCAS content. At high HPMC content, the hydroxyl H-bond donor of HPMC can extensively H-bond with the C=O acceptors of the carboxyl and ester moieties of HPMCAS resulting in the most significant shift of OH stretch to 3437 cm^{-1}. The shifts in the C=O stretch for HPMCAS are much less significant (to 1734 and 1731 cm^{-1}) but still indicate that the strongest intermolecular interactions are likely between the -OH of HPMC and the C=O functionalities of HPMCAS. These favorable H-bonding interactions are likely augmented by hydrophobic interactions that contribute to blend miscibility.

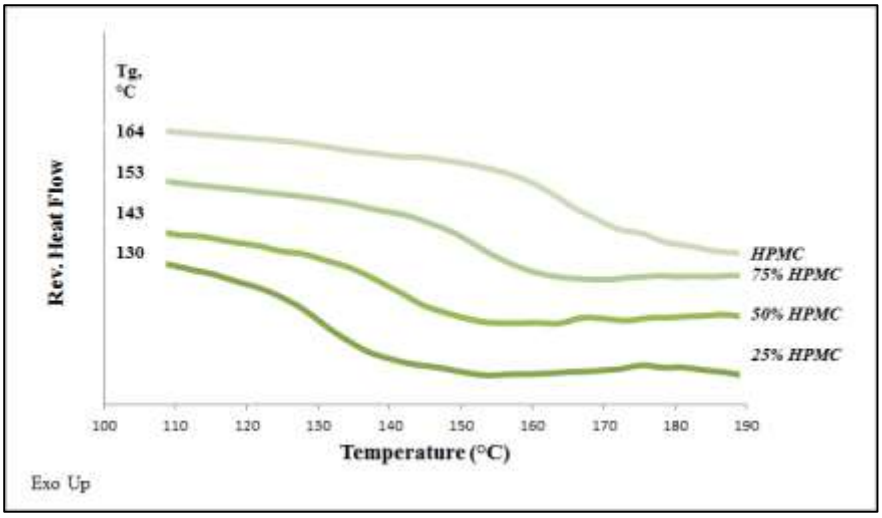

Figure 3.6a: MDSC: Reversing Heat Scans of HPMC/HPMCAS blends

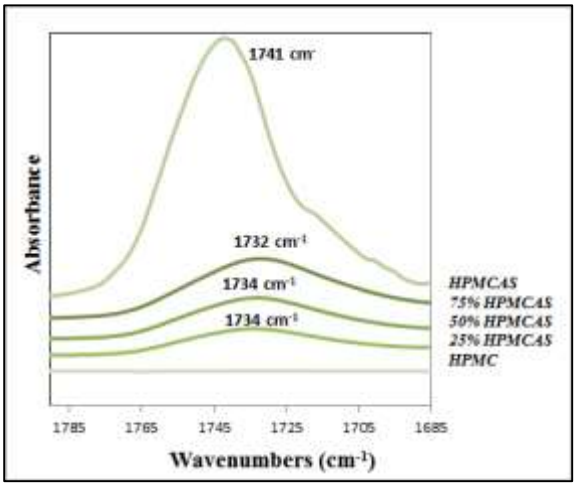

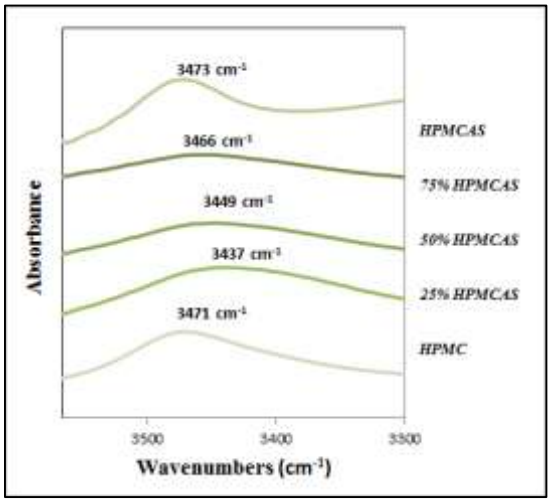

Figure 3.6b: Infrared spectra supporting miscibility of HPMCAS/HPMC blends

HPMC/CMCAB

Similar behavior is demonstrated in the HPMC/CMCAB pairings, with these blends showing increased intermolecular interactions vs. HPMC/HPMCAS. Broadened OH stretch peaks are shifted significantly to 3356 cm^{-1} from 3480 and 3471 cm^{-1} for CMCAB and HPMC respectively. The shifting of the C=O stretch for CMCAB from 1747 to 1636 cm^{-1} with increasing HPMC content indicates extensive H-bonding interactions between the C=O carboxylic acid functionality and the OH donor groups of HPMC. All miscible blends containing HPMC had high T_g values that are promising for ASD formulations. The HPMC/CMCAB blends that demonstrate strong intermolecular interactions are exemplary of a combination of moderately hydrophobic polymer (CMCAB) with a slightly more hydrophilic polymer, that may provide the hydrophobicity balance needed to solubilize the drug, and give enhanced solution and solid state stabilization, while also providing a pH-sensitive release mechanism through the pendant carboxyl groups of CMCAB.

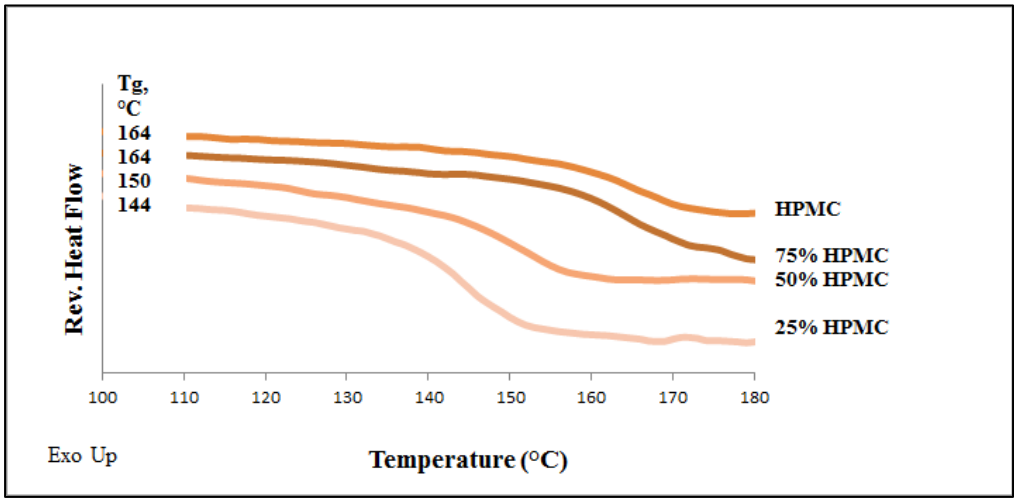

Figure 3.7a: MDSC: Reversing heat scans of HPMC/CMCAB blends

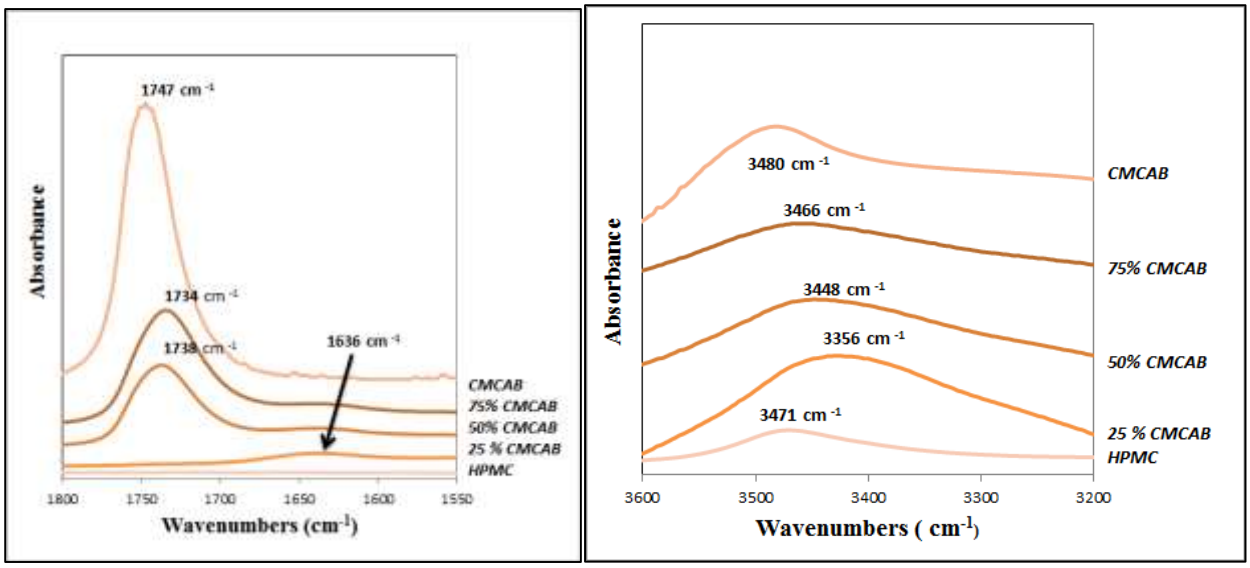

Figure 3.7b: Infrared spectra of CMCAB/HPMC demonstrating H-bonding interactions between HPMC and CMCAB

3.4.5 PVP/HPMCAS

The difference in solubility parameters between PVP and CAAdP is 7.8 $MPa^{1/2}$, higher than for PVP and the other cellulose esters examined. Each of the cellulose esters contains carboxylic acid and/or hydroxyl groups that are strong donor groups that may interact with PVP amide acceptor groups. **Figure 3.8** demonstrates that each blend of PVP/HPMCAS has a single T_g, with decreasing T_g values as % HPMCAS is increased. This combination of strong H-bond acceptor and donor groups affords favorable interactions and leads to PVP/HPMCAS blend miscibility, as also supported by the clear films obtained. The combination also produces blends with the desired high T_g values (138 – 160°C). The combination of HPMCAS, fairly hydrophobic but containing ionizable carboxyl groups, with the hydrophilic PVP, containing no groups ionizable at physiological pH, may significantly improve drug formulations by providing simultaneous pH sensitive release by the cellulose ester and significant solution and solid phase stabilization by PVP.

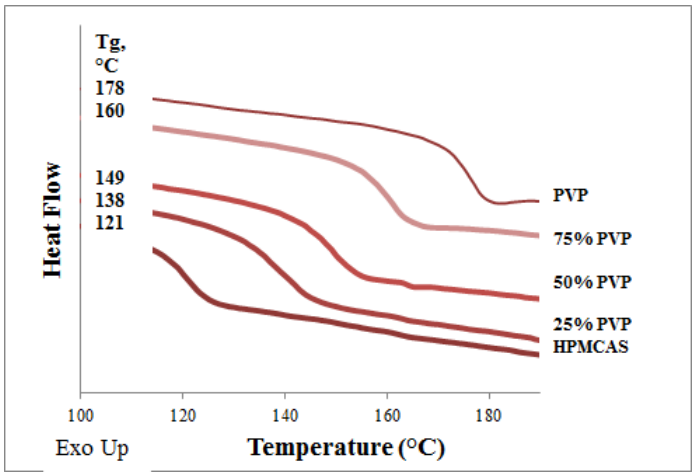

Figure 3.8: Blends of PVP with HPMCAS

3.4.6 CMCAB/HPMCAS

Blends containing two cellulose esters, having only small differences in SP values, may be significantly impacted by the presence of very strong donor groups in each. This could give rise to a predominance of intramolecular H-bonding and reduce miscibility between the pair. With CMCAB/HPMCAS blends, while the values of SP and DP (degree of polymerization) are very similar (DPs of 65 and 64), a DS of 1 for the donor groups on CMCAB and 0.65 for HPMCAS suggests that competitive intramolecular bonding is expected. Thus it was surprising that all CMCAB/HPMCAS blends gave clear films. However, miscibility of these two anionic polysaccharides is impacted significantly by the relative amount of each derivative in the blends. This is clearly demonstrated by the presence of two T_gs in 50/50 w/w blends of the pair that were aged for 21 days (**Figure S3.5a**). Combinations of HPMCAS and CMCAB appear to be only partially miscible.

3.4.7 50% CAAdP blends

Blends of the newly synthesized CAAdP were of special interest since it is an effective stabilizer of amorphous drugs, but has low aqueous solubility[33]. DSC data suggest miscibility of CAAdP with all of the polymers studied in 50:50 (w/w) combinations. DSC data in **Figure 3.9** as well as aging studies conducted on the CMCAB and HPMCAS 50% blends **(Figure S3.6)** show single T_gs and close correlation between expected and observed T_g values in four of the combinations

(with PVP, CMCAB, E100 and HPMCAS). Infrared spectra for these 50 % CAAdP formulations also support the miscibility of the blends (**Figure S3.7** and **Table S3.1**). The prediction of miscibility between CAAdP and HPMCAS appears to be confirmed, while CAAdP miscibility with PVP could be due to interactions between the amide acceptors of PVP and the strong adipate donor groups on CAAdP, despite a difference in SP values (7.8 $MPa^{1/2}$) slightly above the optimum value of 7.0 $MPa^{1/2}$. Despite the presence of strong to very strong donor groups in CMCAB and HPMCAS, their blends with CAAdP appear to be miscible. The strong H-bond donor adipate groups (DS 0.85) on CAAdP appear to interact well with the high DS of medium strength acceptor groups on CMCAB (DS Bu 1.6) and HPMCAS (DS OMe 1.87) in the 50/50 w/w blends. Likewise for E100/CAAdP, the very strong H-bond donor adipate groups (DS 0.85) appear to interact well with the acceptor groups of E100. There appears to be minimal intramolecular H–bonding for CAAdP as all the donor groups would be involved in relatively strong intermolecular H-bonding considering the much lower MW compared to E100 (**Table 3.2**). The evidence for CAAdP miscibility with these polymers in the proportions studied is positive, and will be supplemented in future studies as more CAAdP becomes available.

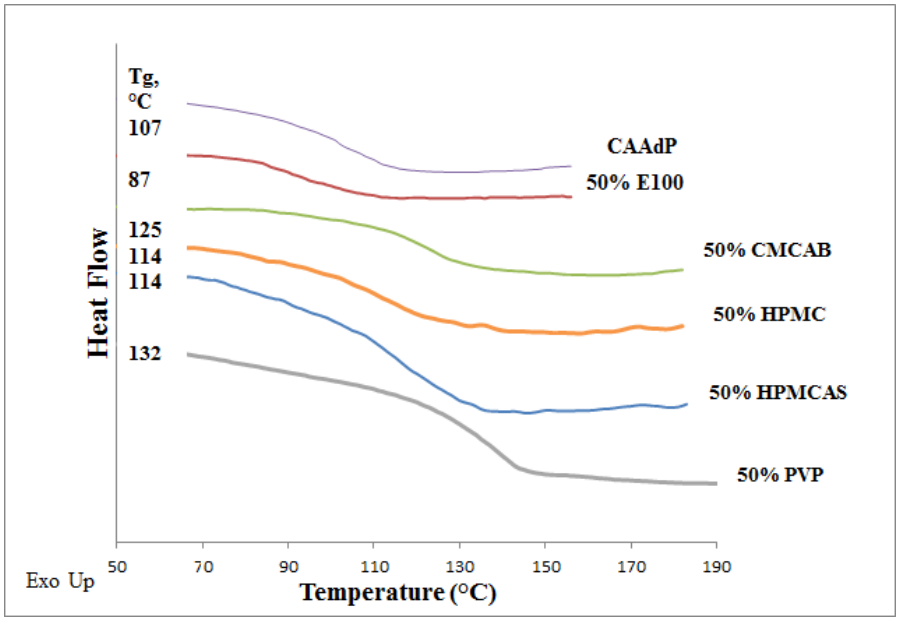

Figure 3.9: Blends containing 50% CAAdP

3.5 Conclusions

The results reveal a number of miscible combinations of cellulose-based polymers with one another as well as with synthetic polymers like PVP. Polymer functional groups play a large part in determining the extent of favorable intermolecular interactions and molecular dispersion to produce miscible blends, and these results are for the most part understandable from such fundamental considerations. Blends containing the water-soluble polymers HPMC and PVP with more hydrophobic polymers like CAAdP, CMCAB, and HPMCAS are shown herein to be miscible. This creates the potential combination of excellent stabilization of amorphous drug often displayed by polymers like CAAdP with the faster release characteristics of the more highly water-soluble polymers. It also creates the possibility of enhancing drug stability against crystallization from solution by providing higher solution concentrations of polymer (HPMC or PVP). Combinations of moderately hydrophobic polymers like CAAdP with more hydrophilic polymers like PVP or HPMC will likely be very useful for *in vitro* studies with poorly soluble, highly crystalline target drugs to achieve enhanced stabilization and release properties of those formulations.

The potential benefits may be exemplified by considering recent studies aimed at enhancing solubility and bioavailability of the natural flavonoid resveratrol, which is highly bioactive, poorly soluble and bioavailable, and shows great therapeutic potential for the prevention of heart disease[48]**.** A recent study from our labs showed promising release and solubility enhancement for resveratrol when formulated using CMCAB, HPMCAS, PVP or CAAdP as matrix polymers at loadings of up to 25 wt% resveratrol[49]. Formulations containing the hydrophobic polymers CMCAB and CAAdP provided effective stabilization against resveratrol crystallization in both solid and solution phases, but suffered from impractically slow rates of drug release. The results herein suggest that the utility of those formulations might be significantly improved by blending CMCAB and CAAdP with even small amounts of PVP or HPMC to give faster resveratrol release, as was observed using the water soluble PVP as sole matrix polymer in the cited study. ASDs containing E100 have also been shown to be effective at inhibiting the crystallization of resveratrol, so the E100 miscible blends described in this study may also have utility for tailoring resveratrol release rates and stabilization[39].

Polymer design is critical to the development of more effective ASD polymers, but its practical impact will always be less than it could be, due to the expense and duration of toxicity

evaluation for new polymers for pharmaceutical use, and of the approval process for formulations containing these new polymers. In short, we will only be able to afford to develop a limited number of new polymers for enhanced ASD. Therefore polymer blending using the data generated in this and related studies will be an essential, beneficial tool for achieving desired ASD properties and performance using a limited set of old and new polymers available for the purpose. We believe that the insights provided from the current study may help drug developers and formulators to construct blend formulations that are well suited to the complex demands of various types of oral delivery methods and the diverse types of therapeutic agents that need to be delivered. We focus in this study on developing miscible polymer blends, but recognize too that some of the immiscible blends, described here and elsewhere may also provide utility in ASD, drug delivery, and other fields[50].

3.6 References

1. (a) Klein, S., Polysaccharides in Oral Drug Delivery - Recent Applications and Future Perspectives. In *Polysaccharide Materials: Performance by Design*, American Chemical Society: 2009; Vol. 1017, pp 13-30; (b) Bolhuis, G. K.; Armstrong, N. A., Excipients for direct compaction--an update. *Pharmaceutical development and technology* **2006,** *11* (1), 111-124.
2. (a) Edgar, K. J., Cellulose esters in drug delivery. *Cellulose* **2007,** *14* (1), 49-64; (b) Liu, J.; Chan, S. Y.; Ho, P. C., Polymer-coated microparticles for the sustained release of nitrofurantoin. *Journal of Pharmacy and Pharmacology* **2002,** *54* (9), 1205-1212; (c) Levine, D. S.; Raisys, V. A.; Ainardi, V., Coating of oral beclomethasone dipropionate capsules with cellulose acetate phthalate enhances delivery of topically active antiinflammatory drug to the terminal ileum. *Gastroenterology* **1987,** *92* (4), 1037-1044.
3. (a) Makhija, S. N.; Vavia, P. R., Controlled porosity osmotic pump-based controlled release systems of pseudoephedrine: I. Cellulose acetate as a semipermeable membrane. *Journal of controlled release* **2003,** *89* (1), 5-18; (b) Schultz, P.; Kleinebudde, P., A new multiparticulate delayed release system.: Part I: Dissolution properties and release mechanism. *Journal of controlled release* **1997,** *47* (2), 181-189; (c) Sinha, V. R.; Kumria, R., Coating polymers for colon specific drug delivery: A comparative in vitro evaluation. *Acta pharmaceutica-zagreb-* **2003,** *53* (1), 41-48.
4. Timpe, C., Drug solubilization strategies: applying nanoparticulate formulation and solid dispersion approaches in drug development. *Am Pharm Rev* **2010,** *13* (1), 12.
5. Huang, L.-F.; Tong, W.-Q. T., Impact of solid state properties on developability assessment of drug candidates. *Advanced drug delivery reviews* **2004,** *56* (3), 321-334.
6. (a) Janssens, S.; Van den Mooter, G., Review: physical chemistry of solid dispersions. *Journal of Pharmacy and Pharmacology* **2009,** *61* (12), 1571-1586; (b) Van den Mooter, G., The use of amorphous solid dispersions: A formulation strategy to overcome poor solubility and dissolution rate. In *Drug Discovery Today: Technologies*, 2012; Vol. 9, pp e79-e85.
7. Newman, A.; Knipp, G.; Zografi, G., Assessing the performance of amorphous solid dispersions. *Journal of Pharmaceutical Sciences* **2012,** *101* (4), 1355-1377.

8. Trasi, N. S.; Taylor, L. S., Effect of polymers on nucleation and crystal growth of amorphous acetaminophen. *CrystEngComm* **2012,** *14* (16), 5188-5197.
9. (a) Ilevbare, G.; Liu, H.; Edgar, K. J.; Taylor, L., Inhibition of Solution Crystal Growth of Ritonavir by Cellulose Polymers–Factors Influencing Polymer Effectiveness. *CrystEngComm* **2012,** *14* (20), 6503-6514; (b) Ilevbare, G. A.; Liu, H. Y.; Edgar, K. J.; Taylor, L. S., Understanding Polymer Properties Important for Crystal Growth Inhibition-Impact of Chemically Diverse Polymers on Solution Crystal Growth of Ritonavir. *Cryst Growth Des* **2012,** *12* (6), 3133-3143.
10. Alonzo, D. E.; Gao, Y.; Zhou, D.; Mo, H.; Zhang, G. G. Z.; Taylor, L. S., Dissolution and precipitation behavior of amorphous solid dispersions. *J. Pharm. Sci.* **2011,** *100* (8), 3316-3331.
11. (a) Vasconcelos, T.; Sarmento, B.; Costa, P., Solid dispersions as strategy to improve oral bioavailability of poor water soluble drugs. *Drug Discovery Today* **2007,** *12* (23–24), 1068-1075; (b) Konno, H.; Handa, T.; Alonzo, D. E.; Taylor, L. S., Effect of polymer type on the dissolution profile of amorphous solid dispersions containing felodipine. *European Journal of Pharmaceutics and Biopharmaceutics* **2008,** *70* (2), 493-499.
12. (a) Ilevbare, G. A.; Liu, H.; Edgar, K. J.; Taylor, L. S., Effect of Binary Additive Combinations on Solution Crystal Growth of the Poorly Water-Soluble Drug, Ritonavir. *Cryst Growth Des* **2012,** *12* (12), 6050-6060; (b) Trasi, N. S.; Taylor, L. S., Effect of Additives on Crystal Growth and Nucleation of Amorphous Flutamide. *Cryst Growth Des* **2012,** *12* (6), 3221-3230.
13. (a) Ilevbare, G. A.; Liu, H.; Edgar, K. J.; Taylor, L. S., Impact of Polymers on Crystal Growth Rate of Structurally Diverse Compounds from Aqueous Solution. *Molecular pharmaceutics* **2013,** *10* (6), 2381-2393; (b) Liu, H.; Ilevbare, G. A.; Cherniawski, B. P.; Ritchie, E. T.; Taylor, L. S.; Edgar, K. J., Synthesis and structure–property evaluation of cellulose ω-carboxyesters for amorphous solid dispersions. *Carbohydr. Polym.* (0).
14. (a) Curatolo, W.; Nightingale, J.; Herbig, S., Utility of Hydroxypropylmethylcellulose Acetate Succinate (HPMCAS) for Initiation and Maintenance of Drug Supersaturation in the GI Milieu. *Pharm. Res.* **2009,** *26* (6), 1419-1431; (b) Friesen, D. T.; Shanker, R.; Crew, M.; Smithey, D. T.; Curatolo, W. J.; Nightingale, J. A., Hydroxypropyl methylcellulose acetate succinate-based spray-dried dispersions: an overview. *Molecular Pharmaceutics* **2008,** *5* (6), 1003-19.
15. (a) Posey-Dowty, J.; Watterson, T.; Wilson, A.; Edgar, K.; Shelton, M.; Lingerfelt, L., Zero- order release formulations using a novel cellulose ester. *Cellulose* **2007,** *14* (1), 73-83; (b) Shelton, M. C.; Posey-Dowty, J. D.; Lingerfelt, L.; Kirk, S. K.; Klein, S.; Edgar, K. J., Enhanced dissolution of poorly soluble drugs from solid dispersions in carboxymethylcellulose acetate butyrate matrices. In *Polysaccharide Materials: Performance by Design*, American Chemical Society: 2009; Vol. 1017, pp 93-113.
16. Pereira, J. M.; Mejia-Ariza, R.; Ilevbare, G. A.; McGettigan, H. E.; Sriranganathan, N.; Taylor, L. S.; Davis, R. M.; Edgar, K. J., Interplay of Degradation, Dissolution and Stabilization of Clarithromycin and Its Amorphous Solid Dispersions. *Molecular Pharmaceutics* **2013**.
17. Pradip; Maltesh, C.; Somasundaran, P.; Kulkarni, R. A.; Gundiah, S., Polymer-polymer complexation in dilute aqueous solutions: poly(acrylic acid)-poly(ethylene oxide) and poly(acrylic acid)-poly(vinylpyrrolidone). *Langmuir* **1991,** *7* (10), 2108-2111.
18. Ilevbare, G. A.; Liu, H.; Edgar, K. J.; Taylor, L. S., Effect of Binary Additive Combinations on Solution Crystal Growth of the Poorly Water-Soluble Drug, Ritonavir. *Crystal Growth & Design* **2012,** *12* (12), 6050-6060.
19. Lyu, S. P.; Sparer, R.; Hobot, C.; Dang, K., Adjusting drug diffusivity using miscible polymer blends. *Journal of Controlled Release* **2005,** *102* (3), 679-687.

20. (a) Goddeeris, C.; Willems, T.; Houthoofd, K.; Martens, J. A.; Van den Mooter, G., Dissolution enhancement of the anti-HIV drug UC 781 by formulation in a ternary solid dispersion with TPGS 1000 and Eudragit E100. *European Journal of Pharmaceutics and Biopharmaceutics* **2008,** *70* (3), 861-868; (b) Goddeeris, C.; Willems, T.; Van den Mooter, G., Formulation of fast disintegrating tablets of ternary solid dispersions consisting of TPGS 1000 and HPMC 2910 or PVPVA 64 to improve the dissolution of the anti-HIV drug UC 781. *European Journal of Pharmaceutical Sciences* **2008,** *34* (4–5), 293-302; (c) Janssens, S.; Denivelle, S.; Rombaut, P.; Van den Mooter, G., Influence of polyethylene glycol chain length on compatibility and release characteristics of ternary solid dispersions of itraconazole in polyethylene glycol/hydroxypropylmethylcellulose 2910 E5 blends. *European Journal of Pharmaceutical Sciences* **2008,** *35* (3), 203-210; (d) Janssens, S.; de Armas, H. N.; Roberts, C. J.; Van den Mooter, G., Characterization of ternary solid dispersions of itraconazole, PEG 6000, and HPMC 2910 E5. *Journal of Pharmaceutical Sciences* **2008,** *97* (6), 2110-2120.
21. Liu, H.; Ilevbare, G. A.; Cherniawski, B. P.; Ritchie, E. T.; Taylor, L. S.; Edgar, K. J., Synthesis and structure–property evaluation of cellulose ω-carboxyesters for amorphous solid dispersions. *Carbohydrate Polymers* **2010,** (0).
22. (a) Coleman, M. M.; Painter, P. C.; Graf, J. F., *Specific Interactions and the Miscibility of Polymer Blends*. Taylor & Francis: 1995; (b) Espi, E.; Fernandez-Berridi, M. J.; Iruin, J. J., An extension of the Painter-Coleman miscibility guide to ternary polymer blends. *Polymer Engineering and Science* **1994,** *34* (17), 1314-1318; (c) Painter, P. C.; Park, Y.; Coleman, M. M., Hydrogen bonding in polymer blends. 2. Theory. *Macromolecules* **1988,** *21* (1), 66-72; (d) Painter, P. C.; Park, Y.; Coleman, M. M., Thermodynamics of hydrogen bonding in polymer blends. 1. The application of association models. *Macromolecules* **1989,** *22* (2), 570-579.
23. Masson, J. F.; Manley, R. S. J., Miscible blends of cellulose and poly (vinylpyrrolidone). *Macromolecules* **1991,** *24* (25), 6670-6679.
24. (a) Williams, R. O.; Williams, R. O.; Watts, A. A. B.; Miller, D. A., *Formulating Poorly Water Soluble Drugs*. Springer New York: 2012; (b) Sharma, A.; Jain, C., Solid dispersion: A promising technique to enhance solubility of poorly water soluble drug. *International Journal of Drug Delivery* **2011,** *3* (2), 149-170; (c) Baird, J. A.; Taylor, L. S., Evaluation of amorphous solid dispersion properties using thermal analysis techniques. *Advanced Drug Delivery Reviews* **2012,** *64* (5), 396-421.
25. (a) Baird, J. A.; Taylor, L. S., Evaluation of amorphous solid dispersion properties using thermal analysis techniques. *Adv Drug Deliv Rev* **2012,** *64* (5), 396-421; (b) Li, B.; Konecke, S.; Harich, K.; Wegiel, L.; Taylor, L. S.; Edgar, K. J., Solid Dispersion of Quercetin in Cellulose Derivative Matrices Influences both Solubility and Stability. *Carbohydrate Polymers* **2010**; (c) Bettinetti, G.; Gazzaniga, A.; Mura, P.; Giordano, F.; Setti, M., Thermal-Behavior and Dissolution Properties of Naproxen in Combinations with Chemically Modified Beta-Cyclodextrins. *Drug Development and Industrial Pharmacy* **1992,** *18* (1), 39-53; (d) Ceschel, G. C.; Maffei, P.; Borgia, S. L.; Ronchi, C., Design and evaluation of buccal adhesive hydrocortisone acetate (HCA) tablets. *Drug Delivery* **2001,** *8* (3), 161-171; (e) Durig, T.; Fassihi, A. R., Identification of Stabilizing and Destabilizing Effects of Excipient-Drug Interactions in Solid Dosage Form Design. *International Journal of Pharmaceutics* **1993,** *97* (1-3), 161-170; (f) Shmeis, R. A.; Wang, Z.; Krill, S. L., A mechanistic investigation of an amorphous pharmaceutical and its solid dispersions, part I: A comparative analysis by thermally stimulated depolarization current and differential scanning calorimetry. *Pharmaceutical research* **2004,** *21* (11), 2025-2030.

26. Jorda, R.; Wilkes, G. L., A novel use of physical aging to distinguish immiscibility in polymer blends. *Polymer Bulletin* **1988,** *20* (5), 479-485.
27. (a) Pham, T. N.; Watson, S. A.; Edwards, A. J.; Chavda, M.; Clawson, J. S.; Strohmeier, M.; Vogt, F. G., Analysis of Amorphous Solid Dispersions Using 2D Solid-State NMR and 1H T1 Relaxation Measurements. *Molecular Pharmaceutics* **2010,** *7* (5), 1667-1691; (b) Aso, Y.; Yoshioka, S.; Miyazaki, T.; Kawanishi, T.; Tanaka, K.; Kitamura, S.; Takakura, A.; Hayashi, T.; Muranushi, N., Miscibility of Nifedipine and Hydrophilic Polymers as Measured by 1H-NMR Spin-Lattice Relaxation. *Chemical and Pharmaceutical Bulletin* **2007,** *55* (8), 1227-1231; (c) Aso, Y.; Yoshioka, S.; Zhang, J.; Zografi, G., Effect of Water on the Molecular Mobility of Sucrose and Poly(vinylpyrrolidone) in a Colyophilized Formulation as Measured by 13C-NMR Relaxation Time. *Chemical and Pharmaceutical Bulletin* **2002,** *50* (6), 822-826.
28. Kar, N.; Liu, H.; Edgar, K. J., Synthesis of cellulose adipate derivatives. *Biomacromolecules* **2011,** *12* (4), 1106-15.
29. Fedors, R. F., A method for estimating both the solubility parameters and molar volumes of liquids. *Polymer Engineering and Science* **1974,** *14* (2), 147-154.
30. Babcock, W. C.; Friesen, D. T.; Lyon, D. K.; Miller, W. K.; Smithey, D. T. Pharmaceutical compositions with enhanced performance. US Patent 8,617,604, 2013.
31. Wise, D. L., *Handbook of Pharmaceutical Controlled Release Technology*. Taylor & Francis: 2000.
32. Ethers, M. C., Technical Handbook. *Dow Chemical Company, Midland, Michingan, USA* **1997**.
33. Ilevbare, G. A.; Liu, H.; Edgar, K. J.; Taylor, L. S., Inhibition of solution crystal growth of ritonavir by cellulose polymers - factors influencing polymer effectiveness. *CrystEngComm* **2012,** *14* (20), 6503-6514.
34. Ilevbare, G. A.; Liu, H.; Edgar, K. J.; Taylor, L. S., Understanding Polymer Properties Important for Crystal Growth Inhibition—Impact of Chemically Diverse Polymers on Solution Crystal Growth of Ritonavir. *Crystal Growth & Design* **2012,** *12* (6), 3133-3143.
35. Ilevbare, G. A.; Liu, H.; Edgar, K. J.; Taylor, L. S., Maintaining Supersaturation in Aqueous Drug Solutions: Impact of Different Polymers on Induction Times. *Crystal Growth & Design* **2013,** *13* (2), 740-751.
36. (a) Sarisuta, N.; Lawanprasert, P.; Puttipipatkhachorn, S.; Srikummoon, K., The influence of drug-excipient and drug-polymer interactions on butt adhesive strength of ranitidine hydrochloride film-coated tablets. *Drug development and industrial pharmacy* **2006,** *32* (4), 463-471; (b) Cui, F.; Wang, Y.; Wang, J.; Feng, L.; Ning, K., Preparation of redispersible dry emulsion using Eudragit E100 as both solid carrier and unique emulsifier. *Colloids and Surfaces A: Physicochemical and Engineering Aspects* **2007,** *307* (1), 137-141; (c) Quinteros, D. A.; Rigo, V. R.; Kairuz, A. F. J.; Olivera, M. E.; Manzo, R. H.; Allemandi, D. A., Interaction between a cationic polymethacrylate (Eudragit E100) and anionic drugs. *European Journal of Pharmaceutical Sciences* **2008,** *33* (1), 72-79; (d) Bharate, S.; Bharate, S.; A., A. B., Incompatibilities of Pharmaceutical Excipients with Active Pharmaceutical Ingredients: A Comprehensive Review. *Journal of Excipients and Food Chemicals* **2010,** *1* (3).
37. (a) Dokou, E.; Brodeur, G. G.; Tauber, M.; Sanghvi, T.; Knezic, D.; Pesha, Y.; Johnston, M. M.; Hurrey, M.; Arekar, S. G.; Penumatcha, R. High potency formulations of vx-950. 2013; (b) Shah, N.; Iyer, R. M.; Mair, H.-J.; Choi, D. S.; Tian, H.; Diodone, R.; Fähnrich, K.; Pabst-Ravot, A.; Tang, K.; Scheubel, E.; Grippo, J. F.; Moreira, S. A.; Go, Z.; Mouskountakis, J.; Louie, T.; Ibrahim, P. N.; Sandhu, H.; Rubia, L.; Chokshi, H.; Singhal, D.; Malick, W., Improved human

bioavailability of vemurafenib, a practically insoluble drug, using an amorphous polymer-stabilized solid dispersion prepared by a solvent-controlled coprecipitation process. *Journal of Pharmaceutical Sciences* **2013,** *102* (3), 967-981.
38. Posey-Dowty, J.; Watterson, T.; Edgar, K.; Kirk, S.; Welty, M.; Yuan, J.; Shelton, M.; Lingerfelt, L.; Wilson, A. Carboxyalkyl cellulose esters for sustained delivery of pharmaceutically active substances. WO Patent 2,007,056,125, 2007.
39. Wegiel, L. A.; Mauer, L. J.; Edgar, K. J.; Taylor, L. S., Crystallization of amorphous solid dispersions of resveratrol during preparation and storage-Impact of different polymers. *J Pharm Sci* **2012**.
40. Laurence, C.; Brameld, K. A.; Graton, J.; Le Questel, J.-Y.; Renault, E., The p K BHX database: toward a better understanding of hydrogen-bond basicity for medicinal chemists. *Journal of medicinal chemistry* **2009,** *52* (14), 4073-4086.
41. Fox, T. G., Influence of diluent and of copolymer composition on the glass temperature of a polymer system. *Bull Am Phys Soc* **1956,** *1* (123), 22060-6218.
42. Nyamweya, N.; Hoag, S. W., Assessment of Polymer-Polymer Interactions in Blends of HPMC and Film Forming Polymers by Modulated Temperature Differential Scanning Calorimetry. *Pharmaceutical Research* **2000,** *17* (5), 625-631.
43. Chokshi, R. J.; Shah, N. H.; Sandhu, H. K.; Malick, A. W.; Zia, H., Stabilization of low glass transition temperature indomethacin formulations: Impact of polymer-type and its concentration. *Journal of Pharmaceutical Sciences* **2008,** *97* (6), 2286-2298.
44. Miller, W. K.; Lyon, D. K.; Friesen, D. T.; Caldwell, W. B.; Vodak, D. T.; Dobry, D. E. Hydroxypropyl methyl cellulose acetate succinate with enhanced acetate and succinate substitution. WIPO Patent 2,011,159,626, 2010.
45. Karavas, E.; Georgarakis, E.; Bikiaris, D., Application of PVP/HPMC miscible blends with enhanced mucoadhesive properties for adjusting drug release in predictable pulsatile chronotherapeutics. *Eur J Pharm Biopharm* **2006,** *64* (1), 115-26.
46. Yang, Z.; Nollenberger, K.; Albers, J.; Craig, D.; Qi, S., Microstructure of an Immiscible Polymer Blend and Its Stabilization Effect on Amorphous Solid Dispersions. *Molecular Pharmaceutics* **2013,** *10* (7), 2767-2780.
47. McPhillips, H.; Craig, D. Q. M.; Royall, P. G.; Hill, V. L., Characterisation of the glass transition of HPMC using modulated temperature differential scanning calorimetry. *International Journal of Pharmaceutics* **1999,** *180* (1), 83-90.
48. (a) Bureau, G.; Longpré, F.; Martinoli, M. G., Resveratrol and quercetin, two natural polyphenols, reduce apoptotic neuronal cell death induced by neuroinflammation. *Journal of Neuroscience Research* **2008,** *86* (2), 403-410; (b) Igura, K.; Ohta, T.; Kuroda, Y.; Kaji, K., Resveratrol and quercetin inhibit angiogenesis in vitro. *Cancer letters* **2001,** *171* (1), 11-16.
49. Li, B.; Wegiel, L. A.; Taylor, L. S.; Edgar, K. J., Stability and solution concentration enhancement of resveratrol by solid dispersion in cellulose derivative matrices. *Cellulose* **2013**, 1-12.
50. Kashdan, D. S. Polymer blends having reverse phase morphology for controlled delivery of bioactive agents. US Patent 4,795,641, 1989.

3.7 Copyright Authorization

JOHN WILEY AND SONS LICENSE TERMS AND CONDITIONS

May 04, 2015

This Agreement between Joyann A Marks ("You") and John Wiley and Sons ("John Wiley and Sons") consists of your license details and the terms and conditions provided by John Wiley and Sons and Copyright Clearance Center.

License Number	3603451239749
License date	Apr 07, 2015
Licensed Content Publisher	John Wiley and Sons
Licensed Content Publication	Journal of Pharmaceutical Sciences
Licensed Content Title	Pairwise Polymer Blends for Oral Drug Delivery
Licensed Content Author	Joyann A. Marks,Lindsay A. Wegiel,Lynne S. Taylor,Kevin J. Edgar
Licensed Content Date	May 13, 2014
Pages	13
Type of use	Dissertation/Thesis
Requestor type	Author of this Wiley article
Format	Print and electronic
Portion	Full article
Will you be translating?	No
Title of your thesis / dissertation	Synthesis and Applications of Cellulose Derivatives for Drug Delivery
Expected completion date	May 2015
Expected size (number of pages)	180

Chapter 4: Cationic Cellulose Derivatives for Drug Delivery: Synthetic Pathways to Regioselectively Substituted Ammonium and Phosphonium Derivatives

(Adapted from Marks, J. A; Fox, S. C and Edgar, K. J. Manuscript to be submitted for publication in Carbohydrate Polymers)

4.1 Abstract:

Cationic polysaccharides are important synthetic targets due to their potential applications in drug and gene delivery, especially through encapsulation of nucleic acids and certain proteins through electrostatic interactions. They have also been sought as paracellular permeability enhancers (PPEs) in an effort to increase permeation across the epithelial membrane especially for hydrophilic macromolecules of therapeutic significance. These PPEs temporarily alter the integrity of tight junctions and allow for more effective transport - a characteristic that has been identified in the amine containing polysaccharide chitosan. Chitosan has been a template for the behavior of cationic polysaccharides and is most heavily investigated. However, its limited positive charge and solubility at neutral pH, added to its inability to target specific areas of the intestine like the ileum or jejunum greatly limit its efficiency in comparison to the best synthetic vehicles available. These drawbacks and others have prompted efforts to functionalize other polysaccharides including cellulose through the addition of permanent positive charges along the polymer backbone. This study explores the synthetic conditions needed to produce ammonium and phosphonium cellulose derivatives regioselectively by halogen displacement at C-6 while maximizing degrees of substitution (DS). Regioselective substitution was successful in each case. Although there were found to be some limitations to the DS and solubility of ammonium derivatives prepared in this way, water-soluble 6-phosphonium cellulose derivatives were produced with DS > 0.5.

4.2. Introduction:

While anionic polysaccharides are very common in nature (e.g. alginate), and anionic polysaccharide derivatives are important items of commerce (e.g. carboxymethyl cellulose, the highest volume commercial cellulose ether), cationic polysaccharide derivatives are much less frequently encountered, in spite of their significant potential value. To cite just a few examples, cationic polymers and lipids have shown great potential for electrostatically binding nucleic acids as vehicles designed to deliver such polyplexes effectively to the cell. These cationic excipients can effectively inhibit the enzymatic degradation of these anionic therapeutics while providing a means to enhance cellular uptake, endosomal escape, and trafficking to the nucleus to provide targeted release [1]. Some of the most commonly used polymers for nucleic acid delivery are amine-containing polymers including polyethyleneimine [2], Superfect, a poly(amidoamine) dendrimer [3], and the polysaccharide chitosan [4]. Phosphonium-substituted macromolecules have shown enhanced thermal stability [5], flame retardancy [6] and biocompatibility [7]. These polymers have also shown decreased cytotoxicity without sacrificing efficacy when phosphonium groups are substituted for ammonium groups [8]. In many cases, these phosphonium-containing macromolecules have shown excellent solution stability as well [1, 9]. In recent years, cationic polysaccharides have been a major area of focus due to their important applications in drug delivery, especially those related to highly insoluble anionic drugs and sensitive anionic species like nuclei acids [8, 10]. Chitosan has been a template for the behavior of cationic polysaccharides and is most heavily studied for such applications. However, recently, other naturally occurring polysaccharides have been derivatized in an effort to produce cationic polymers with performance analogous to that of chitosan; in some cases, materials that are isomeric with chitosan. These include amylose [11], dextran [12], pullulan (Nichifor, Stanciu & Simionescu, 2010) and cellulose derivatives [13].

Commercial chitosan is most often semi-synthetic, prepared from the naturally occurring polysaccharide, chitin; chitin is a linear homopolymer of β-(1→4) linked N-acetylglucosamine. The glucosamine functionality of chitin has been associated with hepatoprotective [14] and antihypoxic effects [15] as well as preventing inflammation [16], all of which are useful biological functions. Recent reports have also linked acetyl glucosamine to having anti-tumor effects [17]. Chitin derived from the waste products of the shrimp and crab industries is

deacylated under very severe alkaline conditions (conc. NaOH, high temperature) to produce linear polymers of β-(1→4) linked 2-amino-2-deoxy-D-glucopyranose, chitosan, with various degrees of deacetylation. This deacetylation product is known as chitosan. Unlike the insoluble chitin, the copolymer-like nature of chitosan, which is not completely deacetylated, promotes reduced crystallinity and increased solubility; the free amine groups may also be protonated, further enhancing solubility [18]. Chitosan and its derivatives have been shown to possess antimicrobial activity, with proven effectiveness against, e.g., *Staphylococcus aureus*, *epidermis*, and *haemolyticus* bacterial strains. These gram-positive bacteria are commonly found in the body in locales that are often susceptible to various types of wounds including the skin and oral cavity [19].

With a pKa of 6.5, chitosan is soluble in aqueous media below this pH, and when protonated is able to increase the permeability of peptide drugs across mucosal epithelia; it acts as an effective absorption enhancer in specific regions of the intestinal lumen [20]. Chitosan amine groups are believed to interact with anionic molecules that are found in mucus or on the surface of cells. For drug and gene delivery applications, chitosan is able to complex and encapsulate anionic nucleic acids and certain proteins through electrostatic interactions. This interaction is capable of protecting these compounds from degradative enzymes within the body [4]. Chitosan is also an excellent film former and mucoadhesive polymer that has been utilized as a coating for alginate beads in a number of controlled release drug delivery applications [21], or as a carrier matrix in the form of chitosan HCl for the controlled release of insulin [22]. Chitosan has also been considered for organ specific drug targeting including liver, colon, kidney and lung. For example, in colonic delivery, chitosan is important as protection for therapeutic agents that will otherwise be susceptible to the harsh conditions of the upper GI tract and be specifically directed to the colon where there are chitinase enzymes that biodegrade the polysaccharide [23].

Chitosan enhances the absorption of these drugs across the epithelial membrane through the opening of tight junctions [20, 24]. Tight junctions are the junctions between columnar cells called enterocytes, which constitute the gastrointestinal (GI) epithelium, separating the GI lumen from the bloodstream. They are important to the functioning of the GI epithelium, as they provide a barrier to the passive movement of fluids, electrolytes, cells, and large molecules through the epithelial membrane. In an effort to increase permeation across the epithelial membrane especially for hydrophilic macromolecules of therapeutic significance, paracellular permeability enhancers

(PPEs) are often sought to temporarily alter the integrity of tight junctions and allow for more effective transport [20, 25].

Illum et al. in 1994 first reported the ability of chitosan to promote absorption of small polar molecules, peptides and proteins including insulin across nasal epithelia in rats and sheep [22b]. A subsequent report by Artursson et al. [26] showed increased paracellular permeability of mannitol across Caco 2 cell monolayers, which mimic in many respects the structure of the GI epithelium. These were among the first studies to describe the absorption enhancement properties of chitosan and attributed these properties to the widening of tight junctions, as well as the bioadhesive properties of chitosan.

While studies have indicated potential for chitosan as a vehicle for therapeutic applications, its limited solubility at neutral pH and inability to target specific areas of the intestine like the ileum or jejunum greatly limit its efficiency in comparison to the best synthetic vehicles available [27]. There are also concerns about the extreme conditions required to convert chitin to chitosan. The fact that natural chitin is typically isolated from crustacean shells, in which it is embedded in a matrix containing marine proteins, is also a concern from the perspective of purity and potential for allergen contamination. In order to solve these problems, researchers have synthesized new derivatives of chitosan, and prepared cationic derivatives of other polysaccharides, in order to achieve beneficial properties similar to those of chitosan [28]. Derivatization of the amine groups on chitosan has produced quaternized chitosan derivatives, having permanent positive charges, that have greater solubility in a wider pH range and show promising capabilities for the absorption enhancement of hydrophilic drugs at pH values similar to the environment of the intestine (pH 6.4-7.5) [20, 25]. *N*,*N*,*N*-Trimethyl chitosan chloride (TMC) has been synthesized and tested for its efficiency as a absorption enhancer compared to chitosan HCl. TMC was tested as a permeation enhancer for the peptide drug buserelin and mannitol across Caco-2-cells at neutral pH values. Confocal laser scanning microscopy was used to show the opening of the tight junctions by TMC to give increased paracellular transport [29].

Quaternized phosphonium derivatives are another potentially interesting and useful family of cationic cellulose derivatives. While there are few reports in the literature of attempts to make phosphonium derivatives of cellulose, such derivatization has been carried out for chitosan and synthetic polymer entities. Phosphonium derivatives of cellulose were reported in 1982 but they have received little or no mention since. In the study, carboxyl containing cellulose derivatives

with 1, 2, or 3 carboxyl groups/anhydroglucose unit (AGU) as well as carboxymethylcellulose (CMC) were reacted with tri(hydroxymethyl)phosphine (THMP) and alkylene oxides or aldehydes, in water and DMF (**Scheme 4.1**).

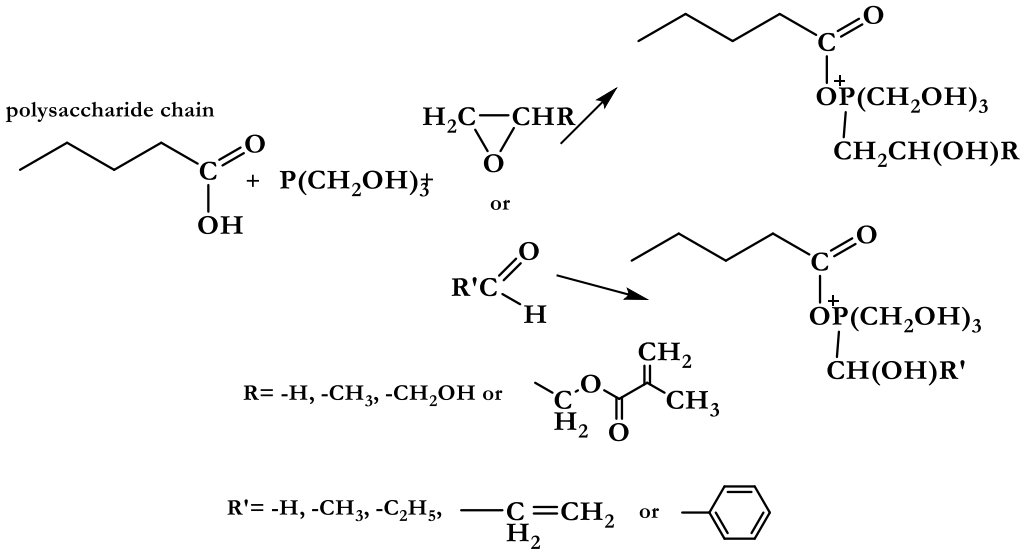

Scheme 4.1: Simplified schematic of the synthesis of phosphonium cellulose derivatives with tri(hydroxymethyl)phosphine (THMP) and alkylene oxides or aldehydes

These reactions were carried out at 0-60°C for 2—6h producing phosphonium derivatives with α and β hydroxyalkyl groups at the phosphorus atom and as high as 9% phosphorus in the resulting products. Higher alkylene or aldehyde and THMP reagent ratios (up to 3 equivalents for each) resulted in greater conversion, increased phosphonium content and increased water solubiility[30]. Synthetic phosphonium derivatives like quaternized triphenylphosphonium-modified polyphenylene oxide (PPh_3 -PPO) have shown excellent antibacterial activity against *Staphylococcus epidermidis* and *Escherichia coli* while some quaternary phosphonium derived compounds have shown anticancer activity [31],[32]. Phosphonium derivatives of poly (acrylic acid) have shown excellent efficacy for promoting transfection of siRNA especially compared to ammonium derivatives of similar structure [8]. Water-soluble phosphonium derivatives of chitosan have been produced by first reacting chitosan with 1-hydroxybenzotriazole (HOBt) in water. The solubilized chitosan is thereafter mixed with (2-carboxyethyl) triphenylphosphonium chloride (CTPC) followed by 1-ethyl-3-(3- dimethylaminopropyl) carbodiimide hydrochloride (EDC·HCl) to produce the quaternized derivative. The water-soluble derivatives synthesized

show low toxicity toward mouse fibroblast cells and are currently being studied for potential drug applications [31].

Regioselective halogenation of cellulose provides an effective means of generating new regioselective derivatives. Furuhata et al. first devised a method of regioselectively brominating cellulose at C-6 without the need for a tosyl cellulose intermediate [33]. This method (cellulose dissolved in DMAc/LiBr, PPh_3, N-bromosuccinimide (NBS)) was found to be completely selective at the C-6 position and yielded a maximum DS of 0.98 [33]. The C-6 primary hydroxyl of cellulose is relatively reactive and the subsequent bromo derivative is not only effective as a C-6 protecting group under certain conditions but can also act as a good leaving group, providing a viable substrate for nucleophilic chemistry at the C-6 position [11, 34]. A number of successful nucleophilic displacement reactions have been reported under heterogeneous reaction conditions. For example, Matsui et al. reported a DS of 0.96 for 6-amino-6-deoxy cellulose synthesized in 2 steps from 6-bromo-6-deoxy cellulose, by initial nucleophilic displacement of the bromide derivative by sodium azide under heterogeneous conditions in DMSO, followed by reduction of the 6-azido derivative with $NaBH_4$ to afford a highly substituted amino derivative [35]. Azide displacement followed by Staudinger reduction and further elaborations have been used by the Edgar laboratory for regio- and chemoselective synthesis of a wide range of 6-amino-6-deoxy derivatives of cellulose [36], pullulan [37] and curdlan [38].

We hypothesize that regioselective nucleophilic halide displacement at C-6 of 6-halo-6-deoxy 2,3, -di-*O*-acyl cellulose esters by trialkylamines and trialkylphosphines will provide an efficient and effective route for synthesis of 6-ammonium and 6-phosphonium derivatives of cellulose. We further hypothesize that the introduction of the positively charged moiety on the cellulose backbone will greatly improve solubility, especially aqueous solubility, of the resulting polysaccharide derivatives, enhancing their potential in drug and gene delivery. Herein we report the results of experiments that test this synthetic hypothesis.

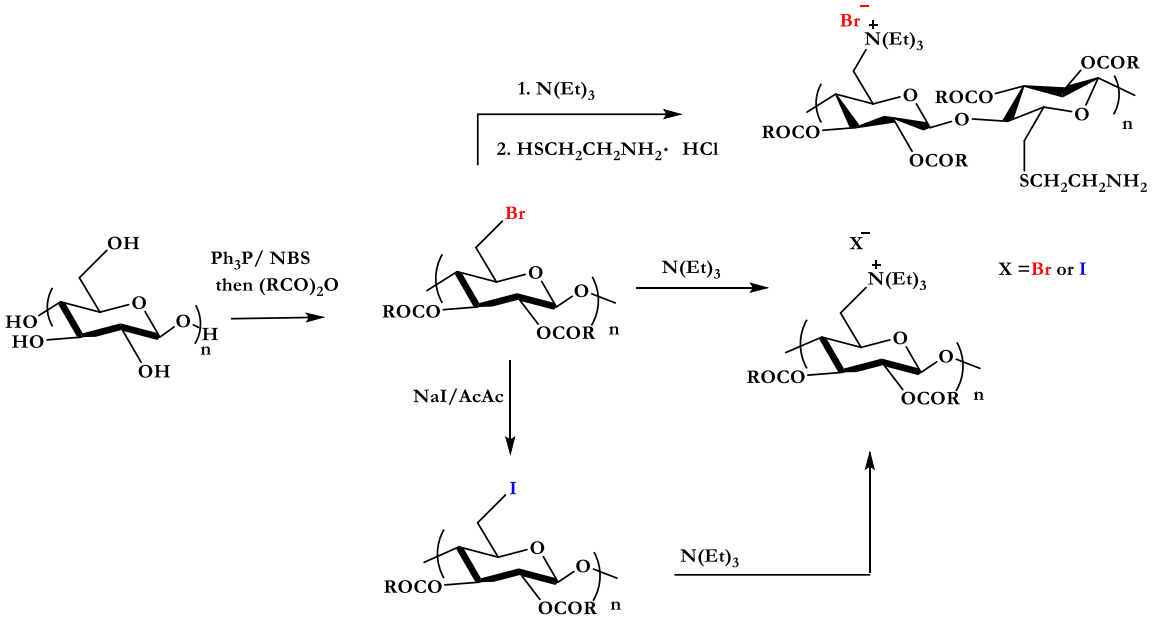

Scheme 4.2: Pathways for conversion of cellulose to 6-ammonium-6-deoxy-2, 3-di-*O*-acyl derivatives.

4.3 Experimental:

4.3.1 Materials:

Microcrystalline cellulose (MCC, Avicel PH-101, Fluka, DP = 80) was dried under vacuum at 50 °C overnight before use. Molecular weight determination for MCC was achieved by gel permeation chromatography in N-methylpyrrolidone containing 0.05% lithium bromide using a Waters 1515 isocratic HPLC pump, Viscotek 270 dual detector, and Waters 2414 refractive index detector. Universal calibration curves were prepared using polystyrene standards. Lithium bromide (LiBr, Fisher) was dried under vacuum at 125 °C. PPh_3 (Strem), all carboxylic acid anhydrides (Acros), triethylamine (TEA, Acros), tributylamine (TBA, 99%, Acros), triethylphosphine (TEP, Aldrich), diethylamine (DEA, Fisher) sodium iodide (NaI,Fisher), NBS (Sigma), acetylacetone (AcAc,), and 2-aminoethanethiol hydrochloride (AET, 98%, Sigma Aldrich) were used as received. Dimethylacetamide (DMAc, Fisher), dimethyl formamide (DMF, Fisher), 1,3-dimethyl imidazolidinone (DMI) and dimethyl sulfoxide (DMSO, Acros) were kept over 4 Å molecular sieves under dry nitrogen until use. Dialysis tubing (3,500 MWCO) was obtained from Fisher and prewet with water prior to use. Methanol, ethanol,

dichloromethane, N-methylpyrrolidone (NMP), acetone, and tetrahydrofuran (THF) were purchased from Fisher Scientific, Pittsburgh, PA and used as received.

4.3.2 Measurements:

NMR spectra were obtained on Varian INOVA 400 MHz or Bruker AVANCE 500 MHz spectrometers in $CDCl_3$, DMF-d_7 or DMSO-d_6. ^{13}C NMR spectra were obtained using a minimum of 5000 scans. Chemical shifts are reported relative to solvent peaks. All elemental analyses were performed by Midwest Microlab, LLC. Carbon, hydrogen and nitrogen contents were determined via combustion at 990°C with an elemental analyzer. Sulfur, bromine and iodine were determined by flask combustion followed by titration. Oxygen analysis was performed via pyrolysis at 1200°C and then determined gravimetrically while phosphorus content was determined by wet oxidation followed by spectrophotometry.

Thermogravimetric Analysis

Thermogravimetric analyses were carried out on a Q500 Thermogravimetric analyzer, TGA (TA Instruments, DE, USA). Approximately 4-6 mg of the sample was heated from 25°C to 600°C at a rate of 10°C/min under a continuous nitrogen flow at 60 mL/min.

Differential Scanning Calorimetry (DSC)

Heating curves of 4-10 mg samples in TA Instruments aluminum hermetic pans were obtained on a TA Instruments Q100 DSC (New Castle, DE). Samples were first equilibrated at -25 °C followed by heating at 20 °C/min to 180 or 190 °C. Samples were quench cooled at 100 °C/min to -25°C, then reheated at 20 °C/min. Second heating scan thermograms were evaluated to obtain sample T_g(s). Temperature modulated DSC (MDSC) was performed with a heating rate of 4 °C/min from -25 °C to 180 or 190 °C and a modulation amplitude of +/- 0.5 °C for 60 s. For these samples reversing heat flow thermograms were evaluated.

Fourier Transform Infrared Spectroscopy

Infrared spectra were obtained on powder samples in absorbance mode using a Bio-Rad FTS 6000 spectrophotometer equipped with a globar infrared source, KBr beam splitter, and DTGS

(d-triglycine sulfate) detector. Spectra of the powdered samples were obtained using a Golden Gate MII attenuated total reflectance (ATR) sampling accessory with a diamond top plate (Specac Inc., Woodstock, GA). Scan range was set from 4000 to 500 cm^{-1} with a 4 cm^{-1} resolution, and 128 scans were co-added. The absorbance intensity of the spectral region of interest was between 0.6-1.2.

4.3.3 Methods:

4.3.4 Regioselective bromination and acylation of MCC

The synthesis and full characterization of 6-bromo-6-deoxy-2,3-di-O-acylcellulose derivatives has been previously published [36]. To a 1 L three-necked flask fitted with a thermometer, nitrogen inlet and overhead stirrer adapter was added dried MCC (5.0 g, 30.8 mmol). To the flask was added 220 mL of DMAc. The slurry was stirred and heated to 160°C. The mixture was kept at 160°C for 1 h during which time about 20 mL of the solvent was distilled from the flask. The mixture was cooled to 80°C and 45 g of LiBr was added and dissolved in the DMAc. The mixture was cooled to room temperature while stirring under N_2 to produce within a few hours a transparent solution that was used within 24 h.

Ph_3P (4 eq. per AGU) was dissolved in 100 mL of dried DMAc and the solution was added dropwise to the reaction mixture. This was followed by the dropwise addition of NBS (4 eq. per AGU) also dissolved in 100mL dried DMAc. The solution was then heated to 70°C for 1 h. After 1 h, 10 eq. per AGU of carboxylic anhydride (acetic, propionic or butyric) was slowly added to the flask and the reaction stirred at 70°C overnight. The reaction mixture was then slowly added to 4 L of a 50:50 (v/v) mixture of methanol and deionized water to precipitate the product followed by filtration. The precipitate was twice dissolved in acetone and reprecipitated in ethanol, before being dried overnight in a vacuum oven at 50 °C to recover the polymer. Yield: 83 % (6-bromo-6-deoxy-2,3-di-*O*-acetylcellulose).

^{1}H NMR (DMSO-d_6, ppm): 1.8-2.2 (CH_3 of acetate), 3.4-5.5 (cellulose backbone)
^{13}C NMR (DMSO-d_6, ppm): 169-170 (C=O of acetate), 100 (C-1), 70–80 (C-2, C-3, C-4, C-5), 32 (C-6), 21 (CH_3 of acetate).

4.3.5 *Regioselective iodination of 6-bromo-6-deoxy-2,3-di-O-acylcellulose derivatives*

6-Bromo-6-deoxy-2, 3-di-*O*-acetyl-cellulose (2.00 g, 6.47 mmol) and 3.88 g sodium iodide (NaI) (4 eq. per AGU) were dissolved in acetylacetone (100 mL) under nitrogen. The solution was heated to 120 °C in an oil bath and stirred for 2 h. After 2 h, the contents of the flask were cooled and added to 900 mL of a 50/50 (v/v) mixture of water and methanol. The filtered precipitate was redissolved in acetone and then reprecipitated in water. The product was collected and dried under vacuum at 50 °C. Yield: 80%

^{1}H NMR (DMSO-d_6, ppm): 1.8-2.2 (CH_3 of acetate), 3.4-5.5 (cellulose backbone)

^{13}C NMR (DMSO-d_6, ppm): 169-170 (C=O of acetate), 100 (C-1), 70–80 (C-2, C-3, C-4, C-5), 21 (CH_3 of acetate), 5 (C-6).

4.3.6 *Kinetic studies with triethylamine*

Approximately 30 mg of 6-deoxy-6-halocellulose ester was dissolved in 0.7 mL of deuterated solvent (DMF-d_7 or DMSO-d_6). The dissolved cellulose derivative was then added to the appropriate number of molar equivalents of triethylamine (5 or 20 molar equivalents). The mixture was then transferred to an NMR tube, and NMR analysis was performed at 80°C for the appropriate experimental time on the instrument, at 64 scans every 15 min for the duration of the experiment. Due to limited solubility of these cellulose derivatives in triethylamine (TEA); it was difficult to perform kinetic experiments in the presence of 100 molar equivalents of the reagent or using TEA as a solvent. Subsequent bench top experiments utilized up to 100 eqs. of TEA in sufficient solvent (DMSO, DMF, DMI or DMAc) to maintain homogeneity over the course of the reaction.

4.3.7 *Preparation of N, N, N-trialkyl-6-amino-6-deoxy-2,3-di-O-acylcellulose derivatives*

6-Bromo- or 6-iodo-6-deoxy-2, 3-di-*O*-acyl-cellulose (0.200 g, 0.56 mmol (I) or 0.65 mmol (Br)) was dissolved in 50 mL anhydrous DMF/DMI/DMAc/DMSO. The solution was added dropwise to 5, 20 or 100 eq. per AGU of TEA. The mixture was then stirred under dry nitrogen and heated to 80°C for 24h. After 24h, the mixture was allowed to cool to room temperature, added to dialysis tubing and dialyzed against ethanol (for 2 d) and then water (for 1 d). Dialyzed samples were transferred to round bottom flasks and the product recovered by rotary evaporation or lyophilization. Samples were dried in a vacuum oven at 50 °C. Yield: 30-45%.

^{1}H NMR (DMSO-d_6, ppm): 1.2 (CH_3 of trialkylammonium), 3.3 (CH_2 of trialkylammonium), 3.4-5.5 (cellulose backbone)
^{13}C NMR (DMSO-d_6, ppm): 100 (C-1), 70–80 (C-2, C-3, C-4, C-5), 62 (C-6 Et_3N^+) 54 (CH_2 of trialkylammonium), 7.8 (CH_3 of trialkylammonium).

Similarly, 6-bromo-6-deoxy-2, 3-di-*O*-acetyl-cellulose (0.200 g, 0.65 mmol was dissolved in 50 mL anhydrous DMF/THF and added dropwise to 100 eq. per AGU of tributylamine (TBA). The reaction mixture was treated and the product recovered as above. Yield: 71%.
^{1}H NMR (DMSO-d_6): 0.98 (CH_3 of tributylammonium), 1.37 ($^{+}NCH_2CH_2\underline{CH_2}CH_3$) 1.63 ($^{+}NCH_2\underline{CH_2}CH_2CH_3$).1.8-2.2 ($CH_3$ of acetate) 3.4-5.5 (cellulose backbone)

To determine the degree of substitution (DS) of the product by ^{1}H NMR, the integral of the N-methyl protons was compared to the integral of the cellulose backbone or methyl protons of the acyl group using the following formula:

$$\mathrm{DS_{Ammonium}} = \frac{\boldsymbol{7\, I_{CH3\ of\ Ammonium}}}{\boldsymbol{9 I_{backbone\ +\ methylene\ Ammonium} - 6 I_{Ammonium}}}$$

4.3.8 *Sequential amination and thiolation of 6-deoxy-6-halo-2,3-di-O-acylcellulose derivatives*
6-Bromo-6-deoxy-2, 3-di-*O*-acyl-cellulose (0.200 g, 0.65 mmol) was first dissolved in 50 mL of anhydrous DMSO. The solution was then added dropwise to 100 equivalents TEA per AGU of cellulose. The mixture was then heated to 80°C and stirred under dry nitrogen for 24h. After 24 h, about 10 mL of the reaction mixture was removed and recovered by dialysis and rotary evaporation while 20 equivalents per AGU of 2-aminoethanethiol hydrochloride (AET) was added to the remaining mixture. The reaction was stirred for another 24 h at 80°C. Then the solution was cooled and added to dialysis tubing, then dialyzed against ethanol (2 d), followed by water (1 d). The product was recovered by rotary evaporation, then dried under vacuum at 50 °C.
Yield: ~40 %.
^{1}H NMR (DMSO-d_6, ppm): 1.0-1.5 (CH_3 of trialkylammonium and -$SCH_2CH_2\underline{NH_2}$), 1.8-2.2 ($CH_3$

of acetate), 3.0 (-$SCH_2\underline{CH_2}NH_2$), 3.1 (-$S\underline{CH_2}CH_2NH_2$), 3.3 ($CH_2$ of trialkylammonium), 3.4-5.5 (cellulose backbone)

^{13}C NMR (DMSO-d_6, ppm): 169-170 (C=O of acetate), 100 (C-1), 70–80 (C-2, C-3, C-4, C-5), 62 (C-6 Et_3N^+), 54 (CH_2 of trialkylammonium), 41 (-$S\underline{CH_2}CH_2NH_2$), 38 (-$SCH_2\underline{CH_2}NH_2$), 35 (C-6-S), 21 ($CH_3$ of acetate), 7.8 (CH_3 of trialkylammonium).

4.3.9 *Synthesis of N, N, N-trialkyl-6-amino-6-deoxy-2,3-di-O-acylcellulose derivatives by* in situ *addition of NaI*

6-Bromo-6-deoxy-2, 3-di-*O*-acyl-cellulose (0.200 g, 0.65 mmol) and NaI (5 equivalent per AGU, 0.485 g) were first dissolved in 50 mL anhydrous DMF/DMSO, then the solution was added dropwise to TEA (100 equivalents per AGU of cellulose). The solution was stirred under dry nitrogen and heated to 80°C for 24h. Then the product solution was added to dialysis tubing, and dialyzed against ethanol (2 d), and then water (1 d). The solution was concentrated by rotary evaporation. The product was collected and dried under vacuum at 50 °C. Yield: 45%.

^{1}H NMR(DMSO-d_6, ppm): 1.2 (CH_3 of trialkylammonium), 3.3 (CH_2 of trialkylammonium) (3.4-5.5 (cellulose backbone)

^{13}C NMR (DMSO-d_6, ppm): 100 (C-1), 70–80 (C-2, C-3, C-4, C-5), 54 (CH_2 of trialkylammonium), 7.8 (CH_3 of trialkylammonium).

4.3.10 *Synthesis of N, N-dialkyl-6-amino-6-deoxy-2, 3-di-O-acetyl-cellulose*

6-Bromo-deoxy-2, 3-di-*O*-acetyl-cellulose (0.200 g, 0.65 mmol) was dissolved in 50 mL anhydrous DMF and the solution added dropwise to diethylamine (DEA) (100 molar equiv/AGU). The reaction solution was then stirred at 50°C for 24h under dry nitrogen. The product was dialyzed against ethanol (2d) and then water (1d), recovered by rotary evaporation and dried in a vacuum oven at 50°C.

^{1}H NMR (DMSO-d_6, ppm): 1.25 (CH_3 of amine), 3.3 (CH_2 of amine), 3.4-5.5 (cellulose backbone).

^{13}C NMR (DMSO-d_6, ppm): 169-170 (C=O of ester), 100 (C-1), 70–80 (C-2, C-3, C-4, C-5), 52.3 (C-6 bonded to N), 49.2 (CH_2 of amine), 21 (CH_3 of acetate), 9.2 (CH_3 of amine).

4.3.11 *Synthesis of P, P, P-triethyl-6-deoxy-6-phosphonium-2, 3-di-O-acyl-cellulose*

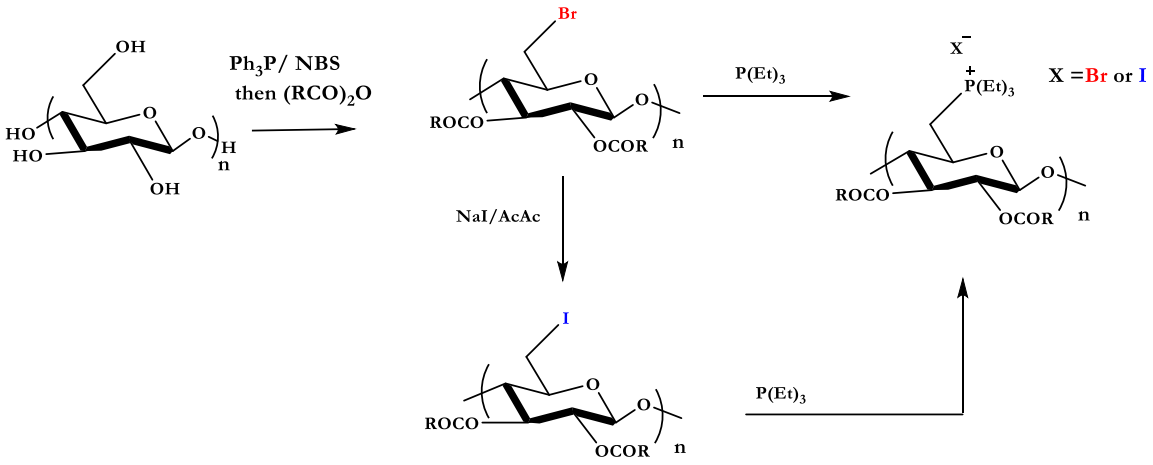

Scheme 4.3: Reaction of 6-deoxy-6-halocellulose esters with triethylphosphine

6-Bromo- or 6-iodo-6-deoxy-2, 3-di-*O*-acyl-cellulose (0.200 g, 0.56 mmol (I) or 0.65 mmol (Br)), was first dissolved in 50 mL anhydrous DMF or anhydrous DMSO. The phosphine reagent (5, 7 or 10 eq. per AGU of triethylphosphine (TEP)) was added first to a 100 mL flask followed by dropwise addition of the polymer solution. The mixture was stirred under dry nitrogen and heated to 80° for 24h. Following the reaction, the mixture was cooled to room temperature and the contents of the flask added to dialysis tubing and then dialyzed against ethanol (for 2 d), followed by water (for 1 d). The dialyzed sample was transferred to a round bottom flask and the product recovered by rotary evaporation. The product was dried in a vacuum oven at 50 °C. Yields: 30-80% (80% yield for *P*, *P*, *P*-triethyl-6-deoxy-6-phosphonium-2, 3-di-*O*-acetyl-cellulose from 10 eqs. TEP in DMSO*).*

^{1}H NMR (DMSO-d_6, ppm): 1.2 (CH_3 of trialkylphosphonium)), 2.45 (CH_2 of trialkylphosphonium) 3.4-5.5 (cellulose backbone)

^{13}C NMR (DMSO-d_6, ppm): 169-170 (C=O of ester), 100 (C-1), 70–80 (C-2, C-3, C-4, C-5), 5 (C-6), 21 (C-6 bonded to P).

^{31}P NMR (DMSO-d_6, ppm): 38.8 (phosphorus bonded to C-6).

To determine the degree of substitution (DS) of the product by ^{1}H NMR, the integral of the P-methyl protons was compared to the integral of the cellulose backbone or methyl protons of the acyl group, in a fashion similar to that described above for the ammonium derivatives.

$$DS_{Phosphonium} = \frac{7\, I_{CH3\ of\ Phosphonium}}{9 I_{\ cellulose\ backbone}}$$

4.4. Results and Discussion

Table 4.1: Starting 6-deoxy-6-halo-2, 3-di-*O*-acylcellulose derivatives

Starting material	DS Ester	DS Halide[1]
6Br23Ac	1.91	1.05
6Br23Pr	1.80	1.05
6Br23Bu	1.93	1.05

[1]Determined by elemental analysis

4.4.1 Preliminary kinetic studies

We carried out kinetic studies in order to determine the appropriate conditions for displacement of the 6-halo substituents by trialkylamines. We were concerned that accumulating positive charge along the cellulose chain might at some point limit the achievable DS of 6-trialkylammonium groups, by analogy to the difficulties many researchers have experienced in achieving carboxymethyl DS of greater than about 1.2 vs. the theoretical maximum of approximately 3.0 when synthesizing carboxymethylcellulose [39]. Kinetic ^{1}H NMR studies of reactions conducted at 60°C showed low DS(R_3N^+) values, < 0.05. Increasing the temperature of the reaction to 80°C provided significant improvement in conversion. Due to the boiling points of some of the trialkylamines used, 80°C was the approximate practical maximum temperature we could use at atmospheric pressure in comparative experiments. Therefore, all further preparative experiments were performed at 80°C. Kinetic studies of bromide displacement by Et_3N were carried out in DMSO-d_6, monitoring by proton NMR, after 15 h producing a product with DS ca. 0.24. Within a few minutes of the reaction, a peak at 1.25 ppm in the ^{1}H NMR (**Figure 4.1**), corresponding to the methyl protons attached to the triethylammonium group at C-6, was evident and grew over the

time scale of the reaction. The peak at 3.28 seen clearly starting at 8h was initially obscured by the HOD peak in the NMR and corresponds to the methylene protons attached to the triethylammonium group at C-6. The integrations from the kinetic experiments are meant to provide relative information about the progression of the substitution reaction since the absolute values of the integrations may not be accurate due to suppression of the triethylamine signals (**Figure 4.1**).

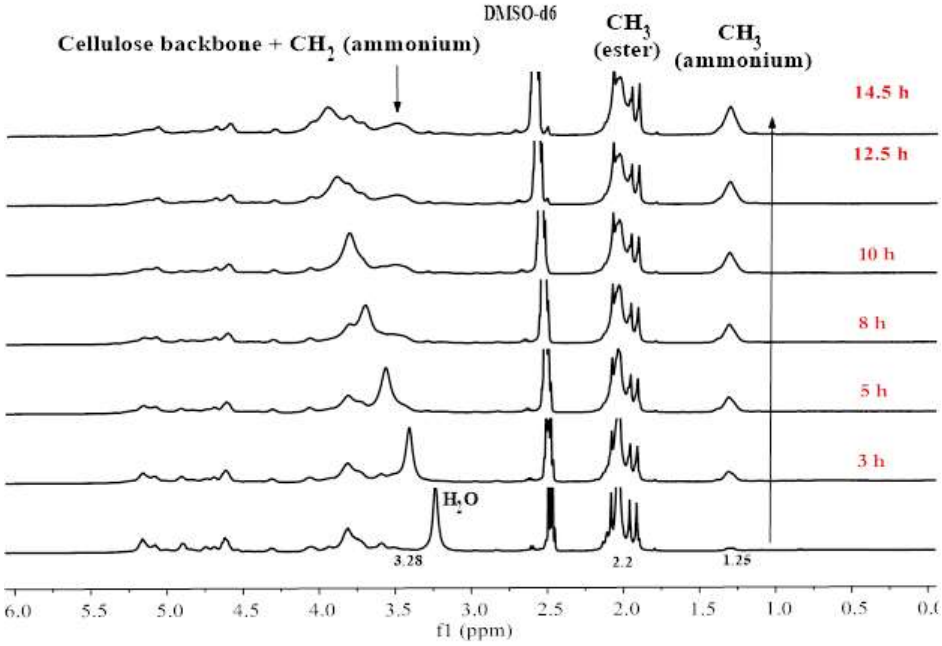

Figure 4.1: Kinetic study of reaction of 6-bromo 2,3 di-*o*-acetyl ester with TEA (5 mol. eq., 15 h, DMSO-d_6, 80°C). (*Note that peaks corresponding to TEA have been suppressed at 0.93 ppm and 2.43 ppm to facilitate better observation of reaction conversion).*

Increasing the proportion of triethylamine to 20 eq. in the kinetic experiments provided only minimal increase in DS(ammonium). The highest DS achieved from the kinetic study was 0.31 for the 6-bromo ester after 15 h at 80°C. Table 4.2 describes the results of kinetic studies of reactions between 6-bromo- and 6-iodo-6-deoxycellulose esters (prepared by Finkelstein reaction of the corresponding 6-bromo derivatives [40]) and triethylamine in DMSO-d_6. Attempts were also made to determine the kinetics of the reaction in DMF-d_7, however reduced miscibility of triethylamine in DMF compared to DMSO and the small total volume of solution required for the NMR experiments gave inconclusive results. Reactions in DMF-d_7 exhibited some heterogeneity and showed very minimal conversion after 15 h, where conversion could be determined. Heterogeneity of the reaction mixture with 100 molar eq. of triethylamine in DMSO-d_6 prevented examination of reaction kinetics at such high reagent excess.

Table 4.2: Results of kinetic studies in DMSO-d_6

Substrate	Mol. eq. TEA	DS Ammonium
6Br23Ac	5	0.24
	20	0.31
6I23Ac	5	0.17
	20	0.28

4.4.2 Limited substitution of ammonium derivatives on the cellulose backbone

Given the results from the kinetic experiments, preparative scale reactions with triethylamine were carried out using a high excess of amine (100 mol eqs.) in anhydrous DMF and DMSO. These reactions were homogeneous because the concentration of triethylamine in the solvent was low enough to prevent immiscibility. The results from the reaction show some increase in the DS attainable vs. the best results in kinetic experiments, as expected given the higher equivalent ratios that were possible in the preparative experiments, with DS(Et_3N^+) = 0.43 being achieved from the 6-bromo-2, 3-di-o-acetyl ester in DMSO. Sodium iodide (NaI) was added to produce the 6-iodo derivative *in situ* in order to utilize the greater leaving group potential of the iodide versus the bromide. In this way, greater substitution of the iodide group for triethylamine could result in higher conversion to the 6-ammonio product[41]. Upon *in situ* addition of 5 molar equivalents of NaI (comparable to that used for the synthesis of 6-deoxy-6-iodo-2, 3-di-*O*-acylcellulose from the brominated derivative under Finkelstein conditions, see experimental section 4.3.3) into the reaction mixture, conversion rose by 12% for the ammonium derivative achieved (maximum DS 0.47 in DMF). These results are described in Table 3. All the derivatives were found to be soluble in DMSO, DMF and methanol but insoluble in water, acetone, THF and ethanol.

Similar modification was performed with tributylamine to test for the influence of a longer chain trialkylamine on the ammonium conversion. The heterogeneous reaction of the amine with 6-bromo-6-deoxy-2,3-di-*O*-acetyl cellulose in THF and DMF produced a derivative with a DS(Bu_3N^+) of ~ 0.06 (**Figure S4.1**). This low DS is likely due primarily to the immiscibility of

the reagent in the solvents investigated (DMSO, THF and DMF, chosen based in part upon the solubility of the starting bromocellulose), as well as to the greater steric demand of the bulkier tributylamine.

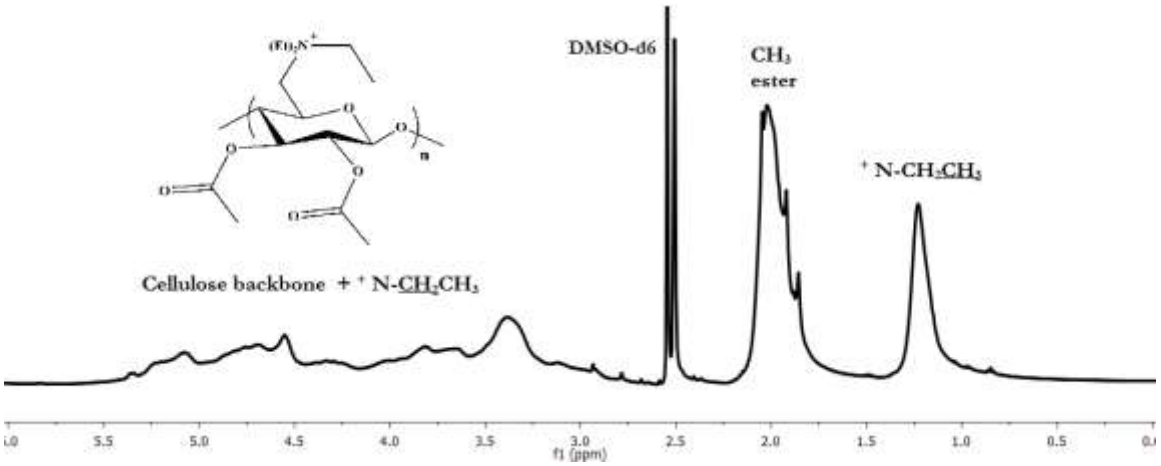

Figure 4.2a: ^{1}H NMR spectrum of DS 0.43 Et_3N^+ derivative of 6-bromo-6-deoxy-2,3-di-*O*-acetyl cellulose using 100 eq. Et_3N

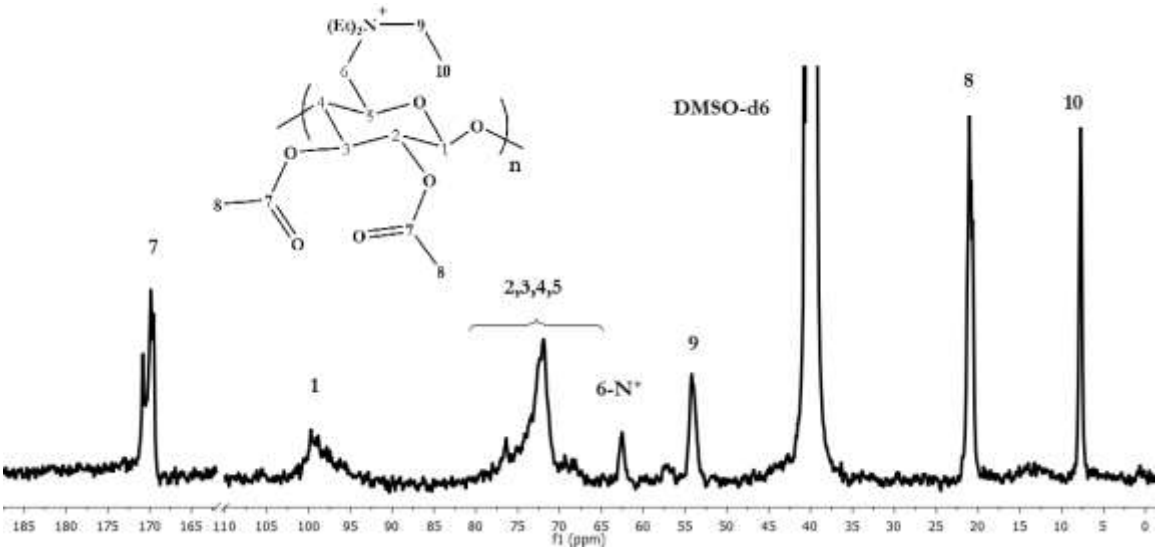

Figure 4.2b: ^{13}C NMR spectrum of Et_3N^+ derivative of 6-bromo-6-deoxy-2,3-di-*O*-acetyl cellulose using 100 eq. Et_3N (DS = 0.43)

Table 4.3. Reaction of Et_3N with 6-halo-6-deoxy-2, 3-di-*O*-acylcellulose derivatives

Product #	Substrate	Solvent	Mol eq. TEA/ (NaI)/(AET)	DS Amm. (Thiol)	DS Ester
1.1	6Br23Ac	DMAc	100/0/0	0.17	1.71
1.2	6Br23Ac	DMI	100/0/0	0.19	1.80
1.3	6Br23Ac	DMF	100/0/0	0.35	1.85
1.4	6Br23Ac	DMF	100/(5)/0	0.47	1.80
1.5	6Br23Ac	DMSO	100/0/0	0.43	1.89
1.6	6Br23Ac	DMSO	100/(5)/0	0.33	1.86
1.7	6Br23Ac	DMSO	100/(10)/0	0.37	1.95
1.8	6Br23Ac	DMSO	100//0/(20)	(0.43)/(*)	1.89
1.9	6Br23Bu	DMSO	100/0/0	0.38	1.93
1.10	6Br23Pr	DMF	100/0/0	0.35	1.80
1.11	6Br23Bu	DMF	100/0/0	0.32	1.75

* DS is difficult to estimate from NMR due to overlapping of the methylene protons of the aminoethanethiol with the backbone and methylene protons of the tetraalkylammonium.and the overlapping of the methyl and amino protons of the ammonium and thiol substituents.

^{1}H NMR confirms the identity of the 6-triethylammonio- -6-deoxy-2, 3-di-*O*-acyl cellulose. The methyl protons of the C-6 Et_3N^+ group are observed at 1.21 ppm. The Et_3N^+ methylene protons overlap the cellulose backbone peaks, but appear around 3.3 ppm. The protons of the methyl peak of the acetyl ester appear between 1.8-2.2 ppm (**Figure 4.2a**).

^{13}C NMR spectrum further confirms identity (**Figure 4.2b);** the methyl and methylene carbons of the N-ethyl groups appear at 7.8 and 54 ppm, respectively. The amine-substituted C-6 peak is predicted by Chemdraw NMR predictor to appear at 58 ppm and appears at 62 ppm in the ^{13}C NMR spectrum. In lower DS(Et_3N^+) products, there is evidence of a small peak at 32 ppm showing residual bromine substituted C-6, but it is not clearly evident in the higher DS product (**Figure 4.2b).** Spectra for the triethylammonium-containing product from 6-bromo-6-deoxy-2, 3-di-*O*-butyryl cellulose can be found in **Figure S4.2.**

The FTIR spectrum of the exemplary ammonium derivative (Product 1.5) shows decreased intensity of the peak at 536 cm^{-1} (Br-CH_2) from the starting material, and new peaks at 1660 (C-$^{+}NEt_3$ stretching) and 1469 cm^{-1} ($^{+}$N-C ethyl bending) confirm the presence of the ammonium substituents **(Figure 4.6).**

4.4.3 Sequential amination and thiolation of 6-deoxy-6-halo-2,3-di-O-acylcellulose derivatives

Due to the limited substitution of the trialkylammonium group, thiolation was devised as a means of replacing residual substituted bromide, since residual alkyl halide may be undesirable in some applications. Similar thiolation had been successfully performed on 6-deoxy-6-bromo cellulose by Aoki et al. [42]. Their reaction of 6-deoxy-6-bromo cellulose with various thiols including 2-aminoethanethiol in the presence of triethylamine, using DMAc as a solvent, gave DS values >0.5 for the thiol substituent. Thiol containing polymers have also become increasingly popular for drug and gene delivery applications [43]. Thiolated polymers have also shown promising results in opening tight junctions for enhanced permeation of hydrophilic drugs[44]. A one-pot reaction was performed on 6-bromo-6-deoxy-2,3-di-*O*-acetyl cellulose in DMSO at 80°C with triethylamine (100 eq., 24h) followed by the thiol (20 eq., 24 h). A portion of the reaction mixture was removed and recovered after 24h before addition of the thiol in order to determine the DS of the trialkylammonium substituent (DS 0.43). The excess triethylamine in the reaction mixture plays dual roles: acting as a base to remove HBr formed during reaction with AET,and helping to convert the thiol groups (pKa 8.32[45]) into more reactive thiolate anions [42]. The thiolated derivative, unlike the solely ammonium substituted derivative, was soluble in water, and also in methanol, DMF, DMAc and DMSO.

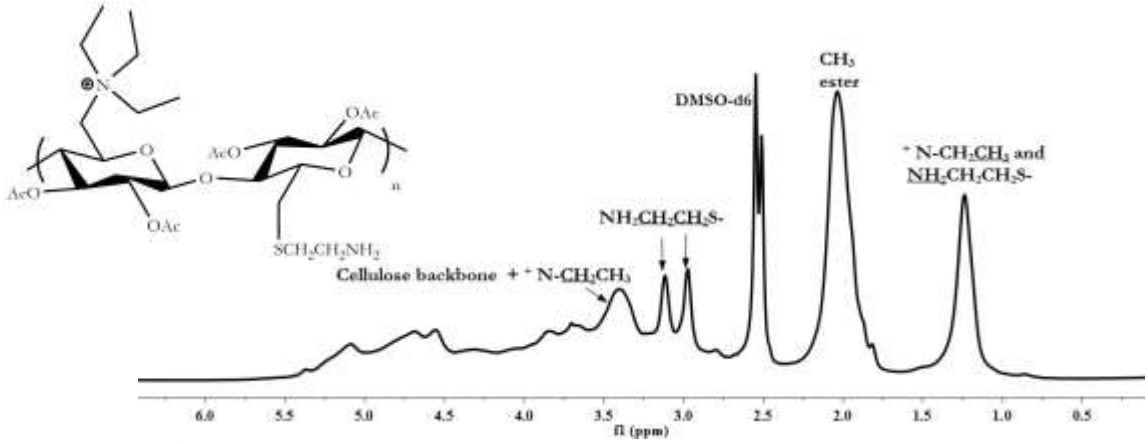

Figure 4.3: ^{1}H NMR spectra of [6-aminoethylthio-co-N, N, N-triethyl-6-ammonium]-6-deoxy, 2,3-di-*O*-acetyl cellulose

The ^{1}H-NMR spectrum of the thiolated derivative is shown in **Figure 4.3.** In comparison with the ^{1}H-NMR spectrum of the tertraakyl ammonium salt, additional resonances appear at 3.0 and 3.1 ppm (methylene peaks of the aminoethylthiol substituent), and a much broader resonance is observed between 1.0 - 1.5 ppm, where the amino protons of the thiol and methyl protons of the ammonium substituent overlap.

The ^{13}C-NMR spectrum in DMSO-d_6 shows the characteristic peaks of the trialkylammonium substituent but also peaks at 35 ppm for thiol substituted C-6, and at 38 and 41 ppm for the -$SCH_2\underline{CH_2}NH_2$ and -$S\underline{CH_2}CH_2NH_2$ methylene carbons, respectively. The methylene carbons are somewhat obscured by the solvent peak in DMSO-d_6 but are more obvious in a spectrum recorded in D_2O.

The FTIR spectrum of the derivative from reaction with 2-aminoethanethiol shows peaks at 1585 and 1650 cm^{-1} due to the protonated amine (**Figure 4.6**). This is similar to spectra observed upon reaction of bromocellulose with 2-aminoethanethiol by Aoki et al. [46].

4.4.4 Reaction of 6-bromo-6-deoxycellulose ester with diethylamine

Due to the incomplete conversion of 6-bromo-2,3-di-*O*-acetylated cellulose to the triethylammonium derivative observed even at very high molar eq. of amine, it was hypothesized that repulsion between accumulating positive charges along the polymer backbone could be a source of this limitation. To investigate this hypothesis, 6-bromo-2, 3-di-*O*-acetylcellulose was reacted with 100 molar equivalents of diethylamine in anhydrous DMSO, with the intent of producing an uncharged trialkylamine cellulose derivative. There was some concern with this reaction that crosslinking could occur, since it might be possible for the initial trialkylamine product to displace halides on other cellulose chains to form bridging tetraalkylammonium salts. In the event this was not a problem, as indicated by spectroscopic analysis of the product as well as its solubility characteristics. We were gratified upon analyzing the product by ^{1}H NMR to learn that DS(NEt_2) was close to 0.9. The large excess of Et_2NH reagent used permitted direct comparison of the results to those reactions with the same molar excess of trialkylamine reagents.

The absence of positive charge along the cellulose backbone does indeed allow for much higher reaction conversion, providing support for the charge repulsion hypothesis. The ^{1}H-NMR spectrum of the trialkylamine derivative is shown in **Figure 4.4**. The methyl protons of the C-6 trialkylamine ethyl groups are observed at 1.5 ppm, while the methylene protons of the amine appear at 3.3 ppm.

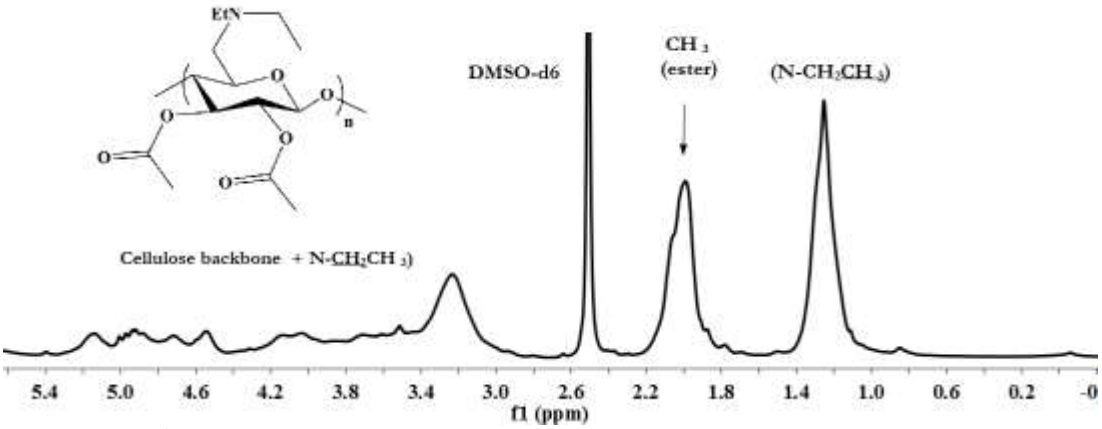

Figure 4.4: ^{1}H NMR spectrum of 6-deoxy-6-diethylamino-2,3-di-*O*-acetylcellulose (DS(NEt_2) = 0.88)

4.4.5 Reaction with trialkylphosphines

We were hopeful that displacement with trialkylphosphines, to afford 6-deoxy-6-phosphonium derivatives, would be more efficient since the larger phosphorus atom would be more able to disperse the positive charge. These phosphonium derivatives were also of strong interest for poly(nucleic acid) delivery and other applications. In the event, 6-bromo-6-deoxy-2,3-di-*O*-acetylcellulose was reacted with triethylphosphine in DMF at 80°C using up to 10 molar equivalents of the reagent. Product 2.1 DS(PEt_3^+) was found to be approximately 0.52(out of a potential DS of 1) with 7 equiv Et_3P, and 0.60 with 10 equiv (Table 4). The derivatives produced were soluble in DMSO, DMF, methanol and water. The ^{1}H NMR spectrum of the phosphonium-containing product is shown in **Figure 4.5a**. The methyl protons of the C-6 Et_3P^+ group are observed at 1.25 ppm and the Et_3P^+ methylene protons at about 2.45 ppm. Figure 5b shows the ^{13}C NMR spectrum of the phosphonium-containing product with peaks at 5.3 ppm and 11.4 ppm confirming the presence of methyl and methylene carbons of the ethyl groups bonded to phosphorus in the cellulose backbone. The phosphine–substituted C-6 peak is predicted by Chemdraw NMR predictor to appear at 18.4 ppm and is likely obscured by the methyl carbon of

the acetate ester in **Fig. 4.5b** but is more visible in the spectrum of the butyryl ester derivative at 21 ppm (**Figure S4.3b**). The peak at 32 ppm in **Fig. 4.5b** is indicative of residual bromine-substituted C-6. The presence of the phosphonium derivative was also verified using ^{31}P NMR. The spectrum in **Fig. 4.5c** shows a single peak at 38.8 ppm corresponding to the phosphorus atom bonded to C-6. For comparison, , the ^{31}P NMR shift of a tetramethylphosphonium chloride hydrate was found to be 37.8 ppm [47]. The phosphonium P of a water soluble derivative of poly(acrylic acid) modified with triethylphosphine has been reported at 39.2 ppm in the ^{31}P NMR [8]. This reference also reported the P-methyl and methylene protons of the phosphonium derivative at 1.22 and 2.3 ppm respectively in the ^{1}H NMR spectrum. Therefore, the ^{31}P and ^{1}H NMR shifts of the 6-phosphonium derivative are consistent with those of comparable compounds in the literature. The phosphorus atom of triethylphosphine (-20 ppm) is not evident in the product ^{31}P NMR spectrum.

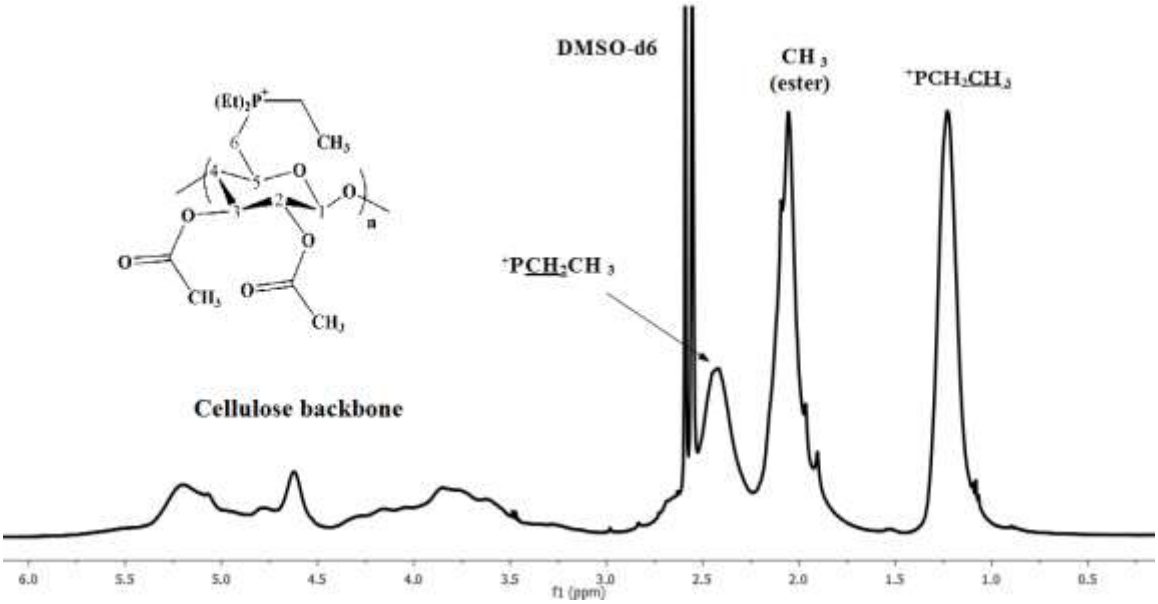

Figure 4.5a: ^{1}H NMR spectrum of Et_3P^+ derivative (DS 0.73) of 6-bromo-6-deoxy-2,3-di-*O*-acetyl cellulose (10 equiv. Et_3P).

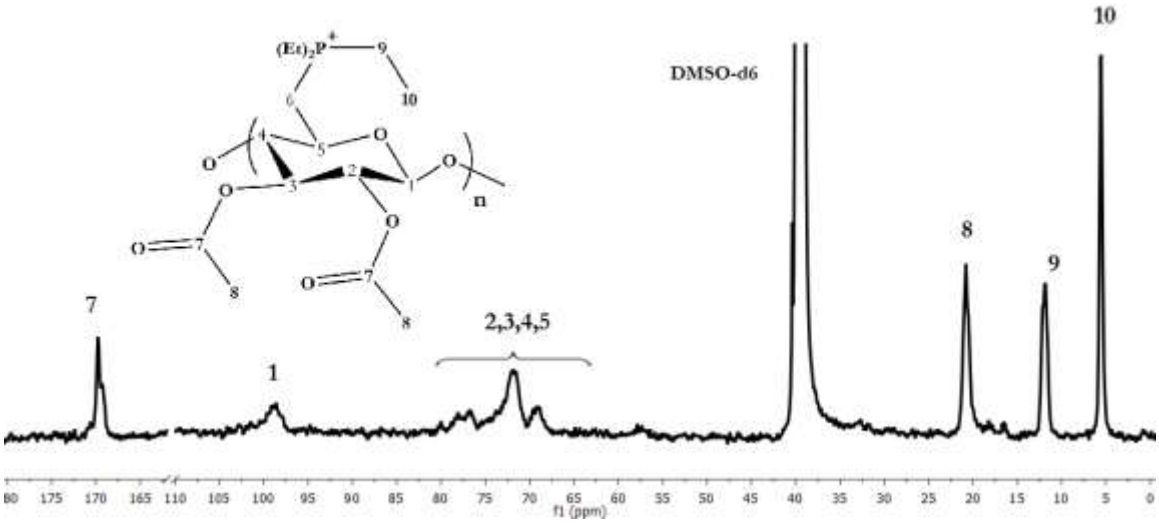

Figure 4.5b: ^{13}C NMR spectrum of Et_3P^+ derivative (DS 0.73) of 6-bromo-6-deoxy-2,3-di-*O*-acetyl cellulose (10 equiv. Et_3P).

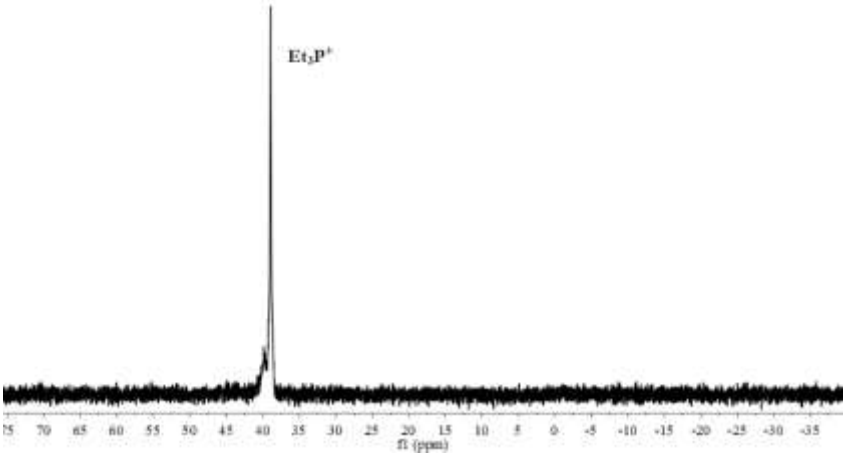

Figure 4.5c: ^{31}P NMR spectrum of *P, P, P*- triethyl-6-deoxy-6-phosphonium-2, 3-di-O-acyl-cellulose

Substituting DMSO for DMF as reaction solvent (6-bromo-6-deoxy-2, 3-di-*O*-acetylcellulose, 10 equiv. Et_3P) afforded slight DS improvement (DS Et_3P^+ 0.73).

Similar reactions of Et_3P with 6-bromo-2, 3-di-*O*-butyryl cellulose showed little sensitivity of conversion to the chain length of the 2,3-*O*-ester groups (DS (Et_3P^+) 0.60 Ac vs. 0.59 Bu in DMF and 0.73 Ac vs. 0.68 Bu in DMSO) as shown in Table 4.4. The corresponding spectra for the butyryl ester phosphonium product can be found in **Figure S4.3**.

Peaks at 1460 (C-$^{+}$PEt$_3$ stretch) and 776 cm^{-1}(P-C ethyl stretch) in the FTIR spectra of product 2.4 **(Figure 4.6)** further confirm successful incorporation of the phosphonium substituent.

Table 4.4: Synthesis of *P, P, P*-triethyl-6-deoxy-6-phosphonium-2, 3-di-*O*-acyl-cellulose

Product #	Substrate	Mol Eq. Et$_3$P	Solvent	DS(Et$_3$P^{+})	DS ester
2.1	6Br23Ac	7	DMF	0.52	1.89
2.2	6I23Ac	7	DMF	0.54	1.88
2.3	6Br23Ac	10	DMF	0.60	1.84
2.4	6Br23Ac	10	DMSO	0.73	1.91
2.5	6Br23Bu	10	DMF	0.59	1.77
2.6	6Br23Bu	10	DMSO	0.68	1.92

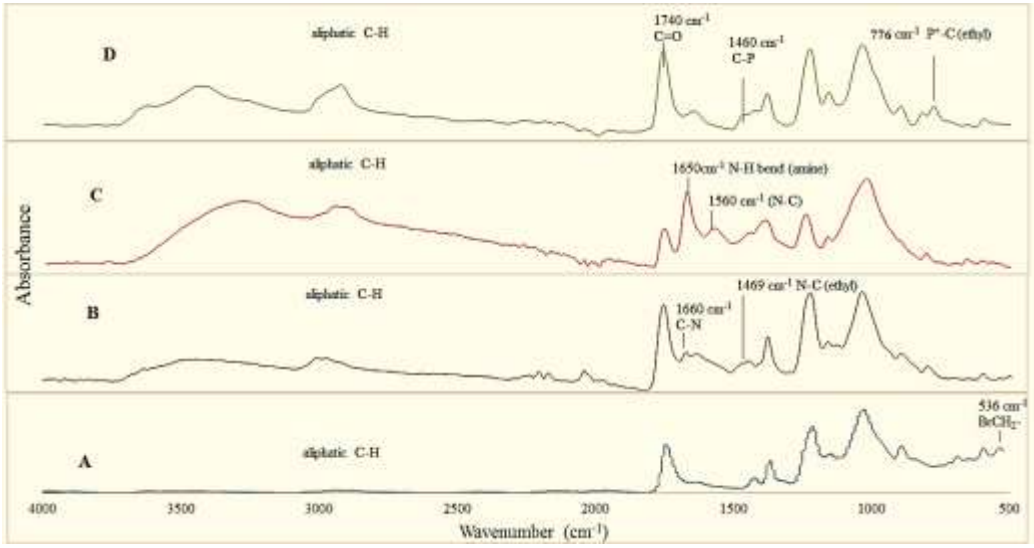

Figure 4.6: Comparison of the FTIR spectra of representative derivatives. 6-bromo-6-deoxy-2,3-di-*O*-acetyl cellulose (A), representative 6-ammonio derivative thereof (Product 1.5, (DS(Et$_3$N^{+}) 0.43) (B), thiolated derivative of (B) (Product 1.8, DS(Et$_3$N^{+}) 0.43, (C) and 6-triethylphosphonio derivative (Product 2.4, DS(Et$_3$P^{+}) 0.73 (D).

4.4.6 Thermal properties of the cationic derivatives

Thermal properties of the derivatives were investigated using TGA and DSC. The ammonium samples of cellulose showed initial degradative weight loss between 220 and 235 °C. This was

typical of all the ammonium derivatives, compared to a onset degradation temperatures between 210°C and 219°C for the starting 6-bromo-6-deoxy-2,3-di-*O*-acyl esters. However, we were surprised to find that the phosphonium derivatives showed initial weight loss between 195 and 200°C. The ammonium and phosphonium derivatives from 6-iodo-6-deoxy-2,3-di-*O*-acyl esters displayed a slightly higher degradation temperature. The thiolated derivative with DS Et_3N^+ 0.43 and its corresponding thiol began to degrade at temperatures > 160 °C, and ca. 11% weight loss was seen between 160 and 180°C. The thiol containing derivative showed the most potential as a flame retardant material[48]. of the derivatives with a total weight loss of just ~ 62 % compared to ~ 75% for the ammonium and phosphonium derivatives. We have not investigated the nature of these decomposition steps in detail. TGA curves of representative samples are shown in **Figure 4.7.** Thermal analyses by DSC did not show any evidence of a T_g before the decomposition temperature for most of the ammonium and phosphonium derivatives analyzed. However, a T_g was visible at 105 °C in the thiol derivative (Product 1.8) by modulated DSC. Similarly, the Et_3P^+ derivative (DS 0.68) and Et_3P^+ (DS 0.38) of 6-bromo-6-deoxy-2,3-di-*O*-butyryl cellulose displayed T_g values at 164 °C and 122°C respectively **(Figure 4.8).**

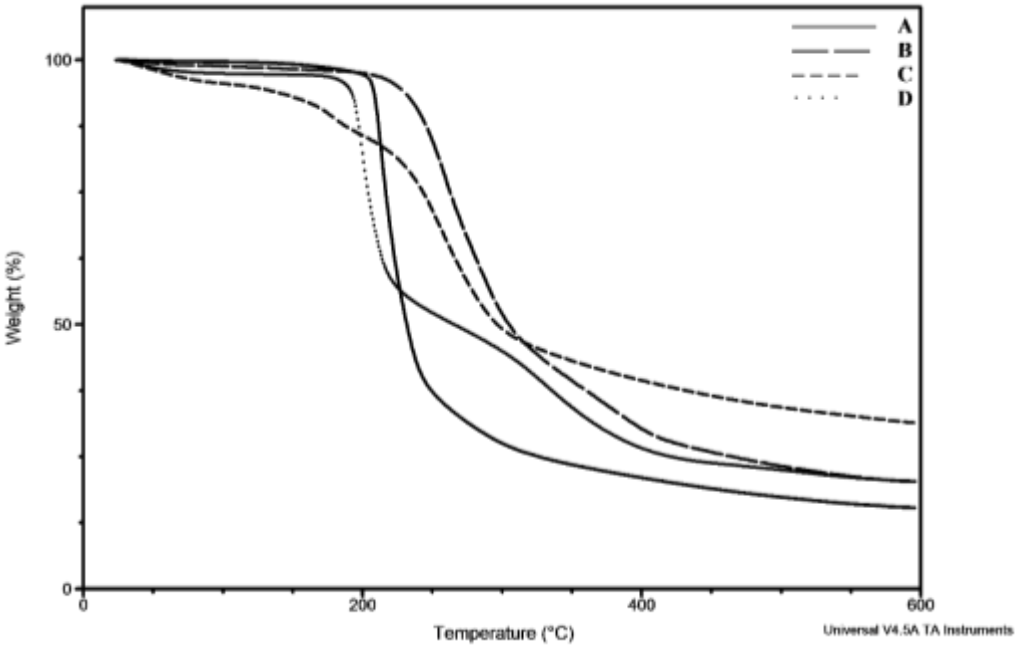

Figure 4.7: Comparison of the thermal degradation profiles of representative derivatives. 6-bromo-6-deoxy-2,3-di-*O*-acetyl cellulose (A) and its representative 6-ammonio (DS(Et_3N^+) 0.35 from 6Br23Ac) (B), thiolated (DS(Et_3N^+ 0.43) (C) and 6-phosphonio (DS(Et_3P^+) 0.73 from 6Br23Ac)(D) derivatives.

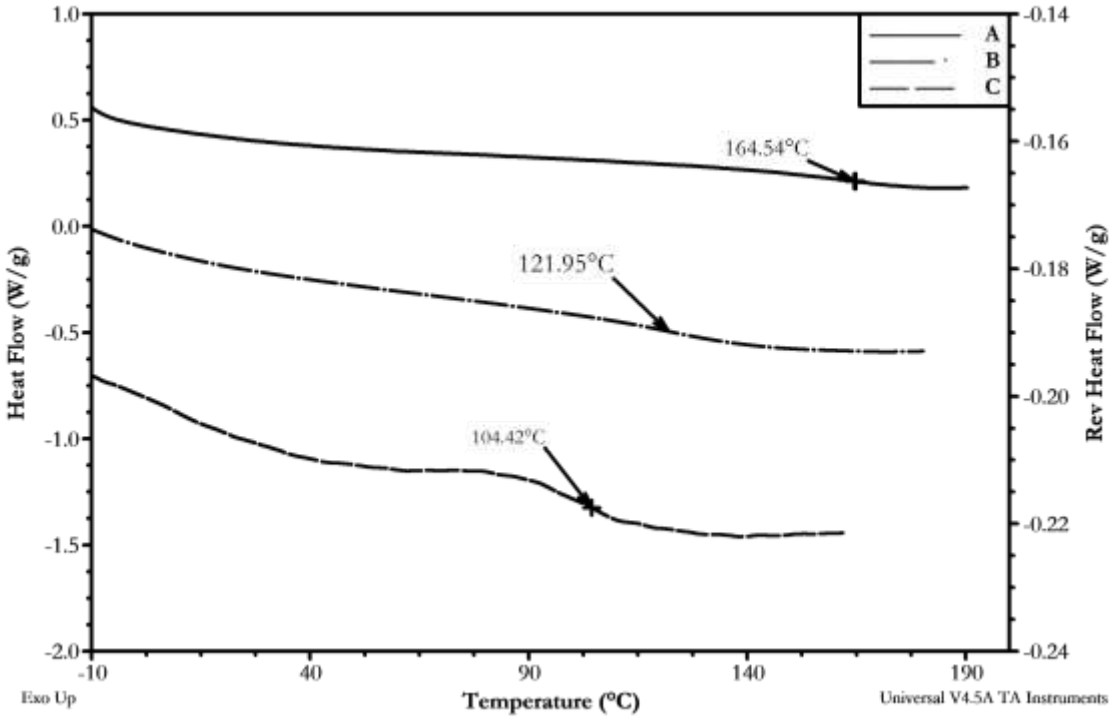

Figure 4.8: DSC thermograms for representative derivatives. A) *P, P, P*-triethyl-6-deoxy-6-phosphonio-2,3-di-*O*-butyryl-cellulose (DS(Et_3P^+) 0.68) , B) *N, N, N*-triethyl-6-deoxy-6-ammonio-2,3-di-*O*-butyryl-cellulose (DS(Et_3N^+) 0.38) and C) thiolated (DS (DS(Et_3N^+) 0.43)) *N, N, N*-trialkyl-6-amino-6-deoxy-2,3-di-*O*-acetyl cellulose derivative.

4.5 Conclusions:

We have established effective new synthetic pathways to cationic derivatives of cellulose by regioselective substitution at C-6 to produce ammonium and phosphonium derivatives. Starting with brominated and iodinated cellulose esters, substantial positive charge could be introduced in fully regioselective fashion, by direct displacement reactions. At the same time, we observed limitations to the degree of substitution attainable. The highest DS Et_3N^+ achieved was ~0.47, while maximum DS Et_3P^+ was ~ 0.73. The limitations in DS were attributed to the accumulation of positive charges along the cellulose backbone during conversion to the cationic derivative. Reactions with dialkylamine reagent supported this theory with a DS as high as 0.9 being achieved for the *N, N*-dialkyl-6-amino-6-deoxy-2, 3-di-*O*-acetyl-cellulose derivative under conditions

identical to those used to make the cationic tetraalkylammonium derivatives. DS of positively charges substituent could be maximized by using a moderate excess of trialkylamine or trialkylphosphine in a polar aprotic solvent. Addition of sodium iodide into the reaction vessel during reactions with trialkylamine afforded a slight increase in conversion to the ammonium derivative. The *O*-acylated ammonium derivatives obtained in this work did not have sufficient DS(R_3N^+) to be soluble in pure water. In order to devise a route to complete removal of the bromide from the cellulose backbone, we first reacted regioselectively substituted bromocellulose esters with trialkylamine followed by reaction of the residual 6-halo substituents with a thiol. We were able to confirm the incorporation of the thiol through elemental analysis, and observed the added benefit that that this further derivatization produced a water-soluble cellulose derivative with appended ammonium and thiol-containing groups. Likely due to the ca. 15-17% higher conversions achieved, all of the phosphonium derivatives exhibited aqueous solubility. There does not appear to be a strong advantage for using 6-iodo- versus 6-bromo-6-deoxycellulose esters; the developing polycationic charge appears to be the more limiting factor, especially for the reactions with trialkylamines. Displacement reactions in DMSO were consistently more effective than in other polar aprotic solvents.

These synthetic methods provide facile access to permanently positively charged cellulose derivatives, substituted regioselectively and in some cases having substantial water solubility. Further exploration of these methods and the cationic derivatives available therefrom are underway in our laboratory and will be of great interest for revealing structure-property relationships with regard to tight junction opening, complexation of poly(nucleic acids) for their delivery to cell nuclei, and effective delivery of anionic drugs, to name just a few aspects of the biomedical application potential of these derivatives.

4.6 References

1. Hemp, S. T.; Allen Jr, M. H.; Green, M. D.; Long, T. E., Phosphonium-containing polyelectrolytes for nonviral gene delivery. *Biomacromolecules* **2011,** *13* (1), 231-238.
2. Grayson, A. C. R.; Doody, A. M.; Putnam, D., Biophysical and structural characterization of polyethylenimine-mediated siRNA delivery in vitro. *Pharmaceutical research* **2006,** *23* (8), 1868-1876.
3. Dufès, C.; Uchegbu, I. F.; Schätzlein, A. G., Dendrimers in gene delivery. *Advanced drug delivery reviews* **2005,** *57* (15), 2177-2202.
4. Lai, W.-F.; Lin, M. C.-M., Nucleic acid delivery with chitosan and its derivatives. *Journal of Controlled Release* **2009,** *134* (3), 158-168.
5. Xie, W.; Xie, R.; Pan, W.-P.; Hunter, D.; Koene, B.; Tan, L.-S.; Vaia, R., Thermal Stability of Quaternary Phosphonium Modified Montmorillonites. *Chemistry of Materials* **2002,** *14* (11), 4837-4845.
6. (a) Ren, H.; Sun, J.; Wu, B.; Zhou, Q., Synthesis and properties of a phosphorus-containing flame retardant epoxy resin based on bis-phenoxy (3-hydroxy) phenyl phosphine oxide. *Polymer degradation and stability* **2007,** *92* (6), 956-961; (b) Ebdon, J. R.; Price, D.; Hunt, B. J.; Joseph, P.; Gao, F.; Milnes, G. J.; Cunliffe, L. K., Flame retardance in some polystyrenes and poly(methyl methacrylate)s with covalently bound phosphorus-containing groups: initial screening experiments and some laser pyrolysis mechanistic studies. *Polymer Degradation and Stability* **2000,** *69* (3), 267-277.
7. Monge, S.; Canniccioni, B.; Graillot, A.; Robin, J.-J., Phosphorus-Containing Polymers: A Great Opportunity for the Biomedical Field. *Biomacromolecules* **2011,** *12* (6), 1973-1982.
8. Ornelas-Megiatto, C. t.; Wich, P. R.; Fréchet, J. M., Polyphosphonium polymers for siRNA delivery: an efficient and nontoxic alternative to polyammonium carriers. *Journal of the American Chemical Society* **2012,** *134* (4), 1902-1905.
9. Floch, V.; Loisel, S.; Guenin, E.; Hervé, A. C.; Clément, J. C.; Yaouanc, J. J.; des Abbayes, H.; Férec, C., Cation Substitution in Cationic Phosphonolipids: A New Concept To Improve Transfection Activity and Decrease Cellular Toxicity. *Journal of Medicinal Chemistry* **2000,** *43* (24), 4617-4628.
10. (a) Hemp, S. T.; Allen Jr, M. H.; Smith, A. E.; Long, T. E., Synthesis and properties of sulfonium polyelectrolytes for biological applications. *ACS Macro Letters* **2013,** *2* (8), 731-735; (b) De Smedt, S. C.; Demeester, J.; Hennink, W. E., Cationic polymer based gene delivery systems. *Pharmaceutical research* **2000,** *17* (2), 113-126.
11. Cimecioglu, A. L.; Ball, D. H.; Kaplan, D. L.; Huang, S. H., Preparation of Amylose Derivatives Selectively Modified at C-6 - 6-Amino-6-Deoxyamylose. *Macromolecules* **1994,** *27* (11), 2917-2922.
12. (a) Nichifor, M.; Stanciu, M. C.; Simionescu, B. C., New cationic hydrophilic and amphiphilic polysaccharides synthesized by one pot procedure. *Carbohydrate Polymers* **2010,** *82* (3), 965-975; (b) Nichifor, M.; Bastos, M.; Lopes, S.; Lopes, A., Characterization of aggregates formed by hydrophobically modified cationic dextran and sodium alkyl sulfates in salt-free aqueous solutions. *The Journal of Physical Chemistry B* **2008,** *112* (49), 15554-15561.
13. Fox, S. C.; Edgar, K. J., Staudinger Reduction Chemistry of Cellulose: Synthesis of Selectively O-Acylated 6-Amino-6-deoxy-cellulose. *Biomacromolecules* **2012,** *13* (4), 992-1001.

14. (a) Santhosh, S.; Sini, T. K.; Anandan, R.; Mathew, P. T., Effect of chitosan supplementation on antitubercular drugs-induced hepatotoxicity in rats. *Toxicology* **2006,** *219* (1–3), 53-59; (b) Santhosh, S.; Sini, T. K.; Anandan, R.; Mathew, P. T., Hepatoprotective activity of chitosan against isoniazid and rifampicin-induced toxicity in experimental rats. *European Journal of Pharmacology* **2007,** *572* (1), 69-73.
15. (a) Lim, C. K.; Halim, A. S.; Zainol, I.; Noorsal, K., In vitro evaluation of a biomedical-grade bilayer chitosan porous skin regenerating template as a potential dermal scaffold in skin tissue engineering. *International Journal of Polymer Science* **2011,** *2011*; (b) Pillai, C. K. S.; Sharma, C. P., Review paper: absorbable polymeric surgical sutures: chemistry, production, properties, biodegradability, and performance. *Journal of biomaterials applications* **2010,** *25* (4), 291-366.
16. (a) Lee, C. G.; Da Silva, C. A.; Lee, J.-Y.; Hartl, D.; Elias, J. A., Chitin regulation of immune responses: an old molecule with new roles. *Current Opinion in Immunology* **2008,** *20* (6), 684-689; (b) Chung, M. J.; Park, J. K.; Park, Y. I., Anti-inflammatory effects of low-molecular weight chitosan oligosaccharides in IgE–antigen complex-stimulated RBL-2H3 cells and asthma model mice. *International immunopharmacology* **2012,** *12* (2), 453-459; (c) Lee, Y. M.; Kim, S. S., Properties of chitin, chitin derivatives and blends with PVA. *Korea Polymer Journal* **1996,** *4* (2), 178-185; (d) Zhou, J. P.; Zhang, L.; Deng, Q. H.; Wu, X. J., Synthesis and characterization of cellulose derivatives prepared in NaOH/urea aqueous solutions. *Journal of Polymer Science Part a-Polymer Chemistry* **2004,** *42* (23), 5911-5920.
17. (a) Jiang, X.; Xin, H.; Gu, J.; Du, F.; Feng, C.; Xie, Y.; Fang, X., Enhanced Antitumor Efficacy by d-Glucosamine-Functionalized and Paclitaxel-Loaded Poly (Ethylene Glycol)-Co-Poly (Trimethylene Carbonate) Polymer Nanoparticles. *Journal of pharmaceutical sciences* **2014,** *103* (5), 1487-1496; (b) Chesnokov, V.; Gong, B.; Sun, C.; Itakura, K., Anti-cancer activity of glucosamine through inhibition of N-linked glycosylation. *Cancer cell international* **2014,** *14* (1), 45.
18. Kumar, M. N. V. R., A review of chitin and chitosan applications. *Reactive and Functional Polymers* **2000,** *46*, 1-27.
19. (a) Krishna, C.; Pillai, S.; Sharma, C. P., Review Paper: Absorbable Polymeric Surgical Sutures: Chemistry, Production, Properties, Biodegradability, and Performance. *Journal of Biomaterials*
Applications **2010,** *25*, 291-366; (b) Dutta, P. K.; Dutta, J.; Tripathi, V. S., Chitin and chitosan: Chemistry, properties and applications. *Journal of Scientific & Industrial Research* **2004,** *63*, 20-31.
20. Thanou, M.; Verhoef, J. C.; Junginger, H. E., Chitosan and its derivatives as intestinal absorption enhancers. *Advanced Drug Delivery Reviews* **2001,** *50, Supplement 1* (0), S91-S101.
21. (a) Prashanth, K. V. H.; Tharanathan, R. N., Chitin/chitosan: modifications and their unlimited application potential - an overview. *Trends in Food Science & Technology* **2007,** *18* (3), 117-131; (b) Bansal, V.; Sharma, P. K.; Sharma, N.; Pal, O. P.; Malviya, R., Applications of Chitosan and Chitosan Derivatives in Drug Delivery. *Advances in Biological Research* **2011,** *5* (1), 28-37.
22. (a) Bernkop-Schnürch, A.; Kast, C. E., Chemically modified chitosans as enzyme inhibitors. *Advanced Drug Delivery Reviews* **2001,** *52* (2), 127-137; (b) Illum, L.; Farraj, N. F.; Davis, S. S., Chitosan as a novel nasal delivery system for peptide drugs. *Pharm. Res.* **1994,** *11*, 1186–1189.

23. (a) Lorenzo-Lamosa, M. L.; Remuñán-López, C.; Vila-Jato, J. L.; Alonso, M. J., Design of microencapsulated chitosan microspheres for colonic drug delivery. *Journal of Controlled Release* **1998,** *52* (1–2), 109-118; (b) Hejazi, R.; Amiji, M., Chitosan-based gastrointestinal delivery systems. *Journal of Controlled Release* **2003,** *89* (2), 151-165.
24. (a) Thanou, M.; Junginger, H. E., *Pharmaceutical Applications of Chitosan and Derivatives.* Marcel Dekker: New York, 2005; (b) Dash, M.; Chiellini, F.; Ottenbrite, R. M.; Chiellini, E., Chitosan: A versatile semi-synthetic polymer in biomedical applications. *Progress in Polymer Science* **2011,** *36* (8), 981-1014.
25. Thanou, M.; Verhoef, J. C.; Junginger, H. E., Oral drug absorption enhancement by chitosan and its derivatives. *Advanced Drug Delivery Reviews* **2001,** *52* (2), 117-126.
26. Artursson, P.; Lindmark, T.; Davis, S. S.; Illum, L., Effect of chitosan on the permeability of monolayers of intestinal epithelial cells (Caco-2). *Pharm. Res.* **1994,** *11*, 1358–1361.
27. Bowman, K.; Leong, K. W., Chitosan nanoparticles for oral drug and gene delivery. *Int J Nanomedicine* **2006,** *1* (1176-9114 (Print)), 117-128.
28. (a) Azzam, T.; Raskin, A.; Makovitzki, A.; Brem, H.; Vierling, P.; Lineal, M.; Domb, A. J., Cationic Polysaccharides for Gene Delivery. *Macromolecules* **2002,** *35* (27), 9947-9953; (b) Nagasaki, T.; Hojo, M.; Uno, A.; Satoh, T.; Koumoto, K.; Mizu, M.; Sakurai, K.; Shinkai, S., Long-Term Expression with a Cationic Polymer Derived from a Natural Polysaccharide: Schizophyllan†. *Bioconjugate Chemistry* **2004,** *15* (2), 249-259; (c) Kamiński, K.; Płonka, M.; Ciejka, J.; Szczubiałka, K.; Nowakowska, M.; Lorkowska, B.; Korbut, R.; Lach, R., Cationic Derivatives of Dextran and Hydroxypropylcellulose as Novel Potential Heparin Antagonists. *Journal of Medicinal Chemistry* **2011,** *54* (19), 6586-6596.
29. Kotze, A. F.; Lueßen, H. L.; de Leeuw, B. J.; de Boer, A. G.; Verhoef, J. C.; Junginger, H. E., N-trimethyl chitosan chloride as a potential absorption enhancer across mucosal surfaces: in vitro evaluation in intestinal epithelial cells (Caco-2). *Pharm. Res.* **1997,** *14*, 1197-1202.
30. Khardin, A. P.; Tuzhikov, O. I.; Lemasov, A. I., New phosphorus containing cellulose derivatives. *Polymer Science U.S.S.R.* **1982,** *24* (9), 2115-2120.
31. Wang, L.; Xu, X.; Guo, S.; Peng, Z.; Tang, T., Novel water soluble phosphonium chitosan derivatives: Synthesis, characterization and cytotoxicity studies. *International Journal of Biological Macromolecules* **2011,** *48* (2), 375-380.
32. Kenawy, E.-R.; Abdel-Hay, F. I.; El-Shanshoury, A. E.-R. R.; El-Newehy, M. H., Biologically active polymers: synthesis and antimicrobial activity of modified glycidyl methacrylate polymers having a quaternary ammonium and phosphonium groups. *Journal of Controlled Release* **1998,** *50* (1–3), 145-152.
33. Furuhata, K.-i.; Koganei, K.; Chang, H.-S.; Aoki, N.; Sakamoto, M., Dissolution of cellulose in lithium bromide-organic solvent systems and homogeneous bromination of cellulose with N-bromosuccinimide-triphenylphosphine in lithium bromide-N,N-dimethylacetamide. *Carbohydrate Research* **1992,** *230* (1), 165-177.
34. Fox, S. C.; Li, B.; Xu, D.; Edgar, K. J., Regioselective esterification and etherification of cellulose: a review. *Biomacromolecules* **2011,** *12* (6), 1956-72.
35. Matsui, Y.; Ishikawa, J.; Kamitakahara, H.; Takano, T.; Nakatsubo, F., Facile synthesis of 6-amino-6-deoxycellulose. *Carbohydrate Research* **2005,** *340* (7), 1403-1406.
36. Fox, S. C.; Edgar, K. J., Synthesis of regioselectively brominated cellulose esters and 6-cyano-6-deoxycellulose esters. *Cellulose* **2011,** *18* (5), 1305-1314.
37. Pereira, J. M.; Edgar, K. J., Regioselective synthesis of 6-amino- and 6-amido-6-deoxypullulans. *Cellulose* **2014,** *21* (4), 2379-2396.

38. (a) Zhang, R.; Edgar, K. J., Synthesis of curdlan derivatives regioselectively modified at C-6: O-(N)-Acylated 6-amino-6-deoxycurdlan. *Carbohydrate Polymers* **2014,** *105* (0), 161-168; (b) Zhang, R.; Edgar, K. J., Water-soluble aminocurdlan derivatives by chemoselective azide reduction using NaBH4. *Carbohydrate Polymers* **2015,** *122* (0), 84-92.
39. Heinze, T.; Pfeiffer, K., Studies on the synthesis and characterization of carboxymethylcellulose. *Die Angewandte Makromolekulare Chemie* **1999,** *266* (1), 37-45.
40. Rahn, K.; Diamantoglou, M.; Klemm, D.; Berghmans, H.; Heinze, T., Homogeneous synthesis of cellulose p-toluenesulfonates in N, N-dimethylacetamide/LiCl solvent system. *Die Angewandte Makromolekulare Chemie* **1996,** *238* (1), 143-163.
41. (a) Hammett, L. P., *Physical Organic Chemistry*. 2nd ed.; McGraw-Hill: New York, 1970; (b) McCortney, B.; Jacobson, B.; Vreeke, M.; Lewis, E. S., Methyl transfers. 14. Nucleophilic catalysis of nucleophilic substitution. *Journal of the American Chemical Society* **1990,** *112* (9), 3554-3559.
42. Aoki, N.; Furuhata, K. I.; Saegusa, Y.; Nakamura, S.; Sakamoto, M., Reaction of 6-bromo-6-deoxycellulose with thiols in lithium bromide-N,N-dimethylacetamide. *Journal of Applied Polymer Science* **1996,** *61* (7), 1173-1185.
43. Liechty, W. B.; Kryscio, D. R.; Slaughter, B. V.; Peppas, N. A., Polymers for drug delivery systems. *Annual review of chemical and biomolecular engineering* **2010,** *1*, 149.
44. Clausen, A. E.; Kast, C. E.; Bernkop-Schnürch, A., The role of glutathione in the permeation enhancing effect of thiolated polymers. *Pharmaceutical research* **2002,** *19* (5), 602-608.
45. Riauba, L.; Niaura, G.; Eicher-Lorka, O.; Butkus, E., A study of cysteamine ionization in solution by Raman spectroscopy and theoretical modeling. *The Journal of Physical Chemistry A* **2006,** *110* (50), 13394-13404.
46. Aoki, N.; Koganei, K.; Chang, H.-S.; Furuhata, K.-i.; Sakamoto, M., Gas chromatographic—mass spectrometric study of reactions of halodeoxycelluloses with thiols in aqueous solutions. *Carbohydrate Polymers* **1995,** *27* (1), 13-21.
47. Margraf, G.; Lerner, H.-W.; Bolte, M., Tetramethylphosphonium chloride hydrate. *Acta Crystallographica Section E* **2002,** *58* (5), o546-o547.
48. Laoutid, F.; Bonnaud, L.; Alexandre, M.; Lopez-Cuesta, J.-M.; Dubois, P., New prospects in flame retardant polymer materials: from fundamentals to nanocomposites. *Materials science and engineering: R: Reports* **2009,** *63* (3), 100-125.

Chapter 5: 6-Carboxycellulose Acetate Butyrate as a Novel Polymer for Amorphous Solid Dispersion and Extrusion

5.1 Abstract:

Amorphous solid dispersions (ASDs) prepared in cellulose derivative matrices are extremely useful for reducing crystallinity, preventing recrystallization, and for giving more sustained release of highly water insoluble, crystalline active pharmaceutical ingredients (APIs). 6-Carboxycellulose acetate butyrate (CCAB) is a new commercial cellulose derivative, recently introduced for use in waterborne coatings applications. The structurally diverse drugs quercetin (Que), ibuprofen (Ibu), loratadine (Lor) and clarithromycin (CLA) were formulated using CCAB as matrix polymer. ASDs were prepared in order to identify the effectiveness of the polymer matrix material at providing solubility enhancement and improved drug release for these chosen drug actives. ASDs were prepared by spray drying. Furthermore, we discovered that unexpectedly CCAB could also be melt extruded to prepare ASDs, in spite of its high DS of both OH groups and carboxyl groups. ASDs were analyzed using powder X ray diffraction (XRD) and differential scanning calorimetry (DSC) for comparison of crystallinity to the pure drugs and for examination of the thermal properties of the resulting ASDs. All the ASDs, both spray dried and extruded, were amorphous up to 25 wt % drug with loratadine showing amorphous character up to 50% of the drug. When examined by dissolution testing, CCAB formulations with 10% drug proved effective at providing solubility enhancement for the very crystalline flavonoid drug quercetin but not for the more soluble ibuprofen and more hydrophobic loratadine. However, there was a noticeable, slower, more controlled release of the drugs from the formulations. Furthermore, we established that CCAB formulations with the very hydrophobic loratadine could be improved by addition of the water soluble ASD polymer PVP, with which CCAB shows good immiscibility. While CCAB did not provide solubility enhancement in all cases, the slower drug release exhibited by CCAB, especially in the stomach, could be especially beneficial, for example in formulations containing known stomach irritants like ibuprofen.

5.2 Introduction:

Over the years, new polymer matrix materials for drug delivery have been continually sought to provide viable commercial materials that can be processed under various conditions while improving the essential characteristics needed for an effective drug formulation[1]. This quest for matrix materials has led to novel synthetic products that provide great insight into the parameters necessary to give great drug stabilization in the solid state and within the aqueous environment of the gastrointestinal (GI) tract[2] and provide better options in areas such as gene delivery[3]. However, in some cases, this search has led researchers to revisit existing materials through pairwise blended formulations, and has led to the discovery of potentially interesting drug delivery applications for other materials that were not previously considered[4].

Cellulose derivatives have been long used in a number of applications including coatings, paper-making, and more recently drug delivery. Cellulose derivatives have been reported in a variety of cases to show favorable drug delivery properties. Some of the most popular and widely known include carboxymethyl cellulose acetate butyrate (CMCAB)[4a, 5], hydroxypropyl methylcellulose acetate succinate (HPMCAS)[6], and hydroxypropylmethylcellulose (HPMC)[7], and more recently novel cellulose esters like cellulose acetate adipate propionate (CAAdP)[8], cellulose acetate suberate (CA Sub) and cellulose acetate sebacate (CA-Seb)[2, 4d, 9] have received more attention in this regard.

Cellulose esters have been very beneficial in drug delivery due to their generally low toxicity, compatibility with various drug actives, and their potential for making micro- and nanoparticles[10]. From a commercial standpoint, cellulose esters have enjoyed great versatility in processing methods including casting films[10-11], spray drying[4a-c, 5b], and extrusion[12]. Certain cellulose esters (for example HPMCAS[4a, 4c, 4d, 10, 13], CMCAB[4a, 4c, 5a, 11a, 13-14], CAAdP[4a, 4c, 4d, 9a, 14] and CASub[2b, 9b]) have been formulated into amorphous solid dispersions with drugs that have poor aqueous solubility. The molecular dispersion of polymer and drug maintains the drug in a high energy amorphous state that can enhance delivery by generating a supersaturated drug solution[15]. The polymer component of the dispersion is incorporated to modify the solubility of the drug, help give greater control over the release rate, and delay drug crystallization from its high energy amorphous state. Favorable interactions between the drug and polymer molecules are essential to delaying recrystallization and improving aqueous solubility[9]. Cellulose ester hydrophobicity is an important consideration for miscibility with the drug and may significantly

impact drug release[2a, 9]. Additionally, the high T_g values of most cellulose esters play an integral role in retarding recrystallization of the drug by limiting drug mobility within the formulation. The high T_g also serves to provide a margin for error against formulation T_g reduction due to plasticization under high humidity conditions and even in the presence of added drug that may have a plasticizing effect.

The modified celluronic acid, 6-carboxycellulose acetate butyrate carboxylate (CCAB) is a relatively new cellulose derivative synthesized by Eastman Chemical Company[16], for which there is no detailed reports on its exploration as an ASD polymer. The ester has a combination of pH responsive carboxyl groups, and small to medium chain length ester groups (degree of substitution (DS) butyryl 1.62, acetyl 0.06). The presence of the carboxy groups (DS O.28) as with derivatives such as CMCAB, CAAdP and others, is important not only for favorable hydrogen bonding interactions with drug actives but also to drive swelling and pH triggered drug release in the intestine. The more hydrophobic butyryl ester chains provide amphiphilicity, and can potentially provide miscibility with hydrophobic drugs. The longer ester chains may also be influential, providing internal plasticization in the processing of these formulations using methods such as hot melt extrusion. Plasticization from added drug and greater mobility of the polymer chains during extrusion may allow for lower processing temperatures.

We have chosen to study the ASD properties of CCAB using several structurally diverse model drugs; ibuprofen (anti-inflammatory)[17], loratadine (anti-histamine)[18], quercetin (anti-oxidant flavonoid)[4a, 19] and clarithromycin (antibiotic)[4c]. Each of these drugs differs significantly from the others in structure, and is important for treatment of a different ailment. More importantly, each drug may benefit from incorporation with the matrix polymer in a unique fashion.

Amorphous formulations can typically be made through a variety of solvent based methods as well as through hot melt extrusion [15c, 20]. However, hot melt extrusion presents the advantages of lower cost due to the absence of solvent, fewer processing steps, and more consistent product once optimal conditions are determined for the extrusion of a particular pharmaceutical product [20c, 21]. Melt extrusion involves the mixing, heating and 'dissolution' of the drug in the polymer in a solvent free environment under pressure. The polymer and drug remain in this state of molecular dispersion as the material hardens. The intense agitation of the material under pressure leads to a more homogeneous dispersion [22]. From a commercial

standpoint, the use of extrusion in converting raw materials by melt processing through a die under controlled conditions to give material of uniform shape and density presents a highly efficient means of production especially as it relates to pharmaceutical products. The complete absence of solvent is advantageous since solvent can not only plasticize the formulations but also act as a contaminant. Extrusion can also be more cost efficient since there is no need for organic solvents and for additional processing to remove such solvents. There are in fact a number of commercial formulations of extruded products ranging from contraceptives to antivirals [23] and the literature cite other successful applications of melt extrusion to enhance the dissolution of poorly soluble drugs [24]. Hot melt extrusion has been utilized with a number of cellulose derivatives including hypromellose (HPMC) and hydroxypropyl methyl cellulose acetate succinate (HPMCAS)[25]. For ester- containing cellulosics there may be some reduction in the ester content and increase in free acid content in the formulation due to degradation[25]. The use of polymer derivatives containing both OH and COOH groups in melt extrusion may be problematic, due to the potential for cross-linking reactions to produce esters between free hydroxyl and carboxylic acid groups[26].

We hypothesize that the amphiphilic cellulose derivative CCAB could prove useful in formulating amorphous solid dispersions with a variety of poorly soluble drug actives and provide solubility enhancement and more effective drug release of the APIs. We further hypothesize that given the high DS of butyryl ester groups, it may be possible to utilize melt extrusion for the formulation of CCAB with lower melting point drug candidates to provide even more complete mixing of the drug/polymer blends, versus other more conventional formulation methods, for enhanced dissolution.

5.3 Experimental:

5.*3.1 Materials*

Dimethylacetamide (DMAc, Fisher), dimethyl formamide (DMF, Fisher), 1,3-dimethyl imidazole (DMI, Fisher) and dimethyl sulfoxide (DMSO, Acros) were kept over 4 Å molecular sieves and stored under dry nitrogen until use. Methanol, ethanol, dichloromethane, N-methylpyrrolidone (NMP), acetone, and tetrahydrofuran (THF) were purchased from Fisher Scientific, Pittsburgh, PA and used as received. 6-Carboxycellulose acetate butyrate (CCAB, MW 252,300 (determined on polymer as received using gel permeation chromatography), degree of substitution, determined

using a Bruker AVANCE 500 MHz by ^{1}H NMR in d_6-DMSO, (DS) (butyrate) =1.62 , DS (acetate) 0.06, CO_2H acid number, determined by the manufacturer to be 56.2 mg KOH/g (DS 0.28)) was from Eastman Chemical Company (Kingsport, Tennessee). Molecular weight determination was by gel permeation chromatography in dimethylacetamide containing 0.1% lithium chloride using a Waters 1515 isocratic HPLC pump, Viscotek 270 dual detector, and Waters 2414 refractive index detector. Degree of substitution (DS) was measured using ^{1}H NMR in DMSO by comparison of integral of the ester protons to the integral of the cellulose backbone. Acid number was provided by the supplier. Ibuprofen (Ibu) and loratidine (Lor) were purchased from LKT Laboratories and Oakwood Chemicals respectively. Quercetin (Que, (hydrate, ≥ 95 %) was purchased from Aldrich Chemicals and clarithromycin (CLA) was purchased from Attix Pharmaceuticals, Toronto, Ontario, Canada. Mesh Sieve (30) was purchased from the Cole Parmer Instrument Company.

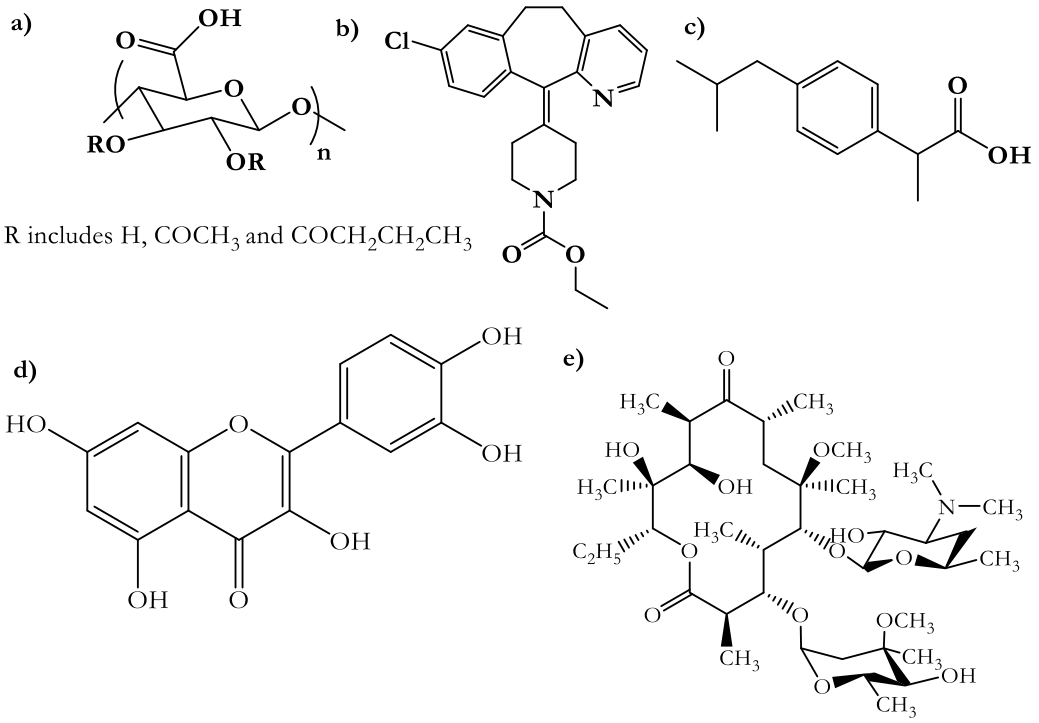

Figure 5.1: Chemical structures of polymer and pharmaceuticals used: a) CCAB b) loratadine c) ibuprofen d) quercetin and e) clarithromycin

5.3.2 Methods:

5.3.3 Preparation of solid dispersions by spray-drying

Powder blend samples were prepared on a Buchi Mini spray dryer B-290. Each polymer/drug pair (1-2 g) was mixed in the ratios 9:1, 4:1, and 1:1 (w:w, polymer:drug) and subsequently

dissolved in 50-100 mL solvent. Spray dryer settings of pump at 45%, aspirator at 100% and inlet temperatures of 90°C were used to produce microparticles of the blended polymers. The temperature was set at least 10 °C above the boiling point of the solvent.

5.3.4 Preparation of solid dispersions by extrusion

Powder mixtures (5 g) containing polymer and drug at varying drug loads were premixed for 1 min in a Micromill grinder (Electron Microscopy Sciences, Hatfield, PA). Melt extrusion was performed on a ThermoScientific Haake Minilab II Micro compounder fitted with a Haake force feeder for powder addition. The co-rotating twin screw microcompounder was first pre-heated. The premixed powder mixtures were then fed through the force feeder and extruded through the barrel. Finally, the extrudate was collected, and allowed to cool before being cryogenically milled using the MicroMill grinder. The milled samples were passed through a 30 mesh sieve (cut off 600 µm) and the powders obtained were subsequently utilized for analyses. The formulations and temperature for extrusion are described in Table 5.1.

Table 5.1: Extrusion temperatures of CCAB with Lor and Ibu

Formulation	Temperature Used
CCAB/ibuprofen	130°C
CCAB/loratadine	140°C

5.3.5 Characterization of solid dispersions

5.3.6 Differential scanning calorimetry (DSC)

Heating curves of 4-10 mg spray-dried powder samples or milled extrudates in TA Instruments Tzero aluminum pans were obtained on a TA Instruments Q2000 DSC or TA discovery DSC (New Castle, DE). Samples were first equilibrated at -75 °C for 5 min followed by heating at 20 °C/min to 150 or 180°C. Samples were quench cooled at 100 °C/min to -75°C, then reheated at the same rate. Second heating scan thermograms were evaluated to obtain T_g values. Where necessary, samples were submitted to temperature modulated DSC (MDSC) with a heating rate of 4 °C/min from -50 °C to 150 or 180 °C and a modulation amplitude of +/- 0.5 °C for 40 s. For these samples reversing heat flow thermograms were evaluated.

5.3.7 Thermal gravimetric analysis

Thermogravimetric analyses were obtained on a Q500 Thermogravimetric analyzer, TGA (TA Instruments, DE, USA). Approximately 4-6 mg of sample was heated from 25°C to 600°C at a rate of 10°C/min under a continuous nitrogen flow at 60 mL/min.

5.3.8 Nuclear magnetic resonance spectroscopy (NMR)

NMR spectra were obtained on Varian INOVA, UNITY 400 MHz, and Bruker AVANCE 500 MHz spectrometers in $CDCl_3$ or d_6-DMSO. Chemical shifts are reported relative to the solvent peaks.

5.3.9 Ultraviolet-Visible spectroscopy (UV-Vis)

All UV-Vis spectra were recorded on a Thermo Scientific Evolution 300 UV-Visible Spectrometer.

5.3.10 Fourier transform infrared spectroscopy (FTIR)

Infrared spectra were obtained on samples in absorbance mode using a Bio-Rad FTS 6000 spectrophotometer equipped with a globar infrared source, KBr beam splitter, and DTGS (d-triglycine sulfate) detector. Spectra of the powdered samples were obtained using a Golden Gate MII attenuated total reflectance (ATR) sampling accessory with a diamond top plate (Specac Inc., Woodstock, GA). Scan range was set from 4000 to 500 cm^{-1} with a 4 cm^{-1} resolution, and 128 scans were co-added. The absorbance intensity of the spectral region of interest was between 0.6-1.2.

5.3.11 X-Ray diffraction (XRD)

Crystallinity was analyzed using X-ray powder diffraction (XRD) on the spray-dried samples or milled extrudate. XRD patterns were obtained using a Shimadzu XRD 6000 diffractometer (Shimadzu Scientific Instruments. Columbia, Maryland). The geometry of the X-Ray diffractometer was the Bragg Brentano parafocusing. The instrument was calibrated using a silicon standard which has a characteristic peak at 28.44° 2θ. The X-ray tube consisted of a target material made of copper (Cu), which emits Kα radiation with a power rating of 2,200 Watts and

accelerating potential of 60 kV. Experiments were performed using a 40 kV accelerating potential and current of 30 mA. Divergence and scattering slits were set at 1.0 mm and the receiving slit at 10 iris. The experiments were conducted with a scan range from 10 to 50° 2θ. Scanning speed was 5º/min.

5.3.12 Gel permeation chromatography

Molecular weight determination was achieved by gel permeation chromatography in dimethylacetamide containing 0.1% lithium chloride using a Waters 1515 isocratic HPLC pump, Viscotek 270 dual detector, and Waters 2414 refractive index detector. Mobile phase flow rate was 0.5 mL/min. Universal calibration curves were prepared using polystyrene standards.

5.4 Drug calibration curves by UV-Vis spectroscopy

Standard curves were generated for each drug in an appropriate solvent (methanol for ibuprofen, ethanol for quercetin and acetonitrile for loratadine and clarithromycin). The standard curves were utilized to calculate the concentration of each drug by UV-Vis absorption. Ibuprofen was analyzed at 230 nm, loratadine at 280 nm and quercetin at 370 nm.

5.5 Calculation of drug load

Drug loading is determined as the percentage of drug in the polymer matrix. To determine the drug load, 10 mg of sample was dissolved in 25 mL of solvent and the concentration of drug determined by UV-Vis analysis using the standard curves generated above.

5.6 Maximum drug solution concentration from the ASDs

ASD sample (drug content of 25 mg) was dispersed in 25 mL of pH 6.8 phosphate buffer at 37 °C with magnetic stirring (200 rpm). The concentration of each drug in solution was measured by collecting 2.0 mL aliquots from the sample every 8 h (every hour for first 2h) until the drug concentration became constant (after 24−30 h). Each 2.0 mL aliquot was centrifuged at 13,000 *g* for 10 min and the concentration of the drug in the supernatant was measured using UV-Vis spectroscopy.

5.7 In vitro drug release from ASDs

Dissolution of each drug from the CCAB matrix was compared to that of the crystalline drug using 2 experimental conditions. These dissolution experiments were performed using 250 mL jacketed flasks with circulating ethylene glycol/water (1:1) to control the temperature at 37 °C.

Dissolution experiment 1: Evaluation of drug release profile from ASDs at pH 6.8

Drug/polymer samples with drug concentration fixed at 0.05 mg/mL were dispersed in pH 6.8 buffer (100 mL) and continuously magnetically stirred (37 °C, 200 rpm). Aliquots (2.0 mL) were withdrawn from the suspension every 0.5 h (during the first 2 h), then every hour for a total of 8 h. Fresh phosphate buffer (2.0 mL) was added to maintain constant volume after each aliquot was taken. The aliquots were centrifuged at 13,000 × *g* for 10 min and the supernatant analyzed using UV/Vis spectroscopy to determine drug concentration (reference calibration curve). Dissolution profiles for each drug/polymer formulation and for crystalline drugs are presented as concentration of drug in solution vs. time (h).

Dissolution Experiment 2: Evaluation of drug release at pH 1.2 followed by pH 6.8

This experiment was designed to mimic the pH conditions during passage through the gastrointestinal tract and evaluates the effect of low pH (stomach pH) during the first 2 h on the dissolution of drug from the ASDs. Formulations were first dispersed in 75 mL 1N HCl (pH 1.2) for 2 h while being magnetically stirred at 200 rpm, with temperature maintained at 37 °C. Two (2.0) mL aliquots were withdrawn every 0.5 h for 2h, centrifuged at 13,000 × *g* for 10 min and the supernatant assayed using UV/Vis spectroscopy for concentration of drug (reference calibration curve). To maintain constant volume, 2.0 mL of pH 1.2 buffer was replenished after each sample is taken. After 2 h, 25 mL of 0.05M pH 6.8 potassium phosphate buffer was added to the flask and the pH of the dissolution medium was adjusted to 6.8 with 5N NaOH. The dissolution experiment was continued for 6h at pH 6.8 with aliquots (2.0 mL) withdrawn every 0.5 h (for the first hour), then every hour. Phosphate buffer pH 6.8 (2.0 mL) was added to maintain constant volume after each aliquot was withdrawn. Each aliquot was centrifuged at 13,000 × *g* for 10 min and the supernatant assayed by UV/Vis for concentration of drug

(reference calibration curve). ASD dissolution profiles were presented as concentration of drug in solution vs. time (h).

5.8 Results and Discussion:

Characterization of spray dried ASDs with CCAB

For this study, we selected four structurally varied drug actives; ibuprofen, loratadine, quercetin and clarithromycin, to be formulated with CCAB. CCAB has a T_g of 134°C which is promising for ASD formulation, since a T_g 40-50°C above the highest possible ambient temperature (ca. 50°C) is usually desired for ASD, in order to provide a margin sufficient to account for the plasticizing effects of both moisture and (potentially) drug, maintaining the formulation T_g above these high ambient temperatures. The polymer drug blends were spray dried to produce microparticles.

Characterization of extruded ASDs with CCAB

In an effort to test the effectiveness of CCAB as an extrudable matrix polymer, formulations of the lower melting point drugs loratadine and ibuprofen were also formulated using melt extrusion. Formulations with 10, 25 and 50% of the drug were extruded at the temperatures indicated in Table 5.1. The extruded formulations were milled and sieved to produce microparticles that were further analyzed similarly to the spray dried particles.

5.8.1 Loratadine

Loratadine is a crystalline antihistamine drug used to treat allergies that displays a melting endotherm at 140°C (Figure 5.2a). CCAB undergoes glass transition at 134°C (Figure 5.2a). The extruded solid dispersions of CCAB with loratadine at 10, 25, and 50 wt% of drug in the dispersion showed only glass transition endotherms, with no evidence for crystallization or melting of the drug. The observed glass transition temperature decreased compared to that of neat CCAB as the percentage of the drug increased. The spray dried blends of CCAB/Lor showed thermal properties comparable to those of extruded blends with T_g values of 124, 101 and 57°C with 10, 25 and 50 wt % drug respectively. The T_g values of the formulation show moderate correlation with the T_g

values calculated using the Fox-Flory equation (108, 83 and 60°C for 10, 25 and 50% loratadine respectively). With some correlation between expected and experimental T_g values for formulations up to 50% Lor, it is not surprising that CCAB/Lor shows mostly amorphous character by XRD up to 50% drug (Figure 5.2c).

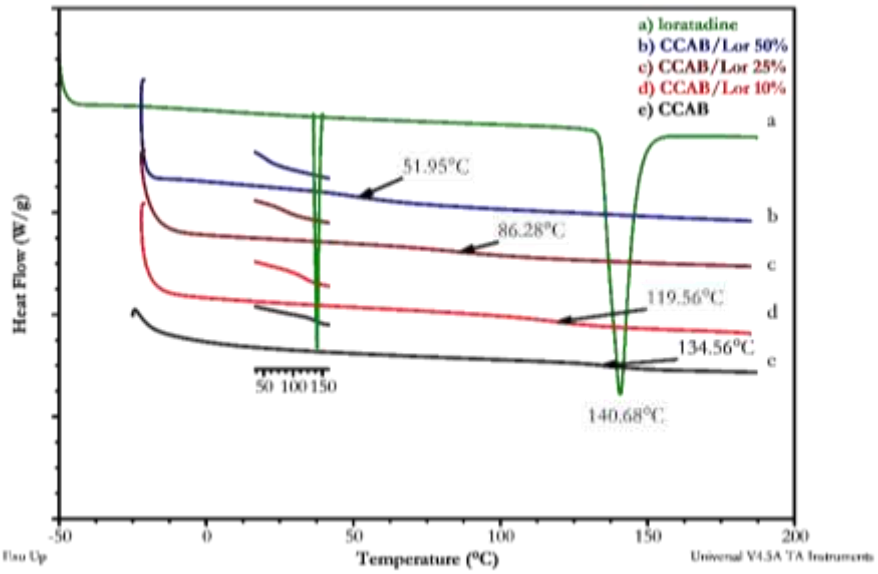

a)

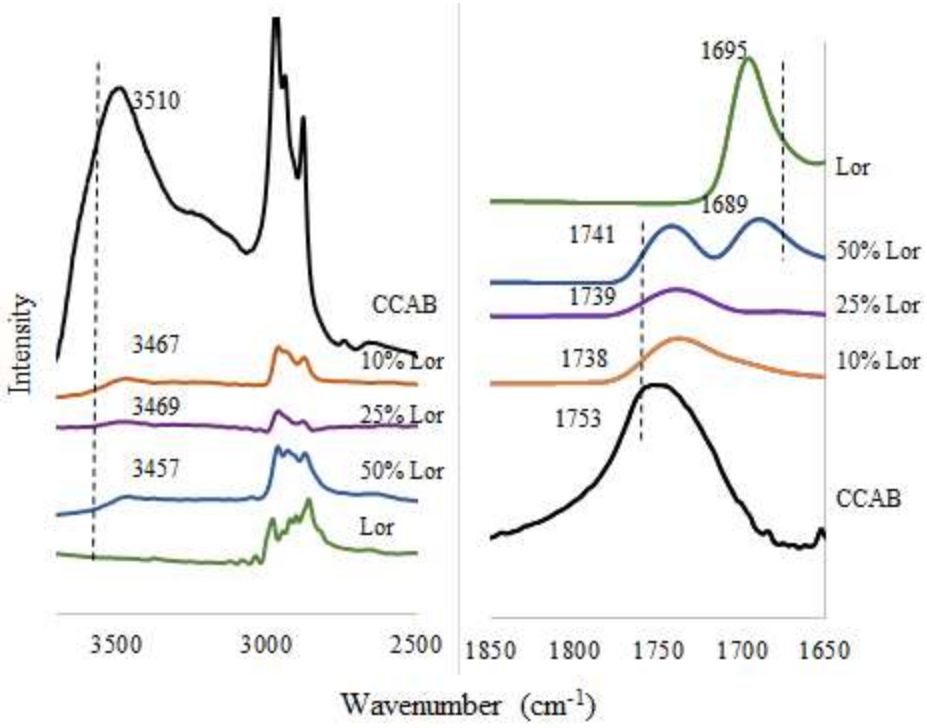

b)

c) 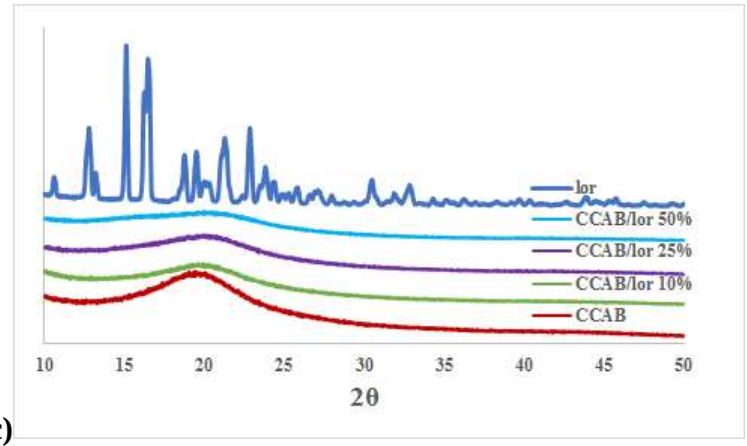

Figure 5.2a: DSC thermograms for CCAB/Lor extrudates. Inset shows expanded areas of transition. b: FTIR spectra of CCAB/Lor extrudate between 1650-1850 and 2500-3500 cm^{-1}. c: X-ray diffractograms of CCAB/Lor blends.

The FTIR spectra of the CCAB/Lor blends show significant broadening in the C=O peak and shifts to lower wavenumbers for the 10 and 25% loratadine blends, indicative of increased hydrogen bonding interactions between the polymer and drug. Significant broadening of the OH stretch peak, present in CCAB but not in pure loratadine, can also be seen with the peak shifting from 3510 cm^{-1} to 3467 and 3469 cm^{-1} for the 10 and 25% ASDs, respectively. However the 50% blend, although DSC provided no indication of the presence of crystalline drug, in the FTIR showed more obvious signs of some immiscibility at this high drug concentration. Two distinct peaks are seen in the C=O stretch region of the blend, at wavenumbers characteristic of the drug (1689 cm^{-1}) and the polymer (1741 cm^{-1}).

5.8.2 Quercetin

The flavonoid quercetin has a much higher melting temperature than the other three drugs used in the study. DSC shows this melting endotherm for pure quercetin at 325°C (Figure 5.3a). The melting point is however so high that it lies above the temperature of decomposition onset for CCAB, thus DSC cannot be used to provide strong indication of the amorphous nature of the dispersion. The quercetin/CCAB/Que formulations do show reductions in measured T_g with increasing drug proportion (Figure 5.3a). XRD diffraction is more revealing, showing that no drug crystallinity is observed for the 10 and 25% drug dispersions compared to the pure crystalline drug (Figure 5.3c), while the 50% Que dispersion does display evidence of significant residual

crystallinity. The FTIR spectrum of the 50% CCAB/Que blend is more characteristic of that of the crystalline drug, especially between 2500-4000 cm^{-1} . In contrast, the 10% and 25% quercetin formulations show characteristic broadening and shift to lower wavenumbers, with increased quercetin content, for the –OH stretch peaks at 3469 and 3467 cm^{-1} respectively (Figure 5.3b), supporting the XRD evidence that these are amorphous dispersions. These interactions result from the five hydrogen bond donor (phenolic OH) groups on each quercetin molecule that are available to interact with the large number of C=O H-bond acceptor groups per CCAB molecule (Figure 5.1).

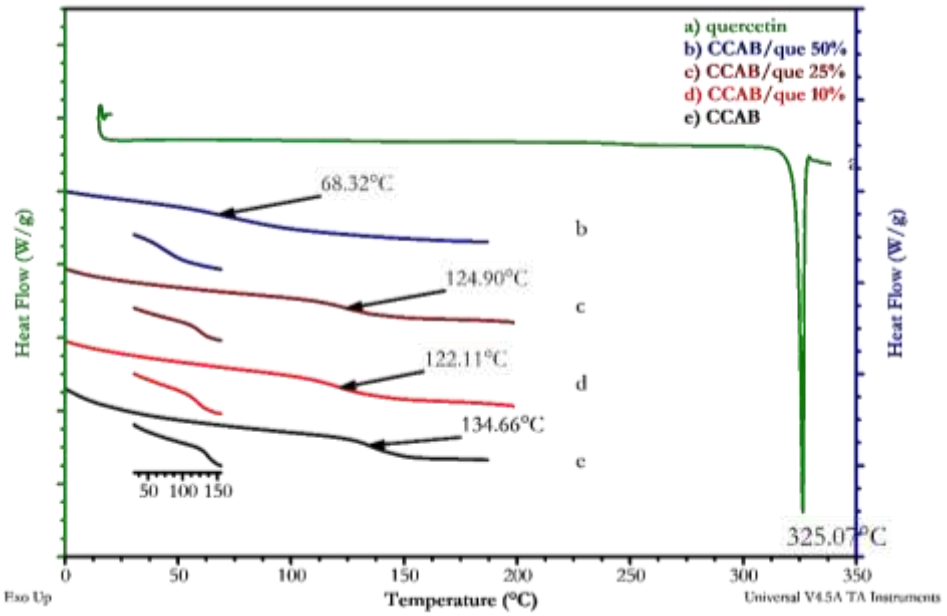

a)

b)

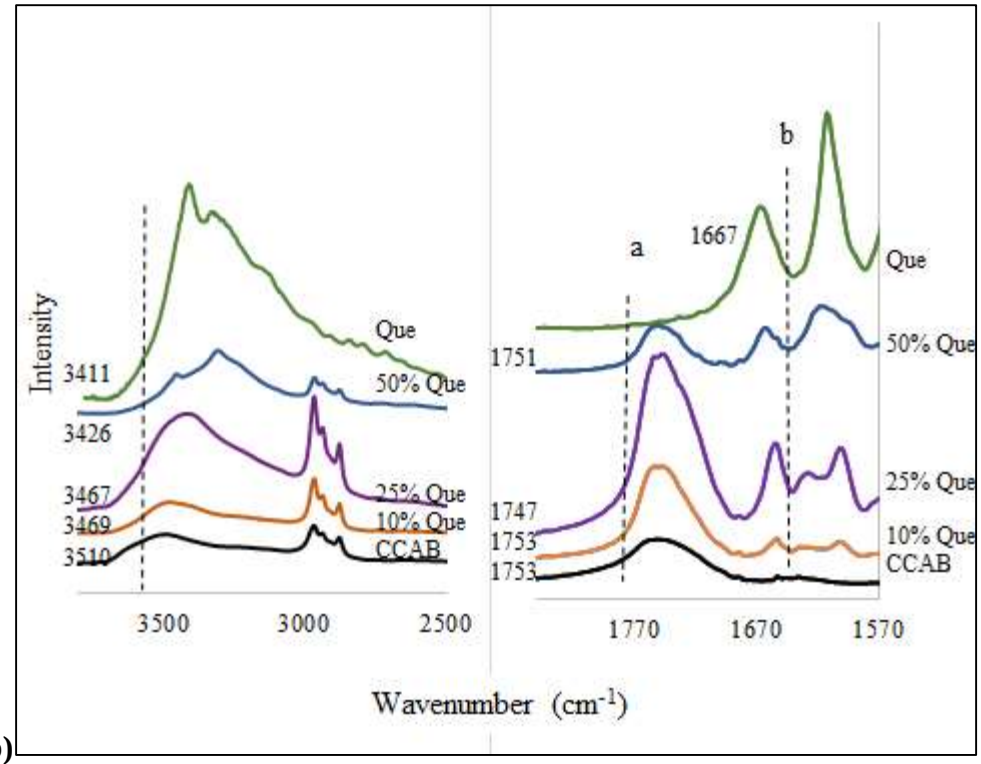

c)

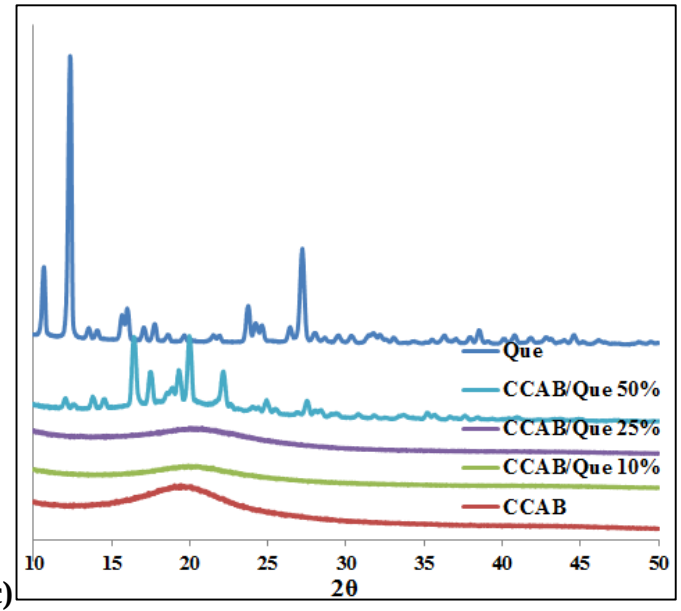

Figure 5.3a: DSC thermograms for CCAB/Que formulations. b: FTIR spectra of CCAB/Que formulations between 1570-1800 and 2500-4000 cm^{-1}. c: X-ray diffractograms of CCAB/Que formulations

5.8.3 Clarithromycin

Clarithromycin is an amino macrolide antibiotic that suffers from poor chemical stability under acidic conditions due to acid catalyzed degradation, exacerbated by the fact that it has much higher solubility at acidic stomach pH than the neutral pH of the small intestine, due to protonation of the clarithromycin amine group[4c, 27]. In order to circumvent clarithromycin instability and provide more effective delivery systems, a number of different approaches have been utilized to enhance clarithromycin delivery including cyclodextrins, lipids and ASDs with cellulose esters[4c].

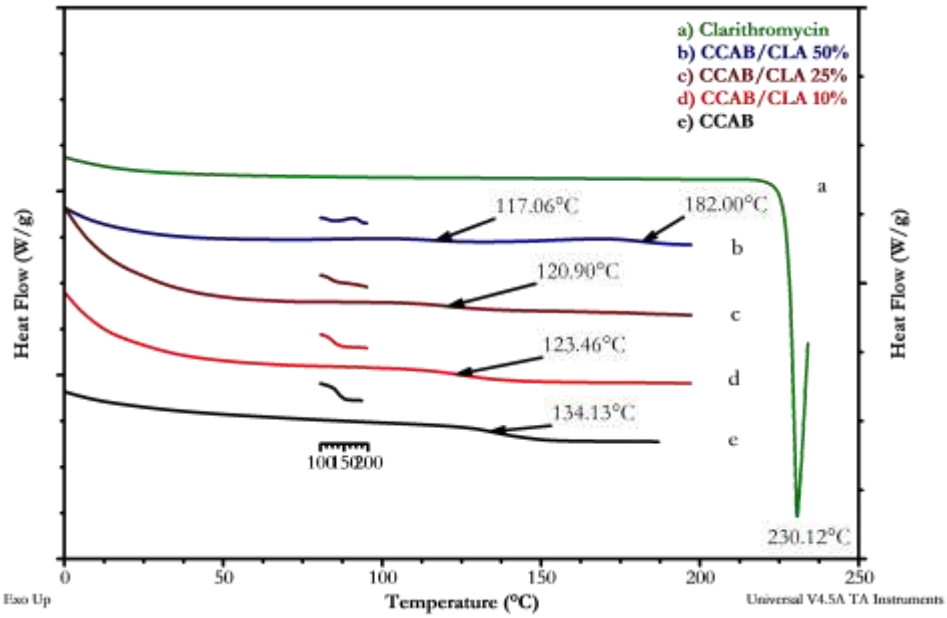

Figure 5.4: DSC thermograms for CCAB/CLA formulations

The DSC thermograms of CCAB/clarithromycin formulations provide evidence for drug/polymer miscibility up to at least 25 wt % drug. The 10 and 25% formulations of clarithromycin in CCAB dispersion show evidence of a single T_g by DSC (Figure 5.4) that are only a few degrees below the predicted Tg values (Table 5.3), while the 50% formulations possess two distinct glass transitions at 117 and 182°C. As would be expected from these results, the XRD diffraction pattern for the 50% formulation shows characteristic crystalline peaks similar to those of the pure drug, while crystallinity is not evident in the 10 and 25% CLA formulations (Figure 5.5b). The FTIR spectra of CCAB/CLA further support this miscibility at

10 and 25% drug showing shifts to lower wavenumbers for the C=O peaks at 1740 and 1745 cm^{-1} compared to 1753 cm^{-1} for CCAB (Figure 5.5a)

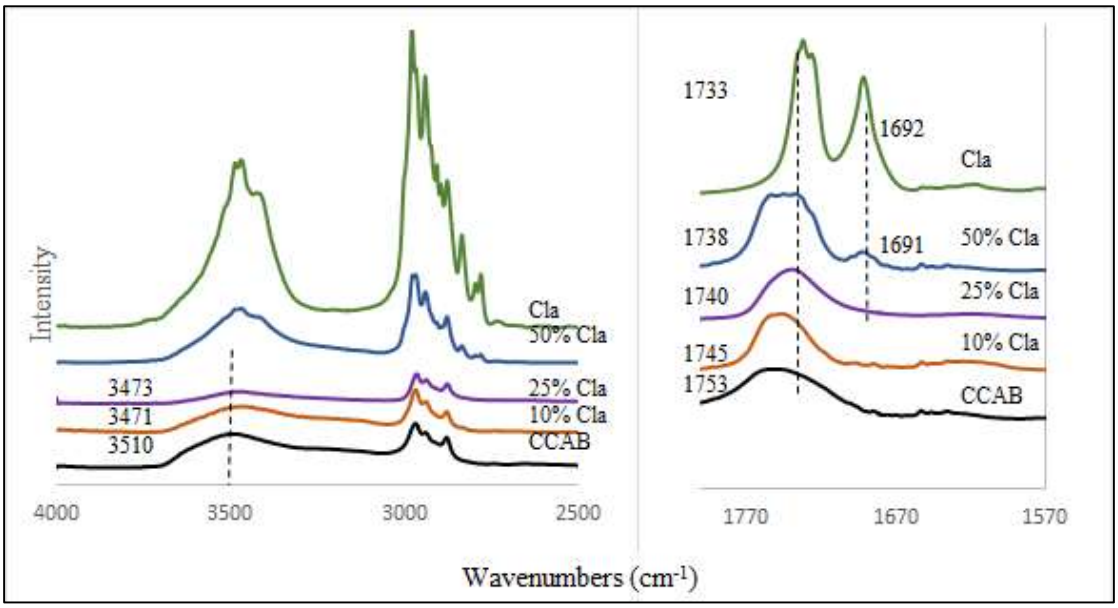

a)

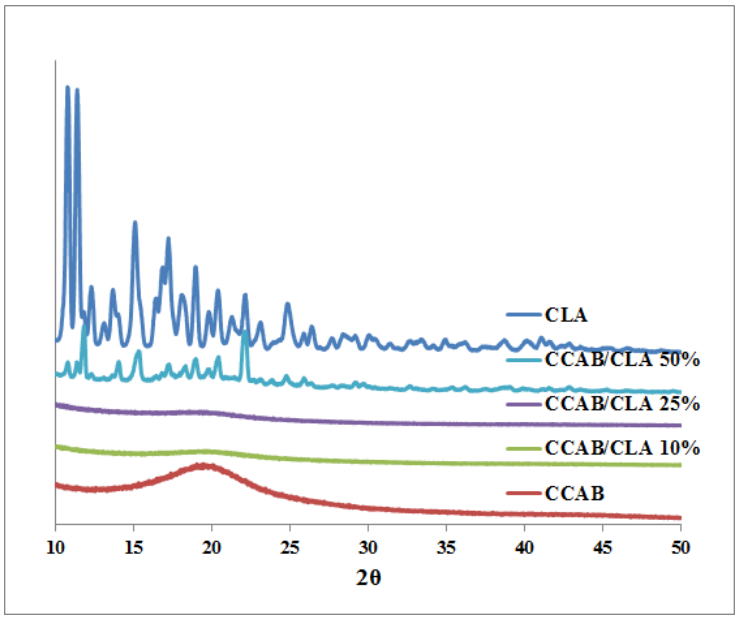

b)

Figure 5.5a: FTIR spectra of CCAB/CLA formulations between 1570-1800 and 2500-4000 cm^{-1}. b: X-ray diffractograms of CCAB/CLA formulations

5.8.4 Ibuprofen

Formulations of CCAB and ibuprofen also showed no evidence of crystallinity up to 25 % of the drug in both spray-dried and extruded formulations (Figure 5.6c). The 10 and 25 % ibuprofen ASDs also displayed single T_gs that were in good correlation to those predicted by the Fox-Flory equation while the 50% blends showed two distinct T_gs including (-24°C) close to the amorphous T_g of pure ibuprofen at -41°C (Figure 5.6a and Table 5.3). FTIR spectra of the ibuprofen formulations also supported these findings with the 10 and 25 % ibuprofen ASDs showing single carbonyl peaks appearing at wavenumbers between those of pure CCAB and pure ibuprofen. For the 50% ibuprofen formulations there appeared two distinct carbonyl peaks at 1722 and 1745 cm^{-1} that were indicative of partially immiscible combinations of ibuprofen and CCAB.

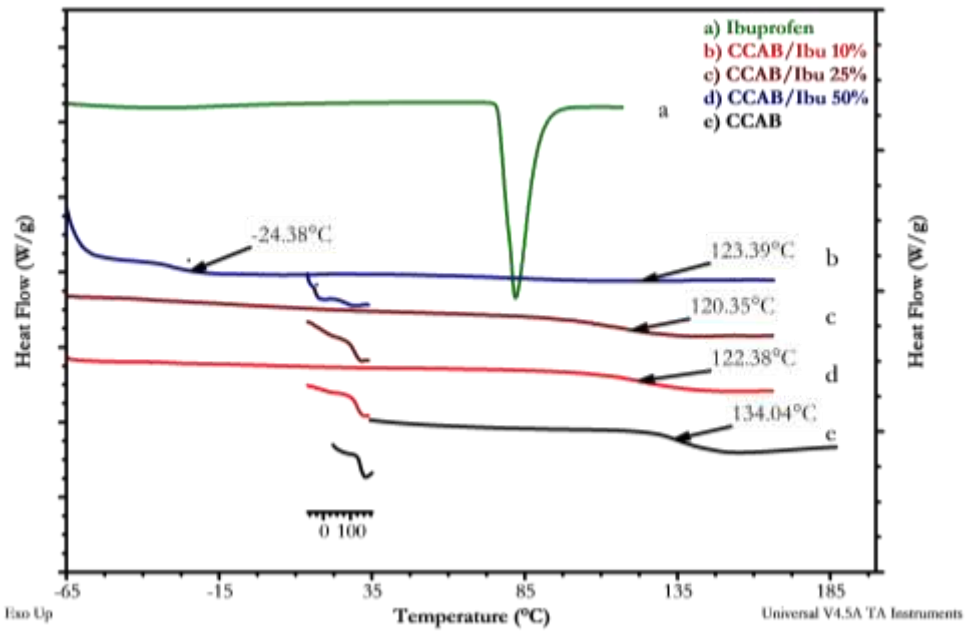

a)

b)

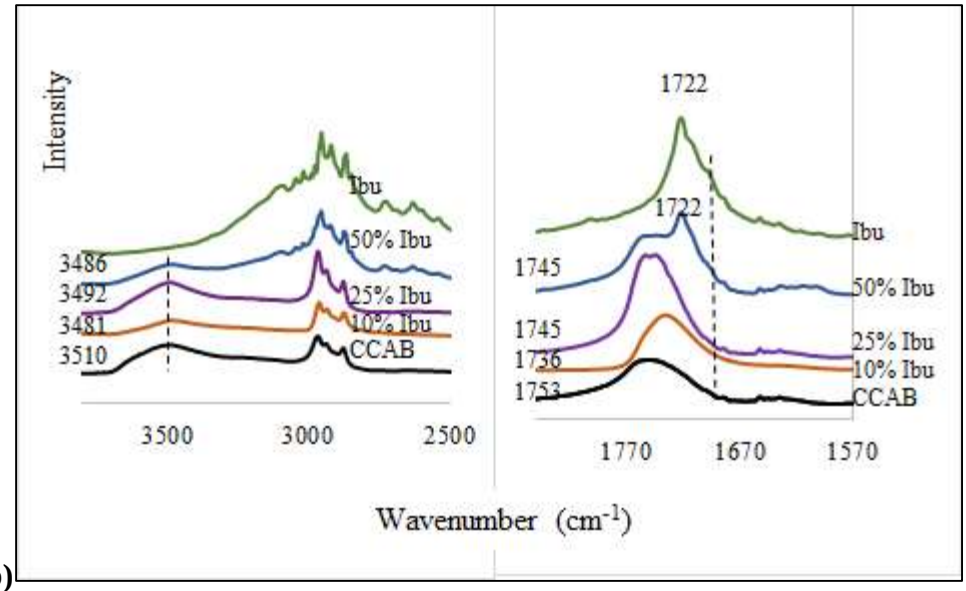

c)

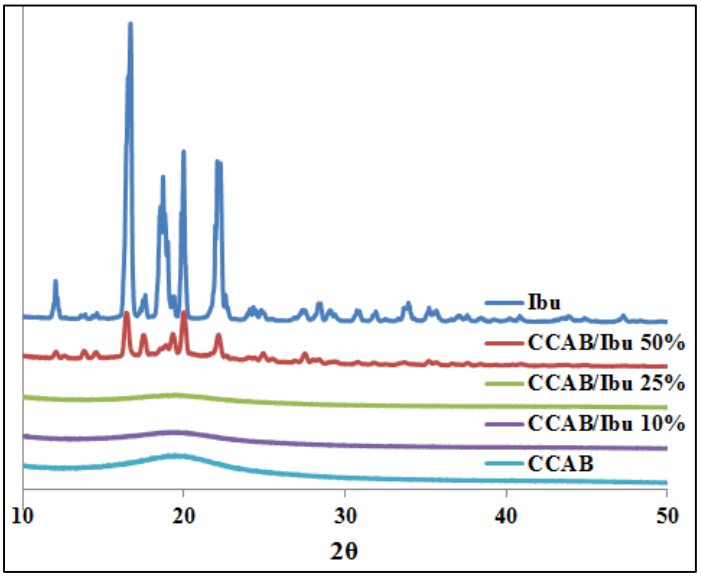

Figure 5.6a: DSC thermograms for CCAB/Ibu formulations. b: FTIR spectra of CCAB/Ibu formulations between 1570-1800 and 2500-4000cm^{-1}. c: X-ray diffractogram of spray dried CCAB/Ibu formulations

5.8.5 Drug loading

UV-Vis analysis was used to determine drug loading using the calibration curves generated as described above (Section 5.4). Relatively high drug loads were achievable with drug loading efficiences between ~70% to > 90% for spray dried samples and more variable drug loads

between ~60% and 90% for extruded samples. Drug loads for spray dried 10 and 25% CCAB/Lor samples were greater than 90% of theory, while for the 10% extruded formulations up to 80% of the theoretical load could be achieved. Extruded 10% CCAB/Ibu had > 90% of the theoretical drug load, while the spray dried 10 and 25% formulations had ~70 and 87% of the theoretical loading respectively. CCAB/Que spray-dried dispersions also showed fairly high drug incorporation with 74 and 92% of calculated loading for the targeted 10 and 25% quercetin formulations. Extruded samples are typically physically mixed before being fed into the extruder. Without vigorous premixing of the polymer and drug, there is some potential for variability in the ratio of polymer and drug as the powder mixture is force fed into the extruder. Thus variability in the drug encapsulation efficiency may be evident between spray dried and extruded formulations. In our work, we have attempted to reduce this variability considerably by utilizing a simple but vigorous premixing process in a Micromill grinder prior to melt extrusion. Drug loads in melt extrusion may also be affected by degradation due to the elevated temperatures needed for processing.

5.8.6 Dissolution testing and solution concentration enhancement

We have calculated the solubility of CCAB to be 430 □g/mL in pH 6.8 buffer; this compares favorably with other useful ASD polymers (Table 5.2) and predicts the possibility of prevention by CCAB of drug crystallization from solution. Calculation of the maximum solution concentrations of Lor, Ibu and Que shows that the solubility of the drugs at pH 6.8 follows the order Ibu > Que > Lor (Figure 5.7).

Table 5.2: Comparison of CCAB Physical Properties to some other Common ASD polymers

Polymer	Solubility (mg/ml)
PVP	>600
HPMCAS	17.7
CMCAB	0.8
CCAB	0.43
CAAdP	0.3

Drug Release Profiles at pH 6 .8

In the measurement of drug release profiles, maximum possible drug concentration was fixed at 50 µg/mL in pH 6.8 buffer solution. Drug concentration was determined by UV-Vis absorption of supernatants from samples centrifuged to remove particles and nanoparticles, by comparison with appropriate standard curves. Drug release and solution concentration enhancement were highly dependent on the drug.

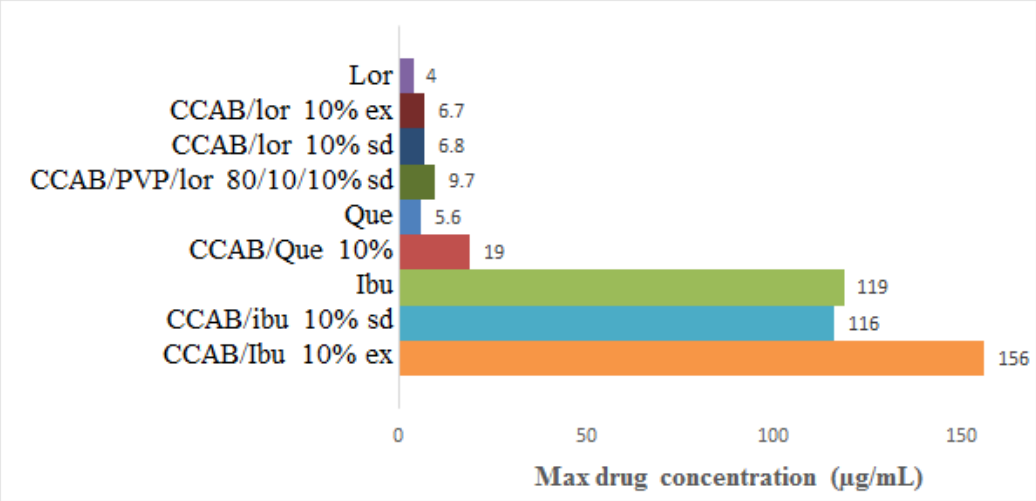

Figure 5.7: Maximum drug solutions concentration from ASDs in pH 6.8 phosphate buffer, 37 °C.

Loratadine

The observed poor solubility of loratadine from these ASDs (Figure 5.7) is not surprising as it is fairly hydrophobic (log P value 4.2[28]). The results of the dissolution study at pH 6.8 with loratadine formulations showed no solubility enhancement for the hydrophobic loratadine from CCAB ASD vs. dissolution of crystalline drug. The similarly high hydrophobicity of CCAB and loratadine likely retards loratadine release and makes it difficult to observe the advantages of amorphous dispersion. Given the poor solubility of loratadine formulated with hydrophobic CCAB, we explored the potential benefits of utilizing a pairwise blended polymer matrix of

CCAB and PVP. Pairwise polymer blends can provide synergistic and beneficial properties to the polymer/drug formulation[4b, 4d]. PVP is a well-known water soluble ASD polymer and was chosen to improve the hydrophilicity of the CCAB/Lor formulation, in hopes of improving Lor dissolution from the ASD. A spray-dried formulation of CCAB/PVP and loratadine in the ratio 8:1:1 (CCAB:PVP:Lor) was analyzed for potential solution enhancement. The formulation containing PVP was shown to be amorphous by XRD and displayed a single Tg by DSC analysis (Figure S5.3 and Table 5.3).The incorporation of 10 wt % PVP provided a 2-fold increase in solubility at pH 6.8 compared to pure loratadine and was superior to the spray dried and extruded formulation with CCAB and loratadine as well. The incorporation of water-soluble PVP also resulted in an expected faster release of the drug to achieve supersaturation within 1 h that was maintained for the remainder of the experiment. Dissolution experiments were also conducted at pH 1.2 for 2 h followed by pH 6.8 for 6 h to mimic the passage of the drug through the gastrointestinal tract. Due to ionization of loratadine at low pH, the pure drug shows high solubility at such conditions. Lor solubility is greatly reduced at intestinal pH, resulting in a 3-fold decrease in solubility at pH 6.8. This is expected of weakly basic compounds like loratadine as they tend to precipitate very rapidly as soon as the stomach acid is neutralized in the small intestine[29]. Given the decrease in concentration of crystalline loratadine observed at the swicch to pH 6.8 (Figure 5.8b), it is expected that Lor would decrease to similar concentrations from the experiment at pH 6.8 only (Figure 5.8a). The CCAB/lor spray dried and extruded formulations and that including 10% PVP show similar results to the experiment conducted at pH 6.8 only, with the 10% PVP containing formulation showing solubility enhancement up to 4 µg/mL. Despite the solution enhancement provided, the resulting concentration of loratadine is still > 2x lower than its predicted amorphous solubility of 11 µg/mL[29].

a)

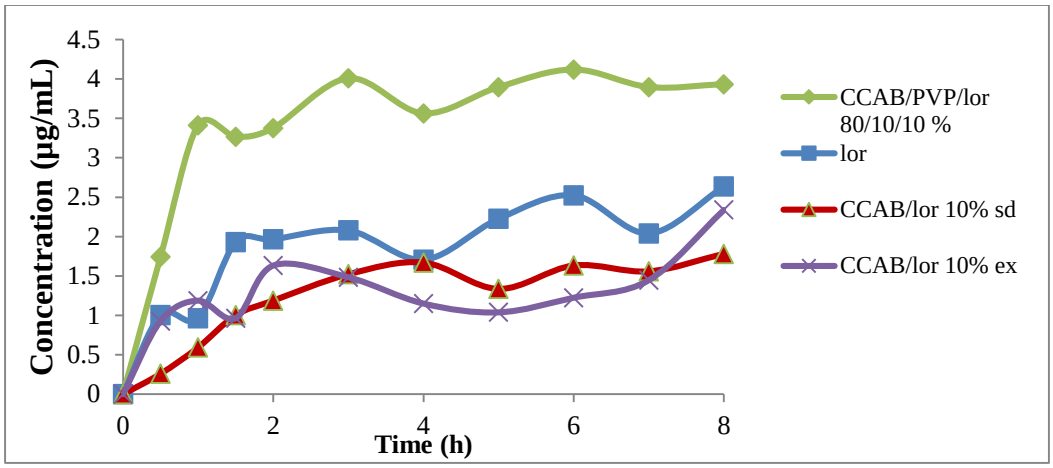

b)

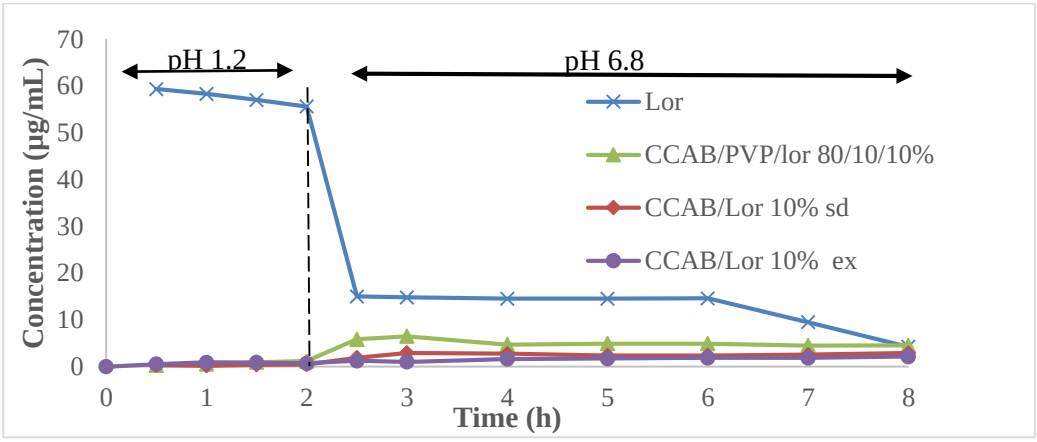

Figure 5.8: Dissolution profiles of CCAB/Lor ASDs. a)10% CCAB and ternary polymer/polymer/drug formulations with loratadine at pH 6.8 and b) at pH 1.2 for 2h then pH 6.8 for 6h (Note: "sd" indicates spray-dried,"ex" denotes extruded formulations)

Ibuprofen

The comparison of dissolution of crystalline ibuprofen at pH 6.8 with ibuprofen release from spray dried or extruded CCAB/Ibu 10% particles shows very fast dissolution of the crystalline drug (~70% of that available) within the first 0.5 h, and maintenance of high drug concentration for the remainder of the 8 h period (Figure 5.9a). Ibuprofen, the most soluble (at pH 6.8) of the drugs used in the study (Figure 5.7) did not exhibit enhanced solution concentration from formulation with CCAB at pH 6.8, however Ibu release was slow and almost constant over the time frame of the experiment, reaching the same maximum concentration as with crystalline

ibuprofen within 7 h. The more compressed extruded formulation at the same ibuprofen concentration (10 wt%) released Ibu more slowly than the spray dried formulation, as is common with denser extruded formulations[30]. The extruded dispersion provided much slower and controlled release compared to the pure drug, as with the spray-dried dispersion. These formulations could be of interest for an extended release version of the painkiller ibuprofen. At pH 1.2 the CCAB formulations, both spray dried and extruded restricted the release of the drug at low pH but showed 2 fold increase in solution concentration versus crystalline Ibu at pH 6.8 due to pH responsive release of the drug from the carboxylate polymer matrix (Figure 5.9b). The much lower concentrations of ibuprofen at gastric pH may however be useful commercially considering the fact that many anti-inflammatory drugs like ibuprofen are stomach irritants[31]. Despite the slower, more controlled pH controlled release of the drug from the CCAB matrix over the time frame of the experiment, the resulting drug solution concentrations are considerably lower than the expected amorphous solubility of ibuprofen, found to be 123 µg/ml by Almeida e Sousa et al[32].

a)

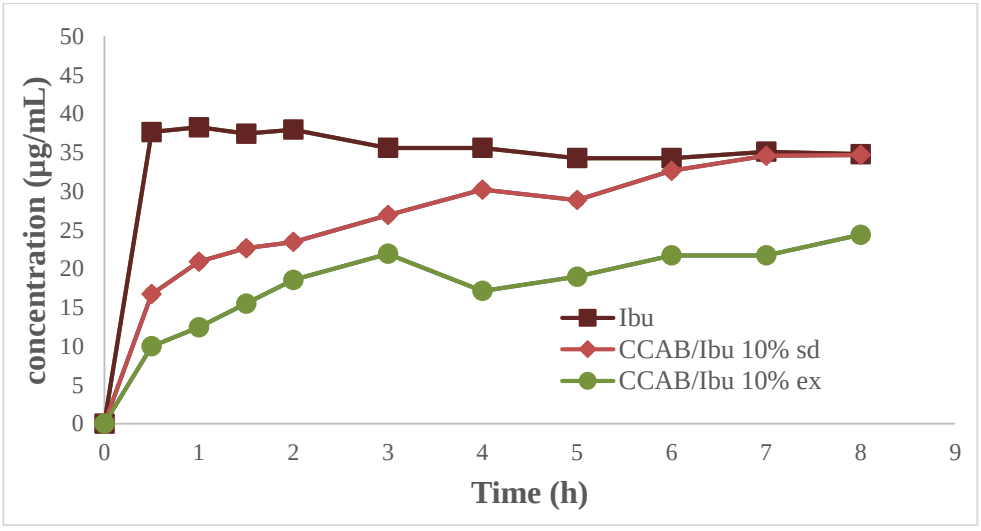

b)

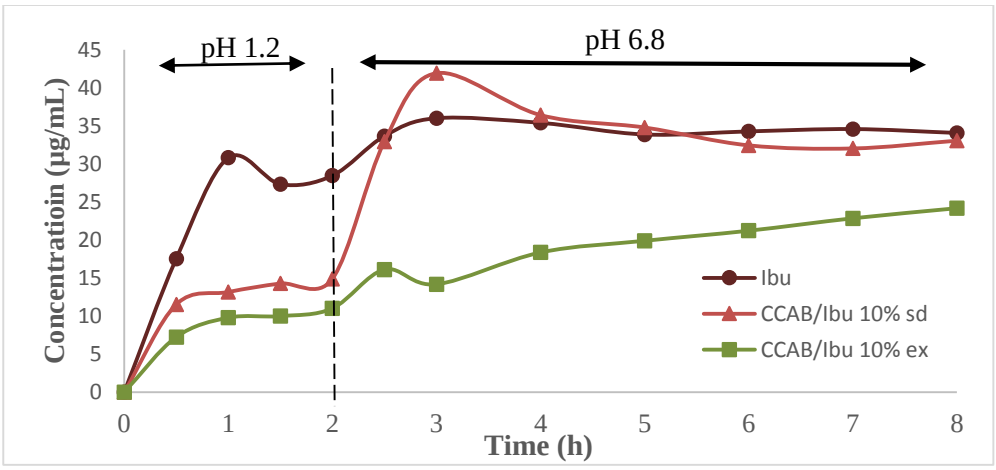

Figure 5.9: Dissolution profiles of CCAB/Ibu ASDs. CCAB formulations with 10% ibuprofen at (a) pH 6.8 and (b) pH 1.2 for 2h followed by pH 6.8 for 6h. (Note: "sd" indicates spray-dried, "ex" denotes extruded formulations)

Quercetin

Quercetin has the lowest log P value (1.82) of the drugs studied. The spray dried formulation of quercetin with CCAB showed about a 3 fold increase in solubility in pH 6.8 buffer (Figure 5.7a). The formulation of the hydrophobic and highly crystalline quercetin into an ASD with CCAB provided much more favorable results than with the other drugs used. In dissolution testing, quercetin solution concentration was enhanced by more than 8-fold from CCAB ASD vs. that from drug only. While dissolution of crystalline quercetin began at about 1h to produce solution concentrations of ~1 µg/mL that were stable over the duration of the 8h experiment, spray-dried ASD of quercetin in CCAB released quercetin slowly to achieve concentrations up to 8 µg/mL after 8h (Figure 5.10a). While there was significant increase in the solution concentration of quercetin from the CCAB matrix, drug release was still low (~20%). Experiments conducted first at pH 1.2 followed by pH 6.8 again showed enhanced dissolution of quercetin from the CCAB matrix (Figure 5.10b). On switching from pH 1.2 to pH 6.8, there is a significant spike in the solubility of pure quercetin as well as that from the CCAB matrix that can be attributed to the increased solubility of the ionized quercetin (pKa of 5.87 for the 4´ OH of quercetin)[33]. This

spike is followed by a noticeable decrease in quercetin concentration that continues for the duration of the experiment for pure quercetin but levels off at ~8 µg/mL for the 10% CCAB/Que formulation. This decline could be attributed to the recrystallization of quercetin[4a] but the oxidative degradation of quercetin is also a likely culprit[33]. The leveling off of quercetin concentrations at ≥8 µg/mL upon dissolution from the CCAB matrix may also indicate the ability of CCAB to provide stabilization of quercetin against oxidative degradation and recrystallization through its favorable interactions with the drug. Some degradation of the drug upon release from the CCAB matrix is not entirely surprising however given results from our labs indicating that degradation of quercetin, the mechanism of which involves non-polar oxygen, may be enhanced from a more hydrophobic matrix compared to a more hydrophilic matrix like PVP[4a]. Over the 8h period, the resulting solution enhancement from the CCAB matrix is still > 2 fold compared to the crystalline drug, which bodes well for the ability of CCAB to improve the release properties of the flavonoid compound. The prediction of theoretical amorphous solubility of the high melting temperature quercetin for comparison to those achieved here is difficult due to the propensity for melt degradation of the drug and so a theoretical value is not currently available in the literature.

a)

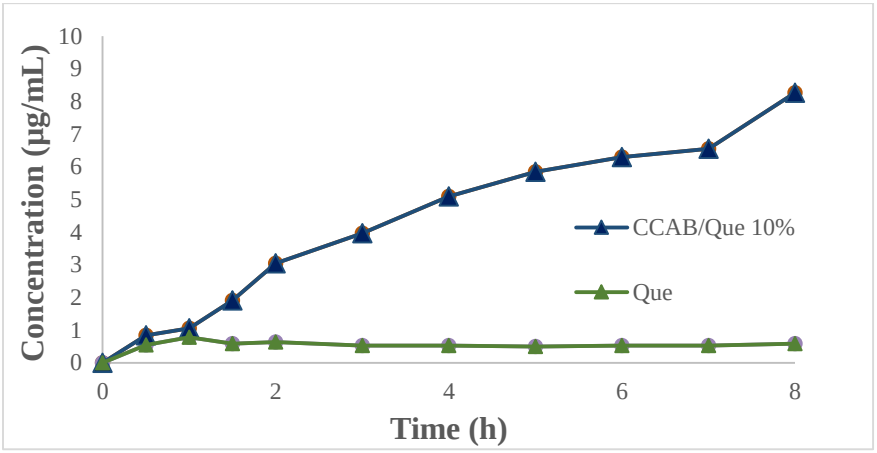

b)

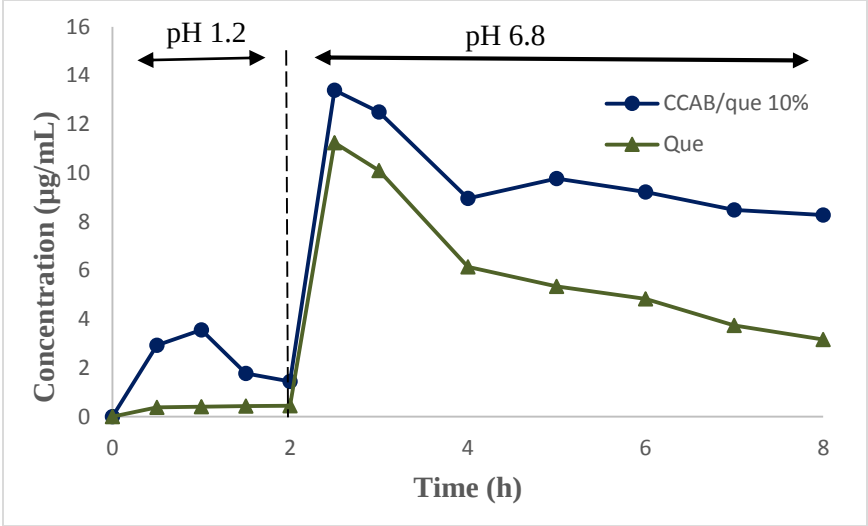

Figure 5.10: Dissolution profiles of CCAB/Que ASDs. Formulations with 10% quercetin at pH 6.8 (a) and at pH 1.2 for 2 h followed by pH 6.8 for 6 h.

Ritonavir

Given the success of polymers synthesized in our lab in providing significant stabilization against recrystallization for the antiviral drug ritonavir[2a, 4d, 9a], we thought it beneficial to test the effectiveness of CCAB in formulating and possibly providing solution concentration enhancement for ritonavir. Spray dried formulation of CCAB with 10% ritonavir (CCAB/Rit) produced an amorphous formulation. Upon dissolution testing, the CCAB formulation provided a 3-fold increase in solution concentration for ritonavir, which is a significant improvement over the crystalline drug. This resulting concentration of ritonavir (13 µg/mL) from the CCAB matrix is 65% of the theoretical amorphous solubility of ritonavir, which is calculated to be 20 µg/mL[15a]. In addition to the solubility enhancement gained from incorporation in the CCAB matrix, the cellulose carboxylate provided slower, more controlled release of the drug for the duration of the experiment as is especially noticeable in Figure 5.11b. Maximum concentration from the CCAB matrix was reached within 4 h and maintained for the duration of the 8h experiment. The higher solubility of ritonavir at pH 1.2 is expected due to the ionization of ritonavir at acidic pH[34]. The solubility of the crystalline drug quickly decreases at pH 6.8.

a)

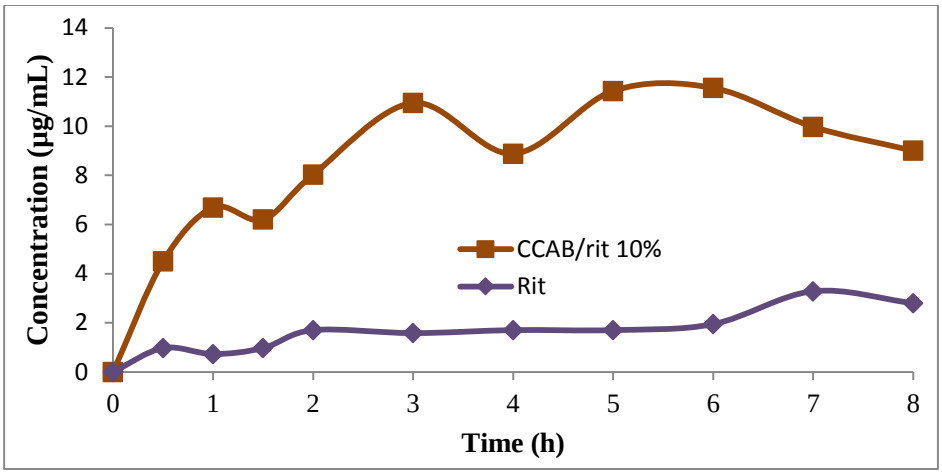

b)

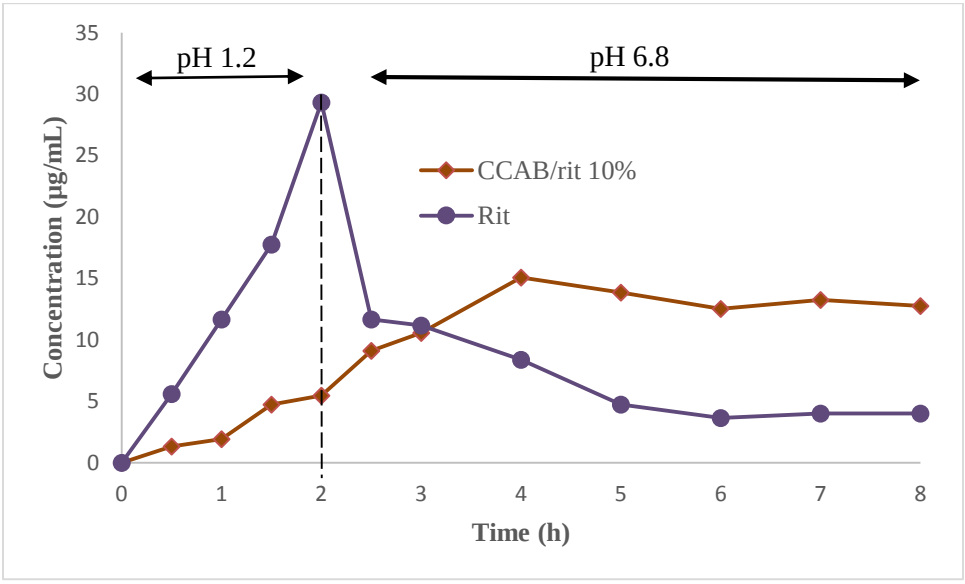

Figure 5.11: Dissolution profiles of CCAB/Rit ASDs. CCAB/10% ritonavir at a) pH 6.8 and b) pH 1.2 for 2h then pH 6.8 for 6h

Comparative experiments with common ASD polymers

While dissolution testing and drug solution concentration experiments can be very enlightening with regard to the potential of a matrix polymer to enhance solution concentration of a particular drug, comparison to commercially available and other matrix polymers that have proven effective, can also provide information about the effectiveness of the polymer being studied. Comparative dissolution experiments of ASDs of 10% loratadine in CCAB, PVP, HPMCAS, CASub, and CAAdP underscored the importance of polymer amphiphilicity in providing greater solution enhancement for a hydrophobic drug like loratadine (Figure 5.12). As expected, the water soluble

PVP provided fast release at gastric pH, releasing close to 100% of the drug. The release profile of loratadine from the PVP matrix was very similar to that of crystalline drug. After 2h, upon switching to pH 6.8, there was a rapid decrease in the drug (recrystallization of drug) and eventually a levelling off at ~ 4 µg/mL for the PVP formulation. The cellulose esters HPMCAS and CAAdP provided far superior solution concentration enhancement for loratadine, with the 10% Lor/CAAdP formulation providing concentrations up to 21 µg/mL (greater than the predicted amorphous solubility of 11 µg/mL) within 2.5h, and maintenance of this concentration for the duration of the study. HPMCAS also provided solution concentration enhancement for loratadine, providing concentrations up to 15 µg/mL with a release profile similar to CAAdP. HPMCAS and CAAdP both are reasonably soluble at pH 6.8 (Table 5.2) and have high DS (CO_2H) (CAAdP DS 0.85 and HPMCAS DS 0.40) that are ionized at pH 6.8 to give pH controlled release. The novel cellulosic CASub provided solution enhancement for the drug up to 20 µg/mL at pH 1.2 but may not be as effective at stabilizing loratadine against recrystallization as CAAdP, HPMCAS and CCAB as there was a slow decrease in drug concentration upon switching to pH 6.8, ultimately down to Lor concentrations of 4 µg/mL. While CCAB does not provide Lor solution concentration enhancement, it appears to prevent recrystallization of the drug and provides a slower release of the drug. This is also supported by the behavior of PVP/Lor compared to the CCAB/PVP/Lor formulation. Whereas loratadine concentration decreases quickly at pH 6.8 with PVP only, there is maintenance of solution concentration with the CCAB/PVP/Lor formulation. It is evident from the miscibility of loratadine and CCAB up to 50% drug loads that the CCAB matrix disperses the drug well but cannot provide solution concentration enhancement due to its relative hydrophobicity.

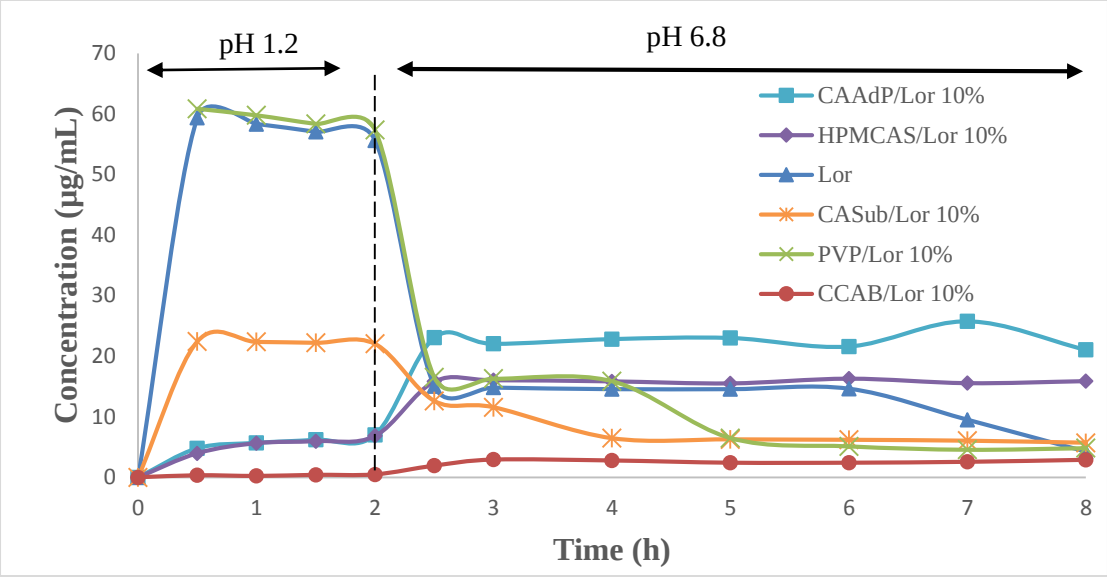

Figure 5.12: Comparison of dissolution profiles of CCAB/Lor 10% ASD to other common ASD polymers at pH 1.2 for 2 h followed by pH 6.8 for 6h.

Comparison of T_g values of ASDs - experimental vs. predicted by Fox equation

Table 5.3 describes T_g values of spray dried and extruded formulation used for the study. The comparison between predicted (by Fox equation) and experimental T_g values shows good correlation for the majority of the formulations including the 50% pairwise blend of CCAB and PVP. Similar T_gs are also demonstrated on comparison of extruded and spray dried formulations of Lor and Ibu with the same loading percentage of the drug. This suggests very little variability in the composition of the dispersions by spray-drying versus extrusion. Additional XRD diffractograms and DSC thermograms are provided in the appendix for some of the formulations described in Table 5.3.

Table 5.3: T_g values of ASDs - experimental vs. predicted by Fox equation

CCAB formulations with:	Experimental T_g	Predicted T_g
10% Ibu (ex)	110	109
25% Ibu (ex)	78	86
50% Ibu (ex)	-41, 62	63
10% Ibu (sd)	122	109
25% Ibu (sd)	120	86
50% Ibu (sd)	-24, 123	63
10% Lor (ex)	120	108
25% Lor (ex)	86	83
50% Lor (ex)	52	60
10% Lor (sd)	124	108
25% Lor (sd)	101	83
50% Lor (sd)	57	60
10% Lor/10% PVP (sd)	130	110
10% CLA	124	131
25% CLA	121	127
50% CLA	117, 182	120
10% Que	122	*
25% Que	125	*
50% Que	68	*
10% Rit	123	115
50% PVP	159	153

- There is no measured amorphous T_g for pure quercetin for calculation of experimental blend T_gs

5.9 Conclusions

It is quite evident that not only is CCAB an excellent matrix polymer for ASDs given its miscibility and ability to produce completely amorphous formulations with a number of highly crystalline drugs including quercetin, ritonavir, ibuprofen, clarithromycin and ritonavir, but it can also provide excellent solution enhancement for hydrophobic APIs including ritonavir and

quercetin. Not only is it possible to formulate these ASDs by spray drying, but the longer chain ester groups of the polymer help to provide significant plasticization to allow for melt extrusion of CCAB with the lower melting point drugs ibuprofen and loratadine. The extruded formulations when milled and sieved to produce microparticles also provide good drug solubility, as evident from the dissolution experiments, however they provide much slower drug release due to the denser particles when compared to spray dried microparticles. When formulated with the most hydrophobic drug loratadine, CCAB provides more controlled, slower release of the drug but does not provide much solution enhancement. However, the addition of a small percentage of a water soluble polymer, PVP, with which CCAB shows good miscibility, provides a 2-fold increase in Lor solution concentration (up to 4 µg/mL). Ibuprofen is one of the more soluble of the drugs utilized in this work and does not achieve solution concentration enhancement from the CCAB matrix, but instead benefits from a slower release of the drug over the residence time along the gastrointestinal tract. This is advantageous for the delivery of ibuprofen since the lower concentrations within the stomach will reduce irritation of the stomach lining often caused by ibuprofen. Formulations of the hydrophobic drugs quercetin and ritonavir with CCAB show much more significant solution concentration enhancement (up to 8 and 13 µg/mL respectively). CCAB provides more controlled release of the drugs and in the case of quercetin shows indications that it may reduce drug degradation compared to that of the crystalline drug. The results from these experiments show that CCAB is a promising matrix polymer for amorphous solid dispersions. Unexpectedly, it can be formulated by melt extrusion to provide extruded microparticles with high drug loads and completely amorphous dispersions of several APIs at concentrations up to 25% drug. The ability of the polymer to provide solution enhancement is influenced by the hydrophobicity of the drugs, and their propensity for degradation, but also provides slower, more controlled release of the drug actives with higher drug solution concentrations at intestinal pH. These results show the utility of CCAB itself, and also provide a good example of the potential benefits of ternary amorphous formulation by pairwise polymer blending.

5.10 References

1. (a) Liechty, W. B.; Kryscio, D. R.; Slaughter, B. V.; Peppas, N. A., Polymers for drug delivery systems. *Annual review of chemical and biomolecular engineering* **2010,** *1*, 149; (b) Uhrich, K. E.; Cannizzaro, S. M.; Langer, R. S.; Shakesheff, K. M., Polymeric systems for controlled drug release. *Chemical reviews* **1999,** *99* (11), 3181-3198; (c) Pillai, O.; Panchagnula, R., Polymers in drug delivery. *Current opinion in chemical biology* **2001,** *5* (4), 447-451.
2. (a) Ilevbare, G. A.; Liu, H. Y.; Edgar, K. J.; Taylor, L. S., Understanding Polymer Properties Important for Crystal Growth Inhibition-Impact of Chemically Diverse Polymers on Solution Crystal Growth of Ritonavir. *Cryst Growth Des* **2012,** *12* (6), 3133-3143; (b) Liu, H.; Ilevbare, G. A.; Cherniawski, B. P.; Ritchie, E. T.; Taylor, L. S.; Edgar, K. J., Synthesis and structure–property evaluation of cellulose ω-carboxyesters for amorphous solid dispersions. *Carbohydrate Polymers* **2014,** *100* (0), 116-125.
3. (a) Ornelas-Megiatto, C. t.; Wich, P. R.; Fréchet, J. M., Polyphosphonium polymers for siRNA delivery: an efficient and nontoxic alternative to polyammonium carriers. *Journal of the American Chemical Society* **2012,** *134* (4), 1902-1905; (b) Hemp, S. T.; Allen Jr, M. H.; Smith, A. E.; Long, T. E., Synthesis and properties of sulfonium polyelectrolytes for biological applications. *ACS Macro Letters* **2013,** *2* (8), 731-735.
4. (a) Li, B.; Konecke, S.; Harich, K.; Wegiel, L.; Taylor, L. S.; Edgar, K. J., Solid Dispersion of Quercetin in Cellulose Derivative Matrices Influences both Solubility and Stability. *Carbohydrate Polymers* **2013,** *92* (2), 2033-2040; (b) Marks, J. A.; Wegiel, L. A.; Taylor, L. S.; Edgar, K. J., Pairwise Polymer Blends for Oral Drug Delivery. *Journal of pharmaceutical sciences* **2014,** *103* (9), 2871-2883; (c) Pereira, J. M.; Mejia-Ariza, R.; Ilevbare, G. A.; McGettigan, H. E.; Sriranganathan, N.; Taylor, L. S.; Davis, R. M.; Edgar, K. J., Interplay of degradation, dissolution and stabilization of clarithromycin and its amorphous solid dispersions. *Molecular pharmaceutics* **2013,** *10* (12), 4640-4653; (d) Ilevbare, G. A.; Liu, H.; Edgar, K. J.; Taylor, L. S., Effect of Binary Additive Combinations on Solution Crystal Growth of the Poorly Water-Soluble Drug, Ritonavir. *Cryst Growth Des* **2012,** *12* (12), 6050-6060; (e) Yang, Z.; Nollenberger, K.; Albers, J.; Craig, D.; Qi, S., Microstructure of an immiscible polymer blend and its stabilization effect on amorphous solid dispersions. *Molecular pharmaceutics* **2013**.
5. (a) Posey-Dowty, J.; Watterson, T.; Wilson, A.; Edgar, K.; Shelton, M.; Lingerfelt, L., Zero- order release formulations using a novel cellulose ester. *Cellulose* **2007,** *14* (1), 73-83; (b) Li, B.; Wegiel, L. A.; Taylor, L. S.; Edgar, K. J., Stability and solution concentration enhancement of resveratrol by solid dispersion in cellulose derivative matrices. *Cellulose* **2013,** *20* (3), 1249-1260; (c) Posey-Dowty, J.; Watterson, T.; Edgar, K.; Kirk, S.; Welty, M.; Yuan, J.; Shelton, M.; Lingerfelt, L.; Wilson, A. Carboxyalkyl cellulose esters for sustained delivery of pharmaceutically active substances. WO Patent 2,007,056,125, 2007; (d) Shelton, M. C.; Posey-Dowty, J. D.; Lingerfelt, L.; Kirk, S. K.; Klein, S.; Edgar, K. J., Enhanced dissolution of poorly soluble drugs from solid dispersions in carboxymethylcellulose acetate butyrate matrices. In *Polysaccharide Materials: Performance by Design*, American Chemical Society: 2009; Vol. 1017, pp 93-113.
6. (a) Miller, J. M.; Beig, A.; Carr, R. A.; Spence, J. K.; Dahan, A., A Win-Win Solution in Oral Delivery of Lipophilic Drugs: Supersaturation via Amorphous Solid Dispersions Increases Apparent Solubility without Sacrifice of Intestinal Membrane Permeability. *Molecular Pharmaceutics* **2012,** *9* (7), 2009-2016; (b) Curatolo, W.; Nightingale, J. A.; Herbig, S. M., Utility of hydroxypropylmethylcellulose acetate succinate (HPMCAS) for initiation and maintenance of drug supersaturation in the GI milieu. *Pharmaceutical research* **2009,** *26* (6), 1419-1431; (c) Shah, N.; Iyer, R. M.; Mair, H. J.; Choi, D. S.; Tian, H.; Diodone, R.; Fahnrich, K.; Pabst-Ravot, A.;

Tang, K.; Scheubel, E.; Grippo, J. F.; Moreira, S. A.; Go, Z.; Mouskountakis, J.; Louie, T.; Ibrahim, P. N.; Sandhu, H.; Rubia, L.; Chokshi, H.; Singhal, D.; Malick, W., Improved human bioavailability of vemurafenib, a practically insoluble drug, using an amorphous polymer-stabilized solid dispersion prepared by a solvent-controlled coprecipitation process. *J Pharm Sci* **2013,** *102* (3), 967-81; (d) Tanno, F.; Nishiyama, Y.; Kokubo, H.; Obara, S., Evaluation of hypromellose acetate succinate (HPMCAS) as a carrier in solid dispersions. *Drug Development and Industrial Pharmacy* **2004,** *30* (1), 9-17; (e) Trasi, N. S.; Taylor, L. S., Effect of polymers on nucleation and crystal growth of amorphous acetaminophen. *CrystEngComm* **2012,** *14* (16), 5188-5197.

7. (a) Varshosaz, J.; Tavakoli, N.; Eram, S. A., Use of natural gums and cellulose derivatives in production of sustained release metoprolol tablets. *Drug Delivery* **2006,** *13* (2), 113-119; (b) Moretti, M. D. L.; Gavini, E.; Juliano, C.; Pirisino, G.; Giunchedi, P., Spray-dried microspheres containing ketoprofen formulated into capsules and tablets. *Journal of Microencapsulation* **2001,** *18* (1), 111-121; (c) Pygall, S. R.; Griffiths, P. C.; Wolf, B.; Timmins, P.; Melia, C. D., Solution interactions of diclofenac sodium and meclofenamic acid sodium with hydroxypropyl methylcellulose (HPMC). *International Journal of Pharmaceutics* **2011,** *405* (1-2), 55-62; (d) Vueba, M. L.; de Carvalho, L. A. E. B.; Veiga, F.; Sousa, J. J.; Pina, M. E., Role of cellulose ether polymers on ibuprofen release from matrix tablets. *Drug Development and Industrial Pharmacy* **2005,** *31* (7), 653-665.

8. Kar, N.; Liu, H.; Edgar, K. J., Synthesis of cellulose adipate derivatives. *Biomacromolecules* **2011,** *12* (4), 1106-15.

9. (a) Ilevbare, G.; Liu, H.; Edgar, K. J.; Taylor, L., Inhibition of Solution Crystal Growth of Ritonavir by Cellulose Polymers–Factors Influencing Polymer Effectiveness. *CrystEngComm* **2012,** *14* (20), 6503-6514; (b) Ilevbare, G. A.; Liu, H.; Edgar, K. J.; Taylor, L. S., Impact of Polymers on Crystal Growth Rate of Structurally Diverse Compounds from Aqueous Solution. *Molecular pharmaceutics* **2013,** *10* (6), 2381-2393.

10. Edgar, K. J., Cellulose esters in drug delivery. *Cellulose* **2007,** *14* (1), 49-64.

11. (a) Edgar, K. J.; Buchanan, C. M.; Debenham, J. S.; Rundquist, P. A.; Seiler, B. D.; Shelton, M. C.; Tindall, D., Advances in cellulose ester performance and application. *Progress in Polymer Science* **2001,** *26* (9), 1605-1688; (b) Kosaka, P.; Kawano, Y.; Salvadori, M.; Petri, D., Characterization of ultrathin films of cellulose esters. *Cellulose* **2005,** *12* (4), 351-359.

12. (a) Wang, P.; Tao, B. Y., Synthesis and characterization of long-chain fatty acid cellulose ester (FACE). *Journal of applied polymer science* **1994,** *52* (6), 755-761; (b) Mohanty, A.; Wibowo, A.; Misra, M.; Drzal, L., Development of renewable resource–based cellulose acetate bioplastic: Effect of process engineering on the performance of cellulosic plastics. *Polymer Engineering & Science* **2003,** *43* (5), 1151-1161; (c) Klemm, D.; Heublein, B.; Fink, H. P.; Bohn, A., Cellulose: Fascinating biopolymer and sustainable raw material. *Angewandte Chemie-International Edition* **2005,** *44* (22), 3358-3393.

13. Wegiel, L. A.; Mauer, L. J.; Edgar, K. J.; Taylor, L. S., Crystallization of amorphous solid dispersions of resveratrol during preparation and storage-Impact of different polymers. *J Pharm Sci* **2012**.

14. Zheng, X.; Gandour, R. D.; Edgar, K. J., Probing the mechanism of TBAF-catalyzed deacylation of cellulose esters. *Biomacromolecules* **2013,** *14* (5), 1388-1394.

15. (a) Ilevbare, G. A.; Liu, H.; Edgar, K. J.; Taylor, L. S., Maintaining supersaturation in aqueous drug solutions: Impact of different polymers on induction times. *Cryst Growth Des* **2013,** *13* (2), 740-751; (b) Zecevic, D. E.; Meier, R.; Daniels, R.; Wagner, K.-G., Site specific solubility

improvement using solid dispersions of HPMC-AS/HPC SSL – Mixtures. *European Journal of Pharmaceutics and Biopharmaceutics* **2014,** *87* (2), 264-270; (c) Van den Mooter, G., The use of amorphous solid dispersions: A formulation strategy to overcome poor solubility and dissolution rate. In *Drug Discovery Today: Technologies*, 2012; Vol. 9, pp e79-e85.
16. (a) Buchanan, C. M.; Buchanan, N. L.; Carty, S. N.; Kuo, C. M.; Lambert, J. L.; Posey-Dowty, J. D.; Watterson, T. L.; Wood, M. D.; Malcolm, M. O.; Lindblad, M. S. Cellulose interpolymers and method of oxidation. US Patent 9,040,684 B2, 2011; (b) Buchanan, C. M.; Buchanan, N. L.; Carty, S. N.; Kuo, C. M.; Lambert, J. L.; Malcolm, M. O.; Posey-Dowty, J. D.; Watterson, T. L.; Wood, M. D.; Lindblad, M. S. Cellulose interpolymers and method of oxidation. US Patent 9,040,685 B2, 2013; (c) Buchanan, C. M.; Buchanan, N. L.; Carty, S. N.; Kuo, C. M.; Lambert, J. L.; Malcolm, M. O.; Posey-Dowty, J. D.; Watterson, T. L.; Wood, M. D.; Lindblad, M. S. Cellulose interpolymers and method of oxidation. US Patent 9,040,683 B2, 2015.
17. (a) Zhang, Y.; Chen, J. J.; Zhang, G. H.; Lu, J. W.; Yan, H. S.; Liu, K. L., Sustained release of ibuprofen from polymeric micelles with a high loading capacity of ibuprofen in media simulating gastrointestinal tract fluids. *Reactive & Functional Polymers* **2012,** *72* (6), 359-364; (b) Vueba, M. L.; Veiga, F.; Sousa, J. J.; Pina, M. E., Compatibility studies between ibuprofen or ketoprofen with cellulose ether polymer mixtures using thermal analysis. *Drug Development and Industrial Pharmacy* **2005,** *31* (10), 943-949; (c) Rivera-Leyva, J.; Garcia-Flores, M.; Valladares-Mendez, A.; Orozco-Castellanos, L. M.; Martinez-Alfaro, M., Comparative Studies on the Dissolution Profiles of Oral Ibuprofen Suspension and Commercial Tablets using Biopharmaceutical Classification System Criteria. *Indian journal of pharmaceutical sciences 74* (4), 312-318.
18. Zeeshan, F.; Bukhari, N. I., Development and evaluation of a novel modified-release pellet-based tablet system for the delivery of loratadine and pseudoephedrine hydrochloride as model drugs. *AAPS PharmSciTech 11* (2), 910-916.
19. Bureau, G.; Longpré, F.; Martinoli, M. G., Resveratrol and quercetin, two natural polyphenols, reduce apoptotic neuronal cell death induced by neuroinflammation. *Journal of neuroscience research* **2008,** *86* (2), 403-410.
20. (a) Timpe, C., Drug solubilization strategies: applying nanoparticulate formulation and solid dispersion approaches in drug development. *Am Pharm Rev* **2010,** *13* (1), 12; (b) Alonzo, D. E.; Gao, Y.; Zhou, D. L.; Mo, H. P.; Zhang, G. G. Z.; Taylor, L. S., Dissolution and Precipitation Behavior of Amorphous Solid Dispersions. *Journal of Pharmaceutical Sciences* **2011,** *100* (8), 3316-3331; (c) Repka, M. A.; Majumdar, S.; Kumar Battu, S.; Srirangam, R.; Upadhye, S. B., Applications of hot-melt extrusion for drug delivery. **2008**.
21. Sarode, A. L.; Sandhu, H.; Shah, N.; Malick, W.; Zia, H., Hot melt extrusion (HME) for amorphous solid dispersions: predictive tools for processing and impact of drug–polymer interactions on supersaturation. *European Journal of Pharmaceutical Sciences* **2013,** *48* (3), 371-384.
22. Repka, M.; McGinity, J.; Zhang, F.; Koleng, J., Encyclopedia of pharmaceutical technology. *Marcel Dekker, New York* **2002**.
23. Shah, S.; Maddineni, S.; Lu, J.; Repka, M. A., Melt extrusion with poorly soluble drugs. *International journal of pharmaceutics* **2013,** *453* (1), 233-252.
24. (a) Feng, J.; Xu, L.; Gao, R.; Luo, Y.; Tang, X., Evaluation of polymer carriers with regard to the bioavailability enhancement of bifendate solid dispersions prepared by hot-melt extrusion. *Drug development and industrial pharmacy* **2012,** *38* (6), 735-743; (b) Liu, J.; Cao, F.; Zhang, C.; Ping, Q., Use of polymer combinations in the preparation of solid dispersions of a thermally

unstable drug by hot-melt extrusion. *Acta Pharmaceutica Sinica B* **2013,** *3* (4), 263-272; (c) Lakshman, J. P.; Cao, Y.; Kowalski, J.; Serajuddin, A. T., Application of melt extrusion in the development of a physically and chemically stable high-energy amorphous solid dispersion of a poorly water-soluble drug. *Mol Pharm* **2008,** *5* (6), 994-1002.
25. Sarode, A. L.; Obara, S.; Tanno, F. K.; Sandhu, H.; Iyer, R.; Shah, N., Stability assessment of hypromellose acetate succinate (HPMCAS) NF for application in hot melt extrusion (HME). *Carbohydrate polymers* **2014,** *101*, 146-153.
26. Dong, Z.; Choi, D. S., Hydroxypropyl methylcellulose acetate succinate: potential drug–excipient incompatibility. *AAPs Pharmscitech* **2008,** *9* (3), 991-997.
27. Ōmura, S., *Macrolide Antibiotics: Chemistry, Biology, and Practice*. Academic Press: 2002.
28. Ilevbare, G. A.; Taylor, L. S., Liquid–liquid phase separation in highly supersaturated aqueous solutions of poorly water-soluble drugs: Implications for solubility enhancing formulations. *Crystal Growth & Design* **2013,** *13* (4), 1497-1509.
29. Hsieh, Y.-L.; Ilevbare, G. A.; Van Eerdenbrugh, B.; Box, K. J.; Sanchez-Felix, M. V.; Taylor, L. S., pH-Induced precipitation behavior of weakly basic compounds: determination of extent and duration of supersaturation using potentiometric titration and correlation to solid state properties. *Pharmaceutical research* **2012,** *29* (10), 2738-2753.
30. Andrews, G. P.; Abu-Diak, O.; Kusmanto, F.; Hornsby, P.; Hui, Z.; Jones, D. S., Physicochemical characterization and drug-release properties of celecoxib hot-melt extruded glass solutions. *Journal of Pharmacy and Pharmacology* **2010,** *62* (11), 1580-1590.
31. Semble, E. L.; Wu, W. C. In *Antiinflammatory drugs and gastric mucosal damage*, Seminars in arthritis and rheumatism, Elsevier: 1987; pp 271-286.
32. Almeida e Sousa, L.; Reutzel-Edens, S. M.; Stephenson, G. A.; Taylor, L. S., Assessment of the Amorphous "Solubility" of a Group of Diverse Drugs Using New Experimental and Theoretical Approaches. *Molecular pharmaceutics* **2014,** *12* (2), 484-495.
33. Ramešová, Š.; Sokolová, R.; Degano, I.; Bulíčková, J.; Žabka, J.; Gál, M., On the stability of the bioactive flavonoids quercetin and luteolin under oxygen-free conditions. *Analytical and bioanalytical chemistry* **2012,** *402* (2), 975-982.
34. Law, D.; Krill, S. L.; Schmitt, E. A.; Fort, J. J.; Qiu, Y.; Wang, W.; Porter, W. R., Physicochemical considerations in the preparation of amorphous ritonavir–poly (ethylene glycol) 8000 solid dispersions. *Journal of pharmaceutical sciences* **2001,** *90* (8), 1015-1025.

Chapter 6: Summary and Future Work

6.1 Pairwise Polymer Blends for Oral Drug delivery

Cellulose derivatives have played a vital role as matrix materials for amorphous solid dispersions (ASDs) over the years. Some of the commercially available polymers for these applications include cellulosics as well as synthetic polymers like PVP and E100. **Chapter 3** of this work examined pairwise blends of some synthetic and cellulosic polymers with the aim of establishing blends that are miscible and display complementary properties for the delivery of poorly water-soluble drugs. The commercial polymers utilized were chosen based on their promising drug delivery capabilities in the literature and in commercial drug applications and a novel cellulose omega carboxy ester (CAAdP)[1], recently synthesized in our laboratories, also presented an exciting possibility given its effectiveness with a number of drug molecules including ritonavir, clarithromycin and some phenolic compounds. The polymers used for the study are depicted in **Figure 6.1.**

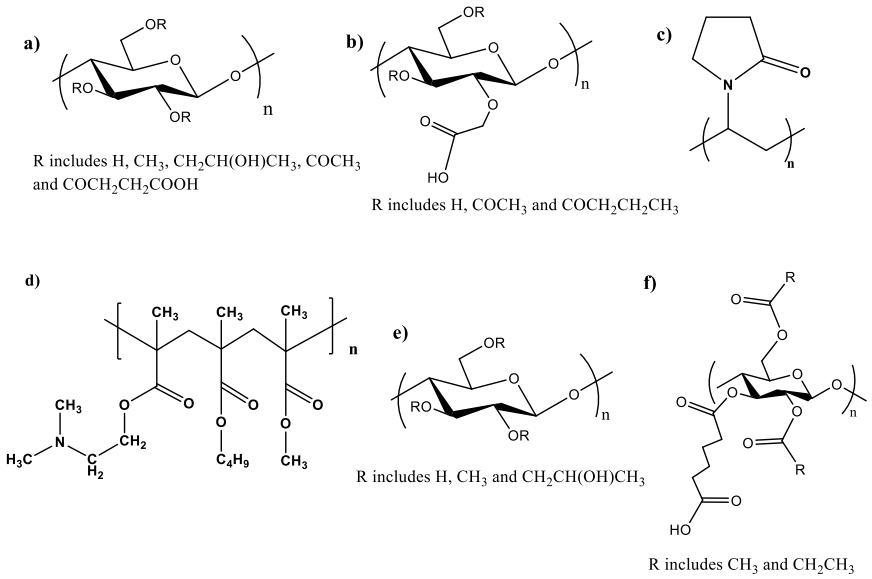

Figure 6.1: Chemical structures of a) HPMCAS b) CMCAB c) PVP d) Eudragit® E100 e) HPMC and f) CAAdP

The blended polymer formulations were film cast as well as spray dried. Film casting was used to give an early estimate of whether any of the blends were immiscible, in which case the film was translucent.. Of the 35 polymer combinations that were examined, only blends of PVP/E100 exhibited immiscibility from this preliminary examination. Further chromatographic and

spectroscopic analyses would further underscore the importance of hydrogen bonding interactions in promoting miscibility between the polymer pairs. The lack of sufficient hydrogen bonding interactions between PVP and E100, which both contain only hydrogen bond acceptor groups, was primarily responsible for the immiscibility of the pair. Comparison of the solubility parameters as well as the presence of hydrogen bond acceptor and donor groups in the polymer blends helped to further understanding of the structural properties of the polymers that would lead to favorable interactions in an amorphous formulation. Single T_g values in a number of these blends coupled with spectroscopic analyses showed that the water soluble polymers PVP and HPMC were miscible with at least four of the other polymers utilized including the novel cellulosic CAAdP. This is significant as not only is increased water solubility critical for favorable release of drug molecules, but studies have highlighted that optimal levels of hydrophobicity/hydrophilicity are necessary to prevent recrystallization of drugs within the ASD. Additionally, many water soluble polymers tend to provide very fast release in the stomach. Addition of a more hydrophobic polymer partner, with which the water soluble polymer is miscible, can be critical for more controlled drug release capabilities. The results of the study are summarized in **Table 6.1**[2]**.**

Due to limitations in the amount of CAAdP available, blends with this polymer were analyzed only in 50/50 (w/w) compositions and coprecipitated instead of spray dried. However, for further utilization of CAAdP in blend formulations, it may be useful to analyze more carefully whether small percentages of CAAdP (on the order of 10 and 15%) may still provide effective miscible formulations for ASD preparation with critical drug molecules. The knowledge of the miscibility of various pairwise blends of these commercially polymers presents a more cost effective means of tailoring formulations with optimal hydrophobicity for utilization with a particular drug. While significant attempts are constantly being made in our lab and others to synthesize a single polymer that is widely effective for ASD formulations, the job can be quite daunting and costly.

While spray drying and other solvent utilizing techniques are very effective for making ASD formulations, extrusion techniques may be an effective means of eliminating solvent involvement and putting these pairwise blends to good use. Extruded materials currently on the market already apply these techniques, for example Kaletra, a drug product of ritonavir/lopinavir that uses PVP/VA as the matrix materials. Given the access to a mini extruder, it may be very beneficial for pairwise blends of some of the commonly extruded polymers like HPMCAS, HPMC

and PVP to be utilized in this regard with small amounts of CAAdP or in other miscible combinations for the study of the effectiveness with common drugs like ibuprofen, loratadine and others.

Table 6.1: Comparison of Expected versus Observed Tg values and Film Clarity of the Blends

Polymer A	% A	Polymer B	% B	*Expected T_g, °C	Observed T_g(s), °C	Film Clarity	Miscibility
CMCAB	25	HPMCAS	75	125	123	Clear	
	50		50	131	122/139	Clear	p
	75		25	137	134	Clear	
CMCAB	25	E100	75	58	82	Clear	**m**
	50		50	72	101	Clear	
	75		25	96	128	Clear	
CMCAB	25	PVP	75	168	167	Clear	**m**
	50		50	159	159	Clear	
	75		25	151	158	Clear	
CMCAB	25	HPMC	75	158	164	Clear	**m**
	50		50	153	150	Clear	
	75		25	148	144	Clear	
HPMCAS	25	E100	75	57	60	Clear	**m**
	50		50	69	94	Clear	
	75		25	87	110	Clear	
HPMCAS	25	PVP	75	159	160	Clear	**m**
	50		50	143	149	Clear	
	75		25	131	138	Clear	
HPMCAS	25	HPMC	75	150	153	Clear	**m**
	50		50	138	143	Clear	
	75		25	129	130	Clear	
E100	25	PVP	75	106	176/48	Translucent	
	50		50	76	175/48	Translucent	**i**
	75		25	59	175/50	Translucent	
E100	25	HPMC	75	102	**	Clear	
	50		50	74	**	Rel. clear	**i**
	75		25	58	**	Rel. clear	
PVP	25	HPMC	75	167	167	Clear	
	50		50	170	171	Clear	**m**
	75		25	174	172	Clear	
CAAdP	50	CMCAB	50	123	125	Clear	**m**
CAAdP	50	HPMCAS	50	113	114	Clear	**m**
CAAdP	50	E100	50	66	87	Clear	**m**
CAAdP	50	HPMC	50	130	114	Rel. clear	**m**
CAAdP	50	PVP	50	134	132	Clear	**m**

Apparent Miscibility	**m**
Immiscible	**i**
Some compositions miscible	**p**

*Expected Tg values are calculated using the Fox Equation[3,4]

6.2 Cationic Cellulose Derivatives for Drug Delivery

Cationic polymers present exciting possibilities for the delivery of anionic drug molecules including DNA and RNA. The oral delivery of such molecules is one area in which more options are needed. Cationic polysaccharides are especially interesting for these applications and many, including chitosan, are of interest as paracellular permeation enhancers (PPEs)[5]. These PPEs are capable of complexing nucleic acids and some proteins through electrostatic interactions and promoting the permeation of hydrophilic macromolecules across the epithelial membrane. The research described in **Chapter 4** established new synthetic pathways to cationic derivatives of cellulose regioselectively substituted at C-6. These derivatives, both ammonium and phosphonium, possess permanent positive charges along the cellulose backbone. This is significant given the limited solubility of the glucosamine-containing polysaccharide chitosan at neutral pH, that limits its efficiency considerably[6].

Regioselectively substituted 6-halo-6-deoxy-2,3-di-*O*-acyl cellulose derivatives were used as starting materials for the ammonium and phosphonium derivatives of cellulose. These starting esters were modified through reactions with trialkylamines and phosphines. The synthetic pathways to the regioselective phosphonium derivatives are described in **Scheme 6.1**. Regioselective substitution with these reagents was successful and produced DS up to 0.4 and 0.7 for the resulting N,N,N-trialkyl-6-deoxy-6-ammonio-2, 3-di-O-acyl-cellulose and P, P, P-triethyl-6-deoxy-6-phosphonio-2, 3-di-O-acyl-cellulose derivatives respectively.

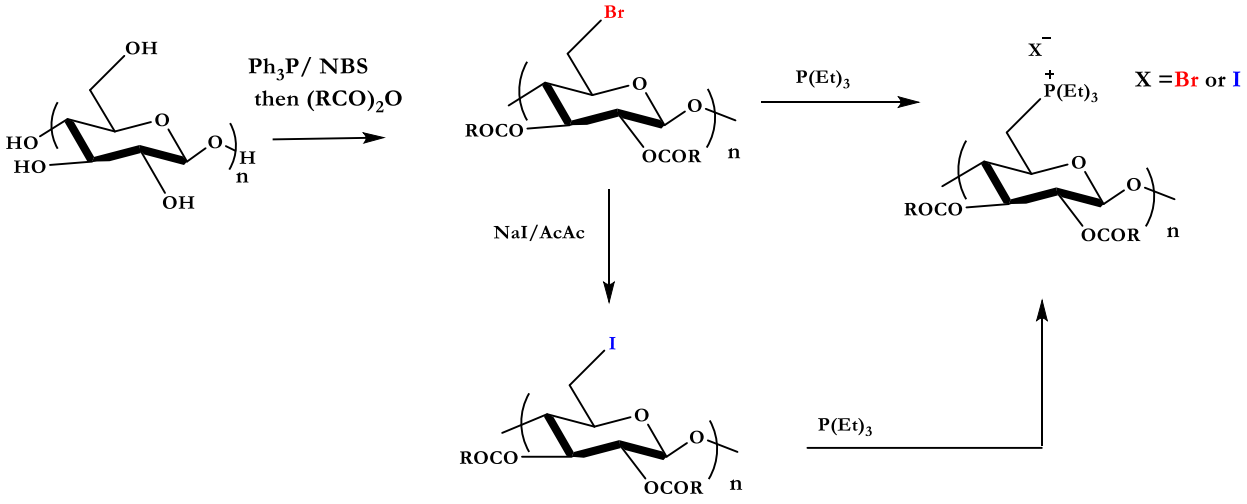

Scheme 6.1: Reaction of 6-deoxy-6-halocellulose esters with triethylphosphine

Early kinetic experiments revealed limitations to the degree of substitution attainable for the ammonium derivatives, and this was thought to be influenced by the propagation of the positive charges along the backbone, and the resulting repulsive forces that limit the highest DS achievable. The highest DS for the ammonium derivatives was 0.43 in DMSO and 0.47 in DMF with the *in situ* addition of NaI as a catalyst[7]. We tested the charge repulsion hypothesis by reacting our starting material with a dialkylamine to test whether the absence of charge in the tertiary amine product would result in higher conversion. This reaction produced a tertiary amine derivative with DS 0.9, giving support to our hypothesis on the limiting nature of the repulsion between positively charged substituents. The examination of the influence of ester chain length at C2 and C3 revealed no significant differences in the DS of the ammonium products.

Additionally, there were also attempts to utilize longer chain trialkylamines to test the influence on the amine chain length and tributylamine was explored for this purpose. This produced a low DS (< 0.1) product, the DS limitation likely being influenced by the bulkiness of the derivative for substitution at C-6, but perhaps primarily due to the relative insolubility of the tributylamine reagent in the solvents explored. The lower DS ammonium derivatives had good solubility in polar solvents but were not soluble in water. Given the ability of the larger phosphorus atom to disperse positive charge more efficiently than nitrogen, we were gratified to find that higher DS levels of phosphonium substituent were achievable upon reaction of our starting material with triethylphosphine. The highest DS achieved was 0.73, with all the phosphonium derivatives prepared displaying DS of positively charged substituent > 0.5, and possessing solubility in water and various other polar solvents. A summary of these reactions is given in **Table 6.2**.

The establishment of synthetic pathways to these positively charged ammonium and phosphonium derivatives will certainly open up new possibilities for their use in drug delivery applications including determining their utility as paracellular permeability enhancers. It will be critical to establish the relative toxicity of these compounds and to establish the influence of cationic DS on toxicity. It is quite possible that lower DS products could find as much utility as their higher DS counterparts since positively charged species are known to often elicit more toxic effects than uncharged species[8]. The use of these derivatives in ASD applications with anionic drugs is certainly a good mode of exploration for these derivatives as well and, in fact, it may also be worthwhile to test the high DS (0.9) tertiary amine derivative as a matrix polymer for ASDs.

For these purposes, it will be important to understand more about the influence of the synthetic process on the molecular weight of these derivatives by utilizing aqueous gel permeation chromatography (GPC) when available.

The unexpectedly low thermal degradation temperatures for the phosphonium derivatives described in **Chapter 4** indicate that more information on the thermal properties of these derivatives may be needed to establish the pathways by which these derivatives degrade relative to their ammonium counterparts[9].

Table 6.2: Regioselectively C-6 substituted cationic cellulose derivatives

Substrate	Solvent	Mol eq. TEA/ (NaI)	DS Ammonium	DS Ester	Product #
6Br23Ac	DMF	100/(5)	0.47	1.80	1.4
6Br23Ac	DMSO	100/0	0.43	1.89	1.5
6Br23Ac	DMSO	100/(5)	0.33	1.86	1.6
6Br23Ac	DMSO	100/(10)	0.37	1.95	1.7
Substrate	**Solvent**	**Mol eq. TEP**	**DS Phosphonium**	**DS Ester**	**Product #**
6Br23Ac	DMF	10	0.60	1.84	2.3
6Br23Ac	DMSO	10	0.73	1.91	2.4
6Br23Bu	DMF	10	0.59	1.77	2.5
6Br23Bu	DMSO	10	0.68	1.92	2.6

6.3 6-Carboxycellulose Acetate Butyrate as a Novel Polymer for Amorphous Solid Dispersion and Extrusion

6-Carboxycellulose acetate butyrate (CCAB) is an untapped matrix polymer resource whose utility has been previously reported only in waterborne coating applications[10]. In chapter 5, we describe the first detailed investigations on the use of CCAB as an ASD polymer. We elected to test the effectiveness of CCAB in reducing the crystallinity and forming miscible combinations with a number of structurally diverse active pharmaceutical ingredients (APIs). These drugs included loratadine, ibuprofen, quercetin, clarithromycin and ritonavir. These CCAB formulations were formulated using both spray-drying and melt extrusion. The longer chain butyryl ester groups on CCAB were hypothesized as potential plasticizers for effective melt extrusion with the lower

melting point drugs ibuprofen and loratadine. CCAB was successfully spray-dried and melt extruded and we established that CCAB was capable of reducing the crystallinity of all the drugs up to 25 wt% and up to 50% for loratadine using X-ray diffraction (XRD). These miscible combinations of polymer and drug were also evaluated by FTIR and DSC to further support the favorable interactions with the drugs tested. Thermal analyses by DSC also revealed moderate correlations of the experimental T_g values with the values predicted using the Fox-Flory equation. Dissolution experiments were conducted at pH 1.2 and pH 6.8 to evaluate the influence of CCAB, as a matrix polymer, on the dissolution behavior of the targeted drugs under the pH conditions along the gastrointestinal (GI) tract. These experiments highlighted the ability of CCAB to moderate the release of the drugs providing slower, more controlled release in most cases and providing solution concentration enhancement; up to 3-fold increase in the solution concentrations of quercetin and ritonavir when 10% drug loaded formulations were examined (**Figure 6.2**).

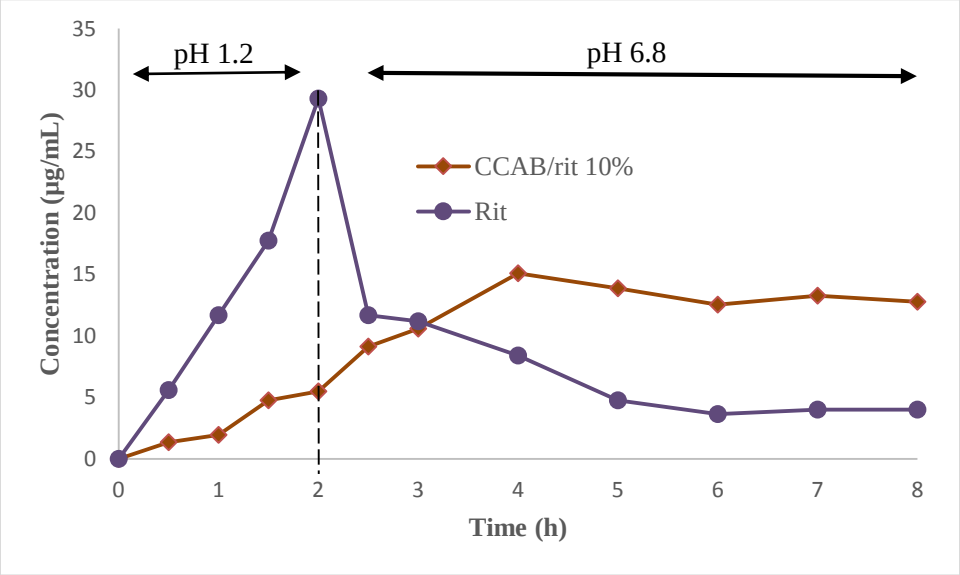

Figure 6.2: Dissolution profiles of 10% Rit in CCAB at pH 1.2 for 2h, then pH 6.8 for 6h

For CCAB/drug combinations resulting in little or no solubility enhancement, hypothesized to be due to the hydrophobicity of CCAB, we also explored the benefits of a ternary polymer/polymer/drug formulation with addition of a water soluble established ASD polymer[2, 11]. This was explored in the case of loratadine, the most hydrophobic and least soluble at pH 6.8 of the drugs in this study. Addition of 10 wt% PVP to the formulation resulted in a 2-fold increase in

solubility compared to the pure drug, spray-dried and extruded 10% loratadine formulations (**Figure 6.3**).

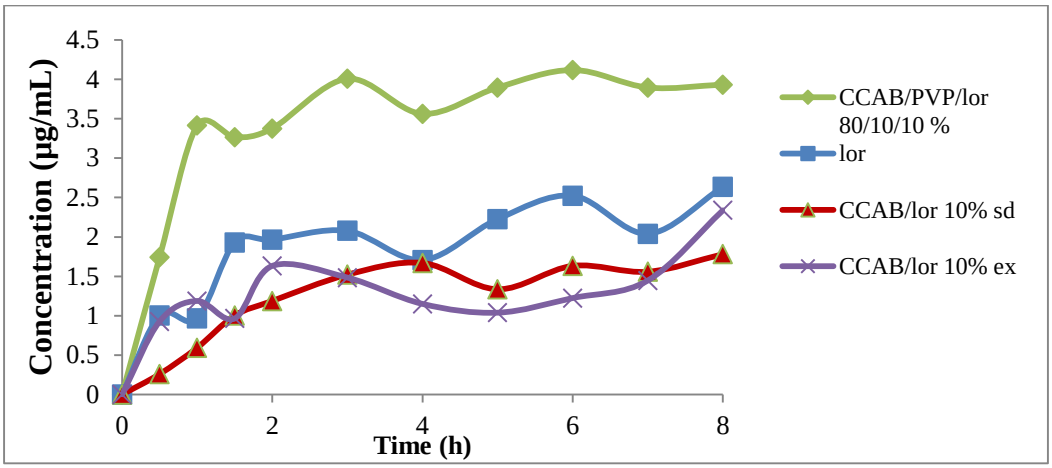

Figure 6.3: Dissolution profiles of 10% Lor in CCAB and ternary CCAB/PVP formulations at pH 6.8. (Note: "sd" indicates spray-dried, "ex" denotes extruded formulations)

Further examination of the potential benefits of CCAB on the solution concentration and degradation reduction for some drugs including clarithromycin[12] are needed and will be further explored. Ester containing cellulosics like CCAB are particularly prone to crosslinking reactions during melt processing. It will be important to further investigate the extent of degradation, if any, and quantify the polymer and drug degradative products for the melt extruded formulations described in this work. This quantification can be explored by utilizing high performance liquid chromatography (HPLC)[13] and potentially HPLC/mass spectrometry (HPLC/MS) if degradation products are detected in the HPLC chromatograms of extruded formulations.

The use of CCAB in the melt extruded formulations described in chapter 5 and the good solubility, drug loading efficiency and dissolution properties resulting will also encourage the exploration of other cellulosics in this regard especially some of the novel omega carboxy esters synthesized in our lab, some of which have already been established as excellent ASD polymers[12, 14]. These high DS long chain carboxy esters including cellulose acetate adipate propionate (CAAdP)[1] and cellulose acetate suberate (CA-Sub)[14a] will likely produce even greater plasticizing effects than that experienced with CCAB.

6.4 References

1. Kar, N.; Liu, H.; Edgar, K. J., Synthesis of cellulose adipate derivatives. *Biomacromolecules* **2011,** *12* (4), 1106-15.
2. Marks, J. A.; Wegiel, L. A.; Taylor, L. S.; Edgar, K. J., Pairwise Polymer Blends for Oral Drug Delivery. *Journal of pharmaceutical sciences* **2014,** *103* (9), 2871-2883.
3. Fox, T. G., Influence of diluent and of copolymer composition on the glass temperature of a polymer system. *Bull Am Phys Soc* **1956,** *1* (123), 22060-6218.
4. Nyamweya, N.; Hoag, S. W., Assessment of Polymer-Polymer Interactions in Blends of HPMC and Film Forming Polymers by Modulated Temperature Differential Scanning Calorimetry. *Pharmaceutical Research* **2000,** *17* (5), 625-631.
5. Di Colo, G.; Zambito, Y.; Zaino, C., Polymeric enhancers of mucosal epithelia permeability: Synthesis, transepithelial penetration-enhancing properties, mechanism of action, safety issues. *Journal of Pharmaceutical Sciences* **2008,** *97* (5), 1652-1680.
6. (a) Hsu, L. W.; Lee, P. L.; Chen, C. T.; Mi, F. L.; Juang, J. H.; Hwang, S. M.; Ho, Y. C.; Sung, H. W., Elucidating the signaling mechanism of an epithelial tight-junction opening induced by chitosan. *Biomaterials* **2012,** *33* (26), 6254-6263; (b) Thanou, M.; Verhoef, J. C.; Junginger, H. E., Chitosan and its derivatives as intestinal absorption enhancers. *Advanced Drug Delivery Reviews* **2001,** *50, Supplement 1* (0), S91-S101; (c) Thanou, M.; Verhoef, J. C.; Junginger, H. E., Oral drug absorption enhancement by chitosan and its derivatives. *Advanced Drug Delivery Reviews* **2001,** *52* (2), 117-126.
7. McCortney, B.; Jacobson, B.; Vreeke, M.; Lewis, E. S., Methyl transfers. 14. Nucleophilic catalysis of nucleophilic substitution. *Journal of the American Chemical Society* **1990,** *112* (9), 3554-3559.
8. Lv, H.; Zhang, S.; Wang, B.; Cui, S.; Yan, J., Toxicity of cationic lipids and cationic polymers in gene delivery. *Journal of Controlled Release* **2006,** *114* (1), 100-109.
9. Xie, W.; Xie, R.; Pan, W.-P.; Hunter, D.; Koene, B.; Tan, L.-S.; Vaia, R., Thermal Stability of Quaternary Phosphonium Modified Montmorillonites. *Chemistry of Materials* **2002,** *14* (11), 4837-4845.
10. (a) Buchanan, C. M.; Buchanan, N. L.; Carty, S. N.; Kuo, C. M.; Lambert, J. L.; Posey-Dowty, J. D.; Watterson, T. L.; Wood, M. D.; Malcolm, M. O.; Lindblad, M. S. Cellulose interpolymers and method of oxidation. US Patent 9,040,684 B2, 2011; (b) Buchanan, C. M.; Buchanan, N. L.; Carty, S. N.; Kuo, C. M.; Lambert, J. L.; Malcolm, M. O.; Posey-Dowty, J. D.; Watterson, T. L.; Wood, M. D.; Lindblad, M. S. Cellulose interpolymers and method of oxidation. US Patent 9,040,685 B2, 2013; (c) Buchanan, C. M.; Buchanan, N. L.; Carty, S. N.; Kuo, C. M.; Lambert, J. L.; Malcolm, M. O.; Posey-Dowty, J. D.; Watterson, T. L.; Wood, M. D.; Lindblad, M. S. Cellulose interpolymers and method of oxidation. US Patent 9,040,683 B2, 2015.
11. (a) Janssens, S.; de Armas, H. N.; Roberts, C. J.; Van den Mooter, G., Characterization of ternary solid dispersions of itraconazole, PEG 6000, and HPMC 2910 E5. *Journal of Pharmaceutical Sciences* **2008,** *97* (6), 2110-2120; (b) Ilevbare, G. A.; Liu, H.; Edgar, K. J.; Taylor, L. S., Effect of Binary Additive Combinations on Solution Crystal Growth of the Poorly Water-Soluble Drug, Ritonavir. *Cryst Growth Des* **2012,** *12* (12), 6050-6060.
12. Pereira, J. M.; Mejia-Ariza, R.; Ilevbare, G. A.; McGettigan, H. E.; Sriranganathan, N.; Taylor, L. S.; Davis, R. M.; Edgar, K. J., Interplay of degradation, dissolution and stabilization of clarithromycin and its amorphous solid dispersions. *Molecular pharmaceutics* **2013,** *10* (12), 4640-4653.

13. (a) Sarode, A. L.; Sandhu, H.; Shah, N.; Malick, W.; Zia, H., Hot melt extrusion (HME) for amorphous solid dispersions: predictive tools for processing and impact of drug–polymer interactions on supersaturation. *European Journal of Pharmaceutical Sciences* **2013,** *48* (3), 371-384; (b) Sarode, A. L.; Obara, S.; Tanno, F. K.; Sandhu, H.; Iyer, R.; Shah, N., Stability assessment of hypromellose acetate succinate (HPMCAS) NF for application in hot melt extrusion (HME). *Carbohydrate polymers* **2014,** *101*, 146-153; (c) Liu, J.; Cao, F.; Zhang, C.; Ping, Q., Use of polymer combinations in the preparation of solid dispersions of a thermally unstable drug by hot-melt extrusion. *Acta Pharmaceutica Sinica B* **2013,** *3* (4), 263-272.
14. (a) Liu, H.; Ilevbare, G. A.; Cherniawski, B. P.; Ritchie, E. T.; Taylor, L. S.; Edgar, K. J., Synthesis and structure–property evaluation of cellulose ω-carboxyesters for amorphous solid dispersions. *Carbohydrate Polymers* **2014,** *100* (0), 116-125; (b) Li, B.; Wegiel, L. A.; Taylor, L. S.; Edgar, K. J., Stability and solution concentration enhancement of resveratrol by solid dispersion in cellulose derivative matrices. *Cellulose* **2013,** *20* (3), 1249-1260; (c) Li, B.; Konecke, S.; Harich, K.; Wegiel, L.; Taylor, L. S.; Edgar, K. J., Solid Dispersion of Quercetin in Cellulose Derivative Matrices Influences both Solubility and Stability. *Carbohydrate Polymers* **2013,** *92* (2), 2033-2040; (d) Ilevbare, G. A.; Liu, H. Y.; Edgar, K. J.; Taylor, L. S., Understanding Polymer Properties Important for Crystal Growth Inhibition-Impact of Chemically Diverse Polymers on Solution Crystal Growth of Ritonavir. *Cryst Growth Des* **2012,** *12* (6), 3133-3143; (e) Ilevbare, G. A.; Liu, H.; Edgar, K. J.; Taylor, L. S., Impact of Polymers on Crystal Growth Rate of Structurally Diverse Compounds from Aqueous Solution. *Molecular pharmaceutics* **2013,** *10* (6), 2381-2393.

Appendix: Supplementary Figures and Tables

Chapter 3: Pairwise Polymer Blends for Oral Drug Delivery

Synthesis of CAAdP

Cellulose acetate propionate (CAP-504-0.2) was obtained from Eastman Chemical. Methyl ethyl ketone (MEK) was dried by refluxing over potassium carbonate. Other purchased reagents were used as received. 10% Palladium hydroxide on carbon PdOH/C was purchased from Sigma Aldrich. Adipic acid, *p*-toluenesulfonic acid (PTSA), 1,3-dimethyl-2-imidazolidinone (DMI), oxalyl chloride, and triethylamine (Et_3N) were purchased from ACROS Organics. Benzyl alcohol, toluene, N,N-dimethylformamide (DMF), dichloromethane were purchased from Fisher Scientific. DMI was dried over 4 Å molecular sieves. Anhydrous tetrahydrofuran was purchased from Sigma Aldrich. All other reagents were synthesized by procedures described below.

Synthesis of Monobenzyl Adipate

Adipic acid (73 g, 0.5 mol), benzyl alcohol (81 g, 0.75 mol), PTSA (0.95 g, 5 mmol), and toluene (400 mL) were combined in a flask equipped with Dean Stark trap and heated at reflux until the theoretical amount of H_2O (13.5 mL, 0.75 mol) was obtained. The solution was then cooled, 300 mL of H_2O was added, and the pH was adjusted to 8 with 6 N NaOH. The aqueous layer was separated and washed with ether (2 x100 mL), 200 mL of fresh ether was added, and the pH was adjusted to 2.0 with 6 N HCl. The ether layer was separated, dried (Na_2SO_4), and concentrated to yield 47 g of monobenzyl adipate (40%) as a colorless oil: ^{1}H NMR ($CDCl_3$) 1.68 (m, 4 H), 2.36 (m, 4 H),5.09 (s, 2 H), and 7.32 (m, 5 H). A similar procedure was followed to synthesize monobenzyl suberate (colorless oil). Yield: 47.5% (31.35 g, 0.12 mol). 1H NMR (CDCl3): 1.33 (m, 4H), 1.63 (m, 4H), 2.33 (m, 4H), 5.11 (s, 2H), 7.34
(m, 5H).

Synthesis of Monobenzyl Adipoyl Chloride

A solution of monobenzyl adipate (20 g, 0.08 mol) and DMF (1 drop) in dichloromethane was cooled to 0 °C, and oxalyl chloride (57.15 g, 0.45 mols) was slowly added. After 30 min at 15

°C, the solvent was removed under reduced pressure. Toluene (200 mL) was added to the resultant oil and again the solvent was removed to yield the acid chloride as an oil that was not purified further.

Reaction of CAP with Monobenzyl Adipoyl Chloride

CAP-504-0.2 (1 g, 3.52 mmol) was dissolved in MEK (10 mL), and the solution was heated to 60 °C with stirring under nitrogen. Et_3N (1.63 mL, 11.6 mmol, 3.3 equiv) was added all at once; then, monobenzyl adipoyl chloride (2.67 g, 10.56 mmol, 3 equiv) was added. An immediate precipitate (presumed to be triethylammonium chloride) was observed. The solution was stirred at 60 °C for 20 h. The reaction mixture was filtered and then added dropwise to isopropyl alcohol at room temperature with stirring. The precipitate was collected by filtration and washed with water. It was redissolved in chloroform and precipitated with hexane. The product was washed with hexane and vacuum-dried at 50 °C.

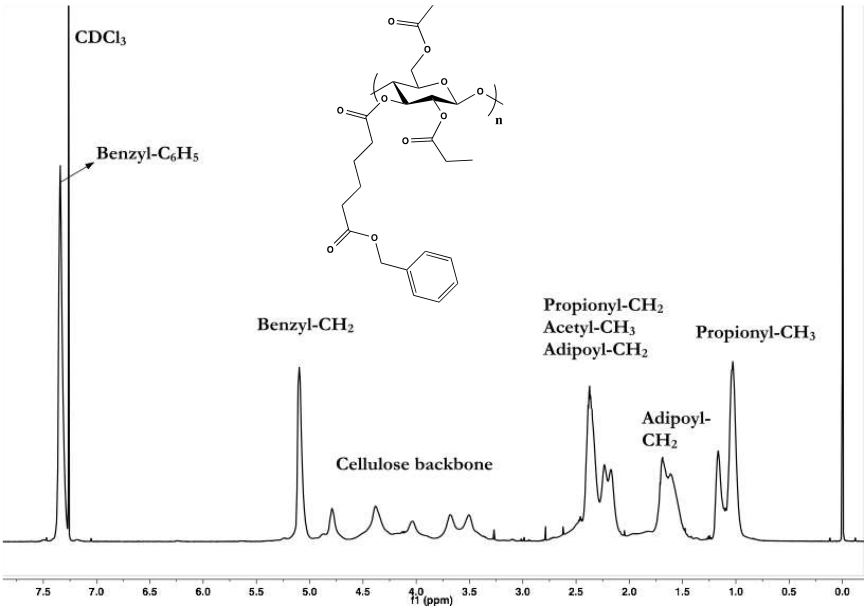

Fig S3.1: Benzyl Cellulose Acetate Adipate Propionate. ^{1}H NMR ($CDCl_3$): 1.02-1.20 (m, $COCH_2C\underline{H_3}$ of propionate), 1.66 (broad s, $COCH_2C\underline{H_2}C\underline{H_2}CH_2CO$ of adipate), 2.16-2.35 (m, $COC\underline{H_2}CH_3$ of propionate, $COC\underline{H_3}$ of acetate and $COC\underline{H_2}CH_2CH_2C\underline{H_2}CO$ of adipate), 3.25-5.24 (cellulose backbone), 5.10 ($C\underline{H_2}C_6H_5$), 7.33 ($CH_2C_6\underline{H_5}$). Degree of substitution (DS) by ^{1}H NMR: adipate 0.85, propionate 2.09, acetate 0.04.

Reaction of CA 320S with Monobenzyl suberoyl Chloride

CAP-504-0.2 (1.00 g, 3.56 mmol) was dissolved in MEK (20 mL), and the solution was heated to 60 °C with stirring under nitrogen. Triethylamine (0.54 mL, 3.92 mmol, 1.1 equiv.) was added to the solution. Monobenzyl sebacoyl chloride (1.11 g, 3.56 mmol, 1 equiv.) or monobenzyl suberoyl chloride (1.02 g, 3.56 mmol, 1 equiv.) was added dropwise and allowed to react at 60 "C for 20 h. The reaction mixture was diluted with ~10 mL of acetone and filtered to remove *in situ* formed triethylamine hydrochloride precipitate. The remaining solution was precipitated into water (250 mL). The precipitate was collected and washed with isopropanol. The filtered product was redissolved in a minimal amount of chloroform and reprecipitated in hexanes.

Representative procedure of Pd/C Hydrogenolysis of the Benzyl Cellulose Ester

The benzyl cellulose ester (200 mg) was dissolved in THF and to this solution was added 10% palladium on carbon (100 mg). The mixture was added to a Parr reactor vessel under hydrogen gas at 80 psi for 1 day. After this time, the mixture was filtered through Celite and evaporated to afford the product. The product was dissolved in chloroform and reprecipitated into hexane. The product was soluble in DMSO and insoluble in water. Additional hydrogenolysis was performed as needed to achieve complete removal of the benzyl groups.

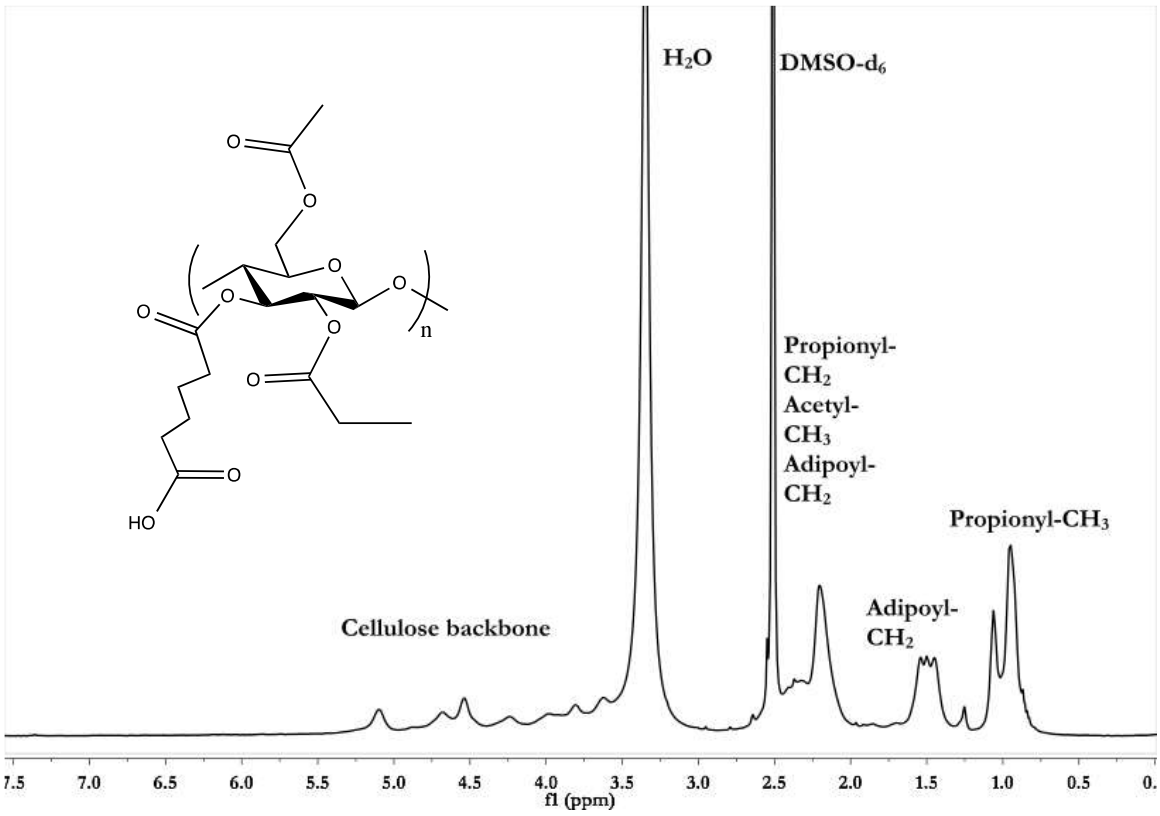

Fig S3.2: Cellulose Acetate Adipate Propionate. ^{1}H NMR (DMSO-d6): 0.95-1.06 (m, COCH$_2$C<u>H$_3$</u> of propionate), 1.50 (broad s, COCH$_2$C<u>H$_2$</u>C<u>H$_2$</u>CH$_2$CO of adipate), 2.21-2.41 (m, COC<u>H$_2$</u>CH$_3$ of propionate, COC<u>H$_3$</u> of acetate and COC<u>H$_2$</u>CH$_2$CH$_2$C<u>H$_2$</u>CO of adipate), 3.50-5.10 (cellulose backbone). DS by ^{1}H NMR: adipate 0.85, propionate 2.09, acetate 0.04.

The degrees of substitution (DS) of the products were assigned from the proton NMR spectra using the ratios of appropriate acyl proton integrations to the backbone proton integration. Yield information is unavailable for the CAAdP of DS 0.85.

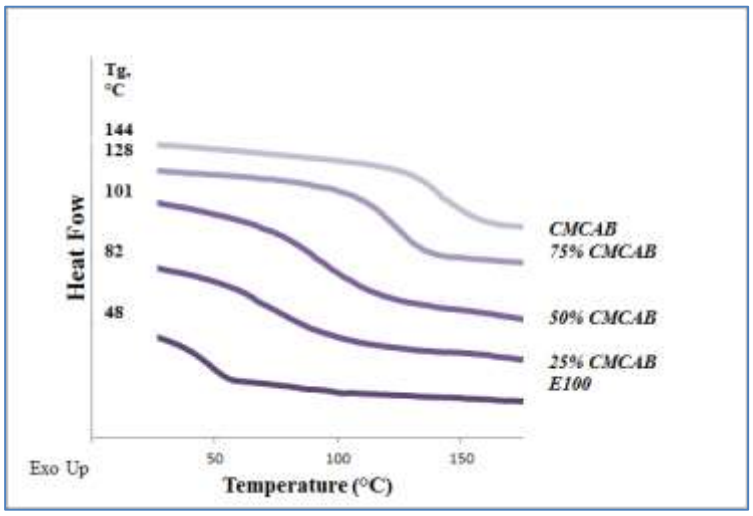

Fig S3.3: 2nd Heat thermograms for CMCAB/E100 blends

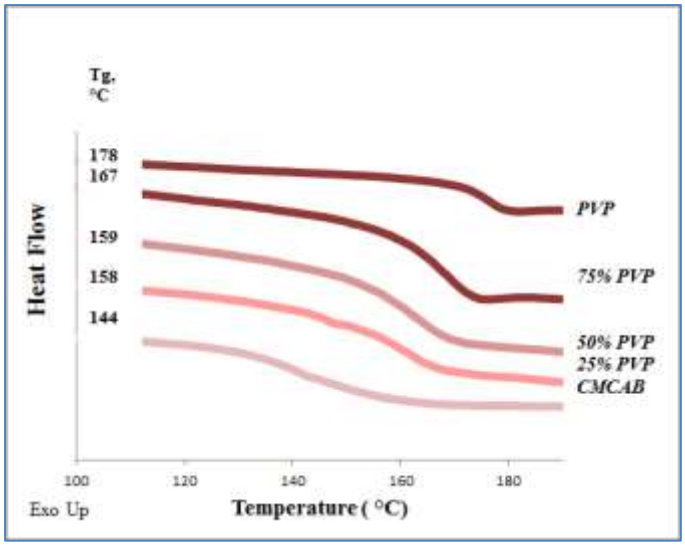

Fig S3.4. 2nd Heat thermograms for PVP/CMCAB

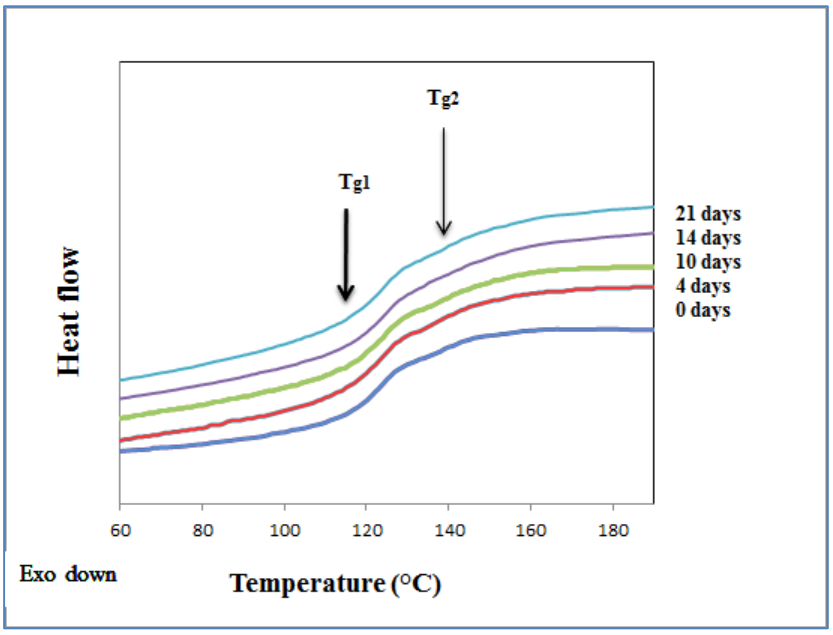
Tg2
Tg1
21 days
14 days
10 days
4 days
0 days
Heat flow
60
80
100
120
140
160
180
Exo down
Temperature (°C)

a) 50/50

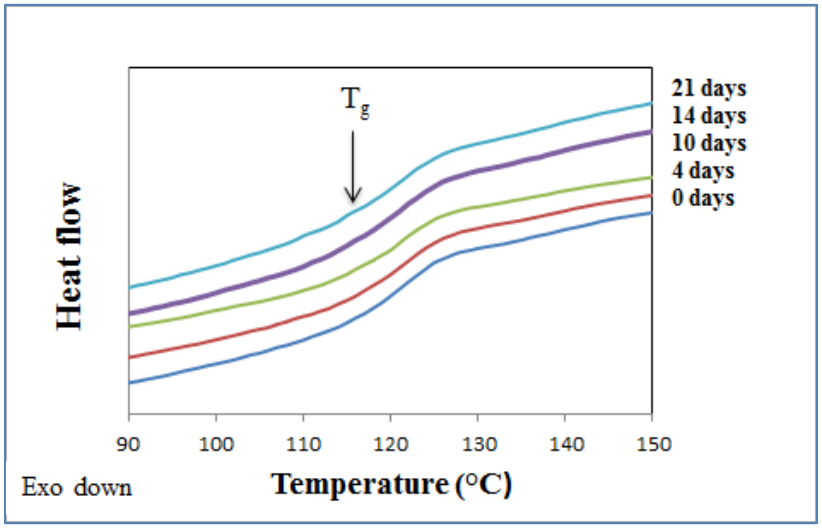
Tg
21 days
14 days
10 days
4 days
0 days
Heat flow
90
100
110
120
130
140
150
Exo down
Temperature (°C)

a) 25/75

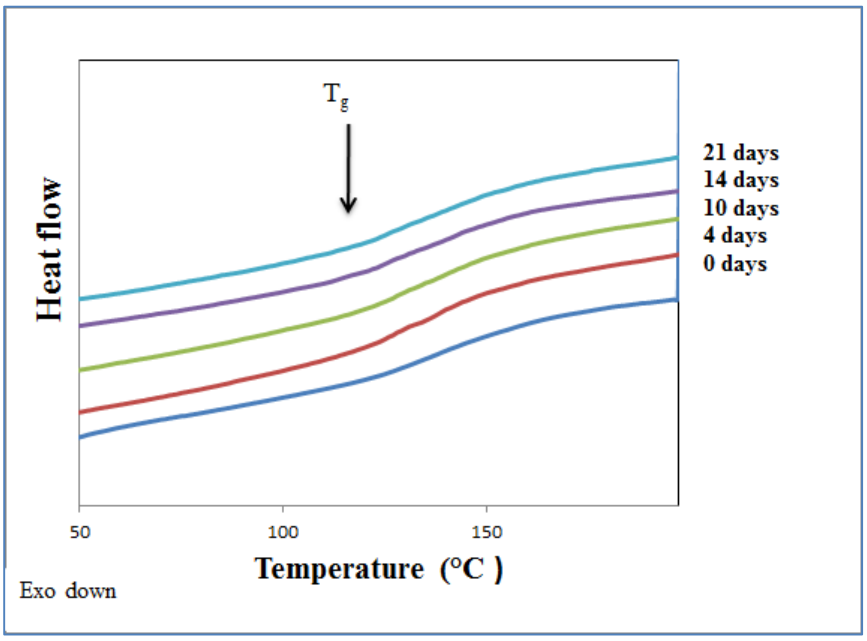

a) 75/25

Fig S3.5. Aging of CMCAB/HPMCAS blends

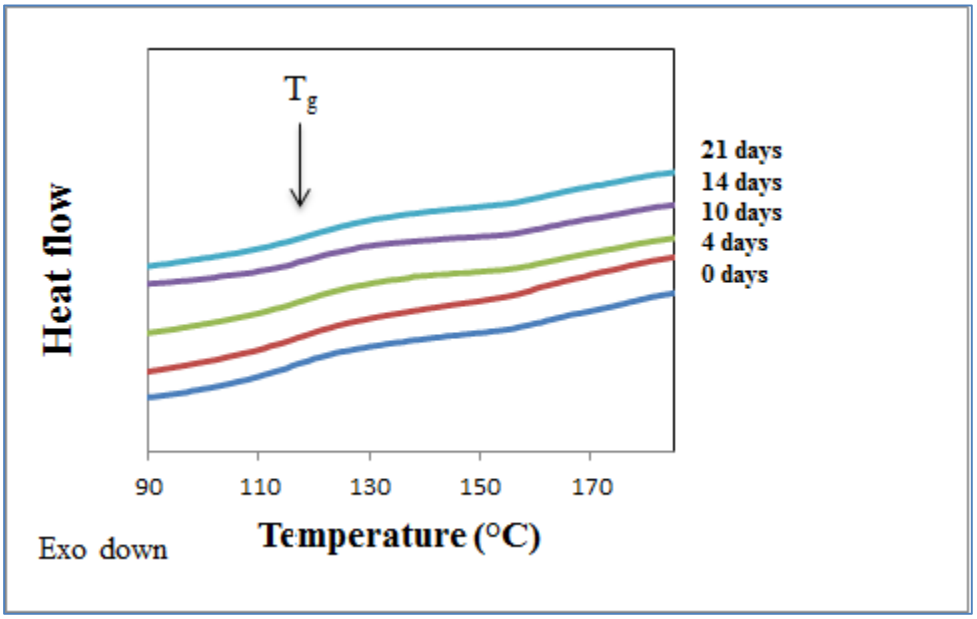

a) 50 % HPMCAS

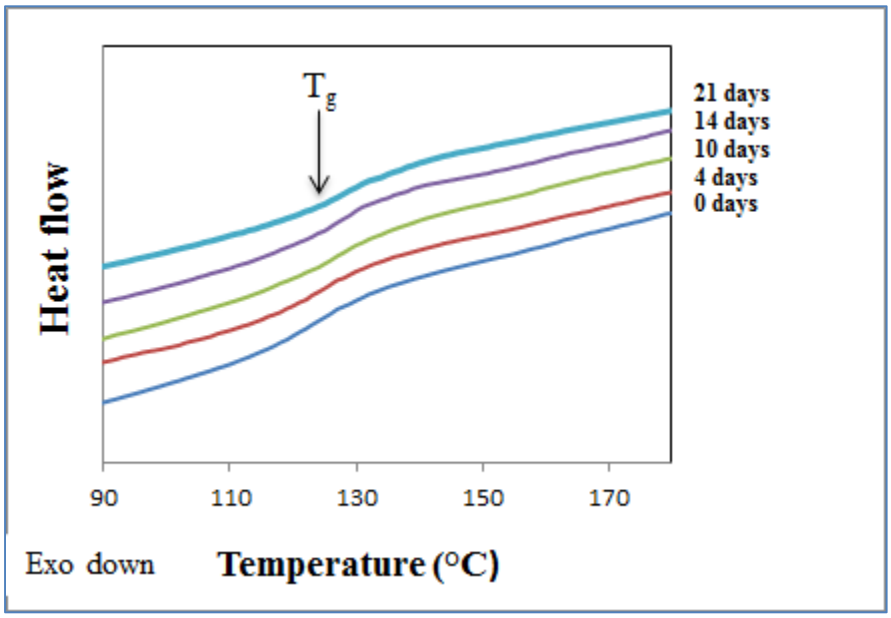

a) 50% CMCAB

Fig S3.6. Aging of CAAdP blends

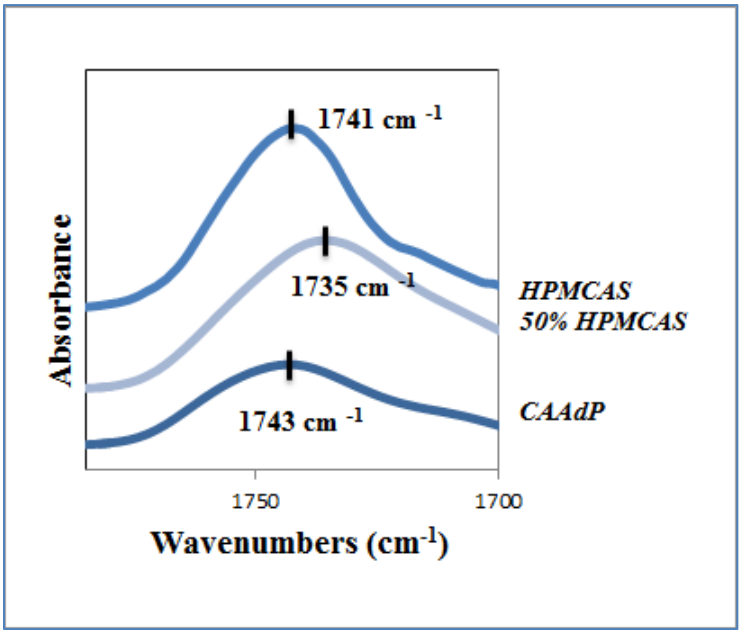

a) HPMCAS/CAAdP

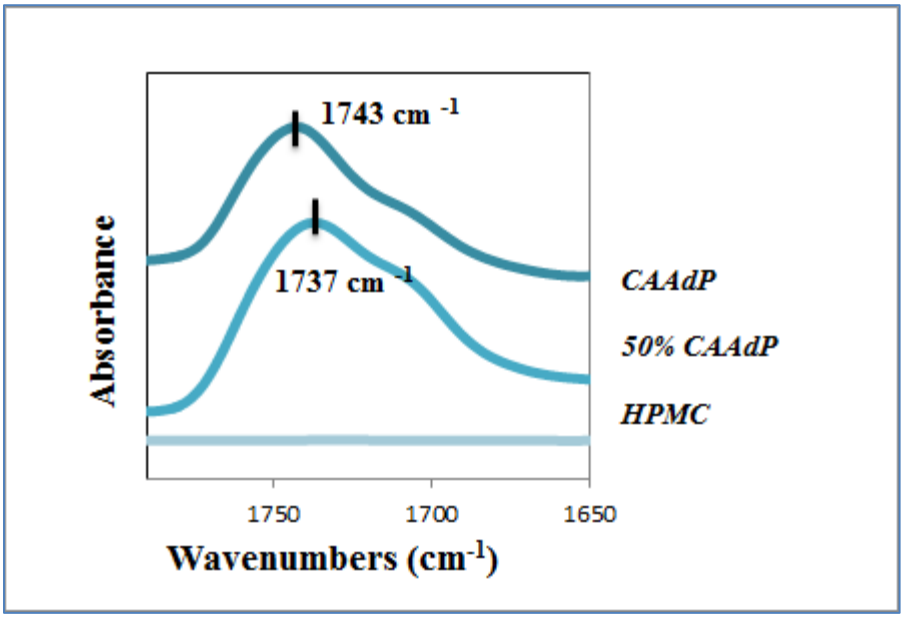

b) HPMC/CAAdP

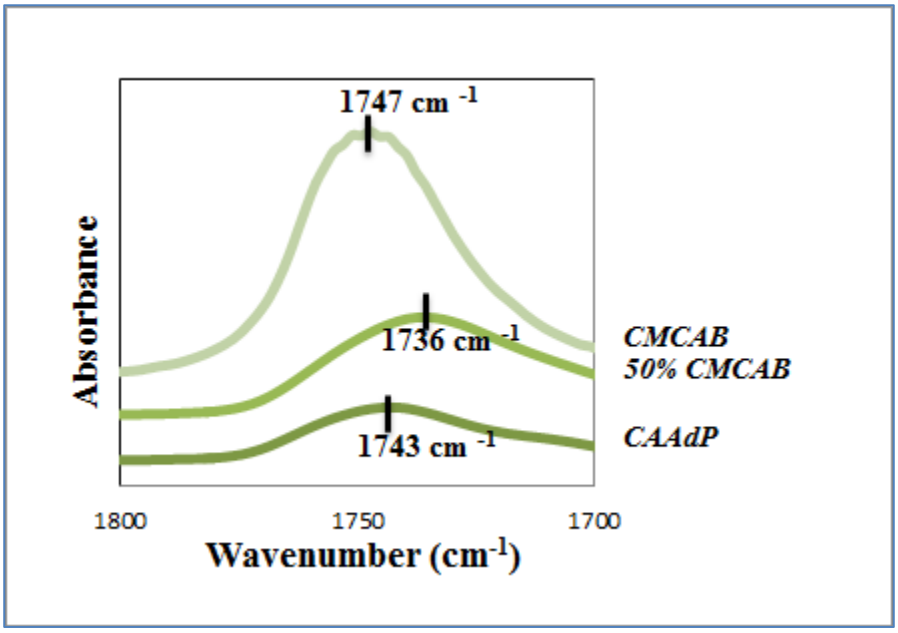

c) CMCAB/CAAdP

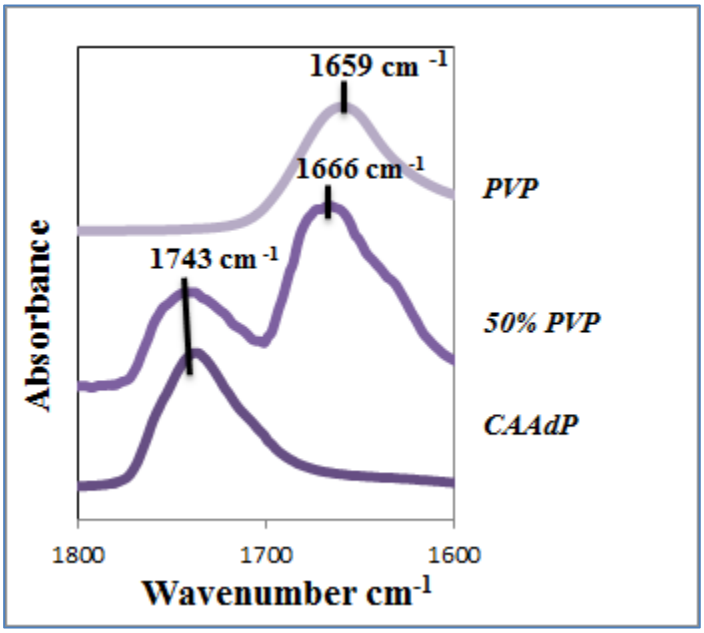

d) PVP/CAAdP

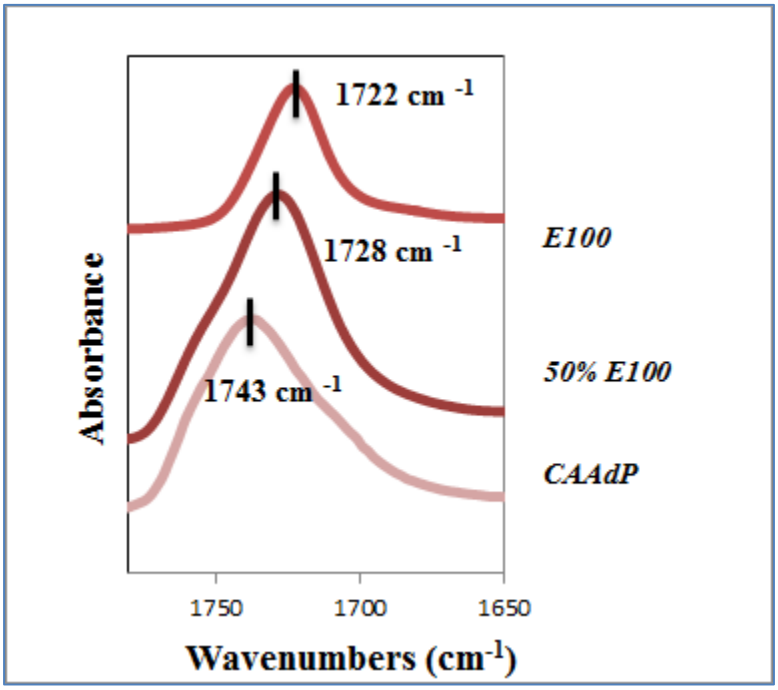

e) E100/CAAdP

Fig S3.7: Infrared Spectra of 50 % CAAdP dispersions showing the carbonyl stretching region.

Table S3.1: Infrared Spectroscopy C=O stretching vibrations of the model polymers used and the shift observed with 50 % CAAdP

Polymer	OH Peak position (cm^{-1})	OH Peak position with 50 % CAAdP (cm^{-1})
Pure CAAdP	**3496**	**-**
PVP	**-**	**3475**
HPMC	**3471**	**3448**
HPMCAS	**3473**	**3467**
CMCAB	**3480**	**3467**
E100	**-**	**3475**

Reaction of 6-bromo-6-deoxy-2,3-di-O-acetyl cellulose with tributylamine

The 6-bromo-6-deoxy-2,3-di-*O*-acetyl cellulose ester was also modified with 100 equivalents of tributylamine to test for the influence of a longer chain trialkylamine on the ammonium conversion. The heterogeneous reaction of the amine with 6-bromo-6-deoxy-2,3-di-*O*-acetyl cellulose in THF and DMF produced a derivative with a DS(Bu_3N^+) of ~ 0.06 (**Figure S4.1**). This low DS is likely due primarily to the immiscibility of the reagent in the solvents investigated (DMSO, THF and DMF, chosen based in part upon the solubility of the starting bromocellulose), as well as to the greater steric demand of the bulkier tributylamine.

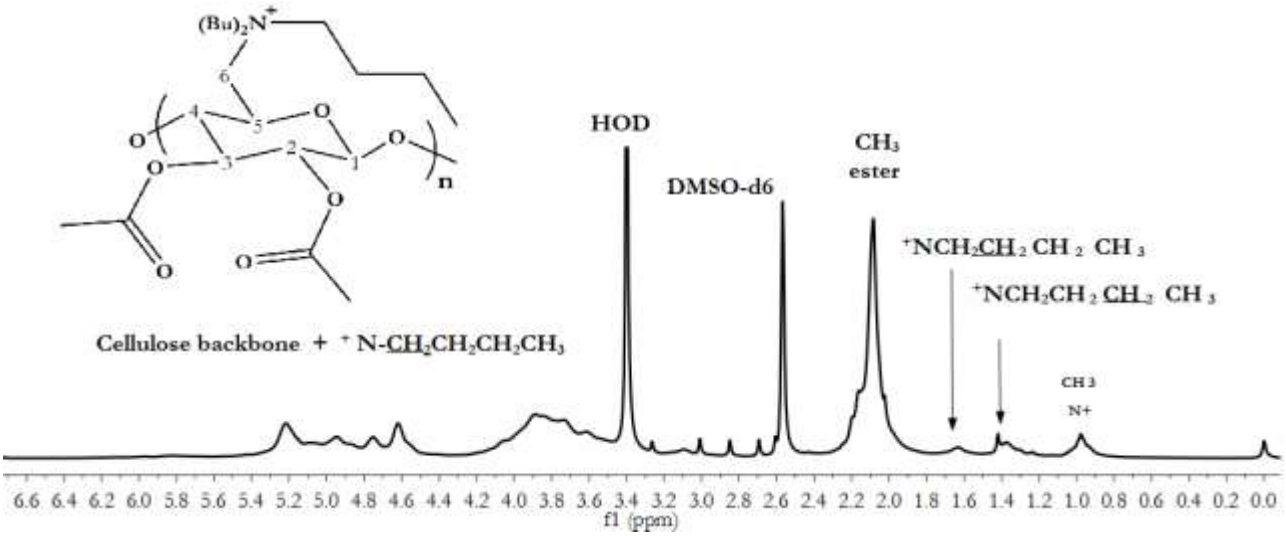

Figure S4.1: ^{1}H NMR spectra of Bu_3N^+ derivative (DS 0.06) of 6-bromo-6-deoxy-2,3-di-*O*-acetyl cellulose using 100 eq. tributylamine in THF.

Reaction of 6-bromo-6-deoxy-2,3-di-O-butyryl cellulose with triethylamine

^{13}C NMR spectrum of Et_3N^+ derivative (DS 0.38) of 6-bromo-6-deoxy-2,3-di-*O*-butyryl cellulose in **Figure S4.2 (top)** shows the methyl and methylene carbons of the N-ethyl groups at 7.8 and 54 ppm, respectively. The amine-substituted C-6 peak appears at 62 ppm in Figure 3 (top). The methyl and two methylene carbons for the butyryl ester appear at 13, 18 and 36 respectively.

The ^{1}H NMR shows the methyl protons of the C-6 Et_3N^+ group at 1.21 ppm the methyl protons of the butyryl ester at 0.8 ppm and the methylene peaks of the ester at 1.5ppm and between 1.8-2.4

ppm. The Et_3N^+ methylene protons are overlapped by cellulose backbone peaks but appear around 3.3 ppm. (**Figure S4.2 (bottom)**).

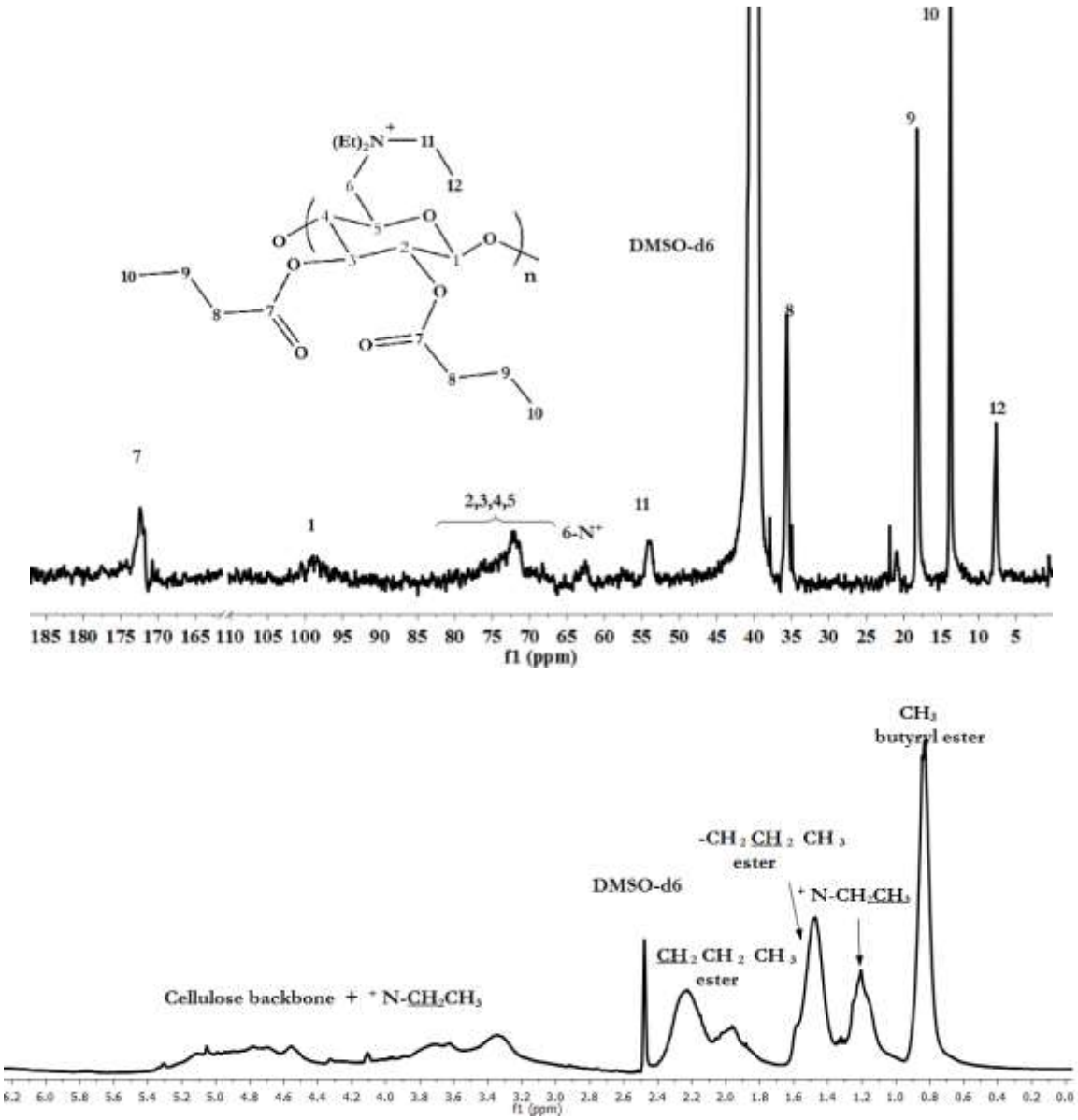

Figure S4.2: ^{13}C NMR (top) and ^{1}H NMR spectra of Et_3N^+ derivative (DS 0.38) of 6-bromo-6-deoxy-2,3-di-*O*-butyryl cellulose using 100 eq. amine.

Reaction of 6-bromo-6-deoxy-2,3-di-O-butyryl cellulose with triethylphosphine

The spectrum of product 2.6 is shown in **Figure S4.3**. The ^{1}H NMR in **Fig. S4.3a** shows the methyl protons for the ethyl groups attached to phosphorus at 1.25 ppm while methylene protons appear together with the methyl protons of the butyryl ester between 2.2 and 2.4 ppm. The methyl protons of the butyryl esters are seen at 0.8 ppm.

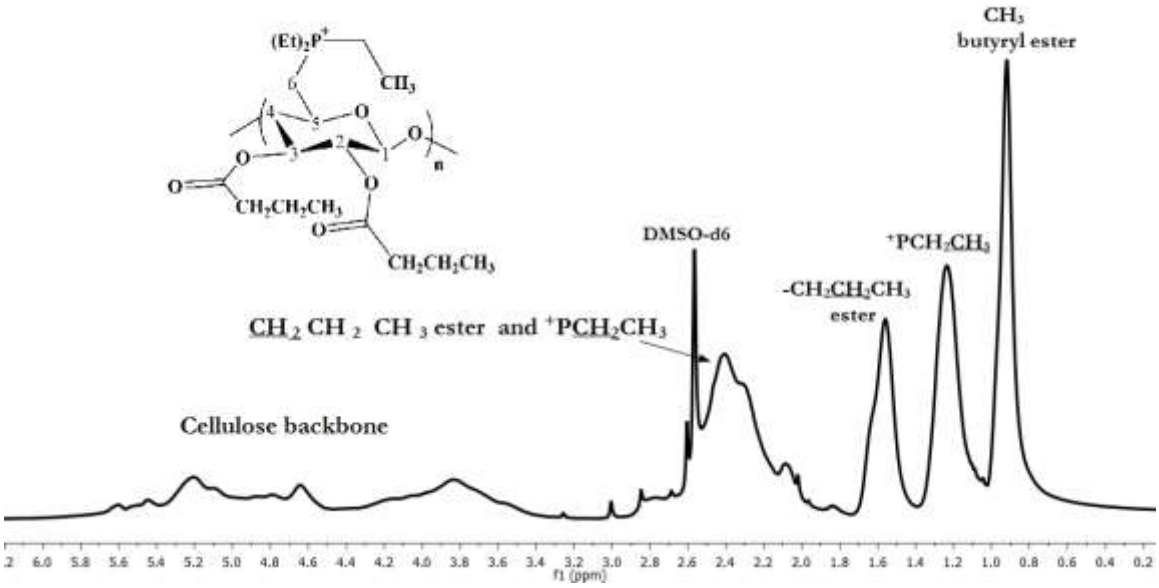

Figure S4.3a: ^{1}H NMR spectrum of the reaction product of Et$_3$P with 6-bromo-6-deoxy-2,3-di-*O*-butyrylcellulose (DS Et$_3$P$^+$ 0.68).

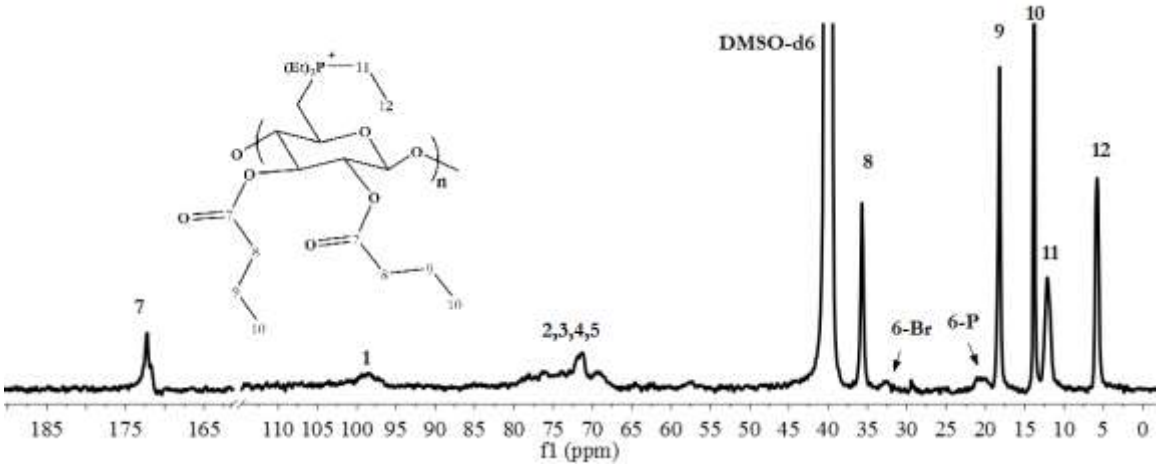

Figure S4.3b: ^{13}C NMR spectrum of the reaction product of Et$_3$P with 6-bromo-6-deoxy-2,3-di-*O*-butyrylcellulose (DS Et$_3$P$^+$ 0.68).

The ^{13}C NMR spectrum in **Figure S4.3b** shows peaks at 5.3 ppm and 11.4 ppm confirming the presence of the methyl and methylene carbons of the ethyl groups bonded to phosphorus in the cellulose backbone. The small peak at 32 ppm is indicative of residual bromine substituted carbon at C-6, while the phosphine-substituted carbon at C-6 appears as a small peak at 21 ppm. The methyl and two methylene carbons of the butyrate ester appear at 13, 18 and 36 ppm respectively. The presence of the phosphonium derivative was also verified using ^{31}P-NMR, which showed a single peak at 38.8 ppm corresponding to the phosphorus atom bonded to C-6.

Chapter 5: 6-Carboxycellulose Acetate Butyrate as a Novel Polymer for Amorphous Solid Dispersion and Extrusion

Synthesis of CAAdP and CA Suberate

Cellulose acetate propionate (CAP-504-0.2) and cellulose acetate (CA 320S) were obtained from Eastman Chemical. Methyl ethyl ketone (MEK) was dried by refluxing over potassium carbonate. Other purchased reagents were used as received. 10% PdOH/C was purchased from Sigma Aldrich. Adipic acid, suberic acid, *p*-toluenesulfonic acid (PTSA), 1,3-dimethyl-2-imidazolidinone (DMI), oxalyl chloride, and triethylamine (Et_3N) were purchased from ACROS Organics. Benzyl alcohol, toluene, N,N-dimethylformamide (DMF), dichloromethane were purchased from Fisher Scientific. DMI was dried over 4 Å molecular sieves. Anhydrous tetrahydrofuran was purchased from Sigma Aldrich. All other reagents were synthesized by procedures described below.

Synthesis of Monobenzyl Adipate and suberate

Adipic acid (73 g, 0.5 mol), benzyl alcohol (81 g, 0.75 mol), PTSA (0.95 g, 5 mmol), and toluene (400 mL) were combined in a flask equipped with Dean Stark trap and heated at reflux until the theoretical amount of H_2O (13.5 mL, 0.75 mol) was obtained. The solution was then cooled, 300 mL of H_2O was added, and the pH was adjusted to 8 with 6 N NaOH. The aqueous layer was separated and washed with ether (2 x100 mL), 200 mL of fresh ether was added, and the pH was adjusted to 2.0 with 6 N HCl. The ether layer was separated, dried (Na_2SO_4), and concentrated to yield 47 g of monobenzyl adipate (40%) as a colorless oil: ^1H NMR ($CDCl_3$) 1.68 (m, 4 H), 2.36 (m, 4 H),5.09 (s, 2 H), and 7.32 (m, 5 H). A similar procedure was followed to synthesize monobenzyl suberate (colorless oil). Yield: 47.5% (31.35 g, 0.12 mol). 1H NMR (CDCl3): 1.33 (m, 4H), 1.63 (m, 4H), 2.33 (m, 4H), 5.11 (s, 2H), 7.34
(m, 5H).

Synthesis of Monobenzyl Adipoyl and suberoyl chlorides

A solution of monobenzyl adipate (20 g, 0.08 mol) and DMF (1 drop) in dichloromethane was cooled to 0 °C, and oxalyl chloride (57.15 g, 0.45 mol) was slowly added. After 30 min at 15 °C, the solvent was removed under reduced pressure. Toluene (200 mL) was added to the resultant oil and again the solvent was removed to yield the acid chloride as an oil that was not purified further. A similar procedure was followed to synthesize monobenzyl suberoyl chloride. Yield: 90.7%

Reaction of CAP with Monobenzyl Adipoyl Chloride

CAP-504-0.2 (1 g, 3.52 mmol) was dissolved in MEK (10 mL), and the solution was heated to 60 °C with stirring under nitrogen. Et_3N (1.63 mL, 11.6 mmol, 3.3 equiv) was added all at once; then, monobenzyl adipoyl chloride (2.67 g, 10.56 mmol, 3 equiv) was added. An immediate precipitate (presumed to be triethylammonium chloride) was observed. The solution was stirred at 60 °C for 20 h. The reaction mixture was filtered and then added dropwise to isopropyl alcohol at room temperature with stirring. The precipitate was collected by filtration and washed with water. It was redissolved in chloroform and precipitated with hexane. The product was washed with hexane and vacuum-dried at 50 °C.

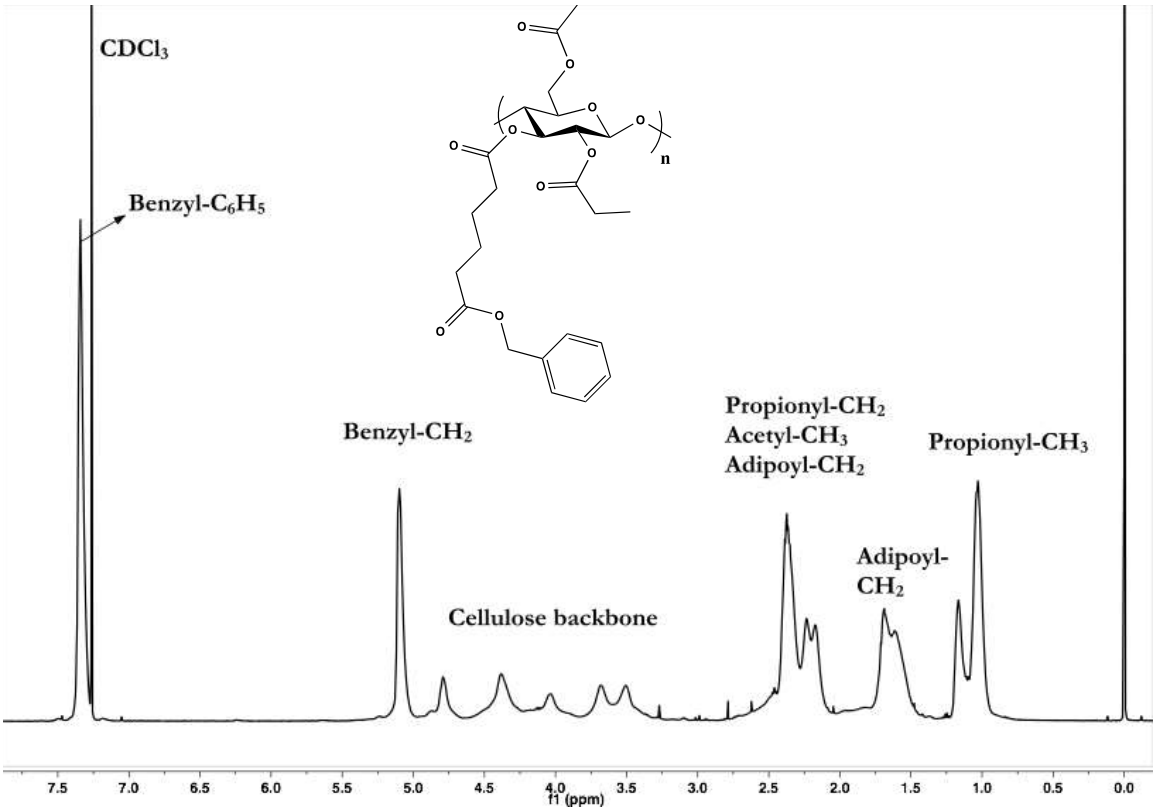

Fig S5.1: Benzyl Cellulose Acetate Adipate Propionate. ^{1}H NMR (CDCl$_3$): 1.02-1.20 (m, COCH$_2$C<u>H$_3$</u> of propionate), 1.66 (broad s, COCH$_2$C<u>H$_2$</u>C<u>H$_2$</u>CH$_2$CO of adipate), 2.16-2.35 (m, COC<u>H$_2$</u>CH$_3$ of propionate, COC<u>H$_3$</u> of acetate and COC<u>H$_2$</u>CH$_2$CH$_2$C<u>H$_2$</u>CO of adipate), 3.25-5.24 (cellulose backbone), 5.10 (C<u>H$_2$</u>C$_6$<u>H$_5$</u>), 7.33 (CH$_2$C$_6$<u>H$_5$</u>). Degree of substitution (DS) by ^{1}H NMR: adipate 0.85, propionate 2.09, acetate 0.04.

<u>Reaction of CA 320S with Monobenzyl suberoyl Chloride</u>

CAP-504-0.2 (1.00 g, 3.56 mmol) was dissolved in MEK (20 mL), and the solution was heated to 60 °C with stirring under nitrogen. Triethylamine (0.54 mL, 3.92 mmol, 1.1 equiv.) was added to the solution. Monobenzyl sebacoyl chloride (1.11 g, 3.56 mmol, 1 equiv.) or monobenzyl suberoyl chloride (1.02 g, 3.56 mmol, 1 equiv.) was added dropwise and allowed to react at 60 °C for 20 h. The reaction mixture was diluted with ~10 mL of acetone and filtered to remove *in situ* formed triethylamine hydrochloride precipitate. The remaining solution was precipitated into

water (250 mL). The precipitate was collected and washed with isopropanol. The filtered product was redissolved in a minimal amount of chloroform and reprecipitated in hexanes.

Representative procedure of Pd/C Hydrogenolysis of the Benzyl Cellulose Ester

The benzyl cellulose ester (1g) was dissolved in 100 mL THF and to this solution was added 10% palladium hydroxide on carbon (1g). The mixture was added to a Parr reactor vessel under hydrogen gas at 90 psi for 1 day. After this time, the mixture was filtered through celite and 1g of fresh catalyst added to the mixture. The mixture was returned to the Parr reactor vessel under hydrogen gas at 90 psi for an additional day after which it was filtered through celite and concentrated under vacuum. The product was precipitated into hexane. For further purification, product could be redissolved in THF and reprecipitated into hexane. The product was soluble in DMSO and insoluble in water. Additional hydrogenolysis was performed as needed to achieve complete removal of the benzyl groups.

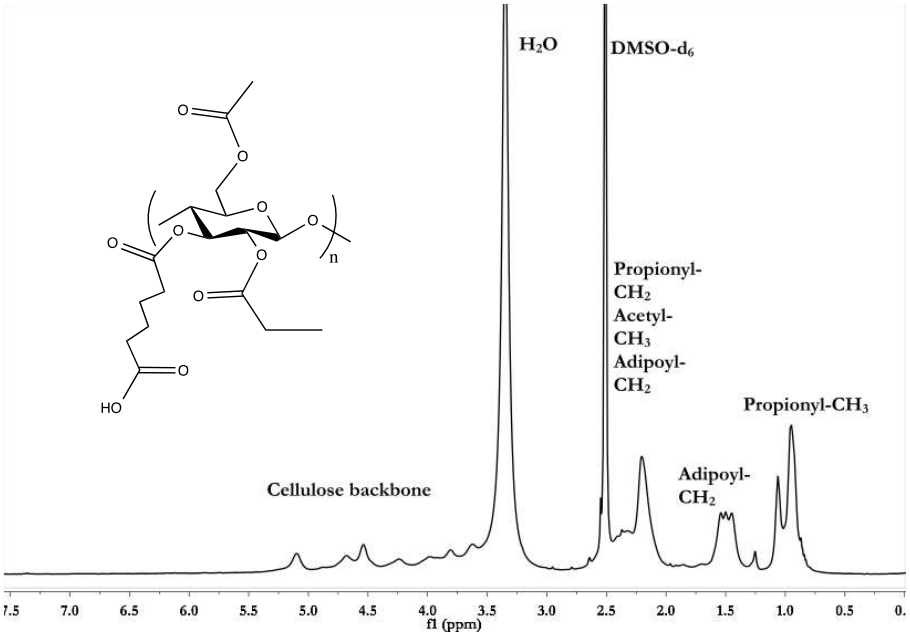

Fig S5.2: Cellulose Acetate Adipate Propionate. ^{1}H NMR (DMSO-d6): 0.95-1.06 (m, COCH$_2$C<u>H$_3$</u> of propionate), 1.50 (broad s, COCH$_2$C<u>H$_2$</u>C<u>H$_2$</u>CH$_2$CO of adipate), 2.21-2.41 (m, COC<u>H$_2$</u>CH$_3$ of propionate, COC<u>H$_3$</u> of acetate and COC<u>H$_2$</u>CH$_2$CH$_2$C<u>H$_2$</u>CO of adipate), 3.50-5.10 (cellulose backbone). DS by ^{1}H NMR: adipate 0.85, propionate 2.09, acetate 0.04.

The degrees of substitution (DS) of the products were assigned from the proton NMR spectra using the ratios of appropriate acyl proton integrations to the backbone proton integration. Yield information is unavailable for the CAAdP of DS 0.85.

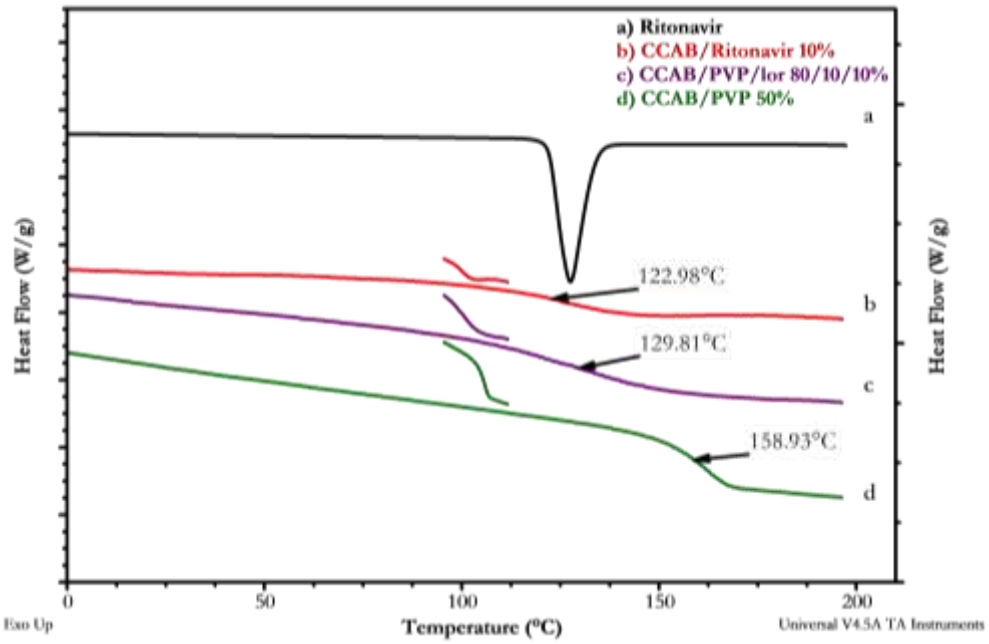

Figure S5.3:DSC thermograms of pure ritonavir, CCAB/Rit 10%, CCAB/PVP/Lor (8:1:1) and binary 50% blend of CCAB/PVP

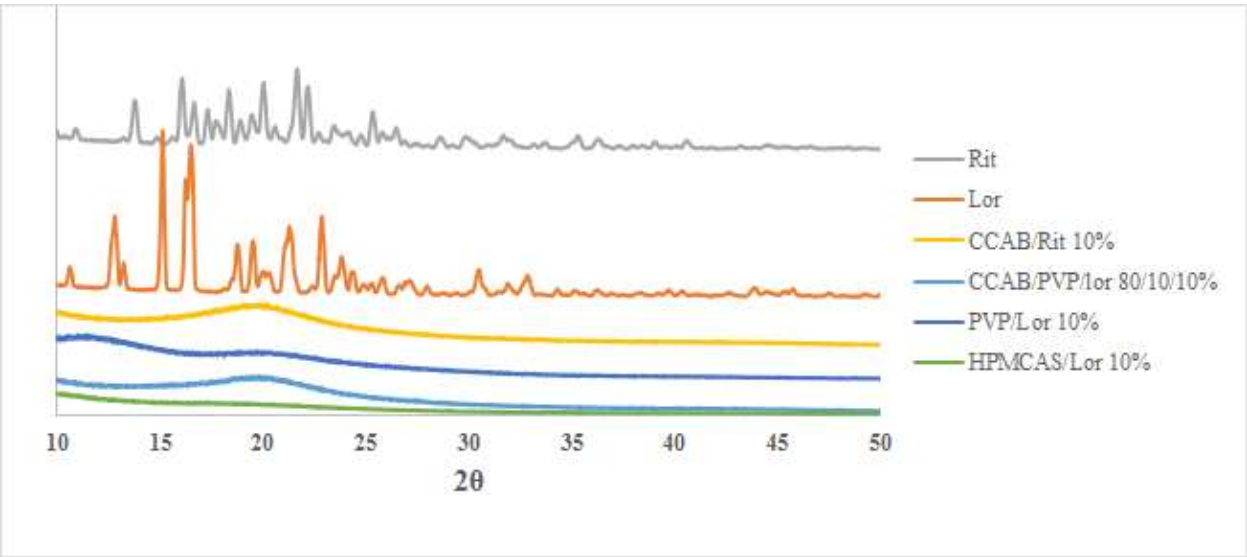

Figure S5.4: XRD Diffractogram of CCAB/PVP/Lor 80/10/10% ASD, ritonavir, loratadine, CCAB/Rit 10%, PVP/Lor 10% and HPMCAS/Lor 10%

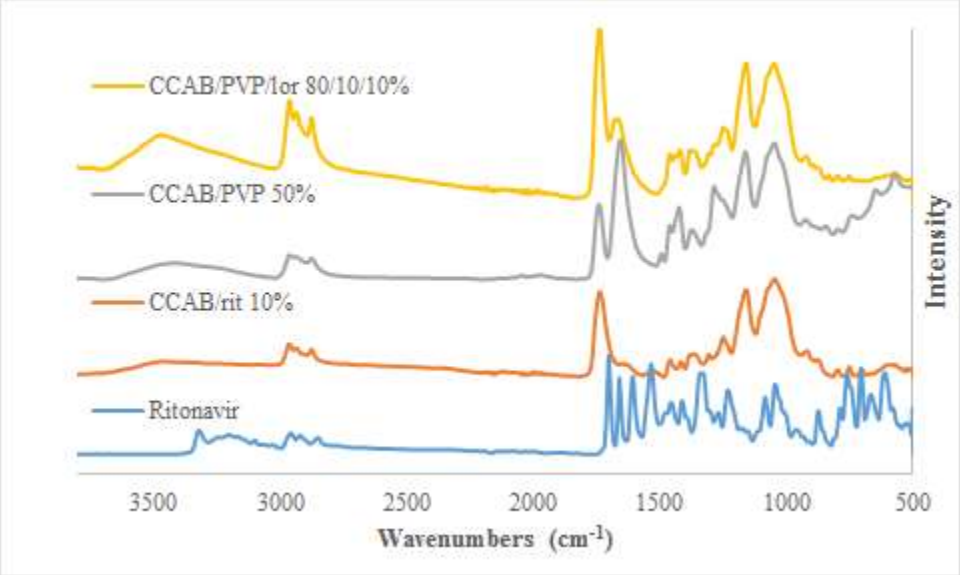

Figure S5.5: FTIR spectra of pure ritonavir, 10% ritonavir in CCAB, CCAB/PVP 50% and CCAB/PVP/Lor 80/10/10% formulations